Fertility preservation in pre-pubertal boys with cancer: a three-dimensional (3D) prepubertal testicular organoid culture system for in vitro spermatogonial stem cell (SSCs) propagation and spermatogenesis

Shiyan Tang
Lincoln College
University of Oxford

Supervisor: **Dr Kevin Coward**
Secondary supervisor: **Professor Anne Goriely**
Nuffield Department of Women's and Reproductive Health

Thesis submitted for the degree of Doctor of Philosophy
Hilary Term 2022

Table of Contents

Abstract

The overall survival rate of childhood cancer has increased over the last decades due to improvements in cancer therapies. However, aggressive cancer treatments, such as chemo- or radiotherapy, can leave young prepubertal boys infertile. Cryogenically 'banking' sperm from prepubertal boys is impossible because spermatogonial stem cells (SSCs) only start to produce sperm after puberty. Thus, to help these patients preserve their fertility, it is recommended to cryopreserve their immature testicular tissues (ITTs) before receiving cancer therapies. To date, there is no standardised procedure for ITT transportation and cryopreservation in clinical practice. Approaches to fertility restoration using frozen/thawed ITTs are in the experimental stages. This thesis aimed to investigate the effects of different cryopreservation methods and potential transportation times on ITTs, and developed a three-dimensional (3D) testicular organoids (TOs) system to support the proliferation and development of SSCs. In Chapter 2, I compared the effects of uncontrolled slow freezing (USF), controlled slow freezing (CSF), and vitrification on the cryopreservation of neonatal gonocyte-containing ITTs using a bovine model. All three methods had similar effects in preserving germ cells, Sertoli cells and proliferating cells in seminiferous cords ($p>0.05$). Vitrified ITTs were found to have lower cell apoptosis but higher cords-basement membrane detachment ($p<0.05$). In chapter 3, I investigated the effects of transportation times of 1 hour, 6 hours, 24 hours, and 48 hours on ITTs. Transportation times up to 48 hours did not affect the viability, percentage of Sertoli cells and proliferating cells, and expressions of selected key genes ($p>0.05$). However, ITTs in the 48-hour group had higher levels of deterioration in terms of the structure of the seminiferous cords (16.43%±2.14%) and decreased percentage of seminiferous cords with germ cells (43.19%±6.45%; $p<0.05$). Next in Chapter 4 and chapter 5, for the first time, a 3D TO model was developed for *in vitro* culturing neonatal bovine testicular cells. Firstly, I optimized the dissociation and enrichment of germ cells in neonatal bovine ITTs. Next, by comparing different extracellular matrix (ECM), I found that Matrigel was optimal in the formation of germ cell aggregations. The TOs emerged from single cell suspensions and developed into 3D structures where germ cells were in the centre with Sertoli cells at the outer layers in neonatal bovine. Furthermore, growth factors glial cell line-derived neurotrophic factor (GDNF), fibroblast growth factor 2 (FGF2), and leukemia inhibitory factor (LIF) were found to promote the transformation of gonocytes into SSCs, while follicle-stimulating hormone (FSH) and testosterone maintained the viability and proliferation of cells in TOs. In summary, this thesis

provided evidence that vitrification could be an alternative method for cryopreservation of ITTs, and tissue transportation times of up to 24 hours does not affect tissue quality and could be used in clinical practice. In addition, a novel 3D TO system was developed in the bovine model, thus offering an *in vitro* platform for the propagation and development of SSCs.

Key words: immature testicular tissues, three-dimensional culture, testicular organoids, fertility preservation, slow freezing cryopreservation, vitrification, *in vitro*, transportation time.

Acknowledgements

Throughout my DPhil journey at Oxford, I have received a great deal of support and help directly or indirectly from these excellent people who I admire and appreciate.

First and foremost, I would like to express my deepest appreciation to my supervisor, Dr. Kevin Coward, for having trusted me and provided me with this golden opportunity to conduct this DPhil project in his laboratory, and for guiding me throughout the journey. My Dphil study could not be possible without Kevin's expertise and trust, valuable and constructive suggestions, patient guidance, enthusiastic encouragement, and unwavering supports academically and personally. I would also like to thank Kevin for sharing his own experiences to me and providing limitless support and helpful advice in my life changing decisions in career.

I wish to show my greatest appreciation to Mrs Celine Jones, our devoted laboratory manager, from whom I have learned a lot from, academically and personally. I would like to thank Celine for helping me to troubleshoot all the unexpected results in my experiments and give me lots of encouragements when my experiment failed. She is an amazing person in many ways; she is patient, positive, kind, and supportive. Her warmness makes Oxford my second home.

I am especially grateful to my second supervisor Professor Anne Goriely, for her support and encouragements. Anne has given me a lot of suggestions in my scientific career since our very first meeting, for which I am truly grateful. I would also like to thank the examiners, Professor Ahmed Ahmed and Dr Muhammad Fatum, for their valuable comments and suggestions in my DPhil transfer and confirmation.

My gratitude extends to all the collaborators and people who have helped me in this project. I would like to thank Future Fertility Programme Oxford and Oxford Cell and Tissue Bank

(OCTB), especially Dr Sheila Lane and Mrs Jill Davis, for providing supports in experiment design and tissue cryopreservation; thank Dr Julian Dye and Dr Cathy Ye from the Department of Engineering, for their help in tissue engineering. I would also like to thank all team members in Kevin's group: Xin, Eisa, Yaqiong, Teresa, and Sally, for all the support and for making my time in laboratory and office enjoyable. In addition, I would like to thank all colleagues at the Nuffield Department of Women's and Reproductive Health for their help in both office and laboratory at the John Radcliffe.

I greatly acknowledge my funding bodies: Oxford Clarendon Scholarship, Lincoln college, SRF and Oxford Medical division for all the financial supports.

I greatly appreciate the supports and accompanies from my dearest friends, especially during the hard time of Covid-19 pandemic, without you I would not be able to have such an unforgettable time at Oxford. Particularly, I would like to thank Junyu, Yiwen, Mengni, Chengcheng, Danlei, Rui, Tianyi, Wenyuan, Hang, Steven and Zhichao for their warmness, cheerfulness, and encouragements throughout the ups and downs in my DPhil.

Last but not least, I would like to express my very profound gratitude to my ever-loving parents: Mr. Maosheng Tang and Mrs. Hongmei Deng, for their unconditional love, continuous supports, encouragements and accompanies during my educational endeavours and beyond.

List of figures

List of tables

List of abbreviations

Abbreviations	Full description
2D	two-dimensional
3D	three-dimensional
AMH	anti-Müllerian hormone
ANOVA	one-way analysis of variance
ART	assisted reproductive technologies
BMP4	bone morphogenic factor 4
BSA	bovine serum albumin
CPA	cryoprotectant agent
CREM	cyclic-AMP responsive element modulator
CSF	controlled slow freezing
DAB	3,3′-diaminobenzidine
DAPI	4′,6-diamidino-2-phenylindole
DMEM/F12	Dulbecco's Modified Eagle's Medium/Nutrient Mixture F-12
DMSO	dimethyl sulfoxide
DNA	deoxyribonucleic acid
dpp	days post-partum
DTM	decellularized testicular matrix
ECM	extracellular matrix
EGF	epidermal growth factor
EHS	Engelbreth-Holm-Swarm
FBS	fetal bovine serum
FGF	fibroblast growth factors
FGF2	fibroblast growth factor 2
FSH	follicle-stimulating hormone
G0	gap 0
G1	gap 1
G2-M	gap 2-mitosis
GC	germ cell
GDNF	glial cell line-derived neurotrophic factor

GFP	green fluorescent protein
GFRα-1	GDNF receptor alpha-1
H_2O_2	hydrogen peroxide
HBSS	Hanks' Balanced Salt Solution
HPG	hypothalamic-pituitary-gonadal
hr	hour
HSCT	hematopoietic stem cell transplant
HSP70-2	heat-shock protein 70-2
ICSI	intracytoplasmic sperm injection
IL1	Interleukin-1
iPSC	induced pluripotent stem cell
ITT	immature testicular tissue
IVF	*in vitro* fertilization
IVS	*in vitro* spermatogenesis
KSR	knockout serum replacement
LH	luteinizing hormone
LIF	leukemia inhibitory factor
LN_2	liquid nitrogen
MAPK/ERK	mitogen-activated protein kinase/extracellular receptor kinase
mTOR	mammalian target of rapamycin
OCTB	Oxford Cell and Tissue Biobank
ORTCP	Oxford Reproductive Tissue Cryopreservation Programme
OWB	organoid wash buffer
PBS	phosphate Buffered Saline
PCR	polymerase chain reaction
PFA	paraformaldehyde
PGC	primordial germ cell
PGCL	primordial germ cell like
PGP9.5	protein gene product 9.5
PI3K/AKT	phosphatidylinositol-3-kinase/AKT
PLGA	poly (D, L-lactic-co-glycolic acid)
PLZF	promyelocytic leukaemia zinc-finger

PMCs	peritubular myoid cells
PreSPG	prespermatogonia
PSC	pluripotent stem cells
PVA	polyvinyl alcohol
qRT-PCR	quantitative real-time reverse transcription-polymerase chain reaction
RA	retinoic acid
RET	rearranged during transfection
RNA	ribonucleic acid
SACS	soft agarose culture system
SCF	stem cell factor
SCs	Sertoli cells
SD	standard deviation
SPG	spermatogonia
SRY	sex determining region Y
SSC	spermatogonial stem cell
STRA8	stimulated by retinoic acid gene 8
TNFα	tumour Necrosis Factor alpha
TO	testicular organoid
TTC	total testicular cells
TUNEL	terminal deoxynucleotidyl transferase dUTP nick end labeling
USF	uncontrolled slow freezing

Chapter 1. General introduction

1.1 Development of testes from the neonatal to the post-pubertal period

Testes, or testicles, are two oval-shaped organs in the scrotum that mainly have two functions: to produce androgens and to produce and store germ cells (GCs). The testicular parenchyma is covered by a fibrous capsule, the tunica albuginea. The septae of the capsule radiate into the parenchyma, forming hundreds of cone-shaped lobules with seminiferous tubules (**Figure 1-1**). The GCs and Sertoli cells in the seminiferous tubules are supported by the basement membrane in the lobules of the testis. These seminiferous tubules become straight and anastomose to make the rete testis in the mediastinum of testis. The tubules in the rete testis drain into the efferent ducts that carry spermatozoa to the epididymis. The epididymis is divided into three segments: the caput proximal (head of the epididymis) to the testis, the corpus (body of the epididymis), and the cauda (tail of the epididymis) (Clement and Giuliano, 2015). The ductus epididymis is formed by the coiled epididymal tubule. The epididymal duct is surrounded by smooth muscle cells, which contract rhythmically according to neural stimulation. The most important function of the epididymis is to help spermatozoa to migrate from the testicular efferent ducts to the ductus deferens and acquire motility and fertility maturity. During pre-puberty, the testes are immature and not fully functional. Spermatogenesis does not begin until after puberty with only mitosis occurring in immature testicular tissues (ITTs). The seminiferous tubules of the prepubertal testis mostly contain spermatogonial stem cells (SSCs) and Sertoli cells, while in the post- pubertal testis, spermatogenesis and GCs are formed in different stages.

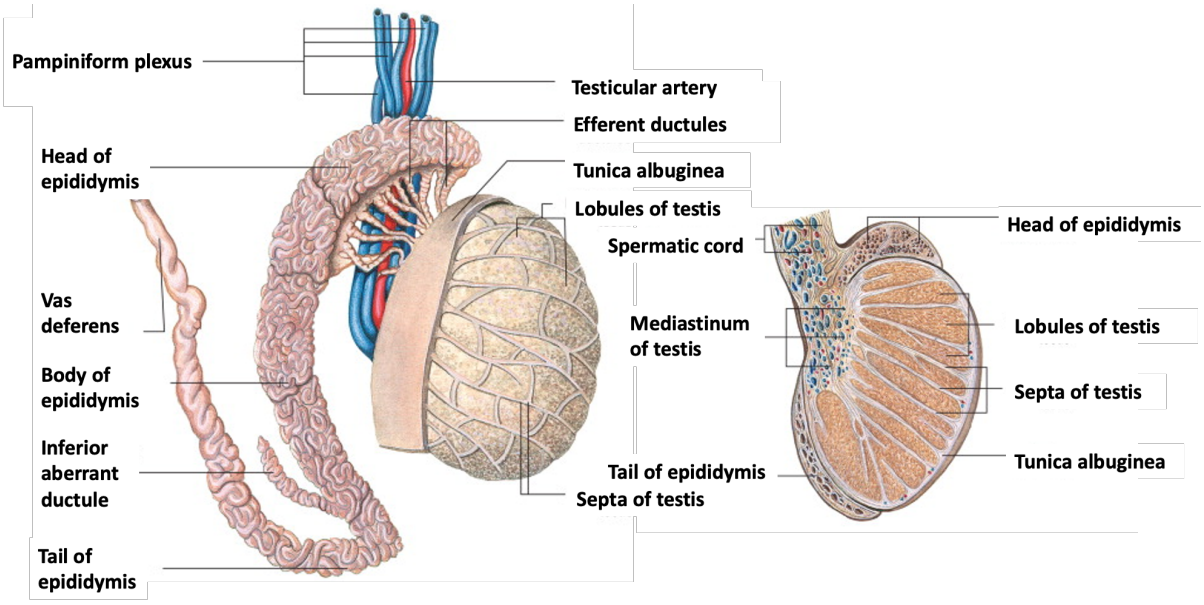

Figure 1-1. Sagittal representation of testes and epididymis. Adapted and modified from (Ellis and Mahadevan, 2014) with permission from publisher.

1.1.1 Hormone changes during mini-puberty and puberty

In males, the hypothalamic-pituitary-gonadal (HPG) axis (**Figure 1-2**) plays a key role in development, sexual maturation, and aging (Corradi et al., 2016). The hypothalamus secretes gonadotropin-releasing hormone (GnRH) in a pulsatile manner, which stimulates the secretion of gonadotropins including follicle-stimulating hormone (FSH) and luteinizing hormone (LH) from the anterior pituitary gland. FSH and LH act on Leydig cell, Sertoli cells, and GCs in the testes. LH induces Leydig cells to synthesize the sex steroid hormone, testosterone, while FSH induces s to produce anti-Müllerian hormone (AMH) and inhibin B, which apply negative feedback on the hypothalamic-pituitary axis and suppress GnRH and LH secretion (Hiller-Sturmhöfel and Bartke, 1998). Testosterone and FSH quantitatively maintain the spermatogenic process in the testis and are essential to this process.

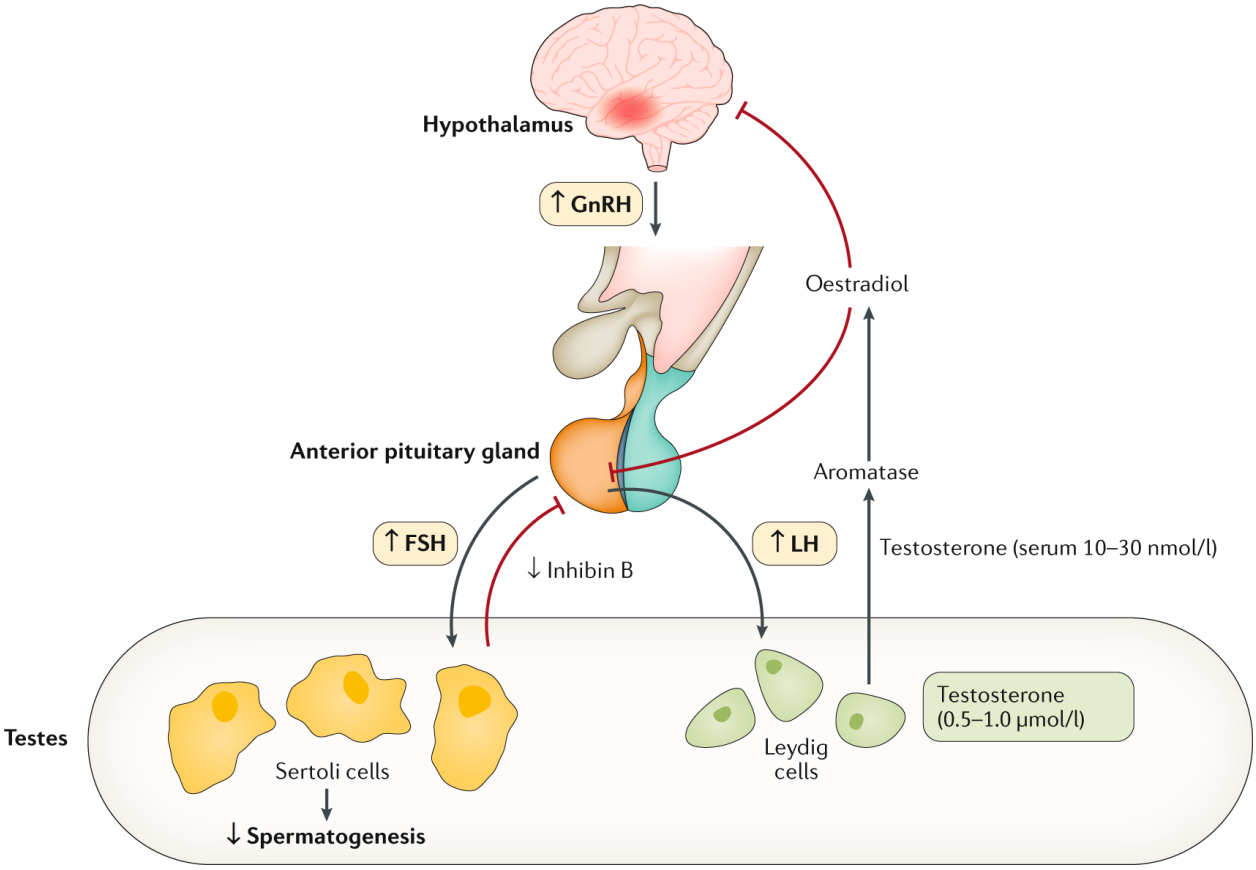

Figure 1-2. The hypothalamic-pituitary-gonadal axis in males. Gonadotropin-releasing hormone (GnRH) triggers the release of luteinizing hormone (LH) and follicle-stimulating hormone (FSH) from the pituitary gland. LH induces Leydig cells to produce testosterone, while FSH induces Sertoli cells to produce inhibin B. Testosterone and inhibin B, in turn, exert negative feedback control on the hypothalamus and pituitary gland. Adapted from Salonia et al. (2019) with permission from publisher.

The development of the testes is closely associated with the regulation of the HPG axis (**Figure 1-3**). Production of testicular hormones starts during the first trimester of the fetal period, and reaches its first peak in the second and third trimester, driving growth of the genitalia and the descent of the testes. In late pregnancy, HPG activity is suppressed by placental estrogens. Gonadotropins surge again during the first 6 months after birth, a period known as mini-puberty

(Forest and Cathiard, 1975). During this time, serum LH increases and peaks between 2-10 weeks after birth, then gradually decreases and maintains low prepubertal values from 6 months of age to the onset of puberty (Winter et al., 1975a, Bergadá et al., 2006). FSH and testosterone increase in the serum and then drop to a low prepubertal level during mini-puberty (Bergadá et al., 2006). During this time, a mild increase of testicular volume resulting from the proliferation of Sertoli cells can be detected by ultrasound (Kuijper et al., 2008, Kuiri-Hänninen et al., 2011). Gonocyte to SSC transformation also happens during mini-puberty and is regulated by gonadotropins and testosterone.

Male puberty is initiated by the re-activation of the HPG axis, with major changes in the physiology of the testis that include increased testicular volume, hormonal and molecular modulation, and the initiation of spermatogenesis (Plant, 2015, Koskenniemi et al., 2017). During puberty, the plasma levels of testosterone, FSH, and LH increase significantly while AMH secretion is suppressed (Salonia et al., 2019). The increased production of testosterone is accompanied by the enlargement of the scrotum and testis, or gonadarche, and the first physical manifestation of puberty (Hiort, 2002). Spermatogenesis starts with the differentiating division of undifferentiated spermatogonia (SPG), followed by spermatocyte meiosis and the formation of round spermatids (Ogawa, 2001) then resulting in sperm production and a visible rise in testis volume.

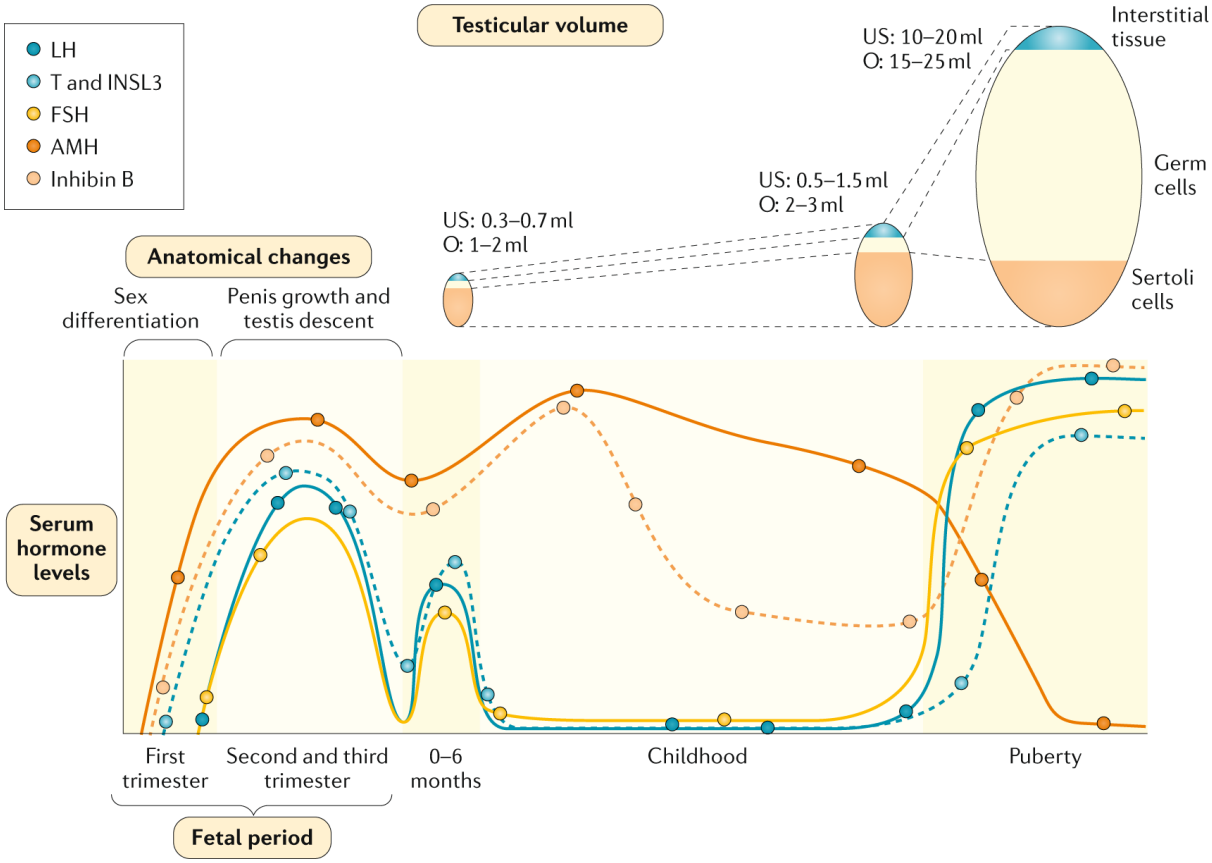

Figure 1-3. Anatomical changes and serum hormone levels from the fetal period to puberty. During the first trimester of fetal period, the secretion of testicular hormones starts to which is independent of pituitary gonadotropins and cause genital differentiation. During the second and the third trimesters, the release of androgen stimulates development of genitalia and testicular descent. Within six months after birth, which is also called 'mini-puberty', volume of testes increases due to the proliferation of Sertoli cells. During mini-puberty, serum levels of anti-Mullerian hormone (AMH) and inhibin B remain at detectable levels, but the levels of gonadotropins and testosterone (T) decrease. Testicular volume grows significantly throughout puberty period due to the spermatogenic development and gonadotropin and T action. Testicular volume grows significantly throughout puberty period due to the spermatogenic development and gonadotropin and T action. At the same time, T inhibits AMH, while follicle-stimulating hormone (FSH) and germ cells upregulate inhibin B. INSL3, insulin-like factor 3; O, testicular volume as measured by comparison to Prader's orchidometer; US, testicular volume as assessed by ultrasonography. Adapted from Salonia et al. (2019) with permission from publisher.

1.1.2 Testicular development

The development of GCs is comprised of two phases: SSC formation and spermatozoa production. SSCs are unipotential stem cells of the seminiferous epithelium in testis that are capable of self-renewal as well as the production of daughter cells to differentiate into spermatozoa. The first phase involves differentiation of primordial germ cell (PGC) into SSC precursor and further transformation into undifferentiated SPG during the neonatal period. The SSC precursors are also called gonocytes or prespermatogonia (PreSPG). The latter phase, spermatozoa production, or spermatogenesis, is the process whereby SPG undergoes mitosis to produce spermatocytes, followed by meiosis to produce haploid cells, which can then differentiate into spermatids. Complete spermatogenesis occurs only in the post-pubertal and adult stages.

Human testes mainly consist of functionally distinct intratubular and interstitial compartment. The intratubular compartment, also called seminiferous tubule, contains GCs, Sertoli cells, and peritubular myoid cells (PMCs). The interstitium contains most of the somatic cells, including Leydig cells, fibroblasts, macrophages, nerve fibers, and capillaries. There are three distinct maturation stages of testicular development in human: neonatal (up to one year after birth), prepubertal (from early childhood to puberty, typically from one to fourteen years), and adult (Guo et al., 2020). During neonatal period, gonocytes migrate from the center of the seminiferous cords in neonatal testes **(Figure 1-4 A)** to the basal membrane and transition into undifferentiated SPG during the first 9 months after birth (Culty, 2009, Oatley and Brinster, 2012). A prepubertal testis lacks an apparent lamina or lumen and no meiosis progression occurs. Individual undifferentiated SPG are located in a specialized microenvironment at the basement membrane of the seminiferous tubules (**Figure 1-4 B**). During the prepubertal period,

typically ages from 1 to 10 years before the start of puberty, SPG and Sertoli cells intermingle in the cord-like structure, and after the initiation of puberty, a lumen begins to form, and Sertoli cells and SPG settle in the basal compartment. Sertoli cells, the only supporting cells in the SSC niche, provide extrinsic signals necessary for self-renewal and spermatogenesis (Oatley et al., 2011). Mature Sertoli cells are larger than immature ones and the proportion declines with age. Tight junctions between Sertoli cells form the blood-testis barrier that separates the basal and luminal compartments of the seminiferous tubules (Yoshida, 2010). Leydig cells reside in the interstitium outside the seminiferous tubule and, along with macrophages and lymphocytes in the intratubular testicular tissues, are an important component of the SSC niche (Miller et al., 1983). Puberty usually starts between 10 and 13 years after birth in human, and this is when primary spermatocytes first appear and spermatogenesis begins (**Figure 1-4 C**). In the adult human testes (**Figure 1-4 D**), complete spermatogenesis happens in seminiferous tubules, where germ cells in different stages occur and spermatozoa are released in lumen for further maturation.

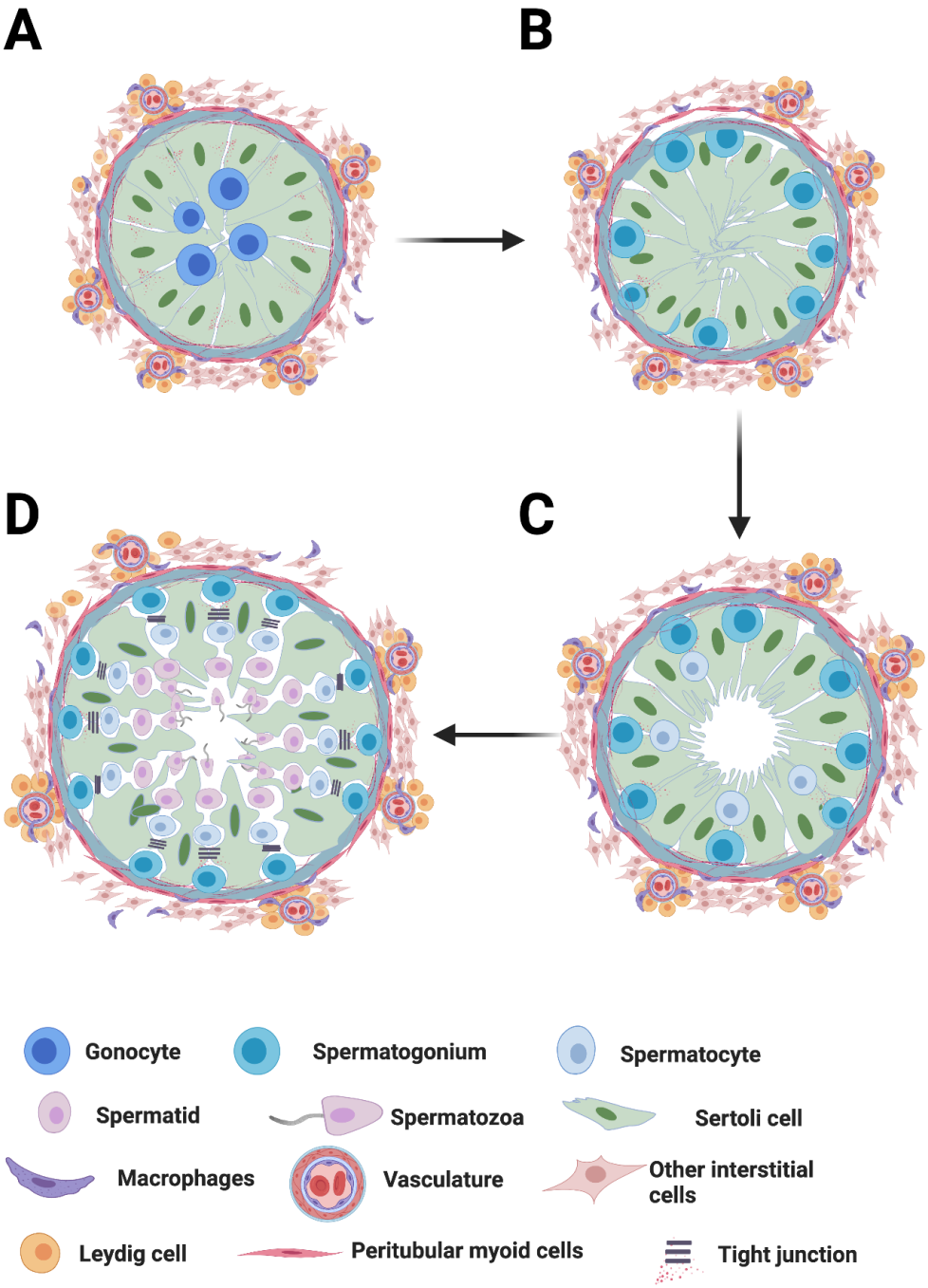

Figure 1-4. Schematic representation of a cross-section of the seminiferous epithelium and germ cell niche in human neonatal (A), prepubertal (B), pubertal (C) and adult testis (D). In the neonatal testis, typically within a year after birth, gonocytes are located at the centre of the seminiferous cords and no lumen is present. Gonocytes gradually migrate to the basement membrane and transform into spermatogonia. In prepubertal testis, typically aged 1 to 10 before initiation of puberty, Sertoli cells and spermatogonia are present at the basal surface with peritubular myoid cells to form the SSC niche. Primary, secondary spermatocytes and spermatids begin to appear during puberty, usually aged 10 to 13 years. Mature Sertoli cells in the pubertal testis are larger than immature Sertoli cells in the prepubertal testis. The volume of testis increases dramatically during puberty. Complete spermatogenesis occurs in the adult testis. Pictures are not to scale. Created with BioRender.com.

Some of the most important cellular changes occur in the GC population (**Table 1-1**). The quantity of SPG in the prepubertal testis varies during testicular development. The number of SPG in each transverse tubular cross-section (S/T) tends to decrease as LH levels decline during the first 3 years of life. This is followed by a two-fold increase at 6-7 years caused by elevated levels of FSH, LH, inhibin B, and testosterone (Winter et al., 1975b). The S/T then remains stable until about 11 years of age. After this point, the S/T increases dramatically to a value of 7 (compared to a value of 1 at 3 years of age) with increasing levels of gonadotropins, thus marking the onset of puberty (Masliukaite et al., 2016). The spermatogonial density per cubic centimeter (cm^3) of testicular volume (S/V) decreases during the first 3 years of life, and increases near puberty (Winter et al., 1975b). Guo et al. also showed that the proportion of SPG increases from 3% of all the testicular cells in 7-year-olds to 10-15% in 11-year-olds (Guo et al., 2020).

Table 1-1. Germ cell content at different testicular development stages. Table created by the Author using published information (Oatley and Brinster, 2012, Masliukaite et al., 2016, Sohni et al., 2019, Guo et al., 2020).

Developmental period	Infant	Juvenile	Adult
Germ cell development	Prospermatogonia proliferate until 5-6 months after birth and differentiate into type A spermatogonia	Undifferentiated spermatogonia only	Complete spermatogenesis
Germ cells according to scRNA-seq results	Three populations: primordial germ cells-like (PGCL) and two prospermatogonial populations, some resembling SSCs	Undifferentiated spermatogonia proliferate and start to differentiate at 10-12 years of age	Complete spermatogenesis
Prepubertal spermatogonial cell counts per seminiferous tubular cross-section (S/T)	A decreasing trend during the first 3 years of life (from 2.5 to 1.2 years)	Plateau until 11 years of age	A sharp increase marks the onset of puberty (to a level of 7)
Spermatogonial numerical density per testicular tissue volume of 1cm^3 (S/V)	A decreasing trend during the first 3 years of life (from $30x10^6/cm^3$ to $19x10^6/cm^3$)	$48x10^6/cm^3$	Approximately $100x10^6/cm^3$

1.1.3 Germ cell development and spermatogenesis

In mice, the PreSPG to SPG transition occurs within 3 days after birth, while in domestic animals such as bovine or humans, this transition period continues for up to 3 months after birth (Paniagua and Nistal, 1984, Fujihara et al., 2011, Sohni et al., 2019, Tan et al., 2020). However, the formation of SPG is complex and remains largely unknown with only a few recent scRNA-seq studies shedding light on human PreSPG development and SSC formation.

Earlier research, based on morphological analysis and protein markers, suggested that only one GC type, PreSPG, also called gonocytes, links PGC and SPG in the human neonatal testes (Fukuda et al., 1975, Gaskell et al., 2004). However, Sohni et al. conducted scRNA-seq analysis on newborn testes on days 2 and 7 and discovered three sub groups in PreSPG states shortly after birth: PGC like (PGCL), PreSPG-1, and PreSPG-2 (**Figure 1-5**) (Sohni et al., 2019). The PGCL cluster had an expression profile that was very similar to that of PGCs in 4- to 19-week-old human fetus, including the expression of pluripotency genes such as *OCT-4* (also known as *POU5F1)* and *NANOG*. Analysis has shown that PGC and PGCL have highly related gene expression patterns. PreSPG-1 and PreSPG-2 lack PGC gene expression but instead have PreSPG gene expression, including the expression of *MAGEA4* and *RHOXF1*. *MAGEA4,* a commonly used gene marker for PreSPG and adult SPG (Hayashi et al., 2012), is also a good marker for distinguishing between PGCL ($MAGEA4^-$) and PreSPGs ($MAGEA4^+$). This suggests that the order of human GC development begins with the differentiation of human fetal PGCs into PGCL, which then differentiate into PreSPG. More advanced PreSPGs are likely to differentiate into undifferentiated SPG. PGCL gradually disappear within the first year after birth, while PreSPG and undifferentiated SPG remain in the human testes until 7 years of age (Guo et al., 2018, Guo et al., 2020).

In humans, SPG (labeled as UTF1+ and FGFR3+) feature three main subsets: undifferentiated SPG, early-differentiated SPG, and differentiating SPG. SSCs, also called undifferentiated or type A SPG, consists of SSC-1, which are more primitive/naïve, and SSC-2, or progenitors, which are more developmentally advanced (Sohni et al., 2019). During prepuberty, SSCs, which remain in the gap 0 (G0) or gap 1 (G1) phases, are the dominant GCs in the human testes. As males' approaching prepuberty, early-differentiating SPG and differentiating SPG gradually appear. While early-differentiating SPG expresses the *NANOS3*, and *L1TD1* genes; differentiating SPG (labeled as KIT+ and largely MKI67+) express the *DMRT1*, *TUBA3D, DNMT1*, and *CALR* genes (Sohni et al., 2019, Guo et al., 2020). Significant expression of the *SYCP3* meiotic marker has only been found in adolescents after 14 years of age (Guo et al., 2020). In post-puberty or adulthood, differentiating SPG go through mitosis and differentiate into spermatocytes (STRA8+), which then undergo further meiosis into spermatids (PRM3+). Early GC development in humans remains largely unexplored and more studies are required to define the relationship between different cell sub-clusters and regulation.

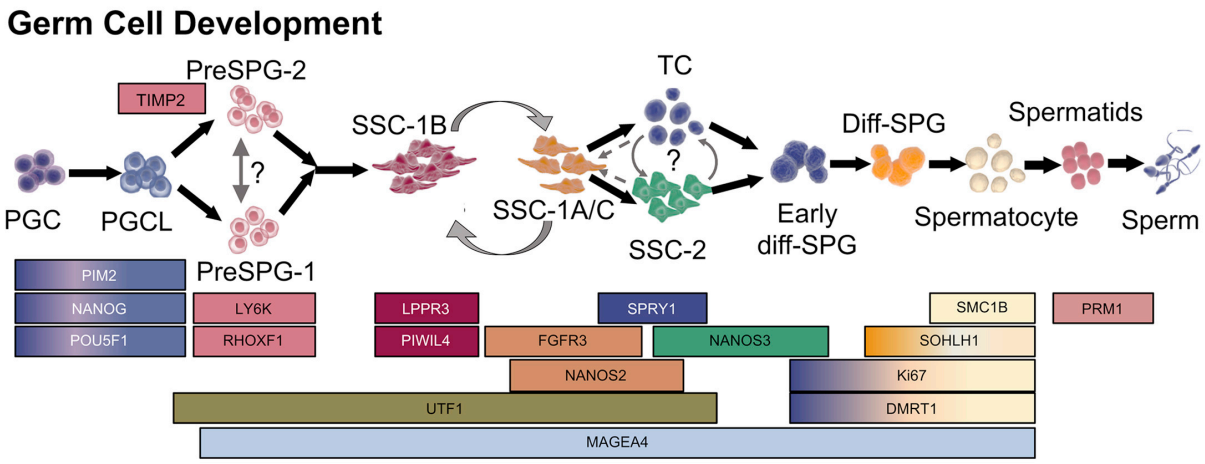

Figure 1-5 Human germ cell development. Black arrows point the direction of differentiation and grey arrows point the transition between different cell states. The expression pattern of key marker genes is indicated by boxes. PGC, primordial germ cells; PGCL, PGC-like; PreSPG, pre-spermatogonia; SSC, spermatogonial stem cell; TC, transition cells, Adapted from Sohni et al. (2019) under a CC BY-NC-ND license.

Spermatogenesis is the regulated process whereby SSCs (diploid) divide into spermatozoa (haploid) through mitosis, meiosis, and spermiogenesis. The time needed to generate an fully mature sperm ranges from 42 to 76 days in a healthy man (Misell et al., 2006). SSCs can either renew themselves to maintain the number of stem cells in the SSC pool or differentiate and form sperm. Type A SPG, with dark nuclei, usually remain in the G0 or G1 phase, without active meiosis. Type B SPG undergo final mitotic division to form primary spermatocytes. These then undergo meiosis I and form secondary spermatocytes. Secondary spermatocytes undergo meiosis II and generate spermatids, which subsequently mature into spermatozoa while moving into the lumen of the seminiferous tubules. After release from the seminiferous tubules, spermatozoa are transported to the epididymis, where they undergo post-testicular maturation and are eventually stored in the cauda to await ejaculation.

1.1.4 SSC niche and regulation

The most important role of tissue stem cells is to maintain the homeostasis of tissues by keeping the constant stem cell pool while producing the differentiated cells to replace those lost tissue cells. The special microenvironment where stem cells located is often called a “niche”, where stem cells can keep the perfect balance of self-renewal and differentiation. The stem cell niche is regulated by multiple elements *in vivo*, including hormones and cytokines, extracellular matrix (ECM) components, biomechanical factors, the physical environment, cellular elements, and neurotransmitters (Köse et al., 2018). There are mainly two types of niche: “closed” (or “definitive”) niche and “open” (or “facultative”) niche(Yoshida, 2018). “Closed” niche refers to a specialized region where stem cells are kept undifferentiated within the niche and will differentiate outside the niche. In an “open” niche, however, stem cells and other differentiating progeny are intermingled. The SSC niche belongs to the “open” niche where SSCs are intermingled with differentiating SPG. It is possible that some early SPG stages can de-differentiate to become SSC and re-enter the niche. The SSC niche, an entity made up of multiple somatic cells and GCs, provides appropriate architectural support and a growth factor milieu (Oatley and Brinster, 2012, Mäkelä and Hobbs, 2019). Different cells in the interstitium and seminiferous epithelium are important for homeostasis (Oatley and Brinster, 2012, Lord et al., 2018) and the regulation of SSC fate (Oatley and Brinster, 2012, Chassot et al., 2017). Thus, identifying components of the SSC niche is critical to understanding the regulation of gonocyte-to-SPG transformation and spermatogenesis *in vivo* and establishing fertility restoration strategies using *in vitro* culture techniques. The SSC niche is essential for the regulation of stem cell self-renewal and differentiation and ensures the balance between these two processes.

Located in the basal compartment of the seminiferous tubule, the SSC niche supports and protects the most primitive SPG (Chiarini-Garcia et al., 2001b, Chiarini-Garcia et al., 2003). However, the location of undifferentiated SPG is not random; they are usually found on the basement membrane adjacent to interstitial tissues and the vasculature (Chiarini-Garcia et al., 2001a, Chiarini-Garcia et al., 2003, Yoshida et al., 2007a). The maintenance and homeostasis of the SSC niche also rely on the vascular network (Oatley and Brinster, 2012), endothelial cells (Bhang et al., 2018), PMCs (Chen et al., 2016), and testicular macrophages (DeFalco et al., 2015). Time-lapse imaging studies show that SPG undergo a transition from undifferentiated SPG to type A SPG while migrating away from the original niche near the intertubular vessels and interstitium. SSC differentiation starts when cells move away from the self-renewing niche into a differentiated niche and disperse over the whole basal compartment region of the seminiferous epithelium. In another experiment involving seminiferous tubule fragment grafting, the relocation of undifferentiated SPG was shown to be closely associated with the branch of blood vessel and interstitium (Yoshida et al., 2007b). Thus, the location of the niche is essential for the fate of SSCs.

Surrounding somatic cells that contribute significantly to the SSC niche include Sertoli cells, PMCs, peritubular macrophages, testicular endothelial cells, Leydig cells, and lymphatic endothelial cells. These cells provide support and produce factors to regulate SSCs directly or indirectly (Juho-Antti and Robin, 2019). Sertoli cells are the most important cellular component of the niche because they are in direct contact with undifferentiated SPG (Oliver and Stukenborg, 2019), and feed and support GCs *via* direct or indirect communication. Sertoli cells secrete numerous paracrine factors, including glial cell line-derived neurotrophic factor (GDNF) (de Rooij, 2009). PMCs provide structural support and also push the luminal fluid towards the rete testis. In the interstitial tissue, testosterone is produced by the Leydig cells and

activates Sertoli cells and indirectly enhances SSC colonization in the testis (Ogawa et al., 1998). The interstitial tissue may also impact SSCs in the niche via secreted factors, such as colony-stimulating factor 1 (CSF1) (Oatley et al., 2009), or by regulating Sertoli cells (de Rooij, 2009). Somatic cell maturation and the establishment of the hypothalamus-pituitary-gonadal (HPG) axis at puberty leads to changes in the niche microenvironment, including the regulation of GDNF and other hormones. These events drive some SSCs into adult-type niches and differentiation (Shinohara et al., 2001, Tadokoro et al., 2002, Ventela et al., 2012).

During the prepubertal period, the levels of FSH, LH, and testosterone remain low. Once puberty starts, AMH levels begin to decline while serum levels of inhibin B, FSH, LH, and testosterone rise, resulting in testicular growth. Male puberty is initiated by activation of the HPG axis, with major changes in the physiology of the testis that include increased testicular volume, hormonal and molecular modulation, and the initiation of spermatogenesis (Plant, 2015, Koskenniemi et al., 2017). Testis size and volume increase and progressive changes in the structure of the tubules leads to clearly defined laminae and lumina (Rey, 1999). GDNF (Naughton et al., 2006b, Chen and Liu, 2015), fibroblast growth factor (FGFs) (Takashima et al., 2015b, Masaki et al., 2018), and retinoic acid (RA) (Raverdeau et al., 2012) are important growth factors that regulate SSC development. Pituitary hormones also affect testicular cells. While FSH stimulates the proliferation of Sertoli cells and SPG, and the production of testosterone, LH stimulates the completion of spermatogenesis. Aged niche cells can also alter SSCs and reduce stem cell regenerative potential, as demonstrated in adult stem cells, while exposure to systemic factors from younger individuals can restore regenerative function (Conboy et al., 2005). The density of SSCs in seminiferous tubules is tightly regulated by the concentration of FGFs produced by lymphatic endothelial cells near the vasculature in the niche environment (Kitadate et al., 2019). Results of scRNAseq on human SSCs niches showed

several important signalling pathways that are highly related to SSC niche environment regulation, including testosterone, RA, WNT, FGF, activin/inhibin, NOTCH, and GDNF pathways (Guo et al., 2018; Guo et al., 2020). These signalling pathways and other factor regulations of human SSC niches have not yet been fully understood and thus additional studies are urgently needed to assess the molecular mechanisms.

In summary, SSC renewal and differentiation are strictly regulated by different cell types and molecular mechanisms within the niche microenvironment. Studies have investigated SSC, SPG, and spermatid gene expression at different ages to gain molecular insights into the transcriptional and epigenetic processes associated with the development of human male GCs. However, the cellular, molecular, biochemical, and genetic mechanisms and signaling pathways in SSC niches in the prepubertal and post-pubertal stages are not yet fully understood and require further research. This is important because understanding the human SSC niches at early stages could enhance our knowledge of the development and regulation of GCs during prepuberty and peri-puberty; there are key stages in the development of the testes and achieving fertility preservation for patients with cancer. Almost all potential approaches to restore fertility would rely on the GCs in testis biopsies, which carry gene heritage and directly affect the health of offspring. Understanding the SSC niche environment could also facilitate the preservation of GCs in testicular tissues by monitoring the changes of structure or homeostasis in stem cell niche. Therefore, in this thesis, I studied the morphology of GCs and Sertoli cells, and the connection between cells in the stem cell niches using histological analysis in **Chapter 2 and 3**. I also investigated the creation of a stem cell niche *in vitro* to study the propagation of GCs and the regulation of growth factors in stem cell niches (**Chapter 4 and 5**).

1.1.5 Bovine animal model

In my DPhil project, I used a 2-week-old neonatal bovine animal model to study gonocytes and prepubertal testicular tissues. Bovine abattoir testicular tissues were collected from slaughterhouse, which would be otherwise discarded. For the ethical aspect, Home Office licensing is not required in this case. Testicular development in bulls is relatively slow from birth to 20 weeks, after which the development begins to accelerate (Wrobel et al., 1986). The seminiferous epithelium in neonatal calves contains gonocytes/SSCs and Sertoli cells but no advanced spermatids for the first 20 weeks after birth. Gonocytes are the predominant GCs in seminiferous tubules until around 20 weeks after birth when they are replaced by SPG. The first SPG are observed at approximately 10 weeks in Holsten bull calves (Al-Haboby, 1986); this could be compared to 8-10 weeks in humans. The initiation of spermatogenesis in Holstein bulls starts at around 16 weeks and ends by 32 weeks (Curtis and Amann, 1981), thus providing a longer pubertal time for research studies.

The bovine model provides some specific advantages. First, the duration of the prepubertal period is similar to humans, and longer than mouse or rat models. Second, bulls have a low efficiency of spermatogenesis ($12x10^6$ sperm per gram of testicular tissue daily), that is similar to that of humans (4 to $6x10^6$ sperm per gram of testicular tissue daily). Third, the duration of spermatogenesis in bulls is approximately 61 days; this is similar to the 74 days duration observed in humans (Amann et al., 1976, Johnson, 1986). Thus bovine ITT represents an ideal animal model for research, considering the limited availability of human testicular tissue.

To study GC development in neonatal bovine testes, I used a range of GC markers, pluripotency-associated markers, and stress- or apoptosis-related markers. Protein gene product 9.5 *(PGP9.5 UCHL-1)*, is a GC marker that is expressed in undifferentiated bovine

gonocytes and SSCs (Wrobel et al., 1995). Promyelocytic leukaemia zinc-finger *(PLZF)*, an established marker for pluripotency, is involved in chromatin remodelling and the transcriptional regulation of SSC maintenance (Buaas et al., 2004; Costoya et al., 2004; Kala et al., 2012). *GFRα-1*, a marker of undifferentiated SPG, is predominantly expressed in gonocytes and SSCs. *GFRα-1* knockdown causes differentiation by inactivating the rearranged during transfection (RET) tyrosine kinase, indicating an essential role for *GFRα-1* in SSC regulation (He et al., 2007). *OCT-4* and *NANOG* are markers of pluripotency while vimentin, which is expressed in the perinuclear area of Sertoli cells, peritubular cells, and a few interstitial cells, has been proposed as a Sertoli cell marker in bovine testis (Devkota et al., 2006). Sex determining region Y(SRY)-box transcription factor 2 (*SOX2*) is a pluripotency marker that is expressed in SSCs; the *SOX2*-positive *C-KIT* negative SSCs can self-renew or undergo differentiation into sperm (Arnold et al., 2011).

Spermatogenesis-related markers include stimulated by retinoic acid gene 8 (*STRA8) and C-KIT. STRA8* is induced by RA and is considered as a meiotic gatekeeper gene because it helps to regulate the initiation of meiosis during spermatogenesis (Bowles et al., 2006; Koubova et al., 2006). SSCs are believed to be negative for *C-KIT*, a known marker for differentiated SPG (Izadyar et al., 2003a).

Cyclic-AMP responsive element modulator (*CREM)* and heat-shock protein 70-2 (*HSP70-2*) are two genes associated with cell apoptosis. *CREM* is involved in the progression of spermatogenesis; the inactivation of *CREM* can result in the upregulation of downstream signalling molecules, thus causing post-meiotic arrest and the promotion of apoptosis (Blendy et al., 1996; Nieschlag, and Schütz, 1996; Matsukawa, 2004; Nantel et al., 1996). The molecular chaperone *HSP70-2* is involved in maintaining protein conformation and

stabilization (Gething and Sambrook, 1992) and is linked to apoptosis inhibition (Dix et al., 1996, Mori et al., 1997) , thus helping to protect the GC proteome from stress and dissociation.

1.2 Cancer in prepubertal boys

Worldwide, approximately 400,000 new cases of cancer are diagnosed annually among children and adolescents 0-19 years of age (World Health, 2021). A microsimulation model has estimated that the current global five-year net childhood cancer survival is 37.4% (Ward et al., 2019b). However, in developed countries, the five-year survival rate has reached 80% and is still increasing as a result of improvements in cancer therapy (Ribeiro et al., 2008, Wasilewski-Masker et al., 2014b). While current cancer treatments are increasingly effective at curing disease, the use of aggressive chemo- or radiotherapy frequently causes irreparable damage, including GC depletion and hypogonadism, to pre-pubertal gonads, which can result in sterility (Tournaye, Dohle and Barratt, 2014). Chemotherapy, involving medications such as alkylating agent, is associated with impaired spermatogenesis and reduced SPG quantity (Poganitsch-Korhonen et al., 2017, Skinner et al., 2017). Exposure to various cytotoxic cancer treatments, such as cyclophosphamide, cisplatin, and doxorubicin, is also shown to induce GC loss in an *in vitro* prepubertal testis model (Smart et al., 2018). Irradiation not only causes direct damage to GCs, it can also have an adverse effect on supporting Sertoli and Leydig cells in the testes (Stukenborg et al., 2018). The prevalence of infertility is 46% among childhood cancer survivors when compared with 17.5% in their siblings (Wasilewski-Masker et al., 2014b).

In adult males, semen can be cryopreserved before cancer therapy; this procedure successfully preserves their fertility by assisted reproductive technologies (ART). Cryopreserving mature sperm from pre-pubertal boys is impossible, however, because puberty is necessary for the

production of functional spermatozoa from the SSCs in the testes. Thus, for childhood cancer patients with a high risk of infertility, ITTs need to be cryopreserved before cancer therapy in order to preserve their reproductive function (Wyns et al., 2010).

1.3 The cryopreservation of testicular tissue

Since the first fertility preservation programme for prepubertal males was launched in 2002, the number of cryopreservation centres worldwide has risen steadily (Picton et al., 2015). Methods for obtaining functional sperm from ITTs are being developed, and primate studies have demonstrated the feasibility of this approach. As a consequence, more clinics are promoting ITT cryobanking as an experimental approach for patients to acquire mature sperm in the future. In 2020, data gathered from 24 coordinating centres around the world showed that more than 1,033 young patients had testicular tissue retrieved and stored for fertility preservation (Goossens et al., 2020).

For childhood cancer survivors, the cryopreservation of testicular tissues prior to initiating gonadotoxic treatment is a potential way for patients to safeguard their fertility. Since the surgical biopsy of ITTs is an invasive procedure and fertility preservation approaches are still in their early stages, cryobanking should be restricted to patients who are at a high risk of cancer treatment-induced testicular damage and subsequent infertility. Not all childhood cancer therapies are associated with a high risk of infertility. In addition, certain first-line chemotherapy drugs, such as antimetabolites, vinca alkaloids, podophyllotoxins, and antitumor antibiotics, are associated with a lower risk of infertility. Therefore, it is not necessary for patients receiving these drugs to bank their ITTs after initial diagnosis (Skinner et al., 2017). For children who have testicular cancer, Hodgkin's disease, non-malignant Hodgkin's

lymphoma, or solid tumours, ITT fragments are usually collected before treatment in most centres because of the high risk of GC damage (Picton et al., 2015). Most testicular tissue biopsies and cryopreservation are performed before the initiation of high-risk cancer treatments such as allogeneic or autologous hematopoietic stem cell transplant (HSCT) and testicular irradiation. However, in some centres, patients who had previously received chemo- or radiotherapy are also included depending on specific inclusion criteria (Wyns et al., 2011, Braye et al., 2019, Valli-Pulaski et al., 2019).

In 2008, the University of Oxford initiated the Oxford Reproductive Tissue Cryopreservation Programme (ORTCP) to help children and adolescents with cancer to preserve their fertility. The ORTCP includes a clinical centre, Oxford Cell and Tissue Biobank (OCTB), and a research programme **(Figure 1-6 A)**. The clinical centre collects reproductive tissue samples from participating patients through minor surgery. Testicular biopsies are transported to the tissue bank where gonadal tissue is then processed and stored (Sadri-Ardekani, 2011). Approximately 10% of tissue from consenting patients is used for research. According to the data provided by the OCTB, testicular tissues from 471 patients had been collected and cryopreserved in the OCTB by June 2021 (unpublished data; **Figure 1-6 B**); 28% and 27% of these patients were diagnosed with leukaemia and bone marrow disorder, respectively (unpublished data; **Figure 1-6 C**). The ORTCP has third-party agreements with most principal cancer treatment centres in the UK and Ireland (**Figure 1-6 D**), thus providing patients with the choice to have their tissue procured at a local centre or in Oxford. There are varying distances between each third-party centre and Oxford, which could result in transportation times of up to 6 hours. The time from procurement to the start of tissues processing is important; therefore the ORTCP aims to process tissue biopsies on the same day as when tissues are collected. However, if the tissues are delivered at night or the cryopreservation

equipment is already in use, tissues may have to be processed the next day. There are some other limitations that might postpone tissue processing in tissue biobanks. For example, testicular tissues cannot be processed at the same time as ovarian tissues in the same machine due to the different cooling programmes; this could cause a few hours delay. Consequently, there is an urgent need to investigate the optimal holding time from ITTs procurement to cryopreservation process, as this might have potential impact on the quality of ITTs. Therefore, in **Chapter 2** of this thesis, I investigated four tissue holding times using neonatal bovine testicular tissues, aiming to explore the effects of holding time before the cryopreservation of ITTs.

A

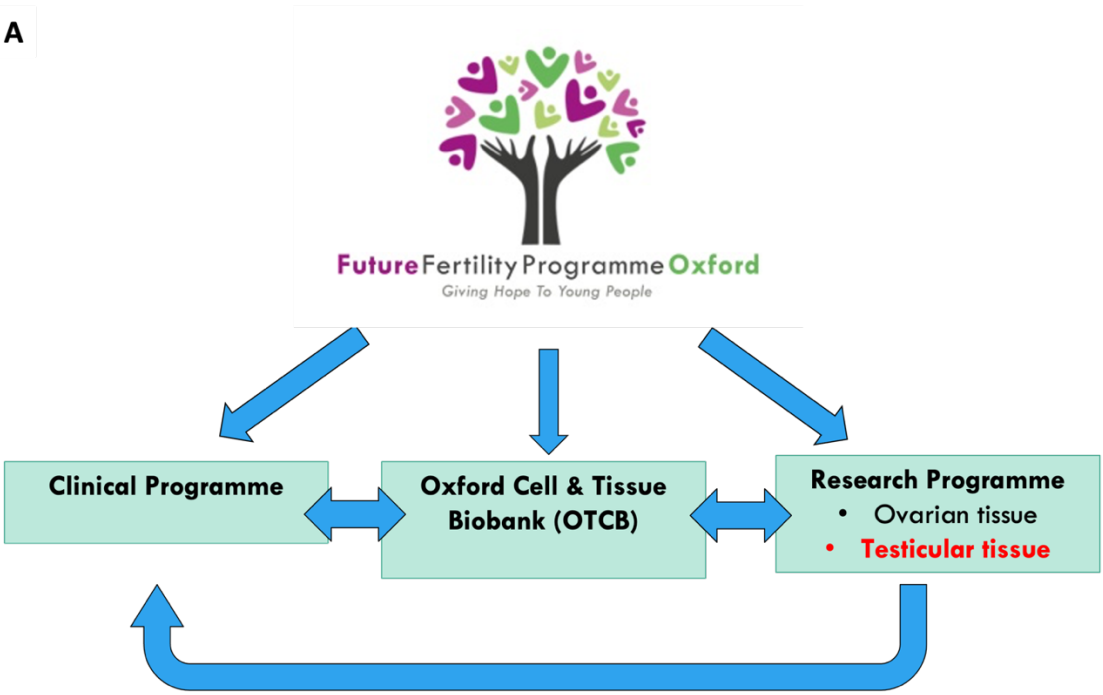
Future Fertility Programme Oxford
Giving Hope To Young People
Clinical Programme
Oxford Cell & Tissue Biobank (OTCB)
Research Programme
• Ovarian tissue
• Testicular tissue

B

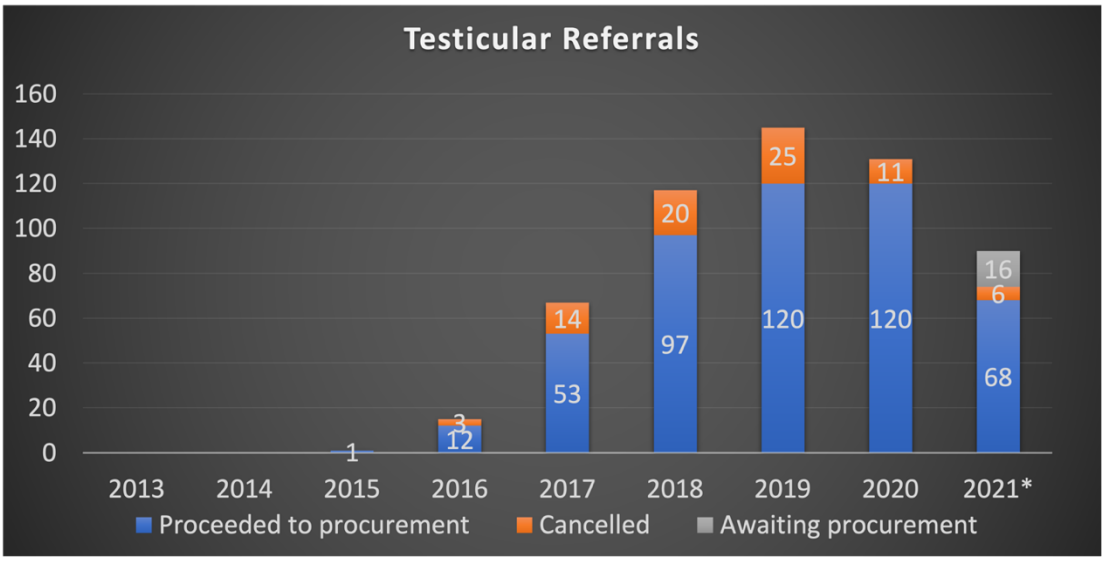
Testicular Referrals
160
140
120
100
80
60
40
20
0
1
12
3
53
14
97
20
120
25
120
11
68
6
16
2013
2014
2015
2016
2017
2018
2019
2020
2021*
Proceeded to procurement
Cancelled
Awaiting procurement

C

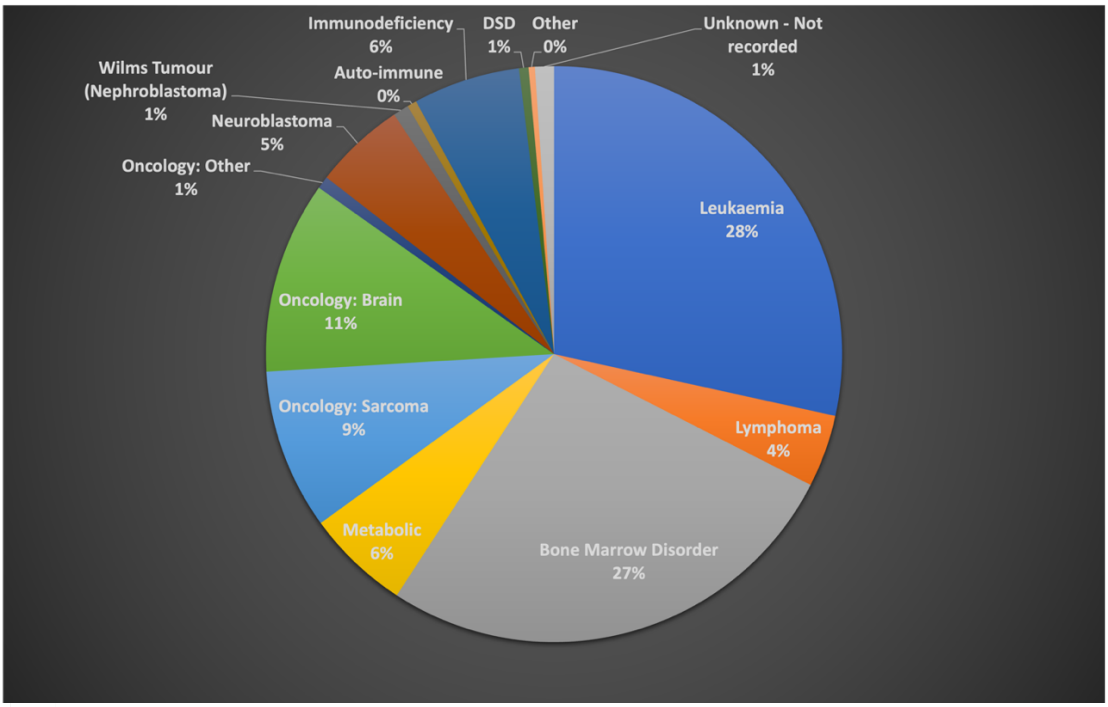

D

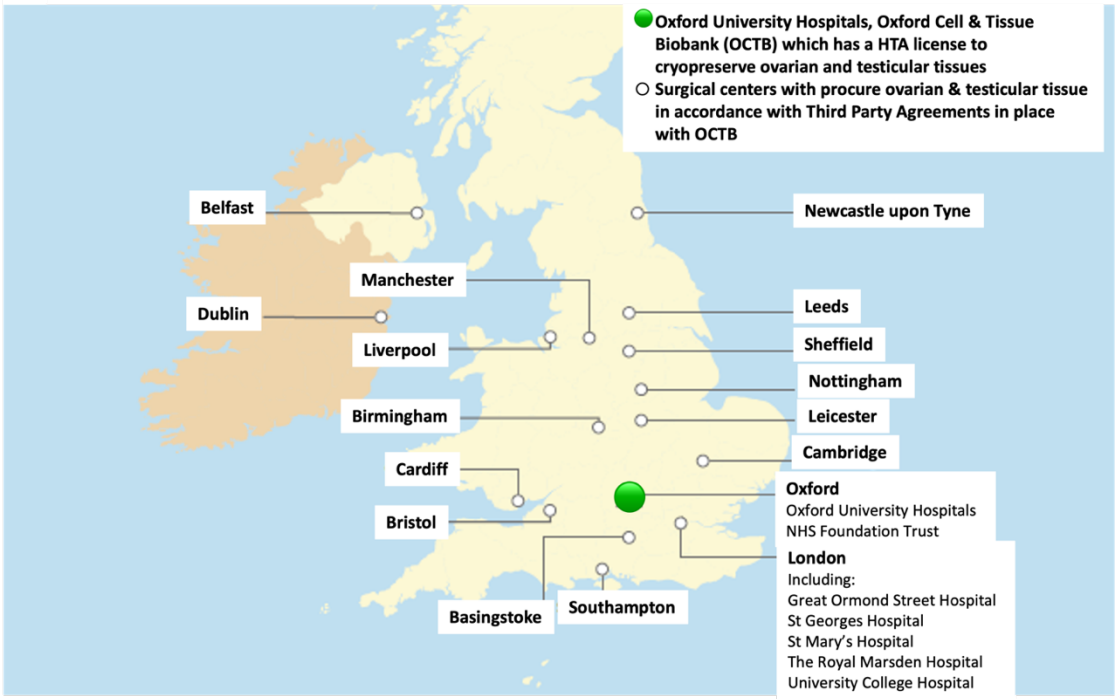

Figure 1-6. Oxford reproductive tissue cryopreservation programme (ORTCP). A) Components of the future fertility trust programme. B) Numbers of testicular referrals that have proceeded to procurement, been cancelled or are awaiting procurement since 2013. *Data collected by 04/06/2021. C) Diagnosis of referral patients. D) A map of Oxford fertility programme ovarian and testicular tissue procurement centres in the UK. The green triangle represents the location of Oxford university hospitals and Oxford cell and tissue biobanks. The white circles are surgical centres that procure ovarian and testicular tissues in accordance with third-party agreements with OCTB. Data provided by Future Fertility Programme Oxford with permission to use.

Controlled slow freezing (CSF) is a commonly used cryopreservation method in prepubertal male fertility preservation programmes (Pietzak et al., 2015, Valli-Pulaski et al., 2019). Programmable freezers have been used to preserve human testicular tissues based on a number of positive findings; these findings include the generation of offspring from cryopreserved ITTs in animal models (Shinohara et al., 2002b), and the observation of proliferation and differentiation in prepubertal human SPG (Wyns et al., 2008). These findings are supportive of clinical applications. Studies also showed that CSF was able to protect good structural integrity in both human adult and prepubertal tissues (Keros et al., 2005, Kvist et al., 2006, Keros et al., 2007). Therefore, CSF has been considered as the first-choice technique for the cryopreservation of human ITTs (Wyns et al., 2011). However, as the computerized machine that CSF requires is expensive, and the procedure of CSF is time-consuming, other cheaper, simpler, and more convenient alternatives would be preferred.

Uncontrolled slow freezing (USF) has been proposed as an effective strategy for the cryopreservation of ITTs in animal models, such as neonatal mice, pigs, and goats (Honaramooz et al., 2002, Ohta and Wakayama, 2005). More recently, vitrification, an ultra-rapid freezing method, has been suggested as an alternative method for ITT cryopreservation because it is a simpler procedure and has the advantage of not forming ice crystals. Despite widespread clinical application of vitrification on the cryopreservation of human embryos and oocytes (Rienzi et al., 2017, Nagy et al., 2020), vitrification has only been used for experimental studies in animal and human testicular tissues but is not yet been widely used in human ITT banking (Curaba et al., 2011a, Baert et al., 2013, Poels et al., 2013). So far, no study has determined whether neonatal testicular tissues can be successfully cryopreserved by USF and vitrification. Therefore, in **Chapter 3**, I designed a study to investigate USF,

vitrification and CSF for bovine neonatal testicular tissues and to compare the efficiency of cryopreservation using these two methods with conventional CSF.

1.4 Strategies for fertility restoration

While ITT collection and cryopreservation has already been launched in clinical practice, there is an urgent need for reliable and clinically safe strategies to restore fertility. Animal models and donated human ITTs have been used to establish three fertility restoration approaches: 1) testicular tissue auto- or xeno-transplantation, 2) GC propagation and auto- or xeno-transplantation for *in vivo* spermatogenesis, and 3) *in vitro* GC spermatogenesis (**Figure 1-7**).

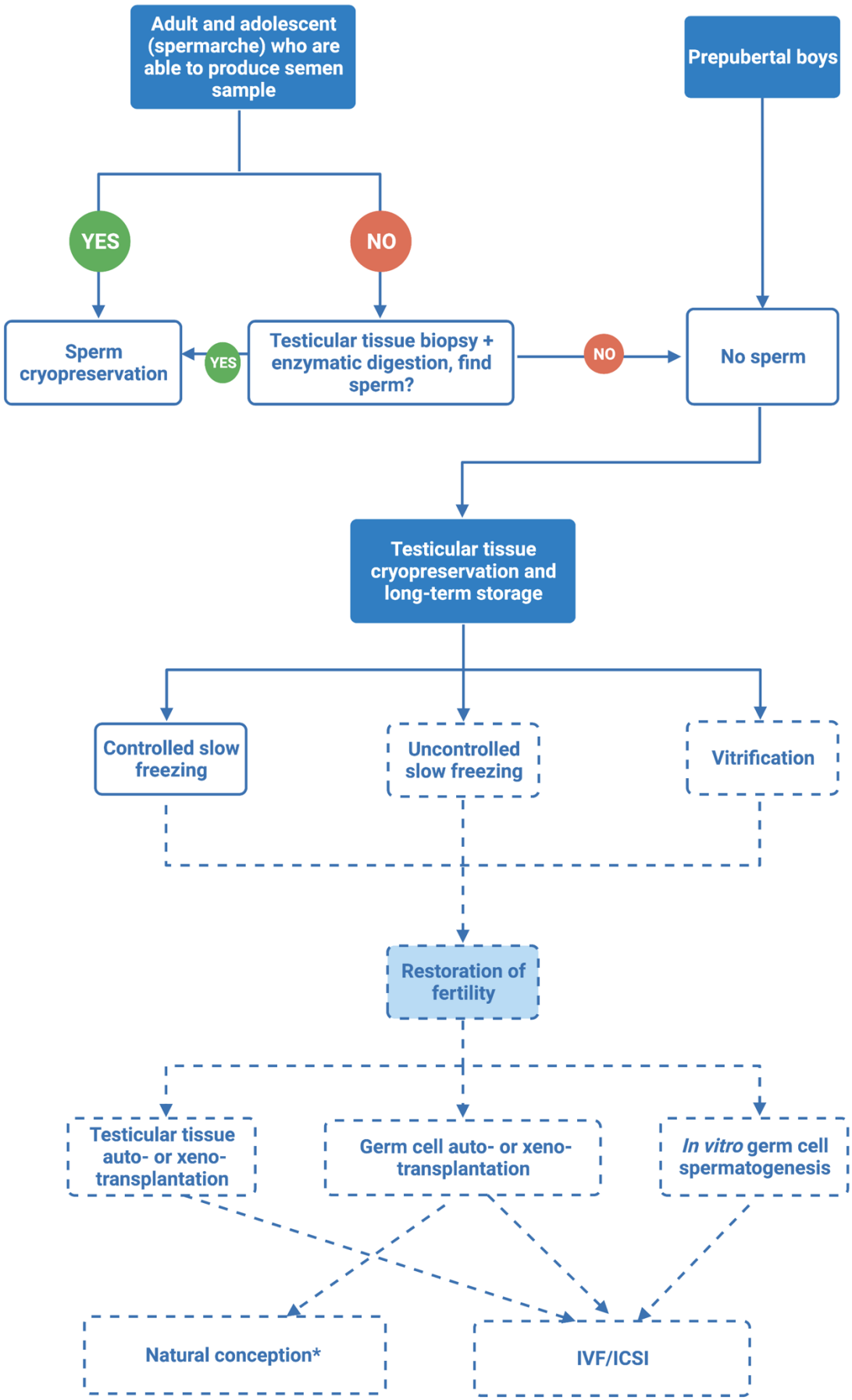
Adult and adolescent (spermarche) who are able to produce semen sample
Prepubertal boys
YES
NO
Sperm cryopreservation
YES
Testicular tissue biopsy + enzymatic digestion, find sperm?
NO
No sperm
Testicular tissue cryopreservation and long-term storage
Controlled slow freezing
Uncontrolled slow freezing
Vitrification
Restoration of fertility
Testicular tissue auto- or xeno-transplantation
Germ cell auto- or xeno-transplantation
In vitro germ cell spermatogenesis
Natural conception*
IVF/ICSI

Figure 1-7. Clinical strategy for the fertility preservation in prepubertal, adolescent and adult patients at high risk of infertility. Strategies in solid boxes indicate they are currently available in clinical practice; strategies in dashed boxes indicate these are experimental cryopreservation or fertility restoration methods. Sperm of testicular tissues are obtained before the initiation of gonadotoxic therapy, based on the age and pubertal stage. For prepubertal patients or adult and adolescent patients who cannot have sperm frozen, testicular tissues are collected and cryopreserved. Three different cryopreservation techniques are being optimized for testicular tissue cryopreservation; these include controlled slow freezing, uncontrolled slow freezing, and vitrification. After the patients have achieved complete remission and fertility restoration treatments are ready for clinical application, frozen tissue fragments may be thawed for i) testicular tissue auto- or xenotransplantation, ii) germ cell propagation and auto- or xenotransplantation for *in vivo* spermatogenesis, and iii) *in vitro* germ cell spermatogenesis. Sperm produced *in vivo* through auto-transplantation of testicular tissues. Sperm produced through xenotransplantation or *in vitro* spermatogenesis could be used for IVF/ICSI. *Purified germ cells could be induced to re-colonise in the testis and produce sperm which provides the possibility to make natural conception. IVF, *in vitro* fertilization; ICSI, Intracytoplasmic sperm injection. Figure reproduced and modified from Fig. 1 in Onofre et al. (2016).

1.4.1 Testicular tissue auto- or xeno-transplantation

Auto- or xeno-grafting of frozen/thawed testicular tissues is a promising strategy for preserving fertility that protects the SSC niche. The autologous grafting of cryopreserved prepubertal testis from a rhesus recently resulted in sperm and offspring production, indicating a possible use for autografting in clinics (Fayomi et al., 2019). In their study, rhesus monkey ITT fragments were autologously grafted under the skin of the back and scrotum for 8 to 12 months; these ITT fragments were found to grow in size and produce testosterone. Testicular tissue fragment transplantation has the advantage of retaining SSCs inside their niches, thus ensuring cell-to-cell interactions and providing the required microenvironment, growth factors and hormones for SSCs. However, the main disadvantage of tissue auto-transplantation is that autografting may have a potential risk of reintroducing cancer cells back into the patients. Therefore, testicular tissue auto-transplantation is not recommended for patients whose ITTs could potentially carry malignant cancerous cells.

Spermatogenesis and healthy offspring have been successfully developed following the xenogeneic transplantation of ITTs from rabbits, mice (Shinohara et al., 2002b), and juvenile monkeys (Liu et al., 2016b). The xenotransplantation of ITTs from 6-month-old marmosets to immunodeficient mice has resulted in complete spermatogenesis (Ntemou et al., 2019). However, spermatogenesis has not yet been observed following the xenotransplantation of human ITT fragments into animal hosts (Del Vento et al., 2018). While this approach avoids the reintroduction of cancer cells into patients, it does carry a risk of viral transmission or epigenetic changes; consequently, this technique is not ready for clinical use.

1.4.2 Germ cell propagation and auto- or xeno-transplantation for *in vivo* spermatogenesis

Since testicular tissue transplantation is not suitable for patients with systemic cancer and/or malignant hematopoietic disorders due to the potential contamination of cancer cells in testicular tissue biopsies. Therefore, *in vitro* GC isolation and propagation, followed by transplantation, is considered a safer strategy for fertility restoration. In prepubertal testicular tissues, the percentage of GCs in total testicular cells is relatively low; thus, undifferentiated GCs are usually needed to be enriched and propagated *in vitro* before being transplanted back into the testes for further spermatogenesis. SSC propagation, followed by transplantation, has been successfully applied to both mouse and primate models, resulting in the generation of functional sperm and healthy offspring or embryos (Brinster and Zimmermann, 1994, Hermann et al., 2012), thus suggesting a potential clinical application for GC transplantation. A study found that the genetic and epigenetic stability of human SSCs could be maintained during *in vitro* propagation (Nickkholgh et al., 2014), which indicatd the well preservation of the

potential functionality of SSCs. in addition, SSC propagation can also provide a useful model to better understand the basic biology and molecules involved in the development of human SSCs. The results of early studies on the epigenetics of *in vitro*-produced gametes are reassuring (Yokonishi et al., 2014b), but further research is required to verify GC quality and functionality prior to clinical application. As mentioned previously in **Section 1.1.4**, undifferentiated SSCs and differentiating SPG are intermingled in an "open" niche in the testis. Therefore, it is possible that the early SPG could be de-differentiated with the right support, which could increase the SSC recovery from each patient. For human tissues, an efficient and safe SSC isolation process is urgently needed, together with suitable *in vitro* culture conditions for GCs at different stages. After purification and propagation, SSCs could be potentially auto-transplanted into patient's testis or be xeno-transplanted to testis of other recipients to re-establish the SSC niches and recover fertility.

In addition, the demand for livestock products will increase due to the growth of the human population over the coming decades, which requires a higher efficiency in livestock production. Cattle are also commonly used as a large animal model for fertility preservation/ re-establishment. "Surrogate sire" technology, an alternative method to artificial insemination, is being developed in farming to transplant the germline from a donor to recipient males to achieve efficient genetic gain from desirable sires(Giassetti et al., 2019). The process of SSC transplantation in surrogate sire also requires good methods for the isolation, purification and propagation of SSCs from donor and re-establishment of SSC niche in the testis of recipient males.

Therefore the strategies developed and optimized in this thesis, including bovine testicular tissue digestion, SSC isolation, SSC enrichment, and *in vitro* SSC maintenance and propagation in two-dimensional (2D) or three-dimensional (3D) systems (**Section 4, 5**), could

potentially provide more guidance for future clinical human GC transplantation as well as improving the efficiency of surrogate sire technology in livestock industry.

1.4.3 *In vitro* spermatogenesis (IVS)

Despite the promising results of different transplantation approaches in animal models, the transplantation of SSCs or ITTs is not yet available in clinical practice. The risk of re-introducing cancer cell is a major bottleneck for clinical transplantation in humans, especially for testicular or non-solid tumours, such as leukaemia. Considerations for the clinical application of these procedures also include the difficulty in isolating and propagating SSCs, and the possible effect of gonadotoxic treatments on the SSC niche (Del Vento et al., 2018). A more promising and safer fertility preservation option is the *in vitro* maturation of freeze/thawed SSCs/ITTs to produce functional spermatids for later ART.

While animal models have been used to study ITTs and spermatogenesis, there are no *in vitro* methods available to generate functional spermatids from human ITTs. Thus, there is a significant need for experimental models that sustain complex SSC niches in human testicular tissues to allow us to study *in vitro* spermatogenesis. To date, many systems have been established for *in vitro* SSC or ITT culture, development, and spermatogenesis. These systems can be divided from low to high physiological relevance into 2D culture, 3D culture, bioreactor culture, 3D printing, organoid culture, tissue sample culture, and testis-on-a-chip (**Figure 1-8**). Generally, the most commonly studied *in vitro* spermatogenesis (IVS) approaches using human tissue are divided into two categories: organ culture and dissociated testicular cell culture. Organ culture maintains the natural SSCs niches in intact testicular tissue fragments but has limitations for long-term culture and cell manipulation. Strategies for the culture of isolated

testicular cells, including conventional 2D culture, 3D culture, organoid culture and testis-on-a-chip, has provided multiple *in vitro* platforms to study testicular tubulogenesis and IVS (Baert et al., 2020, Richer et al., 2020). The 2D and 3D culture of testicular cell suspension allows the initiation of testicular tubulogenesis, which enables the long-term culture of testicular cells and re-establishes a cord-like or tubule-like structure. *In vitro* testicular organoids (TOs) and testis-on-a-chip are recent engineering techniques that provide cells with a microenvironment that mimics *in vivo* conditions for SSCs. In recent years, TO has been used in tissue engineering and refers to the reconstruction of a 3D testicular structure from isolated testicular cells to model testicular architecture and function *in vitro* (Baert et al., 2017). TO provides a platform to study the role of different types of testicular cells, and the regulation of growth factors and hormones *in vitro*, aiming to achieve IVS or provide a drug screening tool for human testicular tissues. TO is described in more detail in Section **1.5.2**. Testis-on-a-chip is a more advanced technology that is based on the formation of organoids and a range of microfluidics techniques, aiming to mimic the organ-level function of human testis and crosstalk between multiple organs on a laboratory developed chip device (Baert et al., 2020). The establishment of testis-on-a-chip is still in a very early stage; further studies are needed.

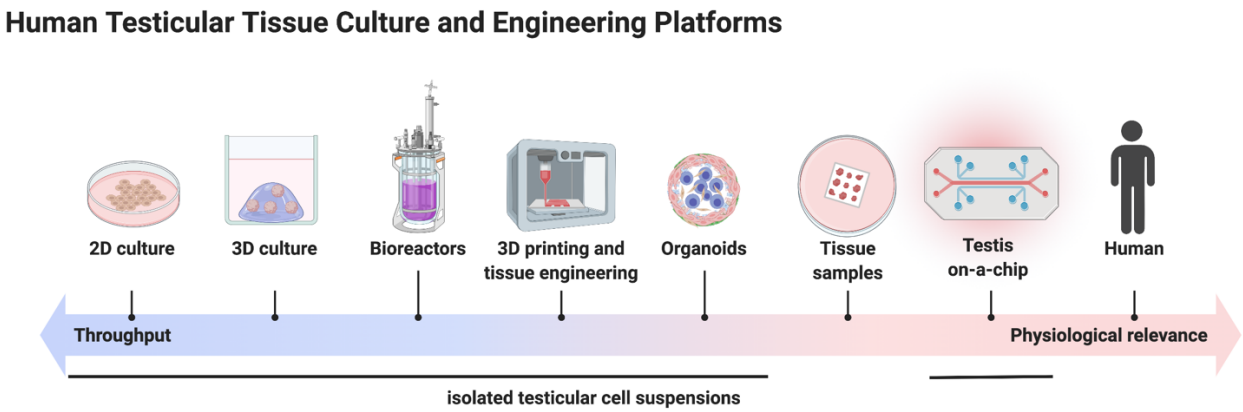

Figure 1-8. *in vitro* engineering techniques for human testicular tissue culture. *In vitro* human testicular cell culture platforms contain two-dimensional (2D) culture, three-dimensional (3D) culture, bioreactors, 3D printing, tissue engineering organoid culture, intact tissue culture, and the testis-on-a-chip platform, in order of their physiological relevance to real *in vivo* human testis. Suspension of isolated testicular cells has been commonly used in most of these *in vitro* culture techniques except tissue sample culture. Figure created by author on Biorander.com.

1.4.3.1 Organ culture

Organ culture involves the cultivation of small ITT segments (1-3 mm^3) to retain the natural histological structure. Several strategies have been explored, including air-liquid interface culture, microfluidic devices, and bioreactor systems (**Figure 1-9**). To provide adequate oxygen, as well as nutrition and support from the culture medium during culture, air-liquid interface cell culture has been used as conventional method for testicular fragments. In 1964, the first organotypic cultivation of rat ITTs was performed using gas-liquid interface culture (Steinberger et al., 1964), leading to meiotic entry and pachytene spermatocyte generation in 12-day-old rats (Steinberger and Steinberger, 1965). Millipore filters (Steinberger and Steinberger, 1971), grid (Boitani et al., 1993), agarose gel (Sato et al., 2013)and hanging drop(Szczepny et al., 2009) have been used to lift the testicular tissue fragments in dish so that tissues could partially contact the culture medium and partially to gas. In 2011, complete

spermatogenesis was observed in freeze/thawed ITTs from neonatal mice that were cultured in an *in vitro* gas-liquid interphase system; these sperm successfully generated healthy fertile offspring (Sato et al., 2011). Complete IVS has been reproduced using adult human ITTs; the production of pachytene spermatocytes (Roulet et al., 2006) and haploid cells (de Michele et al., 2018) has been reported after organotypic culture. The hanging drop method supports the proliferation of GCs from human adult testes (Jørgensen et al., 2014) but not gonocytes from human fetal testes (Jørgensen et al., 2015). Microfluid systems have been used to provide a continuous and controlled supply of oxygen and controllable culture medium, which were beneficial for the long-term culture of ITT fragments (Komeya et al., 2016a, Komeya et al., 2017, Yamanaka et al., 2018). Komeya et al. (Komeya et al., 2016a) constructed a microfluidic system with a constantly running medium channel that maintained mouse ITT and full spermatogenesis for six months. In addition, a bioreactor made of a hollow cylinder of chitosan hydrogel was created for the long-term primary culture of seminiferous tubule segments from prepubertal rats and adult human, and complete spermatogenesis was observed in both tissues (Perrard et al., 2016). Although organ cultures are able to maintain the original structure of testicular tissues, there are some disadvantages of organ culture: i) scale-up is difficult, ii) growth of tissues is slow, iii) the restriction of space inside tissue fragments for cell proliferation, iv) the restriction of nutrition and gas for cells in the centre of tissue fragments, and v) it is difficult to maintain long-term organ culture.

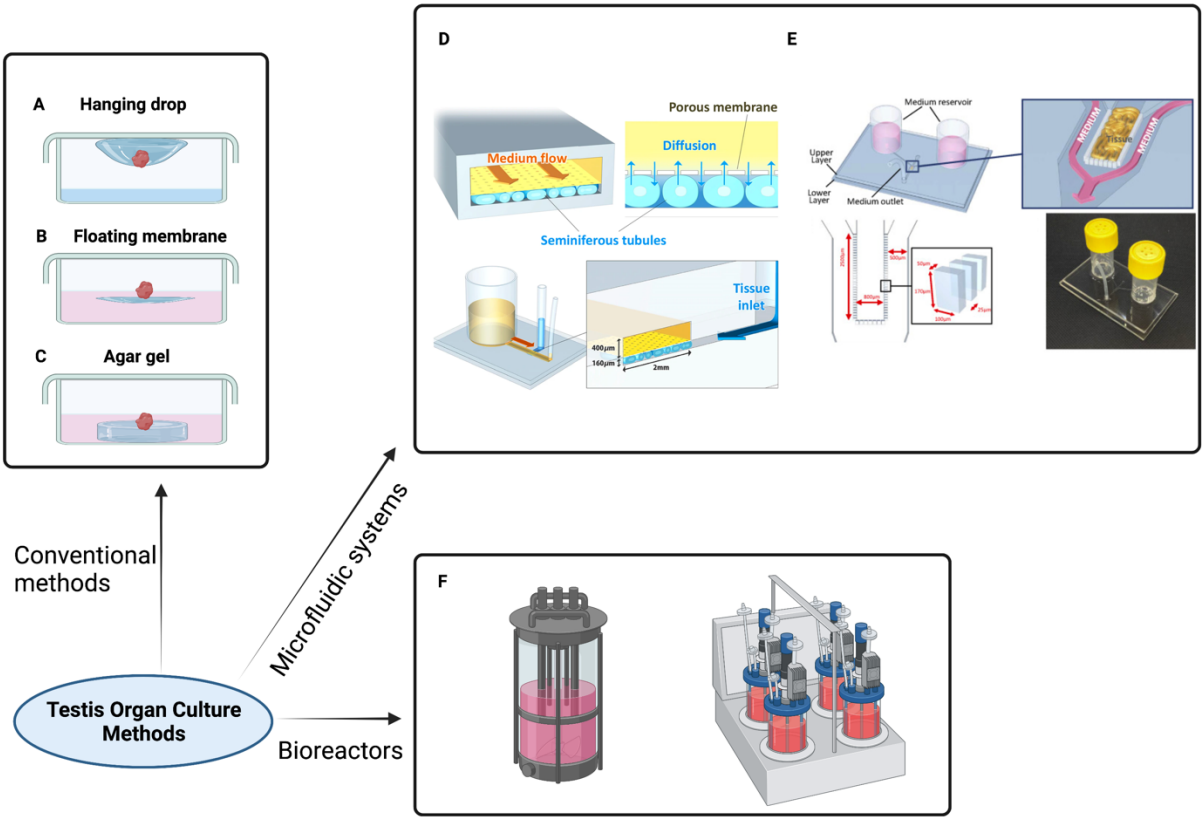

Figure 1-9. Organ culture methods for testicular tissues. Schematic representation of conventional testis organ culture techniques such as A) hanging-drop culture, B) floating membrane, and C) agar gel methods. D) Schematic demonstrating of a pumpless microfluidic device by separating medium flow from tissues. Adapted from Komeya et al. (2016b) under CC BY license. E) A glass bottom and a PDMS overlayer comprised a single layer microfluidic device for testis fragments culture. The culture medium passes through two different medium reservoir tanks that are linked to channels on both sides of the tissue chamber and then combine to produce an output. Adapted from Yamanaka et al. (2018) with permission from publisher. G) Bioreactors have been used for culturation of seminiferous tubule segments. Inspired by Eyni et al. (2021). Created with BioRender.com.

1.4.3.2 Dissociated testicular cells *in vitro*

A standard 2D culture system was initially used for primary testicular cell culture in 1980 (Tung and Fritz, 1980). Since then, important cell-to-cell or cell-to-ECM interactions have been studied in multiple testicular cell types (Hadley et al., 1985, Kierszenbaum et al., 1986). The effect of growth factors, hormones, and culture conditions on GCs or somatic cells has

also been explored (Schlatt et al., 1996, El Ramy et al., 2005). Importantly, immortalized cell lines were generated from murine GCs, Sertoli cells, Leydig cells, and other somatic cell types; these resources allow us to investigate the characteristics and functions of individual cell types (Hofmann et al., 1992). Functional haploid spermatids were successfully generated from the SSCs of adult patients with azoospermia or cryptorchidism after 2D culture *in vitro* (Tesarik and Bahceci, 1999, Yang et al., 2014). Some studies showed that the 2D culture of human GC, feeder cells such as Vero and Sertoli cells, and hormonal supplementation were essential to the spermatogenic process; however, no seminiferous tubular-like structures were observed (Tesarik et al., 2000, Sousa et al., 2002, Tanaka et al., 2003). Digested adult testicular cells can partially rearrange into tubular structures in 2D cultures but cannot support GC maintenance (von Kopylow et al., 2018). While 2D cultures provide certain cellular interactions and structural conditions, the cellular morphology may differ from that of real tissues. In general, the efficacy of 2D cultures for IVS is relatively low. More complicated testicular models that facilitate the interaction between germ and somatic cells are needed to overcome this problem.

Over the last decade, the culture of testicular cells has shifted away from conventional 2D culture models towards more advanced novel 3D culture techniques, such as different types of ECM, organoid, bioreactors, and testis-on-a-chip. The 3D culture mimics the features of the *in vivo* microenvironment and generate complex and sophisticated tissue structures; this has been regarded as an alternative method for studying testicular growth and spermatogenesis *in vitro.* Different 3D models for the culture of testicular cells is described in more detail in the next section.

1.5 *De novo* three-dimensional (3D) models for propagation and spermatogenesis

The stem cell microenvironment is formed by various cell types, ECM, and spatial arrangement, as well as cell-to-cell communication, cooperation, and metabolization, all of which contribute to homeostasis required for survival and function (Moore and Lemischka, 2006). The earliest understanding of the cell microenvironment may originate from the "hematopoietic stem cell microenvironment," created by Raymond Schofield's 1978 "niche" hypothesis (Schofield, 1978). Schofield believed that niches create a specific anatomical structure where the interaction between stem cells and other cells determines their behaviour. Removing stem cells from niches results in cell differentiation.

Over the past few decades, the dynamics and complexity of the stem cell microenvironment have been studied in human bone marrow, skin, small intestine, brain, muscle, and other tissues. As described in **Section 1.1.4**, SSCs reside in niches that are regulated by different cells and factors. 3D culture techniques have provided a better understanding of how the microenvironment is composed during various *in vivo* physiological and pathological processes, including interactions and dynamic changes that occur between cells, ECM, factors, and other active substances. More importantly, a 3D *in vitro* system could facilitate the study of human tissues and cells. As a result, the use of 3D culture systems to mimic the *in vivo* SSC niche environment is a significant area of research.

1.5.1 The *in vitro* cultivation of 3D scaffolds and testicular cells

Both scaffold-free and scaffold-based approaches have been used for the 3D cultivation of testicular cells (Edmondson et al., 2014). Due to the poor meiotic progression observed when using the scaffold-free technique (Yokonishi et al., 2013), most studies have used scaffold-based strategies. A scaffold network of key macromolecules modulates SSC niche maintenance, proliferation, self-renewal, and differentiation *in vitro*. The ECM also directly communicates with stem cells through surface receptors and uses growth factors to regulate SSC activity (Gattazzo et al., 2014). Most commonly used 3D scaffolds have been reported to provide the *in vitro* testicular architecture and lead to the generation of haploid gem cells, including 1) natural scaffolds including those, such as collagen, that are ECM-derived (Lee et al., 2006, Lee et al., 2007b, Reuter et al., 2014), Matrigel (Legendre et al., 2010), decellularized testicular matrix (DTM) (Baert et al., 2015), and seaweed-derived scaffolds, such as calcium alginate (Lee et al., 2001) and soft agar (Stukenborg et al., 2008, Mohammadzadeh et al., 2019), and 2) synthetic scaffolds such as methylcellulose (Stukenborg et al., 2009), and poly (D, L-lactic-co-glycolic acid) (Lee et al., 2011b) (**Table 1-2**).

Table 1-2. Selected *in vitro* 3D models to study testicular physiology and advanced germ cell differentiation.

Culture model	Donor age and species	Growth factor	Maximum culture length	Organization	Propagation/ differentiation of germ cells	Reference
Natural scaffolds						
3D: collagen gel, or collagen + Matrigel	18 *dpp* rats	Testosterone (10^{-7} M)	22 days	Cyst-like structures	Increase in the collagen haploid cell population with or without Matrigel; post-meiotic differentiation of spermatogenetic cells.	(Lee et al., 2006)
3D; 4.3 mg/mL or 2.5 mg/mL Matrigel with or without type I collagen	18 *dpp* peripubertal rats	Retinol ($3.3.10^{-7}$ m) rFSH (100 mIU) Testosterone (10^{-7} M)	22 days	Cluster organization	Round spermatids were detected.	(Legendre et al., 2010)
Laminin, Matrigel, DTM-derived hydrogel	6 *dpp* prepubertal mice; culture of isolated SSCs	Testosterone (10 µM) FSH (100 ng/ml) RA (100 ng/ml)	7 days	Not applicable.	DTM is able to maintain SSC stemness and promote SSC differentiation into round spermatids without SCs.	(Yang et al., 2020)
1:1 Matrigel to cell suspension medium	Adult obstructive azoospermia patients	RA (2 µM) Testosterone (10^{-6} M)	20 days	Not applicable	Round spermatids differentiated fro m human SSCs in the 3D Matrigel system fertilized mouse oocytes, generating embryos with developmental potential.	(Sun et al., 2018)
DTM from sheep testis	18,26,38 years old human	For cell proliferation:	4-6 weeks	Not applicable	Meiotic-related gene expression was	(Ashouri Movassagh

		GDNF (10 ng/mL) EGF (20 ng/mL) LIF (10^3 U/mL) bFGF (10 ng/mL) For differentiation: RA(3.3×10^{-7} M) FSH (2.5×10^{-5} U) Testosterone(10^{-7} M)			higher after 6 weeks of culture.	et al., 2020)
SACS	10 *dpp* and mature (30 *dpp* CD-1 mice	Not applicable	21 days	Colonies	Higher proliferation; round spermatids were observed when all testis cells seed	(Stukenborg et al., 2008)
SACS	Immature (7–9 *dpp*) CD-1 mice	hCG (5 IU/l) rhFSH (5 IU/l)	31 days	Colony formation	GCs underwent spermatogenesis and divided into pre-meiotic, meiotic and post-meiotic stages.	(Stukenborg et al., 2009)
SACS	7 *dpp* mice	Not applicable	14, 30 days	Colonies	Pre-meiotic germ cell expansion and differentiation into spermatozoa.	(Abu Elhija et al., 2012)
SACS	13-33 months old rhesus monkey	FSH (5 ng/ml) Testosterone (10^{-7} m mol/l)	4-8 weeks	Formed colonies/clusters	Meiotic cells and postmeiotic cells were presented after culture.	(Huleihel et al., 2015)
Natural scaffolds with different cultural methods						
Air-liquid interface technique with agarose gel	0.5–5.5 *dpp* neonatal mice	Human rEGF (20 ng/ml) human bFGF (10 ng/ml)	14 days	Irregular and maze-like reconstruction of tubular structure	Reconstructed tubules support germ cell differentiation into	(Yokonishi et al., 2013)

		human rGDNF (10 ng/ml)			pachytene spermatocytes.	
Human testis ECM in hanging drop culture	Adult (ages 56–61) human	RA (2 µM) FSH (2.5 x 10^{-5} IU) Human rSCF (100 ng/ml)	23 days	Compact, tight organoids with GCs being in the centre while somatic cells tend to be in the periphery of the structure.	Diploid to haploid GCs.	(Pendergraft et al., 2017)
Cell-free or cell-laden scaffolds bioprinting with nanocellulose-alginate hydrogel	Prepubertal (<7 *dpp*) and adult (6 months old) mice	Not applicable	Up to 48 days	No restoration of the tubular architecture	Progression of spermatogenesis up to the elongated spermatid stage; cell 59 eorganization into tubular structures was not observed.	(Baert et al., 2019b)
Synthetic scaffolds						
PLGA	18 and 30 *dpp* rats	RA (3.3×10^{-7} M) retinol (3.3×10^{-7} M) rFSH (100 mIU) Testosterone(10^{-7} M) Phytohemagglutinin(100 µg/ml)	18 days	Initial colonization	Differentiation of spermatocytes into spermatids.	(Lee et al., 2011b)
Collagen sponges	7 *dpp* rats	hCG (5 IU/I) FSH	35 days	Detection of tubulogenesis	No detection of haploid cells; maintainance of germ cells	(Reuter et al., 2014)
Agar and polyvinyl alcohol (PVA) nanofibers	3-6 *dpp* neonatal mice	bFGF (10 ng/ml) GDNF (10 ng/ml)	14 days	Formation of spermatogonial stem-like cell colonies	Differentiation of SSCs to meiotic and postmeiotic germ cells.	(Ziloochi Kashani et al., 2020)

PDMS nanotubes	7 *dpp* prepubertal rats	With or without hCG (5 IU/I) and human rFSH (5 IU/I)	14 days	Cord-like structure formation	Not investigated	(Lee et al., 2011a)
Methylcellulose	Immature (Days 7–9) CD-1 mice	hCG (5 IU/l) rhFSH (5 IU/l)	16 days days	Colony formation	Haploid cells	(Stukenborg et al., 2009)
Methylcellulose	13-33 months old rhesus monkey	FSH (5 ng ml−1) Testosterone (10−7 m mol l-1)	4-8 weeks	Formed colonies/clusters	Meiotic cells and postmeiotic cells were presented after culture.	(Huleihel et al., 2015)
Methylcellulose	23–50 years old azoospermic patients	GDNF, LIF, FGF and EGF	3-7 weeks	Colonies	Meiotic and postmeiotic cells were observed after culture.	(Abofoul-Azab et al., 2019)

FSH, follicle-stimulating hormone; RA, retinoic acid; MEM, Minimum Essential Medium; AlbuMAX, bovine serum albumin (BSA) purified with chromatography; DMEM/F12, Dulbecco's Modified Eagle's Medium/Nutrient Mixture F-12; FBS, fetal bovine serum; SCF, stem cell factor; HAS, human serum albumin; KSR, knockout serum replacement; (r)EGF, (recombinant) epidermal growth factor; LIF, Leukemia inhibitory factor; FGF, fibroblast growth factor; SCs, Sertoli cells; GCs, Germ cells; *dpp,* days post-partum; LCs, Leydig cells; DTM, decellularized testicular matrix; BMP4, bone morphogenic factor 4; SACS, soft agar culture system; PLGA , poly (D, L-lactic-co-glycolic acid).

In 2006, Lee et al. showed that rat GCs were able to differentiate on a 3D collagen gel culture system after 22 days and showed high cell viability (Lee et al., 2006). Collagen sponges have also been used successfully for immature rat testicular cell culture (Reuter et al., 2014). A subsequent study reconstructed seminiferous tubule-like structures with GCs on the inside and Leydig cells on the outside of a 3D collagen matrix culture and SPG were shown to successfully differentiate into primary spermatocytes (Zhang et al., 2014). Similarly, Sertoli cells from the transitional zone of adult mice testes organized into cord-like structures when embedded in a collagen matrix (Kulibin and Malolina, 2016). However, complete spermatogenesis has not been reported in 3D culture with collagen. Collagen, as one of the components of the ECM found in real testicular tissues, might not provide enough support for the optimum microenvironment for SSCs *in vitro*. Therefore, in order to mimic the real SSCs niche, a more complex combination of ECM is needed for *in vitro* SSC propagation and differentiation.

DTM is a more natural scaffold with a 3D testicular structure and native ECM compounds such as laminin, fibronectin, collagen, and glycosaminoglycans, that was created to support the attachment and infiltration of dissociated human testicular cells (Baert et al., 2015). In the DTM culture system, testicular cells form organoids that secrete testosterone and inhibin B but do not undergo essential testicular compartmentalization or full GC differentiation (Baert and Goossens, 2018). An innovative DTM-derived hydrogel scaffold was recently developed to support the culture of porcine TOs (Vermeulen et al., 2019). Neonatal mouse testicular cells cultured using the DTM system were shown to generate TOs that were similar to porcine and human organoids but exhibited more advanced SPG differentiation into post-meiotic cells (Rezaei Topraggaleh et al., 2019), indicating that this platform has potential for *in vitro* spermatogenesis. In mouse SSC culture, spermatogenesis was able to continue to the round spermatid stage in DTM hydrogel matrix (Yang et al., 2020); this could be associated with the

natural soluble growth factors binding to nature ECM (Hynes, 2009). These studies suggested that natural testicular ECM components such as collagen, fibronectin, and laminin, as well as a structural organization similar to that seen *in vivo*, would promote testicular cell rearrangement *in vitro*. However, DTM is derived from natural testicular tissues, which requires a large amount of animal testicular tissues and a complex procedure to obtain the DTM. The residual DNA, nucleotides, and other unidentified cellular proteins in the DTM might adversely affect GCs and somatic cells cultured in DTM system. Thus, DTM is not an ideal 3D system for future clinical applications.

In 2009, Stukenborge et al. effectively generated elongated spermatids from mouse testicular cell aggregates in a soft agarose culture system (SACS) and methylcellulose (Stukenborg et al., 2009). More recently, SACS has been used to form 3D cell aggregates of both dissociated somatic and GCs and generate post-meiotic cells from rat (Reda et al., 2014) and rhesus monkey ITTs (Huleihel et al., 2015). However, no advanced human GC differentiation or long-term GC culture has been reported and the effects of SACS on human GCs have not yet been investigated, thus restricting the use of SACS for future clinical application.

Synthetic scaffolds have also been used for *in vitro* testicular cell culture. For example, GCs from neonatal mouse testis developed into the post-meiotic stage in 3D agar and polyvinyl alcohol (PVA) nanofibers culture treated with RA and bone morphogenic factor 4 (BMP4) (Ziloochi Kashani et al., 2020). A 3D bioprinting method based on an alginate-based hydrogel was used as a culture system that allowed for design of the scaffold and cell deposition, and post-meiotic cells were identified in the culture (Baert et al., 2019a). Collagen sponges (Reuter et al., 2014) and carbon nanotubes (Pan et al., 2013) were also used to assess the influence of structural and topographical clues on *in vitro* rat testicular organogenesis, thus resulting in the generation of tubule-like structures. However, these synthetic scaffolds may have one or more

of the following disadvantages when used in cell culture: i) low cell adhesion; ii) low bioactivity; iii) biocompatibility problems; and iv) nondegradability (Reddy et al., 2021). The biocompatibility of these synthetic scaffolds with human GCs is not fully understood; thus, more studies are needed to explore the potential use of a synthetic scaffold on human testicular tissues.

In recent years, a novel organoid technology using Matrigel has been applied to testicular cell culture after its application to numerous animal and human organs, such as lung, liver, and intestine (Kim et al., 2020). Matrigel is one of the most commonly used naturally derived ECM scaffold material that promotes the reorganization of cell suspension into 3D structure *in vitro*. Matrigel is a soluble and sterile extract of basement membrane proteins from Engelbreth-Holm-Swarm (EHS) mouse sarcoma. Furthermore, Matrigel mainly contains laminin, collagen and entactin. Compared to synthetic scaffolds, the components of Matrigel are more similar to the *in vivo* physiological microenvironment which cells normally interact with. Compared to other natural gels, Matrigel has greater versatility to promote the reorganization of a 3D structure. Therefore, Matrigel has been regarded as a suitable ECM for the *in vitro* culture of testicular cells; this is described in more detail in the next section.

1.5.2 Testicular organoids (TOs)

1.5.2.1 Brief development of organoids

An organoid is an *in vitro* 3D cellular cluster produced entirely from dissociated primary tissue cells or induced pluripotent stem cells (iPSC) that is capable of self-renewing and self-

organizing. Organoids could demonstrate organ structure and/or function that is identical to the tissue of origin (Fatehullah et al., 2016). James Rheinwald and Howard Green were the first to develop organoids in 1975 by mixing human keratocytes with irradiated mouse fibroblasts and showed that these organoids could form a stratified self-organized squamous epithelium which had distinct cell types in each layer and resembled stratified skin (Rheinwald and Green, 1975). When an intestinal organoid culture system was first generated in 2009, stem cell research took an extensive technical leap forward in its ability to construct 3D cultures from primary tissues (Sato et al., 2009).

Organoids are generated from two distinct types of stem cells: 1) PSC that includes embryonic stem (ES) cells and induced pluripotent stem cells (iPSC), and 2) organ-specific adult stem cells (aSCs) (Clevers, 2016). When PSCs and aSCs are allowed to differentiate in culture, they are able to self-assemble into structures that closely resemble critical features of their tissues of origin. While PSC-based organoids are established by developmental processes, aSCs form organoids by reproducing the stem cell niche microenvironment during physiological tissue self-renewal or injury repair. Adult stem cells differentiate into tissue-specific cell types *in vivo* and regularly self-renew to refill the stem cell pool (Clevers and Watt, 2018). The novel 3D organoid method allows researchers to create a well-defined, stable *in vitro* culture system resembling the stem cell niche that can provide long-term support for near-physiological epithelia from purified stem cells. Organoids are now generated for a growing number of organs, including the gut (Sato et al., 2009), stomach (Barker et al., 2010), colon (Sato et al., 2011b), kidney, pancreas (Huch et al., 2013), liver (Takebe et al., 2013), mammary glands, prostate, airways, thyroid, retina, and brain (Quadrato et al., 2017). Organoids are a promising tool for advancing personalized treatment and next-generation drug screening, and for reducing the need for animal experiments. Organoids generated from both primary and stem cells

provide simpler and more direct access to study signaling pathways than animal models (Lancaster and Knoblich, 2014, Fatehullah et al., 2016).

1.5.2.2 The generation of testicular organoids (TOs)

Matrigel has been used for immature rat testicular cell culture since SPG progression to pachytene spermatocytes and cord-like structures were first observed in 1985 (Hadley et al., 1985). Hadley et al. stressed the importance of using laminin as a component of Matrigel because it promotes the rearrangement of Sertoli cells into cords (Hadley et al., 1990). Matrigel has been widely utilized to embed testicular cells from neonatal rats and mice (Yu et al., 2005, Gassei et al., 2010) because a higher number of post-meiotic cells are observed in cultures containing a combination of Matrigel and collagen than those with only collagen (Sakib et al., 2019). In Matrigel, neonatal testicular cells can organize into tubule-like structures with a blood-testis barrier in which the differentiation of GCs into round spermatids was observed (Legendre et al., 2010). A recent study also showed that tubule-like structures could be rebuilt in a three-layer Matrigel system using newborn rat testicular cells (Alves-Lopes et al., 2017). These results indicate that Matrigel induces testicular cells to reorganize into tubular-like structures *in vitro*, likely from the complex proteins and growth factors Matrigel contains. The creation of a TO is a novel approach that is considered the most promising method because it could potentially provide an *in vitro* SSC niche environment that mimics the *in vivo* microenvironment and allows designable manipulation.

Research on TOs has increased over recent years (**Table 1-3**). In one of the first studies on TOs in 2017, primary testicular cells from both adult and prepubertal human testes were able to self-organize into functional organoids, where active niche cells and SPG could be maintained for

up to 4 weeks (Baert et al., 2017). These newly formed organoids were able to secrete testosterone, inhibin B, and cytokines, and tight junction proteins were found on the Sertoli cells. Similarly, Pendergraft's 2017 study showed that human organoids from adult GCs and immortalized Leydig and Sertoli cells cultured using the hanging drop method could produce testosterone and generate haploid GCs (Pendergraft et al., 2017). Solubilized human testicular ECM was added to the culture media to imitate native conditions and markers of undifferentiated SPG were continually expressed during a 23-day culture, thus suggesting that the GC pool was maintained (Pendergraft et al., 2017). This 3D human testis organoid model has the potential to be used as a novel testicular toxicity-screening tool. In 2018, TO technology was used to investigate Zika virus infections (Strange et al., 2018), thus indicating a potential clinical application for TOs as a platform to study diseases. More recently, Sakib et al. used a microwell culture system to generate multicellular TOs that presented testis-specific morphology (Sakib et al., 2019). These authors also showed that the GCs in these structures experienced less cellular stress, including having a significantly lower number of autophagosomes, than GCs in 2D cultures. In 2019, Vermeulen et al. generated the first TOs with an exact tissue-specific structure in prepubertal porcine using collagen and hydrogel derived from DTM (Vermeulen et al., 2019). Peritubular and Leydig cells were found on the exterior of the tubule-like structures, while GCs and Sertoli cells were found on the interior. GC proliferation was observed in the organoids, but no further differentiation occurred during the 45 days of culture. In 2020, the self-assembly of tubular-like-structure TOs was shown to be age-dependent; 5-days-postpartum (*dpp*) cells (immature mice) were able to form organoids while 21-dpp cells (adult mice) were not (Edmonds and Woodruff, 2020). In addition, these TOs exhibited long-term (84 days) endocrine function and produce testosterone and inhibin B in response to FSH and hCG, indicating their potential as effective *in vitro* testicular tissue

models. More recently, mouse and chimeric TOs were shown to form in a 3D printed one/two-layer scaffold (Richer et al., 2021). Interestingly, an intact tubule-like structure surrounded by interstitium was observed when culturing a mixture of primary testicular cells and germline stem cells, thus indicating that cell composition can be manipulated on the organoid platform. While the short-term survival of germline stem cells was observed in this organoid system, no GC differentiation occurred.

Table 1-3. Studies reporting the generation of 3D testicular organoids (TOs).

Culture model	Donor age and species	Growth factor	Maximum culture length	Organization	Propagation/ differentiation of GCs	Reference
Human						
DTM	15-year-old and adult human	with or without hCG (5 IU/L) and FSH (5 IU/L)	28 days	Formation of TOs occurs with or without scaffold support in both adult and prepubertal testicular cells.	No progression of spermatogenesis, but spermatogonia were maintained and proliferated in culture.	(Baert et al., 2017)
Human testis ECM in hanging drop culture	Adult (ages 56–61) human	RA (2 μM), FSH (2.5 x 10−5 IU), human rSCF (100 ng/ml)	23 days	Compact, tight organoids with GCs in the centre and somatic cells on the periphery.	Diploid to haploid GCs.	(Pendergraft et al., 2017)
Ultra-low attachment 96-well plate with centrifugation	Adult	-	72 hrs	Organ-like structure containing GCs, SCs, and LCs.	TOs could be infected by the Zika virus.	(Strange et al., 2018)
TOs in microwell culture	6-month-old and 5-year-old human	EGF (20 ng/ml), RA (1 μM)	5 days + 48h of RA stimulation.	Generation of porcine TOs with inverted cell organization (GC and SC were located outside while peritubular myoid cells and LCs were located at the core). Testicular cells containing 50% GCs failed to form organoids.	No progression of spermatogenesis was reported.	(Sakib et al., 2019)
Animal						
Matrigel, three-layer gradient system	5–8-, 20- and 60 days old rats	RA (1 μM),	21 days	Seminiferous tubule-like structures in the organoid	Maintenance and proliferation of SSC Responsiveness of organoids to IL1a, TNFa and RA	(Alves-Lopes et al., 2017)

TOs in microwell culture	1-week-old piglets; P8-P10 mice; 2-year-old rhesus macaque;	EGF (20 ng/ml), RA (1 µM)	5 days + 48h of RA stimulation.	Generation of porcine TOs with inverted cell organization (GC and SC were located outside while peritubular myoid cells and Leydig cells were located at the core). Testicular cells containing 50% GCs failed to form organoids.	No progression of spermatogenesis reported.	(Sakib et al., 2019)
Hydrogel derived from ram decellularized testicular tissues	3-5 days old mouse	RA (10−6 M), hCG (5 IU/l) and FSH(5 IU/l) were added from day 15 to 30	30 days	-	Post-meiotic stage GCs (haploid) were detected in organoids Secretion of testosterone and inhibin	(Rezaei Topraggaleh et al., 2019)
Collagen and hydrogel from DTM	< 7 days old prepubertal pigs	retinol (1 µM) FSH (35 IU/l,) hCG (2 IU/l)	45 days	Reassembled tubule-like structures with SCs and GCs in the middle and LCs and peritubular cells localized outside.	Generation of functional TOs, no spermatogenesis progression; the number of GCs decreased in culture.	(Vermeulen et al., 2019)
3D ECM-free culture (3DF, agarose microwell inserts), and 2D ECM culture (cells on top of 1:1 base medium-diluted Matrigel)	Prepubertal (5 days old), peripubertal (12 or 21 days old) and adult (8-16 weeks old) mouse	FSH (20 mIU/ml), hCG (4.5 IU/ml) starting at day 7of long-term culture	84 days	Self-assembly of *tubule-like* structures Incorporation of all major cell types Structural compartmentalization between tubular and interstitial cells	No meiotic cells were detected Secretion of testosterone and inhibin B over 12 weeks	(Edmonds and Woodruff, 2020)
3D printed scaffolds and air medium interface cultivation	4-5 days old mice	Melatonin (10^{-7} M), retinol (10^{-6} M)	6 weeks	Tubule-like structure	Differentiation of GCs to the meiotic phase	(Richer et al., 2021)

hCG, human chorionic gonadotropin; DTM, decellularized testicular matrix; ECM, extracellular matrix; FSH, follicle-stimulating hormone; SCF, stem cell factor; IL1, Interleukin-1; TNFα, tumour Necrosis Factor alpha; RA, retinoic acid; EGF, epidermal growth factor; GCs, germ cells; SCs, Sertoli cells; SSCs, spermatogonia stem cells; LCs, Leydig cells.

In vitro TOs could potentially be used as long-term models to study GC niche molecular regulatory mechanisms, cell-cell interactions inside SSC niches, and testicular cancer and its microenvironment. TO platforms offer many possibilities to study and manipulate Sertoli cells, GCs, and other essential components of SSC niches for the treatment of male infertility and other conditions. Understanding the SSC niche and its basic mechanisms is important for the design of *in vitro* culture systems that can regulate SSC self-renewal and differentiation for potential clinical application. To date, only a few studies have investigated TOs with limited human tissues or animal models, let alone the use of prepubertal testicular tissues. No complete spermatogenesis has been reported in TO systems in animal models or humans. More studies are needed to explore the optimum microenvironment for the culture of GCs in organoids. Due to the difference of prepuberty period and development of testis in different species, it is important to use suitable animal models with a longer prepuberty period, such as the bovine model, to investigate the optimal *in vitro* microenvironment for GCs before moving to valuable human ITTs. Moreover, no study has investigated TO formation using a neonatal bovine animal model. No study has yet investigated GCs in the postnatal stage, such as the gonocytes, for their *in vitro* maintenance, propagation, survival and differentiation. Therefore, in this thesis, I investigated the *in vitro* isolation, enrichment, and culture conditions of gonocytes, and the formation of neonatal TO using bovine animal model; further details are given in **Chapter 4 and Chapter 5**.

1.6 Gaps in the existing literature, hypothesis, and aims

Increasing attention is being given to infertility caused by childhood cancer treatments and as a result, many fertilities preservation programs have been established for the cryopreservation of reproductive tissues. To date, no standard tissue transportation processes or cryopreservation strategies have been established. Given the importance of maintaining tissue fragment health and quality before and after cryopreservation, the transportation process, including the transport medium and time, requires investigation. It is often not feasible for a patient to come to a fertility preservation center himself, since his condition makes long travels difficult. On the other hand, fresh tissue transport is both expensive and risky to tissue health. Thus, vitrification, a simpler and more efficient cryopreservation method that does not require the use of an expensive and heavy machine, may represent a suitable alternative.

One of the most significant challenges related to the use of stored human ITTs is the production of functional sperm from GCs. Given the differences between prepubertal and pubertal niches, reassembling SSC niches *in vitro* may help to preserve the fertility of prepubertal boys who have been diagnosed with cancer. IVS is the most promising approach to preserving the fertility of these patients given that it requires minimal invasiveness and no risk of transplanting neoplastic cells. However, spermatogenesis is a complex process in a specialized testicular microenvironment *in vivo*, and recreating conditions to support complete GC differentiation *in vitro* is a challenge that has only been achieved in a mouse model thus far. Rebuilding the testicular niche from dissociated cells *in vitro* is an attractive alternative because of the control afforded over the cell culture and the possibility of providing vasculature. Use of this strategy in combination with innovative technologies, such as organoids, microfluidics, or 3D printing, is currently under investigation and may help to create a fully competent IVS culture system.

In vitro organoids could potentially be used as an *in vitro* model to study spermatogenesis and testicular diseases. To date, only limited large mammal models have been used to build TOs. To our knowledge, no bovine TOs have been generated to date. Bovines are commonly used as a large animal model and have a longer prepubertal period to study the development of testes, so could be used to generate TOs before moving to the study of valuable human tissue. In addition, important questions about the efficacy and safety of the developed systems remain unanswered in animal models, let alone in humans. In large animal and non-human primates, complete GC differentiation *in vitro* has relatively low effectiveness and progression beyond the spermatocyte stage remains challenging. There is an urgent need to develop an *in vitro* culture system in large mammal models for the propagation and spermatogenesis of GCs. The use of 3D culture systems is becoming more refined and may provide micro-environment conditions that can support spermatogenesis *in vitro*.

The general aim of my DPhil thesis was to develop an improved 3D culture system as a replicable and easy assessable platform for *in vitro* propagation and differentiation of primary GCs from ITTs. My research was primarily composed of four studies that are linked by the preservation of ITT biopsies and the restoration of fertility.

Aim 1: To investigate the effect of three cryopreservation methods, vitrification, speed-controlled slow freezing, and non-speed controlled slow freezing, on bovine neonatal testicular tissue structure, cell viability, cell apoptosis, and key gene expression (**Chapter 2**).

Hypothesis: Vitrification can be used as an alternative cryopreservation method for bovine ITTs by successfully preserving tissue structure and GCs.

Aim 2: To investigate the effect of four tissue transportation times (1, 6, 24, and 48 hours) on bovine neonatal testicular tissue structure, cell viability, cell apoptosis, and key gene expression (**Chapter 3**).

Hypothesis: Bovine neonatal testicular tissue can retain good condition after a 48-hour transport period.

Aim 3: To optimize the selection and characterization of GCs from dissociated testicular cells (**Chapter 4**). In this section, I optimized the neonatal bovine testicular GC isolation and enrichment protocol and developed basic culture conditions for maintaining GCs *in vitro* using a commonly used 2D culture system.

Hypothesis: The optimized protocols are effective and reliable for GC isolation, enrichment, and short-time *in vitro* maintenance.

Aim 4: To develop a novel 3D organoid culture system for the *in vitro* maintenance and development of GCs from bovine neonatal testicular tissue (**Chapter 5**). To achieve this, I investigated factors including cell types, basic culture medium, cell-seeding methods, and growth factors, that might affect bovine TO generation. I also evaluated the long-term and short-term culture of organoids in this novel 3D system.

Hypothesis: The novel 3D organoid culture system could support GC maintenance and development *in vitro* by providing a niche-like microenvironment.

Chapter 2. A comparison between vitrification and two methods of slow freezing for the cryopreservation of gonocyte-containing neonatal calf testicular tissue

2.1 Introduction

Childhood cancer is a leading cause of death, with an estimated 397,000 cases worldwide in 2015 (Ward et al., 2019a). In many high-income countries, the 5-year survival rate associated with childhood cancer is as high as 80% (Bhakta et al., 2019). However, survival may come at the cost of the long-term side-effects of aggressive anti-cancer therapies; one such effect is infertility. Rapidly dividing cells are the prime target of chemotherapy and radiotherapy; consequently, these cancer treatments may induce a severe loss of GCs, thus resulting in temporary or permanent gonadal toxicity. Consequently, there may be a high prevalence of infertility among adults who survived childhood cancers, including those who suffered from osteosarcoma, Hodgkin's lymphoma, and soft-tissue sarcomas (Wasilewski-Masker et al., 2014a). Increasing evidence shows that chemotherapy with alkylating agents (e.g., cyclophosphamide) or platinum-based agents (e.g., cisplatin or carboplatin) reduces the proliferation of GC populations (Green et al., 2014, Allen et al., 2020). It follows that the survivors of childhood cancer might have a lower chance of having a child than their siblings (Green et al., 2010).

The production of functional sperm begins at puberty; therefore, conventional 'sperm banking' is not practical for the preservation of fertility in prepubertal or adolescent boys. Thus, cryopreserving ITTs represents a promising alternative approach for these patient populations (Keros et al., 2007, Menon et al., 2009). An increasing number of tissue banks have been established in different countries to perform such techniques (Lakhoo et al., 2019b, Valli-Pulaski et al., 2019, Goossens et al., 2020). At present, the most commonly used methods for the preservation of ITTs are controlled slow freezing (CSF), uncontrolled slow freezing (USF), and vitrification. In CSF, the cooling speed and temperature can be controlled using a

programmed machine, whereas USF does not permit such accurate control over the freezing process.

Slow freezing, using dimethyl sulfoxide (DMSO) as a permeating cryoprotectant, is one of the most commonly used methods for the cryopreservation of ITT in human tissue banks (Wyns et al., 2008, Valli-Pulaski et al., 2019). The application of this technique, has led to the production of functional sperm and live offspring from prepubertal grafts in mice (Honaramooz et al., 2002, Shinohara et al., 2002a, Schlatt et al., 2003) and in rhesus monkeys after autologous grafting (Fayomi et al., 2019). These findings indicate that this method offers a potential means of regaining fertility in young people who have undergone cancer treatment. The cooling rate in slow freezing is crucial because it affects the rate of formation and the size of ice crystals (Gurruchaga et al., 2018). Uncontrolled slow freezing (e.g., using the Mr. Frosty system) is a cheap and simple method; however, using this type of system, it is not possible to accurately adjust or design cooling rates that are optimized for testicular tissues. Controlled slow freezing allows the application of optimal cooling rates for testicular tissues during cryopreservation and allow us to monitor the real cooling rate within samples. However, the controlled slow freezing method currently used in clinics for human prepubertal testicular tissues demands complex and costly equipment; these systems are usually owned by large urban hospitals or central tissue banks. Thus, patients may need to travel long distances to specific hospitals to receive this specialized treatment. This may delay their cancer treatment, or alternatively, their tissue biopsy may need to be transported a long distance, which may affect the quality of the preserved tissue.

Vitrification is a physical process in which the liquid in cells/tissues starts to become a solid liquid (also referred to as a glass-like state) without the formation of ice crystals; this occurs because the tissue is cooled rapidly (Wowk, 2010). During this transition, the natural disorder

of water molecules and other dissolved solutes can be largely maintained and preserved inside cells and tissues. Vitrification has been proposed as a clinically safe and efficient fertility preservation technology for use in in vitro fertilization (IVF) laboratories for the cryopreservation of oocytes, embryos (De Munck and Vajta, 2017), blastocyst (Rienzi et al., 2016), sperm (Tao et al., 2020) and ovarian tissues (Suzuki et al., 2015) with full developmental competence. However, vitrification has not been widely used for the storage of testicular tissues. The use of vitrification to cryopreserve ITTs may enable more timely processing of tissues without the need for patients to complete long journeys. Previous research has indicated that vitrification is effective for the cryopreservation of undifferentiated SPG in mice (Curaba et al., 2011b), horses (J Costa et al.), and humans (Curaba et al., 2011a) in terms of preserving tubular morphology. Vitrified testicular tissues from neonatal Aug boars had been proven to produce functional sperm after grafting into nude mice (Kaneko et al., 2020). Furthermore, the completion of spermatogenesis was reported for both controlled rate freeze/thawed and vitrified neonatal mouse testicular tissues (Yildiz et al., 2018). These studies indicate the significant potential of vitrification for preserving male fertility.

ITTs collected from cancer patients (including those suffering from leukaemia, lymphoma, or testicular cancer) before they undergo treatment cannot be used for autologous grafting, as they may contain malignant cells. In such cases, IVS and xenotransplantation are more appropriate approaches. In addition, only a small number of GCs are present in ITTs; *in vitro* culture could facilitate the maturation and development of these GCs. Therefore, the *in vitro* culture of enriched GC populations is important for the isolation and propagation of GCs.

In the early postnatal developmental stage of the mammalian testis, gonocytes, which are located in the centre of the seminiferous cords, are the most prominent type of GC and are surrounded by Sertoli cells (Yang and Oatley, 2014). In bovine and human testes, at

approximately 2 months of age, gonocytes that originate from PGCs gradually begin to migrate to the basement membrane of the seminiferous cords and develop into spermatogonial stem cells (SSCs) (Paniagua and Nistal, 1984, Culty, 2009). This transformation is associated with the capacity of SSCs to self-renew and undergo spermatogenesis; consequently, this process if important for the development of male GCs. Therefore, the preservation of gonocytes during the neonatal period is fundamental to healthy prepubertal testes. However, only a few studies have addressed the cryopreservation of mammalian gonocytes; furthermore, the vitrification of gonocyte-containing testicular tissue has yet to be attempted.

In this study, we utilized the bovine model as an alternative to human tissues. This established animal model has several specific benefits for this type of research. For example, the prepubertal period in the bovine model is similar to that of humans, and longer than in mice or rats. Second, bulls have a lower spermatogenesis efficiency ($12x10^6$ sperm per gram of testicular tissue daily); this is similar to the efficiency of humans (4 to $6x10^6$ sperm per gram daily). Third, spermatogenesis takes 61 days in bulls, compared to 74 days in humans (Amann et al., 1976, Johnson, 1986). The seminiferous epithelium in neonatal calves contains gonocytes/SSCs and Sertoli cells and no advanced spermatids for the first 20 weeks. The initiation of spermatogenesis in Holstein bulls starts at around 16 weeks and ends by 32 weeks (Curtis and Amann, 1981), thus providing a longer pubertal period for research. Given the difficulty in obtaining human ITTs, the bovine model is widely considered to represent an appropriate animal model for this type of research.

In the present study, we investigated the effects of vitrification and two methods of slow freezing on the cryopreservation of neonatal bovine ITTs containing gonocytes. We also assessed the potential of vitrification as an alternative method for cryopreserving neonatal ITTs. The three cryopreservation techniques were compared with regards to tubular histology,

cell viability, apoptosis, and gene expression in neonatal gonocyte-containing ITTs. After thawing, *in vitro* gonocyte cultures were carried out and analysed to evaluate the activity and behaviour of cells after cryopreservation.

2.2 Methods and materials

2.2.1 Collection and preparation of bovine ITTs

Bovine ITTs from 2-week-old Holstein calves (*Bos taurus*) were obtained from Tockenham Corner abattoir (Swindon, UK). All testes were washed in phosphate Buffered Saline (PBS) (Sigma-Aldrich, UK) and immediately transferred to the laboratory on ice in transfer medium containing sterile Hanks' Balanced Salt Solution (HBSS) (Sigma-Aldrich, UK) supplemented with 2% penicillin–streptomycin (Sigma-Aldrich, UK), 0.1 M sucrose (Sigma-Aldrich, UK), and 10 mg/mL bovine serum albumin (BSA, Thermo Fisher, UK). Testes were then immersed in transport medium and transferred on ice immediately to our laboratory. Upon arrival at the laboratory, the adipose tissue and tunica albuginea were removed, longitudinal incisions were made to expose the testicular parenchyma (**Figure 2-1**). Then, ITTs were dissected into fragments that were 1–2 mm^3 in size and then stratified into three groups according to the cryopreservation method: CSF, USF, and vitrification.

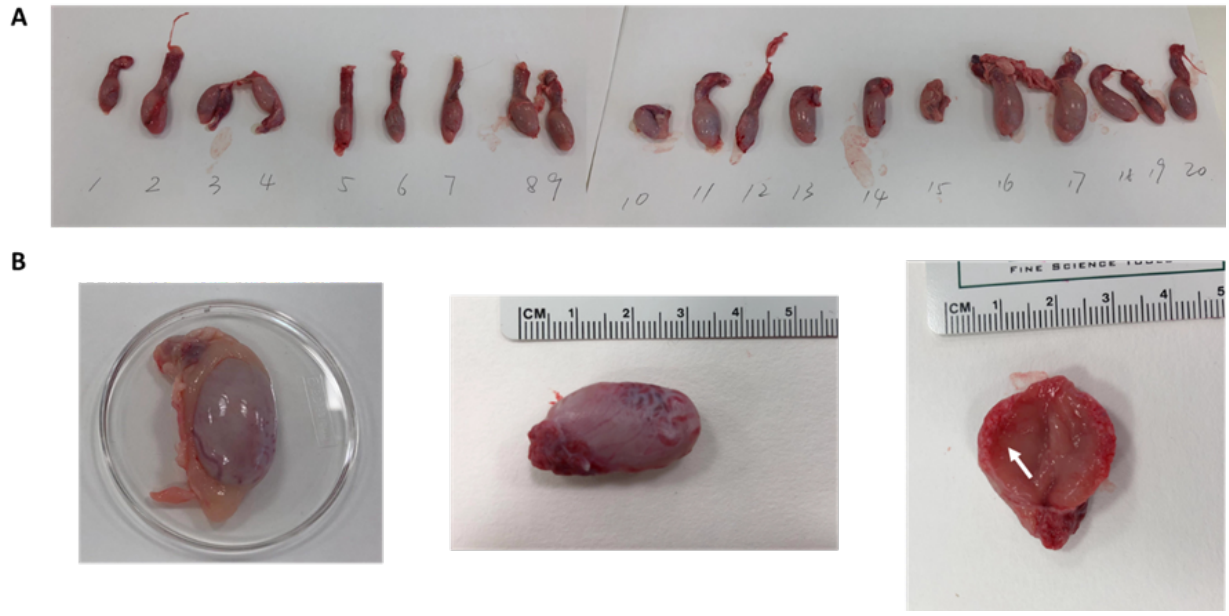

Figure 2-1. Preparation of calf immature testicular tissues (ITTs). A) ITTs were collected and washed with PBS. B) Testis with tunica vaginalis and epididymis (left), after removal of the tunica vaginalis and epididymis (middle), and after a longitudinal incision to expose the testicular parenchyma (right). Tissue fragments of 2 to 5 mm^3 in size were taken from the region indicated by the white arrow for subsequent cryopreservation.

2.2.2 Cryopreservation and thawing

In the CSF group, testicular tissue fragments were processed using the testicular tissue cryopreservation standard operating procedure applied at the Oxford Cell and Tissue Biobank (Oxford, UK) (Lakhoo et al., 2019a) with necessary modifications which were for bovine animal tissues. The individual tissue fragments were transferred to cryovials and equilibrated in 1 mL of premade cryoprotectant agent (CPA) containing HBSS supplemented with 1.5 M DMSO (Sigma, UK), 0.1 M sucrose, and 10 mg/mL bovine serum albumin (BSA). Cryopreservation was performed in a computer-controlled freezer (Ice Cube 14S, SY-LAB, Purkersdorf, Austria) using the testicular tissue cryopreservation programme:

1) Start temperature of 4°C;
2) Cryovials with ITTs were placed into the auto-seeding rack cryovial holders;
3) The initial cooling rate was −1°C/min; cooling was continued until the chamber temperature reached 0°C and then held for 5 min;
4) The cooling rate was −0.5°C/minute until −8°C was reached, and then held for 5 min;
5) The machine automatically seeded the cryovials and the tissues were allowed to soak for 15 min;
6) The cooling rate was −0.5°C/minute until −40°C was reached, and then held for 10 min;
7) A faster cooling rate was applied, of −7°C/minute until −70°C was reached;
8) A much faster cooling rate was applied, of −10°C/minute until −140°C was reached;
9) The cryovials were removed from the chamber and immediately placed in liquid nitrogen for storage.

When the programme was finished, cryovials were removed from the chamber and plunged rapidly into a liquid nitrogen (LN_2)-containing Dewar, where they were stored to await future analysis.

In the USF group, cryovials were placed in a Mr Frosty™ Freezing Container (Thermo Fisher Scientific, Waltham, MA, USA) containing isopropyl alcohol at room temperature, which was then transferred to a −80°C freezer overnight before being placed into LN_2. This unit was designed to provide a cooling rate of approximately 1 °C/min from room temperature to −80°C.

When thawing, the slow-frozen vials were removed from LN_2 and immersed in a 37°C water bath for 2 min. Then, 1 ml of warm transport medium was added immediately to each vial to dilute the cryomedium by 50%; then, all contents were transferred from cryovials to a prepared sterile dish for 3 min. Next, small pieces of testicular tissue were transferred to a fresh dish

containing 3 ml of transport medium for a 5 min incubation with gentle agitation at 37°C. This process was repeated twice.

For vitrification, small pieces of testicular tissue were processed using a vitrification kit according to the manufacturer's instructions (VT601, Kitazato, Shizuoka, Japan). One piece of tissue was placed in 200 µl of equilibration solution for 25 min. After removing the excess equilibration solution, tissue fragments were placed in 200 µl of vitrification solution for 15 min. Next, small pieces of tissue were plunged immediately into fresh LN_2 before being placed into an empty cryovial and stored in LN_2 until further use. To thaw samples after vitrification, tissue fragments were warmed in 1.5 ml of prewarmed thawing solution at 37°C for 1 min incubation, followed by 3 min incubation in 600 µl of dilution solution, and two 5 min incubations in 600 µl of washing solution. All cryovials were stored in LN_2 at −196 °C to await further analysis. Vitrified or freeze/thawed testicular tissues from the three groups underwent immediate fixation for histology, and were evaluated for apoptosis, cell viability, and gene expression.

2.2.3 Histology and immunohistochemical analyses

Freeze/thawed testicular tissue fragments were fixed in 10% formalin (approx. 4% formaldehyde; Sigma-Aldrich, UK) for 24 hours at room temperature before being embedded in paraffin wax. All tissue embedding was performed by the histology facility at the Kennedy Institute of Rheumatology at the University of Oxford. Sections of 5 µm in thickness were obtained using by a microtome (Leica, Germany). At least three section slides from different depths of each of the embedded tissues were used for haematoxylin and eosin (H&E) staining or immunohistochemical staining (**Figure 2-2**). For both H&E staining and

immunohistochemical staining, the sections were dewaxed and rehydrated by xylene and a series of decreasing ethanol concentrations.

Testicular tissue morphological appearance was assessed by H&E staining. For H&E staining, slides were immersed in haematoxylin solution (Sigma-Aldrich, UK) for 30 seconds, followed by eosin solution (Sigma, UK) for 1 minute, and washed in running water for 10 minutes. After mounting and drying, the microscopy images of the stained tissue sections were collected (Nikon, Japan) and seminiferous tubule detachment from the basement membrane was analysed. Based on the main morphological patterns, structural integrity, and architecture, the histology of ITTs was categorized as grades 1, 2, or 3 according to the attachment of tubular cells to the basement membrane (**Figure 2-3 A**). Seminiferous tubules were regarded intact when tubular cells adhered to the basement membrane. Tubules were considered to be grade 1 if there was full cellular adhesion or <30% detachment from the basement membrane, grade 2 if there was partial detachment (30% to 70%) from the basement membrane, and grade 3 if tubules displayed >70% detachment from the basement membrane.

For immunohistochemical staining, after the sectioned tissues have been deparaffinized and rehydrated, 0.3% H_2O_2 was used to inactivate endogenous peroxidase, followed by nonspecific blockade with horse/goat serum blocking solution for 30 minutes at room temperature. Subsequently, ITT sections were incubated with primary antibodies overnight at 4°C. Anti-PGP9.5 primary antibody (1:100 dilution; ab72911; Abcam, Cambridge, UK) was used as a marker of gonocytes and undifferentiated SSCs. Anti-vimentin primary antibody (1:200; sc-6260; Santa Cruz Biotechnology, Santa Cruz, CA, USA) was used as a marker of Sertoli cells. Anti-ki67 primary antibody (1:100; ab15580; Abcam) was employed as a marker for cell proliferation. After washing in PBS, the sections were incubated with the secondary antibody provided in the VectaStain™ ABC kit (Vector Laboratories, Burlingame, CA, USA). After

staining using this kit, signals were visualized using 3,3′-diaminobenzidine (DAB; Novus Biologicals, Littleton, CO, USA). All ITT sections were counterstained with haematoxylin for 30 seconds and washed in running water. After dehydration in a graded ethanol series and clearing in xylene, the slides were mounted and dried. Negative controls were prepared using corresponding concentrations of isotype immunoglobulin G. Images were taken and analysed by ImageJ (National Institutes of Health, Bethesda, Maryland, USA).

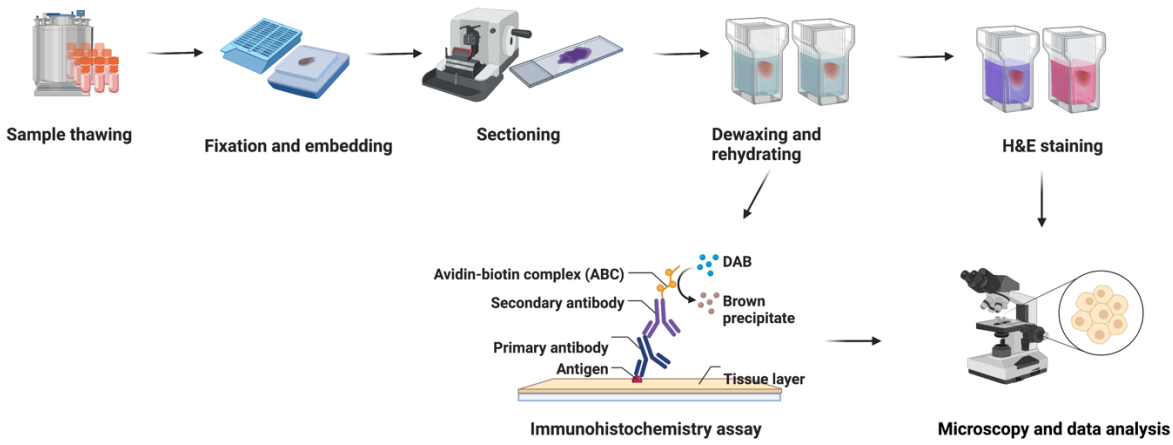

Figure 2-2. Histology and immunohistochemistry procedure. Samples in cryovials were removed from the liquid nitrogen tank and thawed in a water bath. After fixation and embedding, the tissues were sectioned using a microtome, dewaxed, and rehydrated with xylene and ethanol. The slides were then stained with haematoxylin and eosin (H&E) for morphology analysis or with immunohistochemical stains for the analysis of germ cells or Sertoli cells. Figure created by author on Biorander.com.

2.2.4 RNA extraction

The PureLink™ RNA Mini Kit (Thermo Fisher, UK) was used for total RNA extraction for all tissues in accordance with the kit instructions. All samples were lysed with freshly made lysis buffer containing 1% 2-mercaptoethanol (Sigma-Aldrich, UK), and homogenized by 10 passes through a 21-gauge needle using a syringe. A mixture of chloroform and isoamyl alcohol was incubated with lysate for 2 minutes; the colourless aqueous layer containing RNA was then collected. RNA was then bound to the membrane of a spin cartridge and washed with Wash Buffer I and II, allowing the collection of ultrapure total RNA collection after three sequential elutions. Purified RNA was kept on ice for use within a few hours or stored at −80°C for later use. The Qubit® RNA BR Assay Kit (Molecular Probes, UK) was used to quantify the concentration of RNA, and the results were read by a Qubit® 3.0 Fluorometer (Invitrogen, UK).

2.2.5 Quantitative real-time reverse transcription-polymerase chain reaction (qRT-PCR)

Electrophoresis was performed on a denaturing agarose gel to assess the overall quality of the RNA. For electrophoresis, all wells were loaded with 6 µL 2× RNA Loading Dye, 3 µL of eluted RNA samples, and 2 µL of 62.5 µg/mL ethidium bromide (1:10 dilution). The primers for the genes of interest are presented in **Table 2-1**. cDNA was synthesised from 100 ng of RNA using the SuperScript™ IV One-Step RT-PCR Kit (ThermoFisher Scientific, UK) with a thermal cycler programme **(Table 2-3)** for the reverse transcription reaction**.**

The SuperScript™ IV One-Step RT-PCR Kit (Thermo Fisher Scientific, UK) was used for complementary (c)DNA synthesis using a thermal cycler programme with the following settings: reverse transcription at 50°C for 10 min, denaturation at 98°C for 2 min, followed by 40 amplification cycles at 98°C for 10 s, annealing temperature of primers for 10 s at 64.3°C, followed by 72°C for 30 s/kb, and a final extension process at 72°C for 5 min **(Table 2-2)**.

qRT-PCR reactions **(Table 2-3)** were carried out in 96-well plates with a QuantStudio™ 3 system (Applied Biosystems, Foster City CA, USA). In each reaction, a total volume of 20 µl per well was used, containing 4 µl of diluted cDNA templates, 10 µl of Fast SYBR Green Master Mix (Thermo Fisher Scientific), 1 µl each of 10 µM forward and reverse primers, and 4 µl of DNase/RNase free water. The qRT-PCR cycle programme started with pre-denaturation holding stage at 95°C for 20 s, followed by 40 cycles of amplification containing denaturation at 95°C for 3s, annealing/extension at 60°C for 30s, ending with a melt-curve stage at 95°C for 15s and 60°C for 60s. Samples were run in triplicate along with a non-template control. β-actin, which has been identified and validated as a stable gene for qRT-PCR in bovine testes, was used as a housekeeping gene. Data were analysed using Excel™ (Microsoft, Redmond, WA, USA) and the $2^{-\Delta\Delta Ct}$ method (Livak and Schmittgen, 2001).

Table 2-1. Primer sequences used for qRT-PCR in this study.

Gene	Tm (°C)	Forward primer (5'–3')	Reverse primer (3'–5')
B-ACTIN	66.9	TCGCCCGAGTCCACACAG	ACCTCAACCCGCTCCCAAG
STRA8	63.3	TGTACTCCAGAAACCCCAGTCT	TCCTCTTCTTCTTCCTCCTCAA
PLZF	65.2	CCAGCAGATTCTGGAGTATGCA	GCATACAGCAGGTCATCCAAGTC
GFRA-1	64.3	CCACCAGCATGTCCAATGAC	GAGCATCCCATAGCTGTGCTT
THY1	64.6	TTCATCTCCTTGTGACGGGTT	GCAGAGGTGAGGGAATGGC
UCHL-1	63.8	ACCCCGAGATGCTGAACAAAG	CCCAATGGTCTGCTTCATGAA
SOX2	61.0	TTACCTCTTCTTCCCACTCC	TTCTTGCTGTCCTCCATTTC
OCT-4	61.0	AGAGAAAGCGGACGAGTAT	AGTACAGAGTAGTGAAGTGAGG
NANOG	64.9	TAAGCACAGGGGGCAAAAGT	ATGGCTAAAAGGGGTGGAGG
CREM	63.0	TCCGTTATTCAGTCACCACAAA	GAGGGTCTTCGTGAAAGGATTT
HSP70-2	61.9	TTGGGGACAAGTCAGAGAATG	ATCGTGGTGTTCCTTTTGATG

Table 2-2. Reverse transcription (RT) reaction and quantitative PCR reaction components.

	Component	Volume per reaction
Reverse transcription reaction	2× Platinum™ SuperFi™ RT-PCR Master Mix	25 µL
	Template RNA	17.5 µL (100 ng top-up with water)
	Forward Primer [50 µM]	0.5 (×7) µL
	Reverse Primer [50 µM]	0.5 (×7) µL
	SuperScript™ IV RT Mix	0.5 µL
	Total Volume	**50 µL**
qPCR reaction	Fast SYBR Green Master Mix [2×]	10 µL
	RNase-free Water	7 µL
	cDNA Template (Diluted)	1 µL
	Forward Primer [10 µM]	1 µL
	Reverse Primer [10 µM]	1 µL
	Total Volume	**20 µL**

RT-PCR reaction: SuperScript™ IV One-Step RT-PCR Kit was used to reverse transcribe RNA into cDNA, amplifying the key genes with primers in a one-step reaction with a total reaction volume of 50 µL. qPCR reaction: 20 µL total volume reaction mixture was vortexed in a MicroAmp™ Fast Optical 96-well reaction plate and analysed using a QuantStudio™ 3 instrument.

Table 2-3. Reverse transcription reaction and quantitative PCR (qPCR) cycler program.

Program	Step	Temperature	Time	Number of Cycles
Reverse transcription reaction	Reverse transcription	50°C	10 minutes	1
	RT inactivation/initial denaturation	98°C	2 minutes	
	Amplification	98°C	10 seconds	40
		64.3°C	10 seconds	
		72°C	30 seconds/kb	
	Final extension	72°C	5 minutes	1
qPCR reaction	DNA Polymerase UP Activation	95°C	20 seconds	Hold
	Denaturation	95°C	3 seconds	40
	Annealing/Extension	60°C	30 seconds	
	DNA Polymerase UP Activation	95°C	20 seconds	Hold

2.2.6 Tissue digestion

After thawing, tissues from the three groups were dissociated into single cells suspension using a two-step enzyme digestion procedure, adjusted from previously published method (Alves-Lopes et al., 2018). Briefly, each testis fragment was transferred to 2ml of the first digestion solution and then was mechanically desegregated and cut by using needles and scalpel. The suspension was incubated at 37°C for 30 min with shaking, which was followed by 10 min non-shaking incubation for seminiferous tubules fragments to sediment. Supernatant was collected and centrifuged at 400g for 5 min at 4°C, and the pellet containing cells was resuspended in fresh culture medium. Then 2ml of the second digestion solution was added to the sediment of seminiferous tubule fragments, followed by incubation at 37°C for 30 min with shaking. Next, cell suspension was centrifuged at 300g for 5 min at 4°C, and supernatant was disposed and cells were resuspended in fresh culture medium.

2.2.7 Viability

Equal volumes of cell suspension in culture medium or PBS and 0.05% (*w/v*) trypan blue (Gibco, UK) were mixed and incubated at room temperature for 2 min. Then, the numbers of unstained (viable) and stained (non-viable) testicular cells were counted in one set of 16 squares on a hemacytometer under a light microscope (Microscope Nikon Eclipse Ti, Japan). When counting, cells were only counted when they were set within the square or on the right-hand or bottom boundary line of the square. Four replicate counts were done for one sample.

2.2.8 Apoptosis

A fluorometric terminal deoxynucleotidyl transferase dUTP nick end labeling (TUNEL) assay (DeadEnd; Promega, Fitchburg, WI, USA) was used to detect and quantify apoptotic cells by measuring nuclear DNA fragmentation following the kit instruction. Testicular cells adhered to coverslips/slides were fixed by immersion in 4% PFA in PBS for 25 min, followed by permeabilization with 0.2% Triton X-100 solution in PBS for 5 min. After washing, cells/colonies were covered with 100 µl of equilibration buffer for 10 min. A total volume of 50 µl of rTdT incubation buffer was used to replace the equilibration buffer, followed by incubation at 37°C for 1 h in a humidified chamber in the dark. A 2X volume of SSC solution was added, followed by incubation for 15 min at room temperature. After being washed thoroughly three times with PBS, slides were mounted using mounting medium with 4′,6-diamidino-2-phenylindole (DAPI). Samples were analysed under a fluorescence microscope, and 10 random fields from each slide were imaged. A fluorescence microscope (Nikon, Tokyo, Japan) was employed to acquire images of TUNEL-positive cells. Image data were analysed using ImageJ.

2.2.9 *In vitro* culture and proliferation of cells

Testicular cells were cultured in 24-well plates at a density of 5×10^4 cells/well at 37°C in an atmosphere of 5% CO_2. The culture medium for each well contained 1 ml of modified Eagle's alpha medium (MEM-a) supplemented with 10% knockout serum replacement (KSR), insulin (10 µg/ml), L-glutamine (2.5 mmol/l), 1× MEM non-essential amino acids, and penicillin (50 IU/ml). The media in each well was changed every 2–3 days. Details of optimization of culture

conditions for SSCs will be discussed in **Section 4**. Germ cell colonies were identified using immunofluorescence staining with SSC marker PGP9.5 and stem cell marker OCT-4, which will be detailly described in **Section 4.3.2** and representative staining images will be showed in **Figure 4-11**.

2.2.10 Data analyses and statistical methods

The Shapiro–Wilk test was used to test the normality of quantitative data. Data with a normal distribution are presented as a mean ± standard deviation (SD), whereas data with a non-normal distribution are presented as a median (25% percentile, 75% percentile). Significance was determined using the Student's *t*-test or by one-way analysis of variance (ANOVA). $P<0.05$ was considered significant. Statistical analyses were undertaken using Prism 9 (GraphPad, San Diego, CA, USA).

2.3 Results

Bovine abattoir testicular tissues were collected from slaughterhouse, which would be otherwise discarded. For the ethical aspect, Home Office licensing is not required in this case.

2.3.1 Effects of the three cryopreservation methods on histological changes in bovine neonatal ITTs after thawing

The structure of bovine seminiferous tubules in H&E-stained sections was evaluated under a light microscope. A total of 672, 743, and 603 seminiferous tubules were examined in the USF, CSF, and vitrified groups, respectively. No fresh-fixed control group was included in this study mainly due to the COVID-19 pandemic lockdown. Two-week-old bovine testicular tissues contained interstitial tissue and seminiferous cords without lumina. Seminiferous cords consisted of gonocytes located in the centre, which were surrounded by Sertoli cells. The integrity of the seminiferous tubules was preserved after freeze/thawing in all groups, with continuous adhesion to Sertoli cells and clear identification between Sertoli cells and GCs (**Figure 2-3B**). No necrosis was observed in any of the tissue sections. All seminiferous tubules were categorized into grades 1, 2, and 3 according to adherence between the tubules and the basement membrane, which was described in details in **Section 2.2.3**. The percentage of grade 1 cords in vitrified tissues was significantly lower than in the CSF or USF tissues ($P<0.05$), while the proportion of grade 3 cords was significantly higher in vitrified than USF and CSF-treated tissues ($P<0.05$ **Figure 2-3C**). The CSF group had the highest proportion of grade 2 cords.

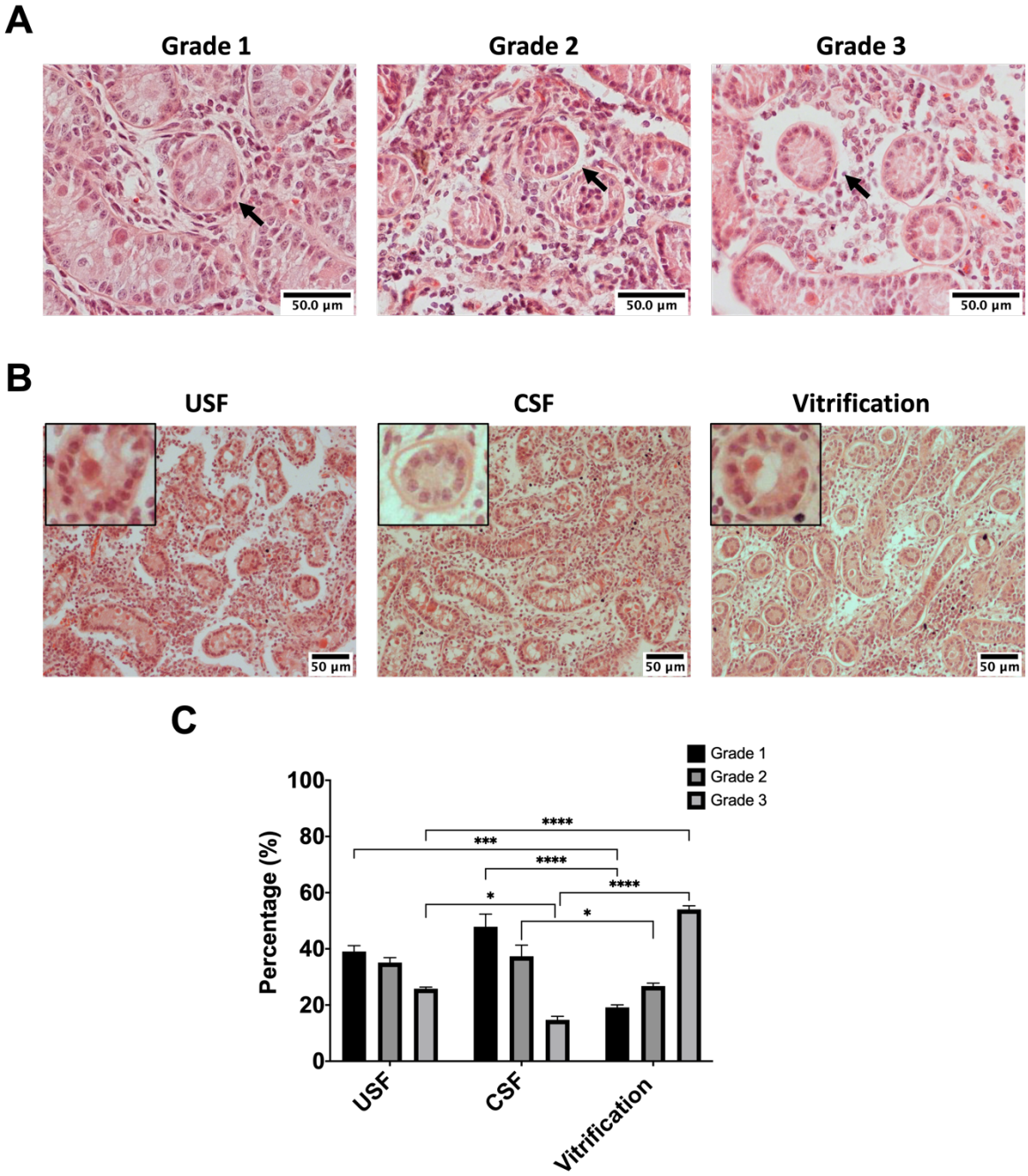

Figure 2-3. Tissue integrity and histology after vitrification, controlled slow freezing (CSF) and uncontrolled slow freezing (USF). A) Cross-sectional images of testicular tissue graded 1, 2, or 3 according to adhesion to the basement membrane. Grade 1 – 'Good': seminiferous cords with <30% detachment of cellular adhesion to the basement membrane. Grade 2 – 'Satisfactory': partial detachment (30–70%) detachment from the basement membrane. Grade 3 – 'Detached': >70% detachment from the basement membrane and disrupted cell-to-cell adhesion. B) Representative haematoxylin and eosin (H&E) images for tissue frozen using the three different cryopreservation methods. The inset in each image displays seminiferous cords at a higher magnification. C) Percentage of seminiferous cords classified as grade 1, 2, or 3 in all seminiferous cords that counted. Data are the mean ± standard deviation (SD; n = 3). G = gonocyte; SCs = Sertoli cells; M = peritubular myoid cell. Scale bar = 50 µm. *P<0.05, ** P<0.01, ***P<0.001, ****P<0.0001.

2.3.2 Effects of the three cryopreservation methods on gonocytes, Sertoli cells and cell proliferation

A total of 495, 520, and 511 seminiferous tubules with positive staining for the germ-cell marker protein gene product 9.5 (PGP9.5; also known as UCHL-1) were analysed in the USF, CSF, and vitrified groups, respectively. PGP9.5-positive cells had a low cytoplasm-to-nuclear ratio. In 2-week-old bovine testes, PGP9.5-positive cells were located in the centre of the seminiferous tubules and were in contact with a single layer of surrounding cells (**Figure 2-4A**). Some PGP9.5-positive cells were located between basement cells or located at the basement membrane. The proportion of seminiferous cords that contained PGP9.5-positive cells per tissue section was 56.44 ± 3.89%, 56.24 ± 6.26%, and 57.10 ± 3.87% in the USF, CSF, and vitrified groups, respectively (**Figure 2-4B**). In gonocyte-containing seminiferous cords, the number of gonocytes per 10^4 μm^2 was 7.75 ± 1.75 in the USF group, 7.89± 1.83 in the CSF group, and 7.92 ± 1.23 in the vitrified group (**Figure 2-4C**): these differences were not significant.

A total of 348, 401, and 394 seminiferous tubules were stained with vimentin (an SC marker) and analysed in the USF, CSF, and vitrified groups, respectively. Vimentin-positive cells were found throughout most of the single cell layer at the basement membrane of seminiferous tubules and in some interstitial cells (**Figure 2-4D**). The proportion of vimentin-positive cells within the seminiferous tubules was 90.61 ± 4.12% in the USF group, 91.11 ± 3.95% in the CSF group, and 89.87 ± 4.19% in the vitrified group (**Figure 2-4E**).

A total of 294, 305, and 311 seminiferous tubules stained with a marker of cell proliferation, Ki67, were analysed in each group. Ki67-positive cells were observed mainly in the nuclei of proliferating Sertoli cells located at the basement membrane of seminiferous tubules and in

some interstitial cells (**Figure 2-4F**). Only some gonocytes were Ki67-positive. The proportion of seminiferous tubules that contained Ki67-positive cells did not differ significantly when compared between the groups (**Figure 2-4G**). The proportion of Ki67-positive cells within the seminiferous tubules was 87.05 ± 3.30 % in USF, 86.9 ± 2.40 % in CSF, and 88.12 ± 2.61 % in the vitrified group.

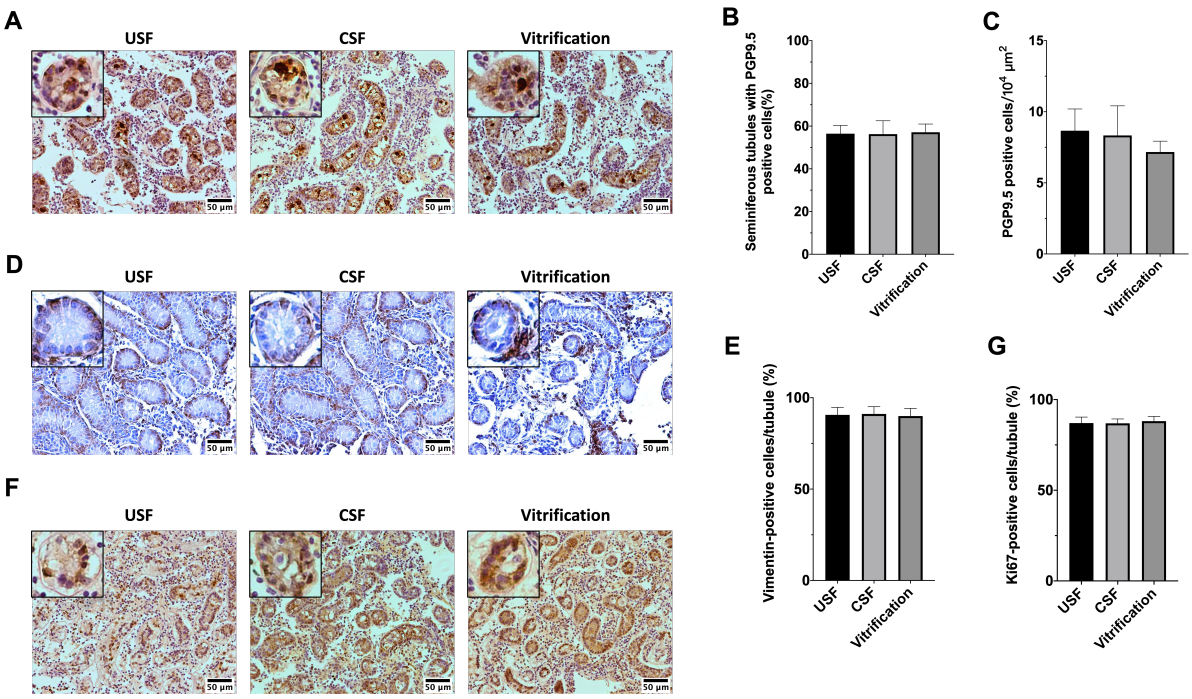

Figure 2-4. Immunohistochemistry of neonatal testicular tissues after cryopreservation. A) Representative image of bovine neonatal tissue stained immunohistochemically with the germ-cell marker PGP9.5. B) The proportion of tubules containing PGP9.5-positive cells. C) Average number of PGP9.5-positive cells per 10^4 µm^2 seminiferous tubules. D) Representative image of bovine neonatal tissue stained immunohistochemically with the Sertoli-cell marker vimentin. E) Proportion of vimentin-positive cells per seminiferous tubule. F) Representative image of bovine neonatal tissue stained immunohistochemically with Ki67, a marker of cell proliferation. G) Proportion of seminiferous tubules containing Ki67-positive cells. H) Proportion of Ki67-positive cells per seminiferous tubule. The inset in each image displays seminiferous cords at a higher magnification. G = gonocyte; SCs = Sertoli cells; M = peritubular myoid cell. Scale bar = 50 µm. Error bars represent the standard deviation (SD) among biological replicates (n = 3). *P<0.05, ** P<0.01, ***P<0.001, ****P<0.0001.

2.3.3 Effects of the three cryopreservation methods on changes in the expression of selected genes in bovine ITT

According to qRT-PCR, the expression of gonocyte/SSC marker genes (*GFRα-1*, *PLZF*, *UCHL-1,* and *THY1*), stem-cell markers (*OCT4, NANOG,* and *SOX2*), spermatogenesis-related markers (*STRA8* and *CREM*), and the apoptosis-related gene *HSP70-2*, were used to evaluate the effect of the three cryopreservation methods on ITT quality. No statistically significant differences were detected in the expression levels of any of these genes when compared between the three cryopreservation methods (all $P>0.05$) (**Figure 2-5**). A high variance was noticed in vitrification group, which was mainly due to one single outlier value.

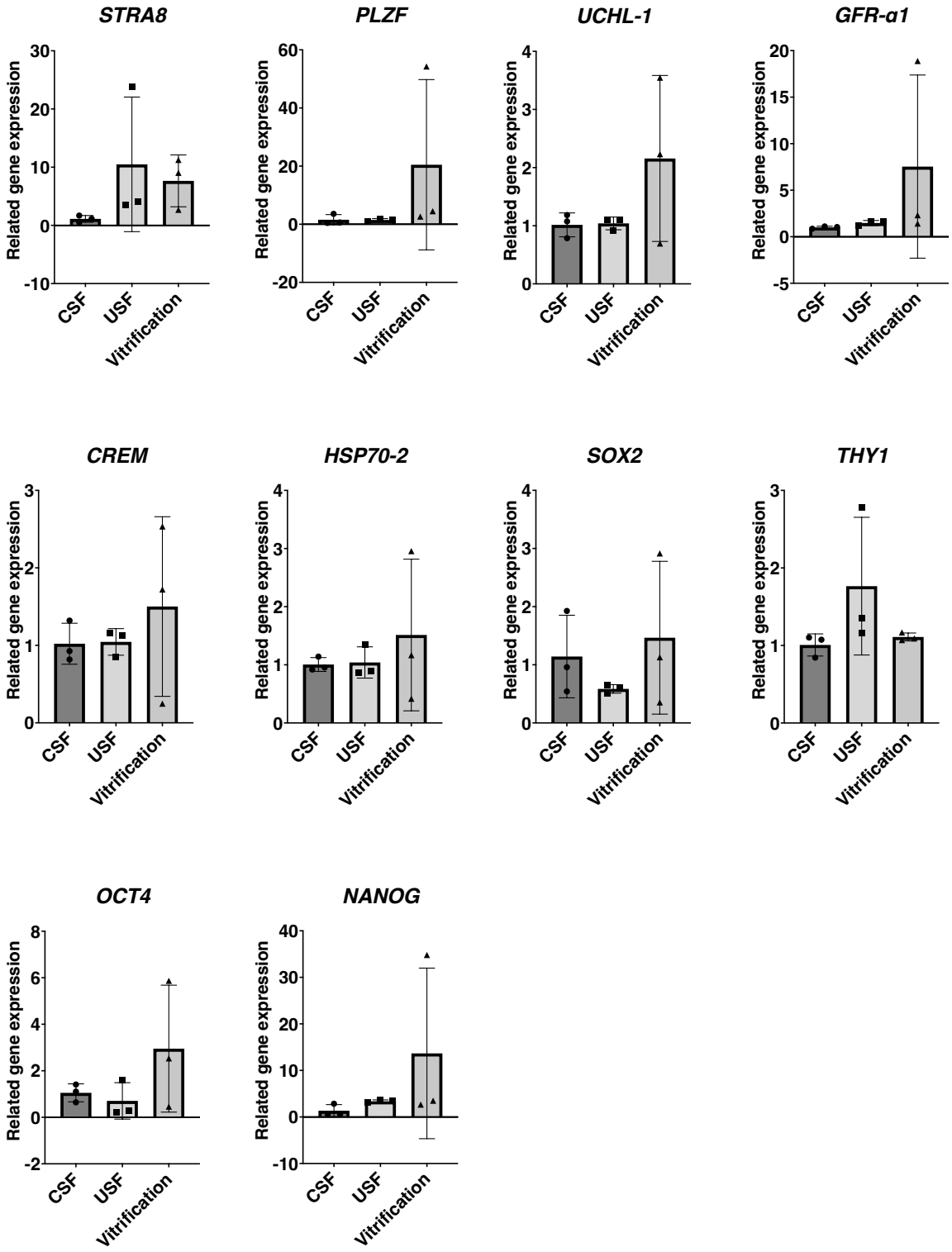

Figure 2-5. Relative gene expression in immature testicular tissues (ITTs) cryopreserved using three methods. The effects of the three cryopreservation methods (controlled slow freezing (CSF), uncontrolled slow freezing (USF), and vitrification were evaluated by comparing the expression of related genes (*STRA8, PLZF, UCHL-1, GFRα-1, CREM, HSP70-2, SOX2, THY1, OCT4, and NANOG*) in frozen/thawed bovine ITTs. No significant differences in expression between genes were observed. Error bars represent the standard deviation (SD) among biological replicates (n = 3). *P<0.05, ** P< 0.01, ***P<0.001, ****P<0.0001.

2.3.4 Effects of the three cryopreservation methods on the proportion of membrane-intact live cells and cellular apoptosis

The viability of isolated testicular cells was assessed immediately after tissue digestion and cell dissociation. The proportion of viable cells was 89.0 ± 2.0% in fresh tissue (**Figure 2-6A**), which was significantly higher than in the USF group (64.0 ± 3.6%), CSF group (71.8 ± 2.1%), and vitrified groups (70.0 ± 2.0%). There was no significant difference in viability when compared between the three cryopreserved groups.

A TUNEL assay was used to evaluate the extent of apoptosis in testicular cells. The percentage of testicular cells that had undergone apoptosis in the CSF and USF groups was significantly higher than in the fresh tissue group ($P<0.05$) (**Figure 2-6B**), but no difference was found between the vitrified and fresh tissue groups ($P>0.05$).

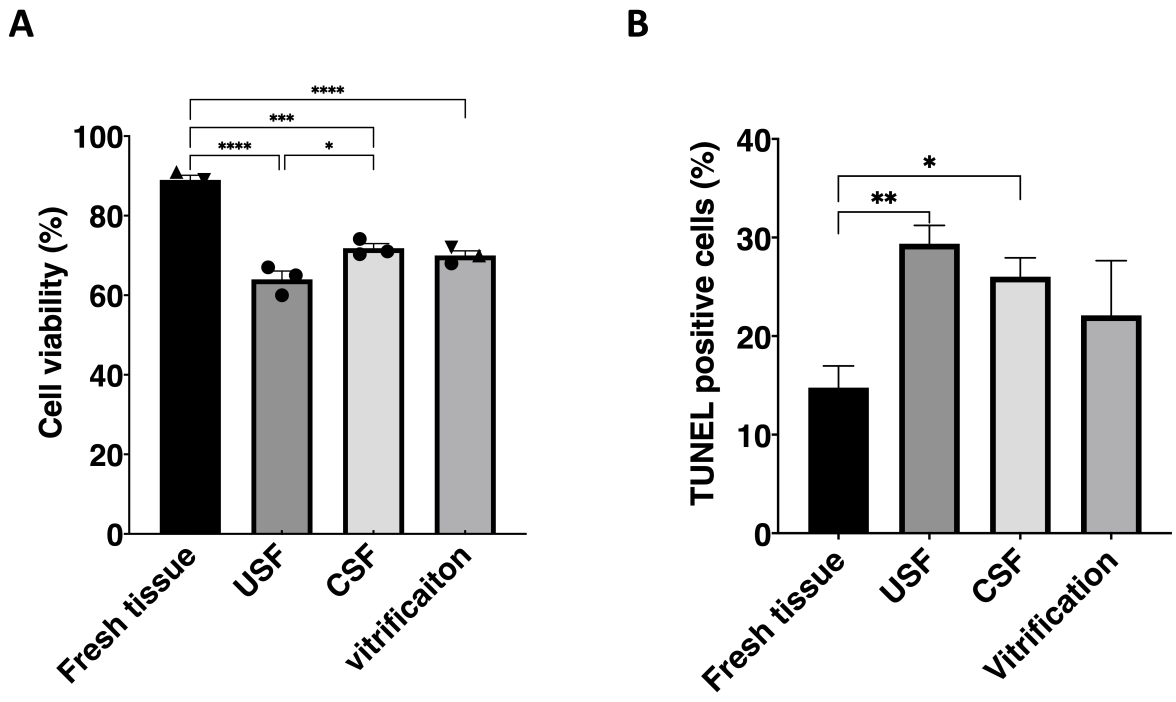

Figure 2-6. Total cell viability and apoptosis in testicular cells from neonatal bovine immature testicular tissue (ITT) samples immediately after collection (fresh) and after cryopreservation by vitrification or controlled/uncontrolled slow freezing (CSF/USF). A) Viability of cells was evaluated before and after cryopreservation using trypan blue staining. B) Percentage of TUNEL-positive cells in each of the four groups. Values are the mean ± standard deviation (SD) of three replicates from three donors. $P<0.05$ was considered significant. Three biological replicates were carried out (n=3). *$P<0.05$, ** $P< 0.01$, ***$P<0.001$, ****$P<0.0001$.

2.3.5 Short term in vitro culture of bovine neonatal testicular cells from frozen/thawed ITTs

Dissociated testicular cells were cultured *in vitro*, and cell activity was evaluated. The formation of gonocyte colonies was observed 7 days after *in vitro* culture, and no differences in the size and numbers of GC colonies were observed. To quantify the effect of the three cryopreservation methods on the formation of GC colonies, colony numbers were counted, and the diameter of colonies was measured on day 7. The number of GC colonies was $5.58 \pm 1.02/cm^2$ in the fresh tissue group, $4.95 \pm 1.18/cm^2$ in the vitrified group, $6.91 \pm 1.50/cm^2$ in the CSF group, and $5.4 \pm 2.2/cm^2$ in the USF group 7 days after *in vitro* culture (**Figure 2-7B**). The morphology and proliferation patterns of GC colonies were similar in cells taken from fresh ITTs and frozen/thawed ITTs. The mode of cryopreservation did not significantly affect colony formation in the enriched GC cultures. The colony diameter was 126.2 ± 35.15 µm in the fresh-tissue group, 115.8 ± 26.22 µm in the CSF group, 124.3 ± 28.75 µm in the USF group, and 128.2±28.91 in the vitrified group. A growth curve was drawn for selected cells from ITTs cryopreserved using the three methods: percentage proliferation was found to be similar among the groups and the difference between groups was not significant (**Figure 2-7D**).

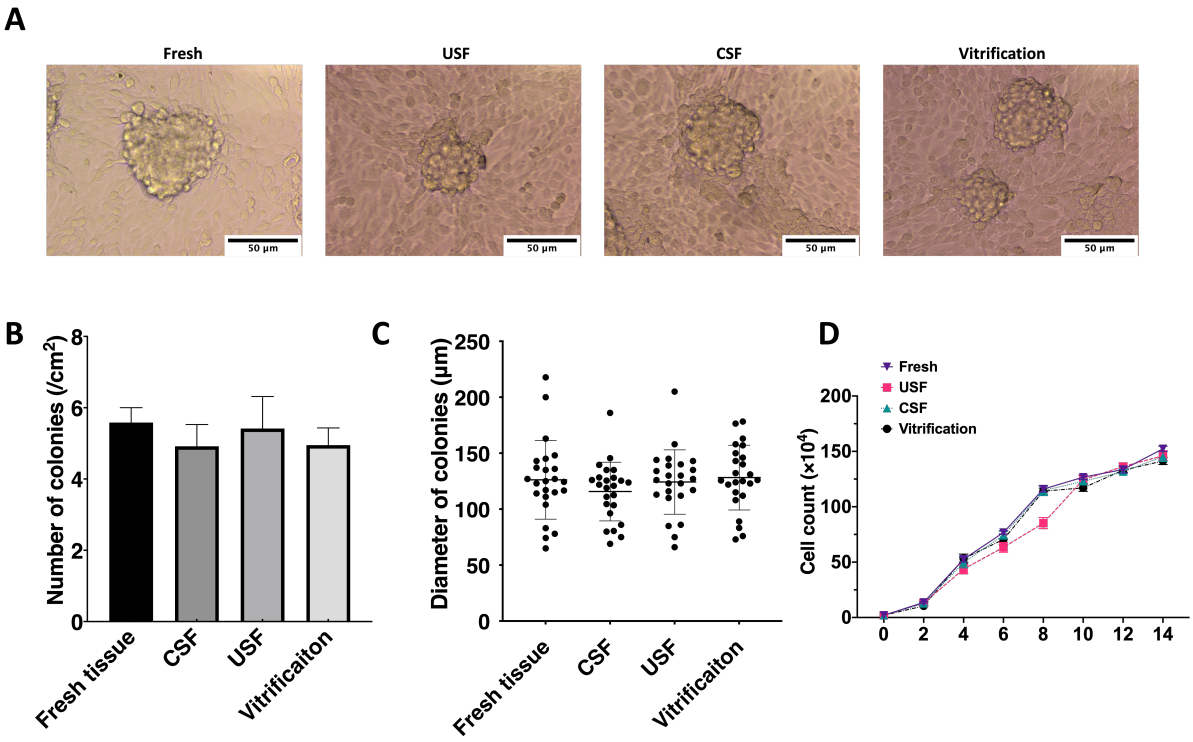

Figure 2-7. *In vitro* culture of dissociated testicular cells from tissues cryopreserved using uncontrolled/controlled slow freezing (CSF/USF), and vitrification. Representative bright field images of germ cell colonies at day 7 of *in vitro* culture; scale bar = 50 µm. B) Number and C) diameter of germ cell colonies; ●▲▽represent different biology replicates. D) Growth curve of *in vitro* cultured testicular cells from tissues cryopreserved using different methods. Values are the mean ± standard deviation (SD) of three replicates from three donors. Three biological replicates were carried out (n=3). *P<0.05, **P<0.01, ***P<0.001, ****P<0.0001

2.4 Discussion

The cryopreservation of ITTs may be used to preserve fertility in male patients for whom sperm cryopreservation is not an option. Cryopreserved ITTs can be used for grafting or IVS to generate mature sperm at a future date.

Testes have a complex architecture and cellular interactions and provide SSCs with a unique microenvironment for self-renewal and differentiation. Both the size and structure of immature testes develop with age, and the different cell types and tissues present at different stages may require different freezing methods. During the early embryonic/foetal period in mammals, male germline stem cells begin as PGCs, which develop into gonocytes to represent a transitional population between PGCs and SSCs. In the current study, we used the bovine model to study neonatal testicular tissues because the structure of the seminiferous cords and early GC development are similar to that in humans. Testicular development in the bovine model is relatively slow from birth to 20 weeks (Wrobel et al., 1986), thus providing a longer time period for investigating the early development of the testes. In the testes of both humans and the bovine model, during the first 3 months after birth, gonocytes are the dominant GCs in seminiferous cords, and will gradually start to change into SSCs. The first SSCs develop at around 3–4 months after birth in both humans and the bovine model, and mainly consist of seminiferous cords without a central lumen (Ibtisham et al., 2020). In a rodent study, slow-frozen and vitrified testicular tissues in neonatal mice produced sperm after *in vitro* culturing, and the use of these sperm resulted in healthy offspring (Yokonishi et al., 2014a). However, few studies have explored cryopreservation of neonatal testicular tissue using gonocytes in domestic animals or humans (Pukazhenthi et al., 2015).

CSF, USF, and vitrification are the most common methods applied for the cryopreservation of testicular tissues. Slow freezing has been used to preserve ITTs with SSCs in tissue biobanks in both the USA and UK (Lakhoo et al., 2019b, Valli-Pulaski et al., 2019). Glycerol, ethylene glycol, and DMSO are used as cryoprotective agents for testicular cryopreservation. Calf testicular tissue frozen with 10% DMSO has been found to be more viable than other concentrations of DMSO or other cryoprotectants (Zhang et al., 2017). Thus, in our study, 10% DMSO was used as the cryoprotectant for slow freezing. The use of an appropriate cryoprotective agent and controlled speed of freezing have been suggested to diminish cell damage and thus avoid tissue injury; CSF enables modification of the cooling rate and thus optimizes cell dehydration and reduces the risk of ice formation in cells.

However, during CSF and USF, ice formation within cells is not entirely avoidable, which could cause germ cell damage. Vitrification uses a small volume of solution and ultrarapid liquid solidification, thus avoiding ice formation in cells (Yavin and Arav, 2007). Therefore, vitrification has been proposed as an alternative method for the cryopreservation of testicular tissues. The production of live offspring from vitrified testicular tissues has been achieved in Japanese quail (Liu et al., 2013), piglets (Kaneko et al., 2013), and neonatal mice (Yokonishi et al., 2014a), thereby indicating its efficacy and safety as a cryopreservation method for ITTs. The maintenance of proliferating SSCs from vitrified non-human primate ITTs has been demonstrated in xenografted mice (Poels et al., 2012). In addition, vitrified human ITTs (in boys aged 6 and 12 years) have similar spermatogonial and histologic tubular structures, thus enabling their survival and proliferation from frozen and fresh samples (Curaba et al., 2011a). Vitrification is simpler and less expensive than other methods, and elicits less damage to cells, thus producing similar results as slow freezing in the cryopreservation of adult and late-prepubertal human testicular tissues (Curaba et al., 2011a, Curaba et al., 2011b, Baert et al.,

2013). Moreover, portable vitrification devices are available, which make immediate cryopreservation possible for patients in remote areas. This may help to avoid damage to tissue caused by transportation, or the inconvenience and potential treatment delays associated with long-distance travel.

The morphology and structure of seminiferous tubules are commonly assessed as indicators of cryopreservation success. In our study, the structure and health of cells in bovine ITTs were compared between the three cryopreservation techniques using histology. Intact tubule structures with clear boundaries were well preserved in all cryopreserved tissues, regardless of the method used. The connections between gonocytes, located in the centre of seminiferous cords, and Sertoli cells at the basement membrane were well protected among all three groups. In addition, no large gaps were observed between gonocytes and Sertoli cells. These results indicate that slow freezing and vitrification can maintain the structure of seminiferous tubules. An increase in the gaps between seminiferous cords and interstitial tissue was found in vitrified tissues, thus suggesting that neonatal seminiferous cords are more likely to shrink if cryopreserved using this method. In a study by Curaba and colleagues, the main damage to the structure of mouse ITTs resulting from cryopreservation was the formation of small gaps, and an increase in the number of pyknotic cells in the centre of seminiferous tubules; however, the authors did not specifically examine the detachment of the tubular basement membrane (Curaba et al., 2011a). It is unclear that if the freezing process directly causes separation from the basement membrane, or if it alters tissue properties so they are more susceptible to fixation artefacts. It is also possible that the way tissues were fixed in the current study (formalin fixation) induced the shrinkage of the seminiferous tubules in testicular tissues (McLachlan et al., 2006). In future study, bouin's fluid or modified Davidson's fluid could be used to reduce

the shrinkage of seminiferous tubules in testicular tissues and increase the morphology in immunohistochemistry.

The preservation of GCs is crucial for successfully preserving ITTs for reproductive purposes. In this study, we evaluated gonocytes in seminiferous tubules using the germ-cell marker PGP9.5. Gonocyte degradation was not detected after cryopreservation using CSF, USF, or vitrification. The latter was found to exert similar effects on the preservation of GCs in seminiferous tubules compared with the traditional slow-freezing methods. Sertoli cells were connected directly to GCs in the seminiferous tubules and occupied most of the space in the seminiferous tubules in neonatal testes, thus providing gonocytes with support and nutrition. We also showed that the structure and GC related gene expression in the Sertoli cells was well-preserved in thawed tissue after CSF, USF, or vitrification. Cell proliferation was evaluated using immunohistochemical staining for Ki67; some Sertoli cells were found to be Ki67-positive, indicating active proliferation. Some gonocytes expressed Ki67, and some were negative for this marker, indicating that only some gonocytes were actively proliferating. This is similar to previous findings in rats (Zogbi et al., 2012). Together, these results suggest that vitrification, USF, and CSF have similar effects on the preservation of proliferating cells within seminiferous tubules.

We investigated the expression of gonocyte/SSC markers (*GFRA-1, PLZF, UCHL-1,* and *THY1*) stem-cell markers (*OCT4, NANOG,* and *SOX2*), spermatogenesis-related markers (*STRA8, C-KIT,* and *CREM*), and the apoptosis-related gene *HSP70-2* following cryopreservation. Our results indicated that CSF, USF, and vitrification had comparable protective effects on the propagation, self-renewal, pluripotency, differentiation, and stress in gonocytes/SSCs in neonatal bovine ITTs.

Testicular cell activity was evaluated using an *in vitro* culture assay. We investigated cell viability, apoptosis, proliferation, and development. Cell viability was decreased, and apoptosis was increased after cryopreservation regardless of the cryopreservation technique used; these findings were consistent with those of Milazzo and colleagues (Milazzo et al., 2008). These data reflected the degradation of testicular tissue throughout cryopreservation. DNA fragmentation in neonatal testicular cells, an indicator of apoptosis, increased slightly after a freeze/vitrified-thaw procedure within a normal range; this was consistent with previous findings in ferret testes (Lima et al., 2020), cat testes, and ovarian tissue (Mouttham and Comizzoli, 2016, Lima et al., 2018). Lima and colleagues found that DNA fragmentation can return to similar levels as in fresh tissue after *in vitro* culture, which may be due to DNA repair mechanisms during culture (Lima et al., 2020). Our data on cell viability and apoptosis, together with our histological findings, demonstrated that ITTs were healthy after cryopreservation. In addition, testicular cells from cryopreserved tissue could form GC colonies and propagate at a similar rate as those from fresh testicular tissue regardless of the cryopreservation technique used, indicating that all the techniques preserved GCs effectively.

Our study found that vitrification has similar preservation effects as slow freezing methods on the viability of testicular tissues. In addition, vitrification could protect GCs from damage by avoiding the formation of ice crystals during cryopreservation. These studies were conducted using the bovine model; therefore, the use of human neonatal tissues is required to fully evaluate the safety and efficiency of vitrification in preserving prepubertal human gonocyte-containing testicular tissues. If this is successful, vitrified tissue grafting/gonocyte transplantation could be used to restore fertility in infertile men. In this case, vitrification could be potentially provided as a faster, cheaper and more accessible method for the cryopreservation of testicular tissue as this technique already available in for the

cryopreservation of embryos and oocytes in IVF clinics. This practice will avoid the risk of potential tissue degradation or damage during long-term transportation, or unnecessary patient transport. This technology could also be beneficial to adult patients who cannot produce sperm and need to store testicular tissues.

In this study, we demonstrated similar effects of vitrification and CSF on the preservation of gonocytes and SC structure in the seminiferous tubules of neonatal tissue. Vitrification had a similar impact on cell viability and apoptosis as CSF and USF. Dissociated bovine testicular cells from vitrified and slow-frozen tissues exhibited similar rates of proliferation. The formation of gonocyte colonies during *in vitro* culture was similar among all three cryopreservation techniques.

These findings suggest that vitrification could be used as an alternative method to traditional slow-freezing cryopreservation techniques for the long-term storage of early-stage gonocyte-containing bovine ITTs. Our protocol should now be investigated for clinical applications in humans.

2.5 Key findings

- The vitrification of neonatal bovine testicular seminiferous tubules preserved gonocyte numbers and the structure of the seminiferous tubules despite a higher prevalence of detachment from the basement membrane.
- Vitrification preserved testicular cell viability and the gene expression of key genes in the GCs
- Vitrified GCs were able to form healthy and viable cell colonies *in vitro*

Chapter 3. The impact of transportation time on immature testicular tissue (ITTs)

3.1 Background

3.1.1 Childhood cancer and preservation

In recent decades, the five-year net survival rate for children diagnosed with cancer has risen dramatically due to significant progress in cancer therapy and research. The five-year survival rate of childhood cancer patients has reached over 80% in high-income countries, such as the United States and the United Kingdom (Phillips et al., 2015, Lam et al., 2019, Ward et al., 2019c). However, both cancer and the necessary treatments may have adverse effects on male reproduction. As the survival rate continues to improve, it is essential to consider the infertility risk caused by cancer or aggressive cancer treatments. Infertility, caused by GC depletion and hypogonadism, is one of the long-term side effects of cancer therapy that is associated with adult survivors of childhood cancer (Tournaye et al., 2014). Exposure to various cytotoxic cancer treatments, such as cyclophosphamide, cisplatin, and doxorubicin, was proven to induce GC loss in an *in vitro* model of the prepubertal testis (Smart et al., 2018). In adult men, semen can be cryopreserved before cancer therapy, and fertility can therefore be successfully preserved *via* ART. In contrast, immature boys have not yet started to make sperm. Consequently, the only option is to store testicular tissue prior to the initiation of therapy.

3.1.2 Tissue banks and transfer processes

Over the past decades, several international centres have established reproductive tissue cryopreservation programmes to preserve fertility for childhood cancer survivors. In 2000, it was reported that two boys had testicular tissue cryopreserved before cancer therapy for malignant illness (Bahadur et al., 2000). In the US, testicular biopsy and cryopreservation has

been provided for patients who were at risk of infertility by a coordinated network of medical centres, including the University of Pittsburgh Medical Centre (Valli-Pulaski et al., 2019). At the University of Oxford, the ORTCP was established in 2008 with the aim of helping children with cancer to preserve their fertility by providing tissue cryopreservation alongside a dynamic research programme (Lakhoo et al., 2019a)**.** The ORTCP has third-party agreements with most principal cancer treatment centres in the UK and Ireland, which give patients the choice to either have their tissue procured at a local centre or in Oxford. However, the distance between a third-party centre and Oxford varies enormously which results in different transportation times. If a patient receives biopsy surgery in a distant hospital, the biopsied tissue may need to be transported to tissue bank centre to undergo the standardized cryopreservation procedure. Appropriate transport conditions and period of transport are essential for maintaining high quality of the biopsied tissue. Within the UK, the tissue transit time varies from half an hour to up to 6 hours. In addition to the transit time needed on the road, sometimes tissues are needed to be held for longer time period due to the availability of freezing machines. In some cases, the overall transportation time (transit time plus holding time, counting from the time of tissue collection to the time when tissues are started to undergo cryopreservation) could be up to 48 hours. Therefore, it is necessary to investigate the effects of tissue transportation time on the health of ITTs. Moreover, owing to the difference in structural morphology between ITTs and adult testes, there is a need to study the effects of transportation period on ITTs in appropriate animal or human models.

The aim of this study was to explore the effects of different transportation times (1 hour, 6 hours, 24 hours, and 48 hours) on bovine ITTs preserved for fertility preservation using standardized clinically relevant processes.

3.2 Methods

3.2.1 Experimental design

ITTs from three calves were divided into four groups; each group was subject to different transportation times prior to the assessment. In the control group, ITTs were processed within 1 hour, whereas in the remaining three groups, the tissues were subjected to processing after a delay of 6 hours (corresponding to a short transportation time), 24 hours, and 48 hours (corresponding to a long transportation time). These time points were selected to replicate the real-world transportation times of human tissue in fertility preservation programs. All tissues were cryopreserved using the testicular cryopreservation procedure of the ORTCP and stored in liquid nitrogen (LN_2). The tissues were then thawed and characterised by viability, apoptosis, histological, and immunohistochemistry analyses, and RT-qPCR. (**Figure 3-1**)

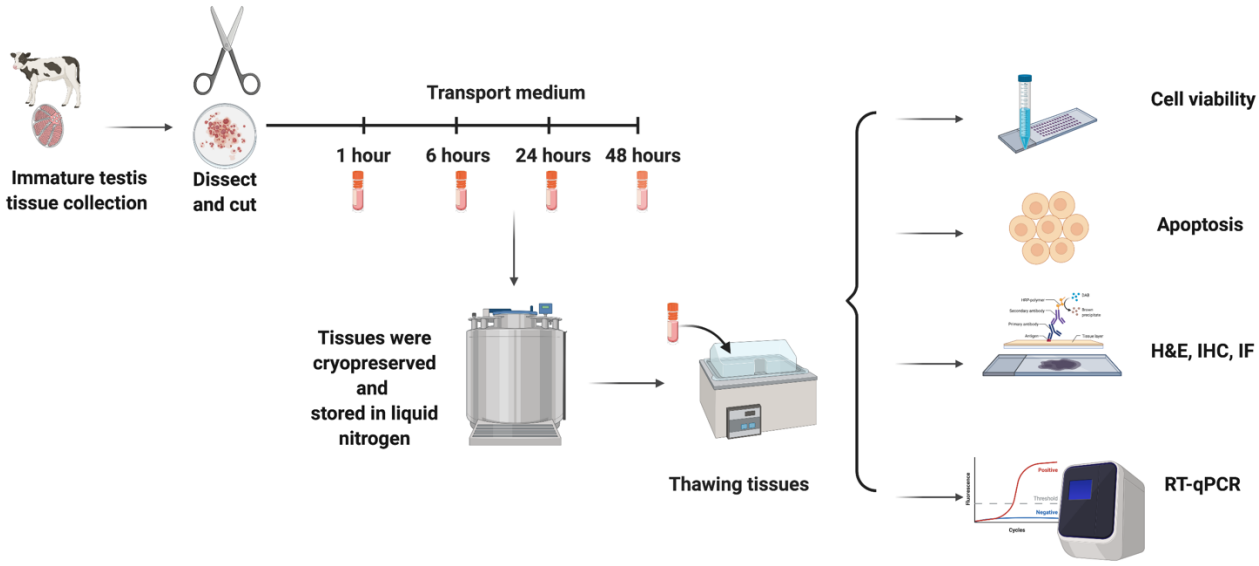

Figure 3-1. Experimental design for transportation time experiment. Bovine immature testicular tissues were collected and transferred to the laboratory, which was followed by dissection into small fragments and storage in transport medium for 1 hour, 6 hours, 24 hours, or 48 hours. Tissue fragments were cryopreserved using the testicular tissue cryopreservation procedure of the Oxford tissue biobank and then stored in liquid nitrogen. After thawing, testicular cell viability, apoptosis, histological and immunohistochemical analyses, and gene expression (RT-qPCR) were assessed for each group. Three biological replicates were carried out (n=3). Created with BioRender.com.

3.2.2 Collection and preparation of testicular tissues

The collection and preparation of neonatal bovine testicular tissues was described in **section 2.2.1.** Testicular tissue fragments were then divided into four groups and subsequently processed at four different time points (1 hour, 6 hours, 24 hours, and 48 hours). After the sections were cut, they were submerged in transfer medium for different time periods at 4°C to mimic the transport conditions used for human tissue, and were then dissected into 2–5 mm^3 fragments before the cryopreservation procedure. Multiple pieces of tissue fragments from

each testis were processed for cryopreservation without delay within 1 hour after tissue collection in the 1-hour group.

3.2.3 Cryopreservation and thawing of bovine testicular tissue fragments

Testicular tissue fragments were cryopreserved using speed-controlled slow freezing method which was described in **Section 2.2.2**.

3.2.4 Histology and immunohistochemistry

Histology and immunohistochemistry analysis were described in **Section 2.2.3**.

3.2.5 Viability

Trypan blue stain was used to assess cell viability, which was described in **Section 2.2.6**.

3.2.6 RNA extraction and quantitative real-time PCR (qRT-PCR)

Details of RNA extraction and qRT-PCR was described in detailed in **Section 2.2.4** and **Section 2.2.5.** The changes in the expression of gonocyte/SSC marker genes *GFRA-1*, *PLZF*, *UCHL-1*, C-kit, and *THY1*, stem cell markers (*OCT4*, *NANOG*, and *SOX2*), spermatogenesis-related markers (*STRA8* and *CREM*) and the apoptosis-related gene *HSP70-2* were used to evaluate the effect of the transportation time.

3.2.7 Statistical analysis

The Shapiro–Wilk test was used to test quantitative data for normality. If the data passed the normality test, ANOVA was used for statistical analysis; otherwise, the Kruskal–Wallis test was performed. A post hoc test and ANOVA were performed to identify differences between groups. All statistical analyses were performed by GraphPad Prism version 9.3.0 for Mac software (GraphPad Software, San Diego, California, USA), with p values of <0.05 considered to indicate statistical significance. Normally distributed data are presented as mean ± SD, whereas non-normally distributed data are presented as median with 25% and 75% percentiles.

3.3 Results

Bovine abattoir testicular tissues were collected from slaughterhouse, which would be otherwise discarded. For the ethical aspect, Home Office licensing is not required in this case.

3.3.1 The effects of transportation time on cell viability and tissue morphology

Tubular morphology was assessed by H&E staining. Histological evaluation showed that neonatal bovine testes contained undeveloped seminiferous tubules with no lumen. Representative structures of the seminiferous cords and interstitium are shown in **Figure 3-2 A.** There were two main cell types in the seminiferous cords: GCs and immature Sertoli cells; these were distinguished by their morphology. GCs have a higher nuclear/cytoplasmic ratio than immature Sertoli cells, and were characterized by their large size, round shape, pale cytoplasm, and presence of one or two prominent nucleoli in the nucleus. In 2-week-old neonatal bovine immature testes, there were two types of GC, gonocytes and SPG, in the seminiferous cords. Gonocytes, located in the centre of seminiferous cord, comprised the majority of GCs shortly after birth, although a few SPG were found in the seminiferous cords, interacting with the basal lamina. Immature Sertoli cells mostly occupied the seminiferous epithelium, with basophilic nuclei observed. Flat PMCs were found in the interstitium surrounding the seminiferous cords. Leydig cells were also found in the interstitium.

The cell viability of the four groups was not statistically significantly different (**Figure 3-2 B**). The viability of testicular cells from freeze/thawed testicular tissues was 83.1%±2.1% in the 1-

hour group, 82.8%±4.88% in the 6-hour group, 78.59%±6.15% in the 24-hour group, and 72.4%±3.24% in the 48-hour group.

The results showed that there was a significant overall difference in the distribution of Grade 1, 2, and 3 tubules between the four groups ($p<0.05$; **Figure 3-2 C**). The testicular tissues processed after 48 hours contained 29.53%±3.66% Grade 1 intact tubules; this was significantly lower than in the 1-hour group (65.61%±6.26% Grade 1 tubules; $p<0.05$). A significantly higher proportion of Grade 2 cords with partial detachment from the basement membrane was observed in the 48 hours group (54.04%±3.51% *versus* 27.21%±4.54% in the 1-hour group; $p<0.05$). The percentage of Grade 3 cords was 7.18%±1.94% in the 1-hour group, 14.10%±3.47% in the 6-hour group, 15.87%±1.87% in the 24-hour group, and 16.43%±2.14% in the 48-hour group ($p<0.05$). The shape, size, colour, and integrity of the seminiferous tubules indicated that they remained healthy in the 1-hour, 6-hour, and 24-hour groups (**Figure 3-2 D**). However, the seminiferous tubules in tissues from the 48-hour group were shrunken and partly ruptured.

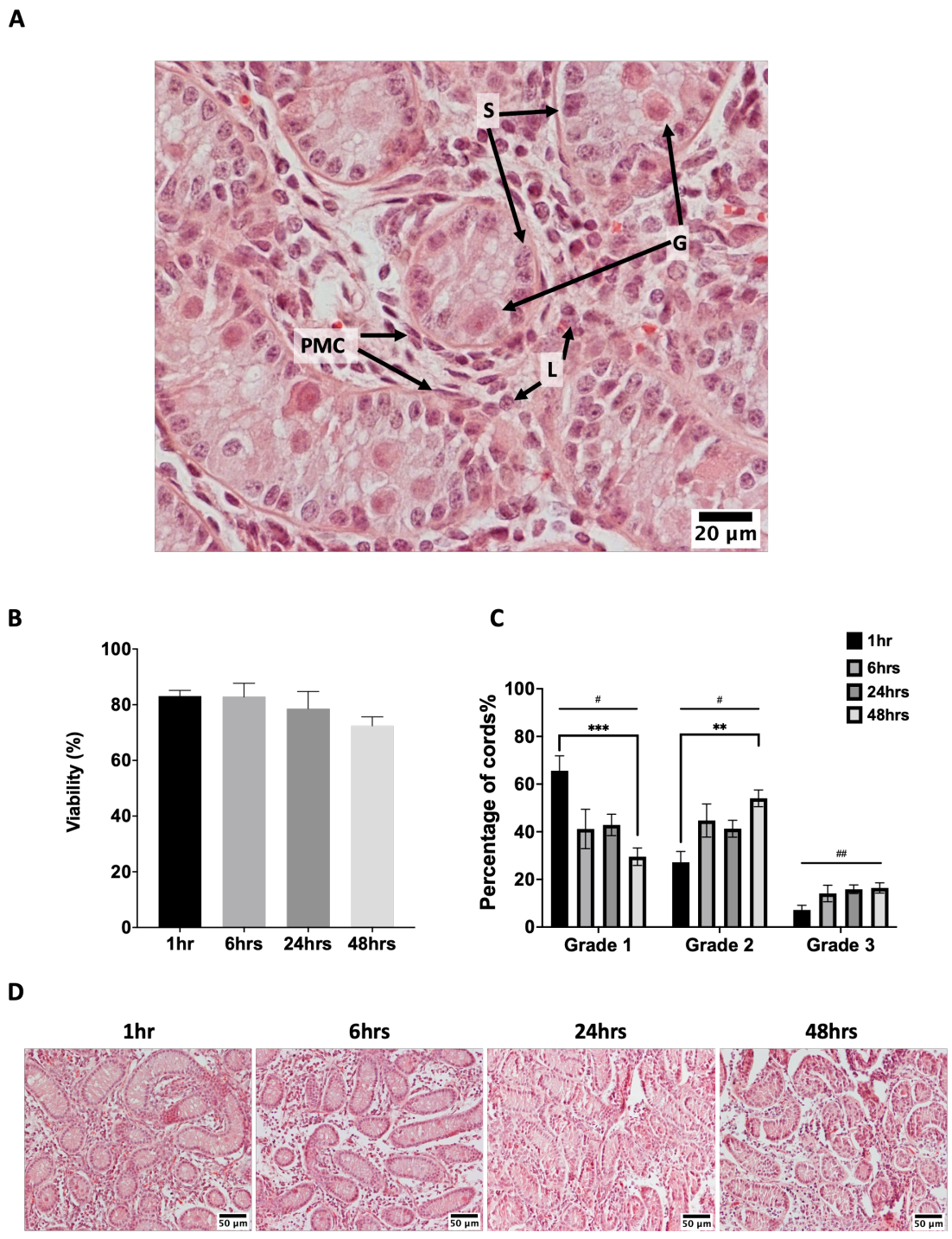

Figure 3-2. Histological analysis and cell viability. A) Representative histology image of bovine neonatal testicular tissues stained by haematoxylin and eosin (H&E). G, germ cells; S, Sertoli cells; L, Leydig cells; PMCs, peritubular myoid cells. B) Cell viability in freeze/thawed neonatal testicular tissues processed after 1 hour, 6 hours, 24 hours, and 48 hours. C) Percentage of seminiferous cords categorized as Grade 1, 2, or 3. Overall significance of differences between four groups: # $p<0.05$; ## $p<0.01$. Significant difference between two groups shown in the hoc test: ** $p<0.01$; *** $p<0.001$. D) Representative images of H&E staining of tissues processed after 1 hour, 6 hours, 24 hours, and 48 hours. Scale bars = 50 µm. Three biological replicates were carried out (n=3).

3.3.2 The effects of transportation time on germ cells

The presence of GCs, including gonocytes and all subtype of SSCs in seminiferous tubules in 2-week-old bovine testes, was detected by PGP9.5 immunohistochemical labelling. To assess the effect of delayed time on GCs, immunohistochemical staining with the GC marker PGP9.5 was applied to tissues with different process time (**Figure 3-3 A**). PGP9.5-positive cells were mainly found in the middle of tubules (gonocytes); only a small proportion have migrated to the basement membrane (SSCs). In the 1 hour and 6-hour groups, PGP9.5-positive cells were round and well connected to/touching PGP9.5-negative cells. In the 48-hour group, PGP9.5 cells were of irregular shape and gaps between PGP9.5-positive cells and the surrounding PGP9.5-negative cells were observed. The percentage of tubules containing PGP9.5-positive cells in the testes tissue sections was significantly different ($p<0.05$) for each group: 53.30%±10.38% in the 1-hour group, 50.17%±6.18% in the 6-hour group, 43.05%±6.96% in the 24-hour group, and 43.19%±6.45% in the 48-hour group (**Figure 3-3 B**). When comparing the two groups in the post hoc test, a significant difference in tubules with PGP9.5-positive cells was found between the 6-hour and 48-hour groups ($p<0.05$). The number of PGP9.5-positive cells per 10^4 μm^2 of seminiferous tubules recorded to have a median of 5.3 and 25%-75% quantiles [5, 10] cells in the 1-hour group, 5.0[4.0, 10.0] in the 6-hour group, 5[3.3, 6.7] in the 24-hour group, and 10[6.7, 12.9] in the 48-hour group (**Figure 3-3 C**). The number of PGP9.5 cells per unit tubular area was significantly higher in the 48-hour group than in the other three groups ($p<0.05$).

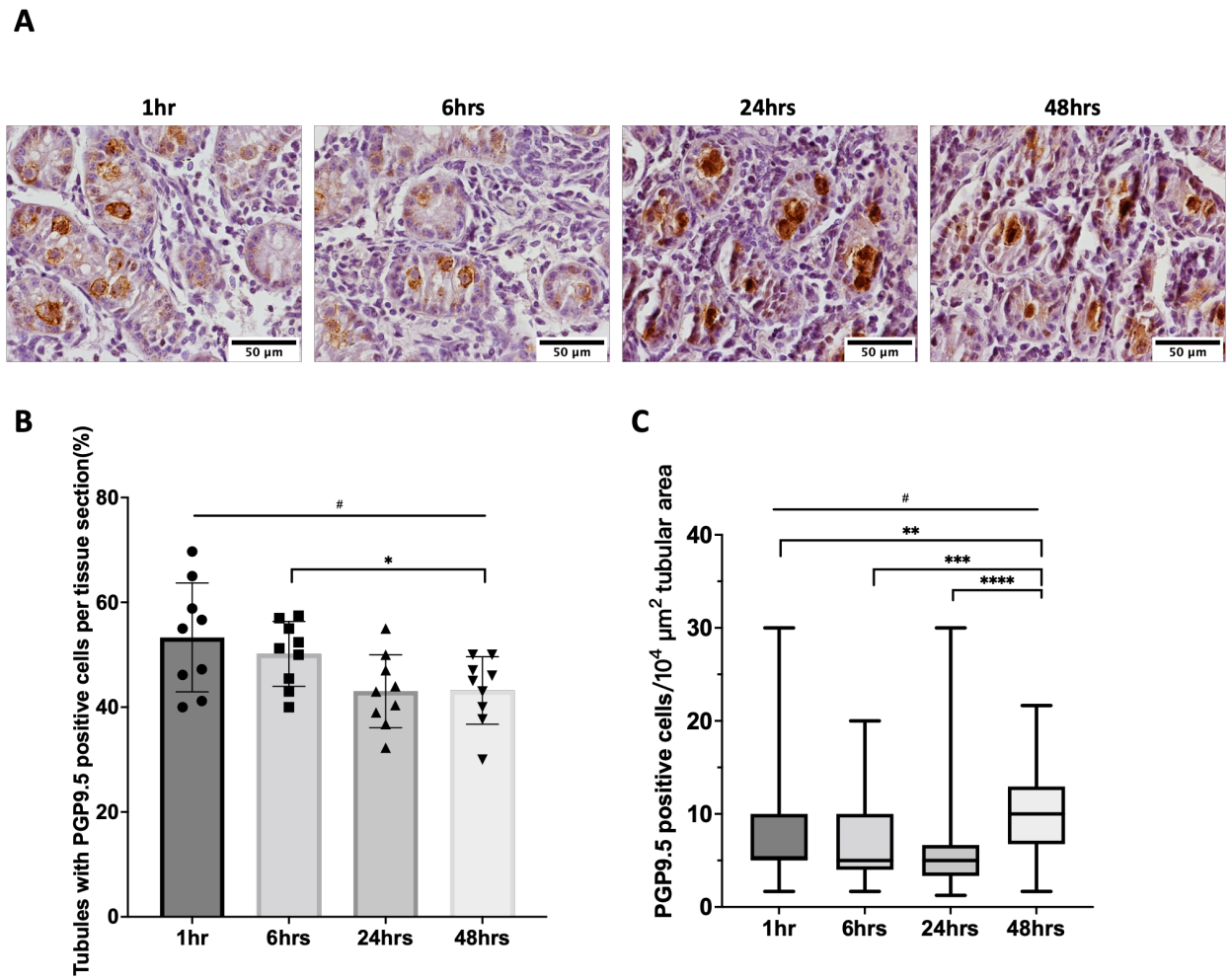

Figure 3-3. Analysis of immunohistochemistry staining of the germ cell marker PGP9.5. A) Representative images of immunohistochemical staining for PGP9.5 shows the gonocytes inside the bovine neonatal seminiferous tubules in samples processed after 1 hour, 6 hours, 24 hours, and 48 hours. Scale bar = 50 µm. B) Percentage of tubules with PGP9.5-positive cells per tissue section. The data were normally distributed, and one-way ANOVA was performed. C) Number of PGP9.5-positive cells per 10^4 μm^2 within seminiferous tubules. The data are presented as median, 25% and 75% quantiles, or min/max. The data were not normally distributed and therefore the Kruskal–Wallis test was performed. For B and C, overall significance between the four groups is denoted by # $p<0.05$. Significant differences between the two groups are shown, as determined by post-hoc test: *$p<0.05$; ** $p<0.01$; *** $p<0.001$; ****$p<0.0001$. Three biological replicates were carried out (n=3).

3.3.3 The effects of transportation time on Sertoli cells

Vimentin-positive areas in the testes included Sertoli cells and some interstitial cells. The perinuclear region of the cytoplasm of Sertoli cells in seminiferous tubules was stained positive for vimentin, with higher intensities observed on the basement side compared with the lumen side (**Figure 3-4 A**). GCs with a higher nuclear/cytoplasmic ratio were not stained with vimentin. The percentage of vimentin-positive cells in seminiferous tubules was evaluated and no difference was found between the four groups (**Figure 3-4 B**).

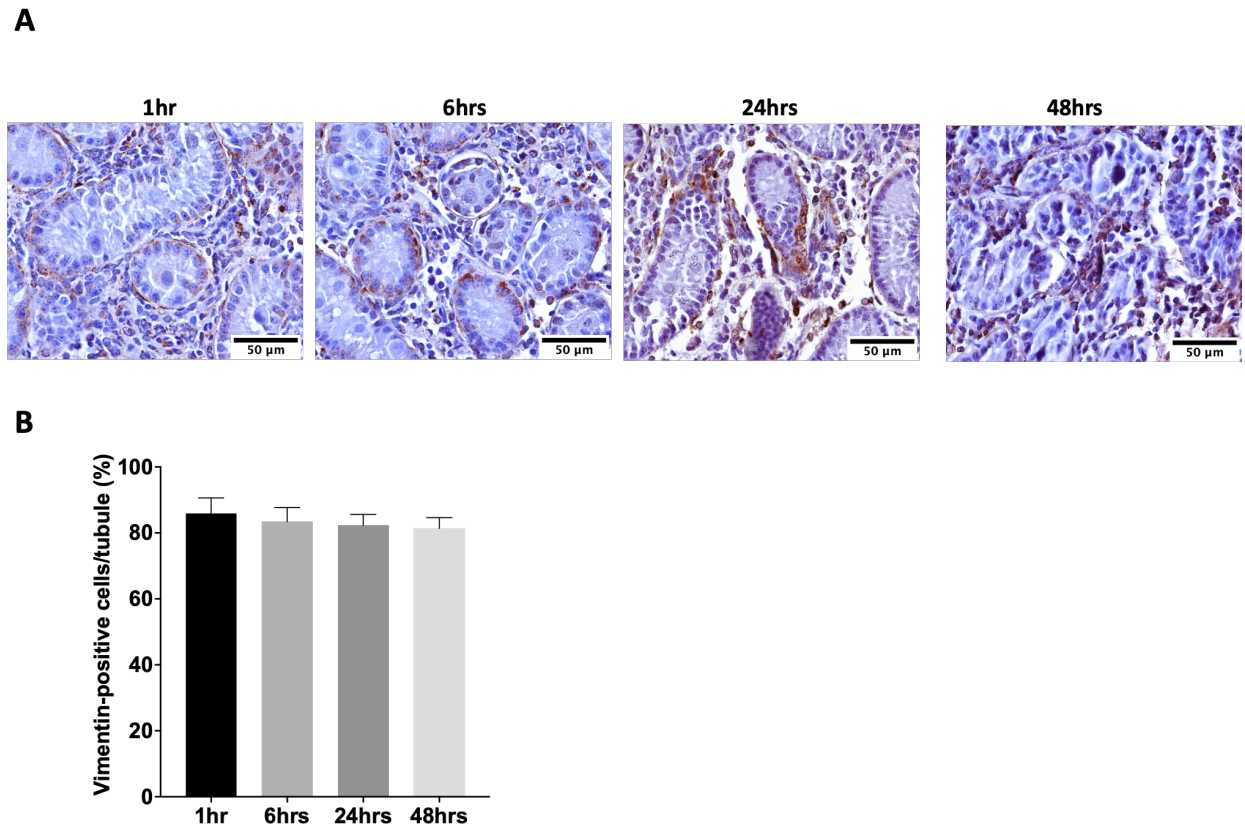

Figure 3-4. Analysis of immunohistochemical staining of the Sertoli cell marker, vimentin. A) Representative images of immunohistochemical staining of vimentin showing Sertoli cells inside bovine neonatal seminiferous tubules in samples processed after 1 hour, 6 hours, 24 hours, and 48 hours. Scale bar = 50 µm. B) Percentage of vimentin-positive cells in tubular cells. Three biological replicates were carried out (n=3).The data are presented as the mean± SD; significance was determined by one-way ANOVA. *p<0.05; ** p<0.01; *** p<0.001; ****p<0.0001.

3.3.4 The effects of transportation time on proliferating cells

Ki67 was used to label proliferating cells in neonatal testicular tissue. Ki67-positive cells were mainly found within seminiferous tubules and some interstitial cells (**Figure 3-5 A**). Most gonocytes located in the centre of seminiferous tubules were ki67-negative. Ki67-positive cells within seminiferous tubules were mainly located at the basement membrane. No difference in the percentage of ki67-positive cells per tubule was found in tissues processed after different delays (**Figure 3-5 B**).

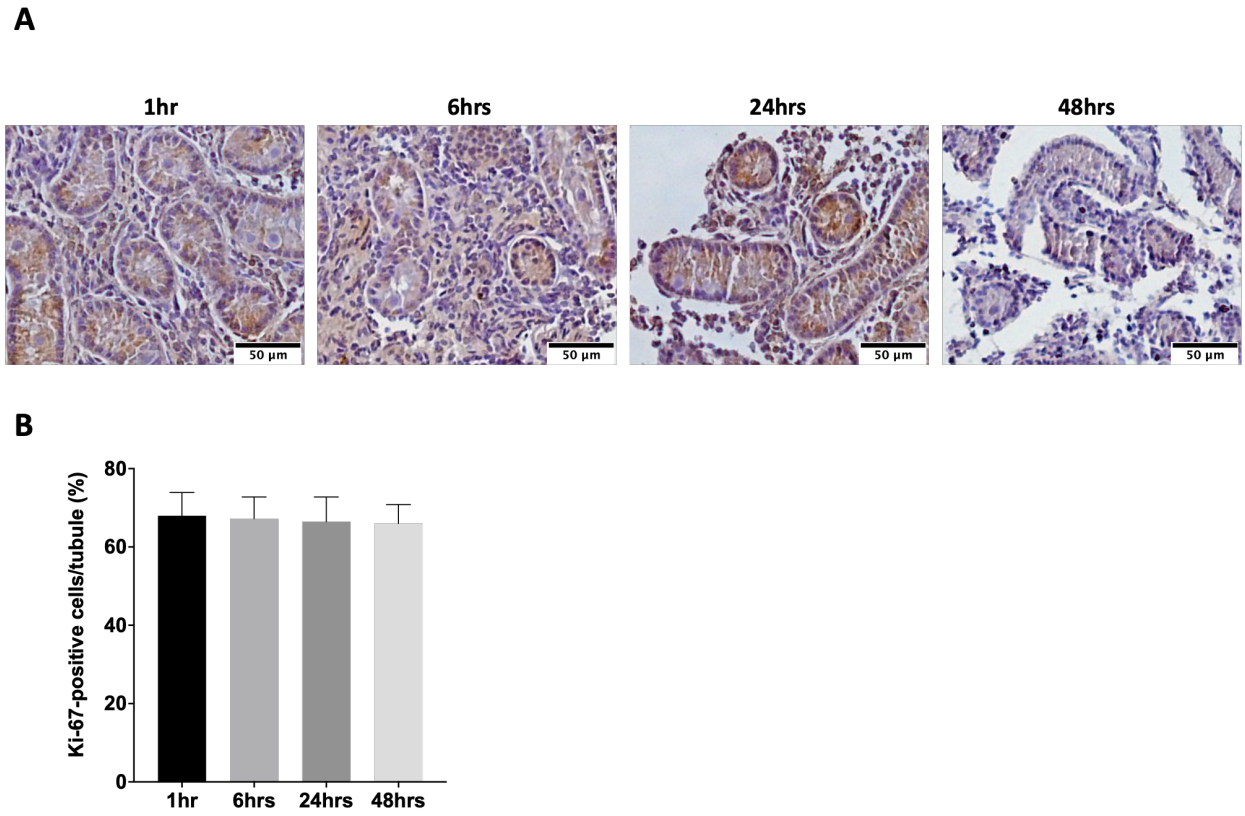

Figure 3-5. Analysis of immunohistochemical staining of the proliferating cell marker Ki67. A) Representative images of immunohistochemical staining of ki67 showing the proliferating cells in testis tissue processed after 1 hour, 6 hours, 24 hours, and 48 hours. Scale bar = 50 µm. B) The quantification of ki67-positive cells in one seminiferous tubule. Three biological replicates were carried out (n=3). The data are presented as the mean ± SD, with one-way ANOVA performed to determine the significance of differences. *p<0.05; ** p<0.01; *** p<0.001; ****p<0.0001.

3.3.5 The effects of transportation time on gene expression: RT-qPCR results

The expression levels of gonocytes/SSC markers (*STRA8*, *PLZF*, *GFRA-1*, *THY1*, *UCHL-1*), a marker of differentiation (*C-KIT*), and apoptosis-related genes (*CREM* and *HSP70-2*) were used to evaluate the effect of different transportation times on the quality of freeze/thawed bovine ITTs by real-time quantitative polymerase chain reaction (RT-qPCR).

The changes in the expression of key genes in bovine ITTs in relation to transportation time are shown in **Figure 3-6**. No statistically significant differences were observed in the expression levels of the selected genes tests, except for *C-KIT*, including GC-related, spermatogenesis-related, and apoptosis-related genes. There was a significant difference in *C-KIT* gene expression between the 1-hour group and the 6-hour and 24-hour groups ($p<0.05$).

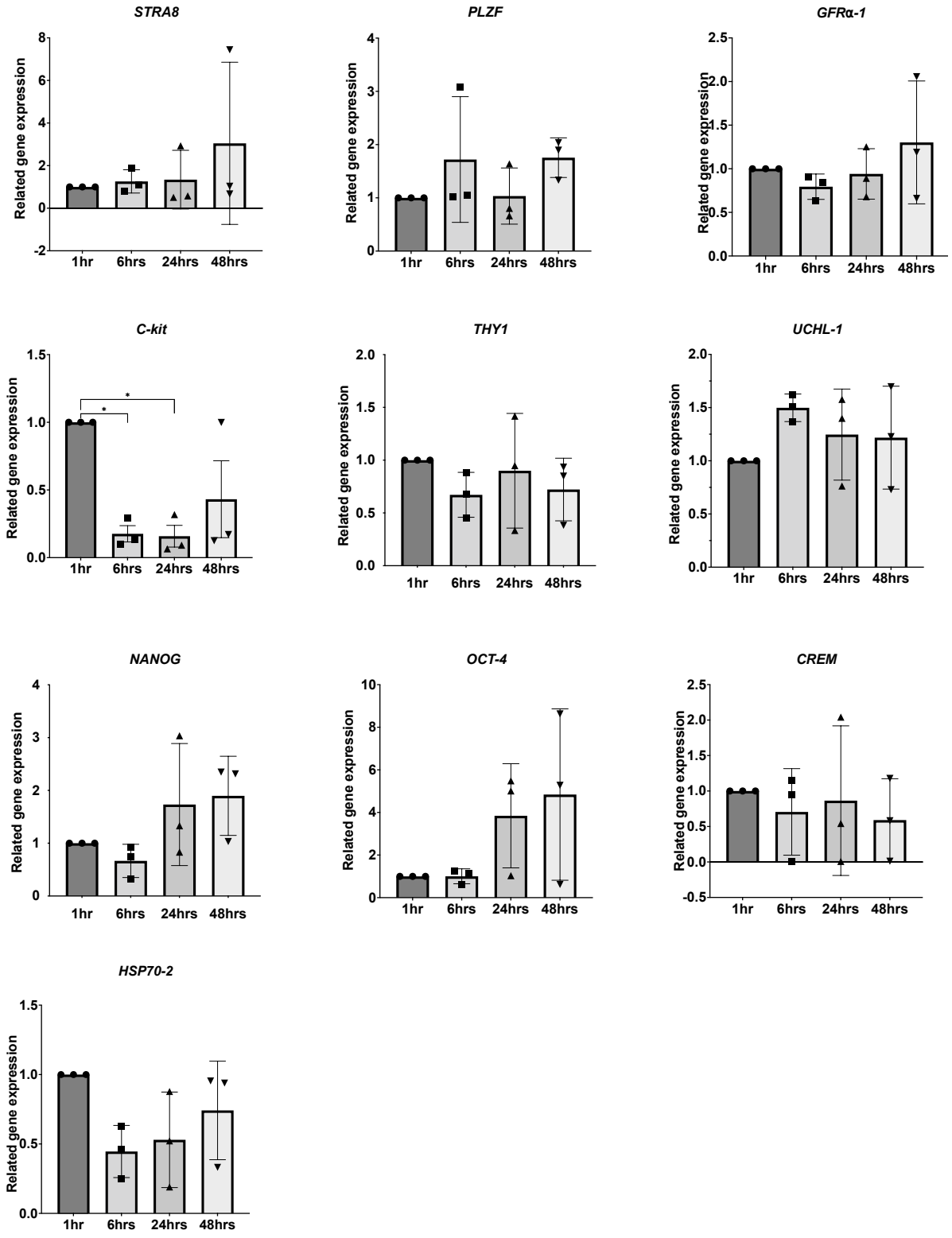

Figure 3-6. Effect of transportation time on the expression of selected genes. The effects of various delay in processing on the expression of STRA8, PLZF, C-KIT, GFRA-1, THY1, UCHL-1, NANOG, OCT-4, CREM, and HSP70-2 in freeze/thawed bovine ITTs. Three biological replicates were carried out (n=3). Error bars represent the standard deviation among biological replicates (N=3). * $p<0.05$ in post-hoc test from one-way ANOVA.

3.4 Discussion

Cell viability has been used as an important evaluation parameter and a reliable predictor for the health and potential development of tissues after cryopreservation (Abrishami et al., 2010). The results of the current study revealed that viability remained high after storage at 4°C for 48 hours, with no statistically significant differences compared with tissues processed within 1 hour; this indicated that immature testicular fragments could be transported in certain conditions for up to 48 hours at low temperature before undergoing cryopreservation procedures without a high proportion of cell death. These results are consistent with a previous study on porcine testis tissue, which showed that the viability of total testicular cells and GCs in fresh tissues remained high when stored at 4°C for 48 hours, but was significantly decreased after storage at 72 hours (Zeng et al., 2009). Another study showed that cell viability remained high even after storage for 8 days in storage medium at 4°C (Faes and Goossens, 2017). The viability of ITTs is believed to be affected by the transport or holding medium and tissue preserving. Previous research showed that the viability of testicular cells from 1-week-old piglets varied significantly when preserved in different holding media (Yang et al., 2010). The viability was significantly decreased, to around 50%, after preservation as whole tissue fragments, but was maintained at up to 80% when preserved in cell suspension after being stored at 4°C for 3 days (Yang and Honaramooz, 2010, Yang et al., 2010). The temperature at which tissues were stored before cryopreservation was essential and was reported to affect the viability of cells; for example a study using mouse ITTs showed that viability also remained high after 24 hours at 4°C, but decreased significantly if stored at 22°C–24°C for 24 hours or 34°C for 6 hours (Salian et al., 2021). It is believed that the use of 4°C, a hypothermic temperature, can preserve biological tissue samples for short periods because the low temperature suppresses metabolism and reduces the activity of catabolic enzymes; as such, 4°C

is often recommended for tissue transportation. The metabolic rate is demonstrated to be lowered by 50% for every 10°C decrease in temperature, with 10%–12% metabolism remaining at 4°C (Southard and Belzer, 1995). In conclusion, the viability of testicular tissues was maintained at a high level after 48 hours of storage at 4°C before the cryopreservation procedure.

The unique complex structure of testicular tissues provides support for GC growth and survival. During the first 3 months after birth, the lumen is not detectable in the seminiferous cords. The majority of GCs in the seminiferous cords are gonocytes, which subsequently migrate to the basement membrane and become undifferentiated SPG as the testes grow. In the current study, the structure of seminiferous cords was evaluated and compared in tissues stored for different transportation times. The results of H&E staining showed that the gap between the tubules and basement membrane increased after 48 hours of storage in transport medium at 4°C before the cryopreservation procedure. Disordered tubular structure and rupture were observed in tissues from the 48-hour group. These observations indicated that tissues structures could be preserved well and remained healthy over a 24-hour transport period, with a high viability and good seminiferous cord structure retained, whereas a transport period of 48 hours was more likely to result in abnormal structures. The rupture and increasing gap between seminiferous cords to the basement membrane observed in testicular tissues could disrupt the original GC niche and affect cell–cell interaction and support to the gonocytes. Salian et al. also provided evidence that 24 hours storage at 4°C did not affect tissue morphology and appearance (Salian et al., 2021). In a previous study, adult human testicular tissues were shown to maintain high cell viability, good tubular structure, and appropriate numbers of SPG for 3 days at 4°C (Faes and Goossens, 2017). Significant deterioration of seminiferous tubular morphology was identified on day 5 of storage, with a destroyed tubular structure, ruptured basement membranes, and the

loss of the germinal epithelium. It is possible that ITTs are more sensitive to changes in the environment than adult tissues, which caused structural changes to occur sooner. However, Faes's study used an average scoring system combining several parameters, which did not specify when the early signs of tissue deterioration were apparent or which signs were specifically observed. The health classification criteria of testicular tissues varies between different studies; in the current study, the attachment of seminiferous cords and the basement membrane was strictly categorized and evaluated. I found that the earliest change in morphology was the increasing gap between the tubules and the basement membrane, which was first observed, although only at a very low level, in the 6-hour group, and significantly increased after 48 hours of storage. As the gap increased, the structure of the seminiferous cords is more likely to change, and the cells are more likely to be disordered and shrunken. Therefore, to better preserve the structure of seminiferous cords, it is recommended that ITTs are transported within 24 hours after tissue collection.

For fertility preservation, GCs are the most important cells that we want to preserve in the testicular tissues. I evaluated the GCs in ITTs by analysing PGP9.5 (a GC marker) using immunohistochemistry and the expression of selected genes, including gonocyte/SSC markers *STRA8, PLZF, C-KIT, GFRA-1, THY1, UCHL-1, NANOG, OCT-4, CREM.* PGP9.5 was present in gonocytes and type A SPG in neonatal bovine ITTs, as determined by immunohistochemistry (Cai et al., 2016). My study showed that a delay in processing of 6 hours or 24 hours had no significant effect on GC number and GC related gene expression. However, the proportion of tubules with GCs decreased after 48 hours of storage in transport medium at 4°C, whereas the number of GCs per seminiferous tubular area increased. These results might be caused by changes in the tubule structures, including tubular rupture and shrinkage, after extended exposure to transport medium. Healthy and normal GCs are

characterized by their large round shape with high a nuclear/cytoplasmic ratio. However, I observed changes in the shape of GCs stored for 48 hours; this indicated that the morphology of GCs is affected by a long transportation time. It is promising that the health and structure of GCs could be well maintained after storage for 24 hours. a previous study showed that the proportion of gonocytes did not differ after 3 days of storage (Yang et al., 2010). The functions of GCs were assessed by xenografting in Zeng's study (Zeng et al., 2009); the survival of testis grafts for tissues with a 48-hour cooling period remained high, and complete spermatogenesis and mature spermatozoa were detected. Overall, the condition of GCs could be maintained effectively for 24 hours prior to cryopreservation, with no statistically significant negative effects found. Further investigations of GC function will require grafting or *in vitro* culture.

Sertoli cell proliferation was assessed by immunohistochemistry using vimentin and ki67 labelling. Ki67 has been used previously to label proliferating SSCs in ITTs (Poels et al., 2012). Most of the proliferating cells within the seminiferous cords of 2-week-old bovine ITTs were immature Sertoli cells. During the first 3 months after birth, gonocytes migrate to the basement, where they gain the ability to self-renew; during the transformation period, most gonocytes were Ki67-negative. The proportion of Sertoli cells and proliferating cells in seminiferous cords did not change significantly over the 48-hour storage period. Furthermore, the morphology of Sertoli cells did not notably differ. These results were consistent with the previous findings showing that the morphology of Sertoli cells in human adult testicular tissues started to deteriorate from day 8 (Faes and Goossens, 2016). It is believed that during the first 48 hours, the transportation time after tissue collection would not have adverse effects on Sertoli cells and cell proliferation.

For gene expression, the expression of *CREM* in testicular tissues is believed to be related to the potential ability of GCs to undergo spermatogenesis (Blendy et al., 1996). The expression

of *HSP 70-2* is known to be associated with the maintenance of GC viability and a reduction in apoptosis (Eddy, 1999). The results of the current study showed that the expression of the spermatogenesis-related genes *CREM* and *HSP70-2* remained similar after storage for 48 hours. The expression of *C-kit* during foetal gonadal development is associated with the survival, migration, and proliferation of PGCs (Izadyar et al., 2002a). A previous study showed that *C-kit* regulated the onset of the differentiation process of GCs (Zhang et al., 2011). Testes undergo complex changes during the embryonic and postnatal stages. In 2-week-old neonatal testes, gonocytes (identified by stem cell marker OCT-4) migrate to undifferentiated SSCs; thus, two types of GCs (identified with germ cell marker PGP9.5) are present. Some SSCs are already exist in the seminiferous cord; these can self-renew and are prepared for differentiation. The reduction in *C-kit* gene expression observed in the current study may be associated with the suppressed activity of GCs during the 48 hours of storage at low temperature. Overall, it is believed that a 48-hour transport process would not adversely affect the spermatogenesis potential of GCs in neonatal testes.

In the current study, the tissues were sectioned into small fragments before immersion in the transport medium, which is in similar size to human biopsy tissues collected from patients in clinic. The transportation time, storage conditions, and testicular tissue cryopreservation procedure strictly followed the human tissue procedures that are used routinely in the Oxford Tissue Biobank, and therefore our results are reliable for clinical purposes.

In conclusion, testicular tissue may be kept in transport medium for up to 48 hours without altering viability, tissue morphology, Sertoli cell morphology, or the number of SPG.

3.5 Key findings

- The viability of neonatal bovine testicular cells remained high after simulation of a 48-hour transport process in medium at 4°C.
- The space and gap between seminiferous cords and the basement membrane increased significantly in bovine neonatal testicular tissues stored in transport medium for 48 hours, with a deterioration in the structure of seminiferous cords.
- Changes in the morphology and location of GCs were observed with a 48-hour delay prior to processing, including the presence of seminiferous cords with GCs and the shape of GCs.
- SCs and proliferating cells were well preserved during 48 hours of transportation.
- The expression of selected GC-related, spermatogenesis-related, and apoptosis-related genes was unaffected during the simulation of a 48-hour transport period.

Chapter 4. Optimization of dissociation, enrichment, and culture conditions for bovine gonocytes and spermatogonial stem cells (SSCs)

4.1 Introduction

The early stage of development in neonatal testes includes a short period of around 3 months called mini-puberty. During this stage, the dominant GCs are gonocytes, located in the centre of the seminiferous cords. Gonocytes develop from primordial GCs and transform to SSCs; thus, gonocytes can be detected based on most GC markers, pluripotency stem cell markers, and certain surface protein markers (Awang-Junaidi and Honaramooz, 2018). *PGP9.5, PLZF,* and *GRFα-1* are expressed in both gonocytes and SPG (Wrobel, 2000, Costoya et al., 2004, Luo et al., 2006, Kim et al., 2019, Zhang, 2021). *Nanog* and *Oct 4* are pluripotency stem cell markers that are also expressed in fetal gonocytes (Hoei-Hansen et al., 2005, Goel et al., 2008, Mitchell et al., 2014).

In vivo and *in vitro* culture are the two main approaches by which cryopreserved prepubertal testicular tissues can be induced to produce functional sperm, thereby restoring fertility. The main *in vivo* methods are SSC transplantation, tissue autografting, and xenografting. Although these approaches have led to promising progress, the risks of transplanting residual malignant cells by autografting or infections of animal origin by xenografting cannot be neglected. Therefore, *in vitro* GC maintenance, propagation, and spermatogenesis are recommended as safer methods, especially in patients with leukaemia (Yokonishi et al., 2014a). The development of 2D cultures and 3D organoids for the *in vitro* study of SSCs was described earlier in **Section 1.4.3** and **Section 1.5**. Mouse ITTs cultured *in vitro* have been used to successfully produce functional sperm and offspring (Yokonishi et al., 2014a), indicating the promising future of this approach. Although no such results have yet been achieved in domestic animal models or humans, some progress has been made in this direction. GCs represent a unique and small population of cells with self-renewing and differentiating potential in prepubertal testicular tissues. The failure of gonocytes to undergo normal development could

lead to testicular GC cancer (Rajpert-De Meyts, 2006); therefore, the study of normal fetal GCs is fundamental to GC cancer research. Understanding how gonocytes behave in these culture systems could provide new opportunities to use gonocytes as a model to study male germline stem cells.

4.1.1 Dissociation and isolation of bovine gonocytes

Various methods have been proposed for the isolation and purification of SSCs from total testicular cells. Mechanical disruption, together with trypsin dispersion, is used for SSC isolation; however, this method can cause damage to and the loss of SSCs. Another technique, two-step enzymatic dissociation after removal of the tunica albuginea (Bellve et al., 1977, Izadyar et al., 2002b) is an effective, economical, and simple method for SSC isolation. In brief, collagenase is used to disperse seminiferous tubules, after which hyaluronidase and DNase I are used to digest cell–cell junctions and genomic DNA to obtain a high-quality suspension (Aponte et al., 2008, Kofman et al., 2013).

In vivo, SSCs are located in niches supported mainly by Sertoli cells in seminiferous tubules to maintain their undifferentiated state. During *in vitro* culture, SSCs in long-term culture will finally disappear owing to the extensive growth of Sertoli cells. The proportions of SSCs in total testicular cells are relatively low. Thus, the balance between Sertoli cells and SSCs needs to be adjusted to achieve better *in vitro* maintenance of SSCs. Various SSC purification methods have been established, including physical and immunological methods (He et al., 2015). Physical methods for SSC purification include differential plating, Percoll density gradient centrifugation selection, morphology-based selection, and gravity sedimentation

selection. Immunological methods include fluorescence activated cell sorting and magnetic-activated cell sorting.

Percoll density gradient centrifugation selection, differential plating, and morphology-based selection are the three most commonly used physical methods for SSC purification. Cells are tracked in different Percoll fractions depending on their density. The differential plating selection method is based on the different adherence speeds between cell types; normally, high-activity stem cells adhere to the plate faster than SSCs. Isolated GCs form colonies during culture, which makes it possible to identify and enrich SSCs under a microscope by mechanical collection. However, there have been limited studies of methods for the isolation and purification of bovine gonocytes. No standard methods have been established for this purpose, nor has any systematic study investigated the effects of different culture conditions on the formation of gonocyte colonies.

4.1.2 2D culture of enriched bovine gonocytes

In vitro culture systems provide a platform for cell studies that cannot be performed *in vivo*. For instance, gonocytes only exist for a short time in male mammals at an early stage after birth. Thus, the lack of an *in vitro* culture system for calf gonocytes makes it difficult to study the molecular mechanisms underlying the functions of bovine gonocytes and their transformation into SPG. The postnatal maintenance of bovine gonocytes, and their ability to colonize and proliferate, has not been fully investigated. This chapter describes the optimization of methods for the isolation and enrichment of gonocytes from neonatal bovine testicular tissues, as well as optimization of *in vitro* culture conditions for their maintenance and proliferation (**Figure 4-1**).

In this Chapter, I aim to optimize the isolation of GCs from bovine testicular tissues and optimize GC culture condition on a 2D culture systems. Firstly, **section 4.3.1** discusses the isolation, enrichment, and characterization of gonocytes from 2-week-old bovine testicular tissues. Then, **section 4.3.2** describes the optimization of a stepwise approach of several culture conditions for the maintenance and colony formation of neonatal bovine gonocytes: culture medium, fetal bovine serum (FBS) or knockout serum replacement (KSR), incubation temperature (34 °C *versus* 37 °C), cell seeding density (1.0×10^4 *versus* 5.0×10^4 *versus* 1.0×10^5 cells/well), and choice of ECM support (laminin *versus* collagen IV *versus* Matrigel *versus* fibronectin).

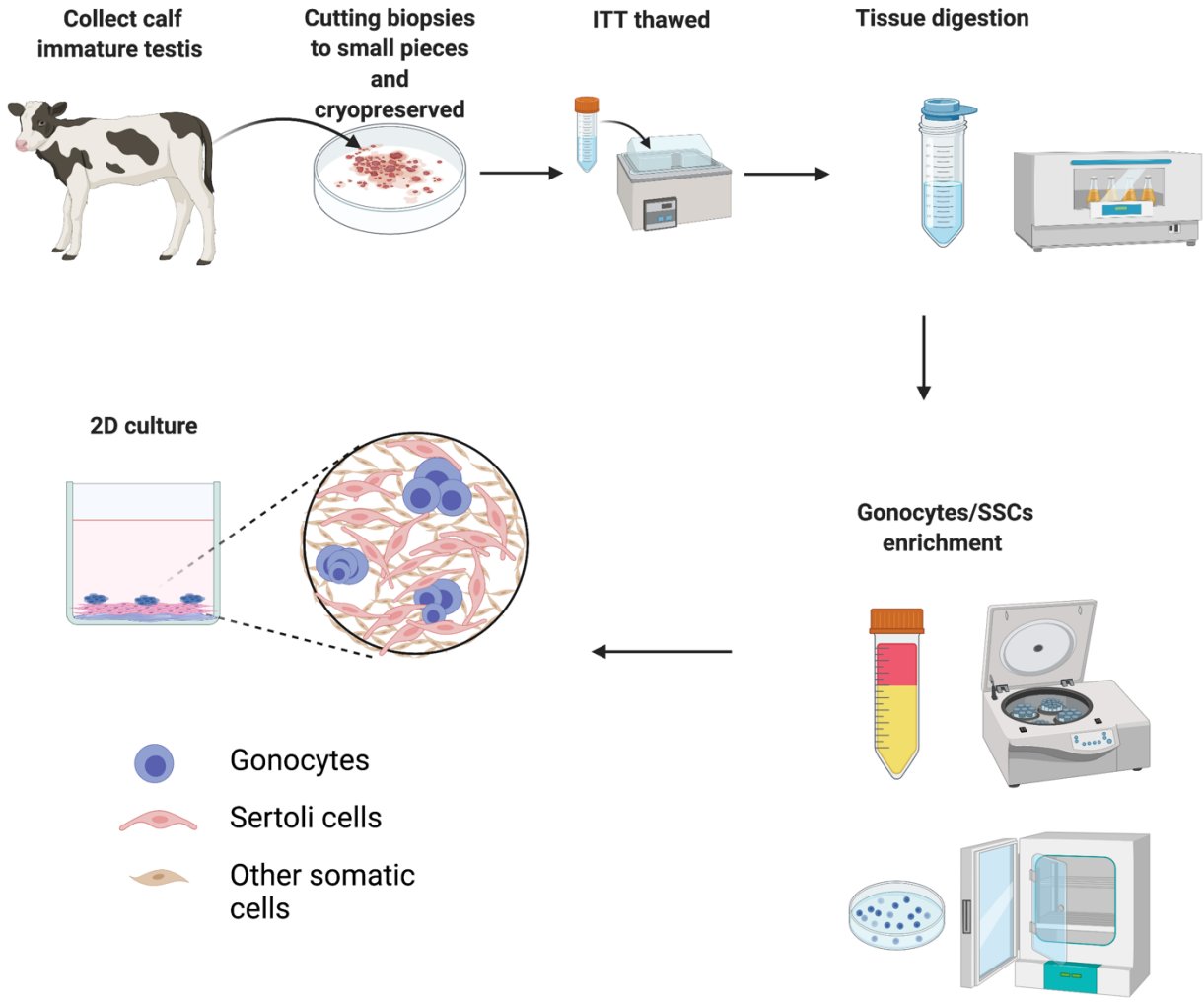

Figure 4-1. Optimization of tissue digestion, germ cell enrichment, and *in vitro* culture conditions for gonocytes from neonatal bovine testes. Neonatal calf testes were collected, sectioned, and cryopreserved in liquid nitrogen. After thawing, tissues were digested using a two-step enzymic digestion method. Germ cells were enriched using the Percoll density gradient centrifugation method or differential plating before seeding. Culture conditions were then optimized for *in vitro* culture of gonocytes. Figure created by author on Biorander.com.

4.2 Methods

The collection of neonatal bovine testicular tissues was described in **section 2.2.1.** The methods used to perform tissue digestion were described in **section 2.2.8**.

4.2.1 Enrichment of gonocytes

4.2.1.1 Comparison of different Percoll gradient concentrations

Testicular cells were collected after dissociation by a two-step enzymic digestion method and suspended in a 5% Percoll density gradient (Hunter Scientific, Saffron Walden, UK). The Percoll gradients were created by layering 2 ml each of 50%, 45%, 40%, 35%, 30%, and 20% Percoll in a 15-ml Falcon tube. The cell layer was carefully moved onto the layers of Percoll density gradient in a 15 ml Falcon tube, followed by centrifugation for 25 min at 1000 x g and 34 °C. Cells within and between different Percoll density phases were collected, washed with 4–5 volumes of phosphate-buffered saline (PBS) and thoroughly mixed by inversion before centrifugation at 700 x g for 5 min at 34 °C. After removal of the supernatant, cells in the pellets were ready for further processing. Cell viability was assayed with trypan blue and counted on a haemocytometer, which was described in **Section 2.2.7**. The Percoll gradient concentrations resulting in the highest proportion of PGP-positive gonocytes/SSCs were then used in further experiments.

4.2.1.2 A comparison of different incubation times and coating method for differential plating

In order to determine the most effective incubation time and coating method for gonocyte enrichment by differential plating, freshly isolated testis cells were seeded on plates either coated or uncoated with 2% Matrigel at a density of 1×10^5 cell/well. Testicular cells were fed with 10% KSR-minimum essential medium (MEM)-α and cultured at 34°C with 5% CO_2 for 3 h or overnight. Non-adherent cells suspended in the culture medium were collected by brief centrifugation at 1200 rpm at room temperature for 5 min. Adherent cells were observed under a microscope. The proportions of gonocytes/SSCs were then determined by immunocytochemical staining with PGP9.5.

4.1.3 Cell culture

Gonocytes collected by different enrichment methods were analysed for cell viability using trypan blue dye before being seeded for further experiments. Laminin, collagen IV, Matrigel, and fibronectin were diluted in PBS to make 5 μg/cm² coating solutions, which were then used to coat plates or glass coverslips, followed by incubation for 1 h. Cells were cultured in 24-well culture dishes with or without glass coverslips coated with different ECMs. The culture medium was MEM-α or Dulbecco's Modified Eagle's Medium/Nutrient Mixture F-12 (DMEM/F12), supplemented with 10% KSR or 10% FBS, presented in **Table 4-1**. The medium was changed every 2 days.

Table 4-1. Culture media and supplements.

Components (of all culture media)		Concentration
Base medium	MEM-α	
Serum or serum replacement		
	FBS	10%
or	KSR	10%
Other supplements		
	Penicillin–streptomycin	1%
	Gentamicin	20 μg/ml
	Insulin–transferrin–selenium	0.1X
	Vitamin C	10^{-4} M
	Vitamin E	10 μg/ml
	Sodium pyruvate	1 mM
	Non-essential amino acids	1X
	Glutamine	2 mM

FBS, fetal bovine serum; KSR, knockout serum replacement.

4.1.4 Immunocytochemical staining

Floating cells collected were fixed on poly-L-lysine-coated slides for immunocytochemical staining. Cells or GC colonies adhered to coverslips/slides were washed with PBS and fixed by 4% paraformaldehyde (PFA) for 20 min at room temperature. Cells were washed three times with PBS, permeabilized with 0.1% Triton X-100 (v/v) (Sigma) in PBS for 15 min, washed three times with PBS again, then blocked using 1% bovine serum albumin (BSA) dissociated in PBS for 1 h at room temperature. Cells were then stained with primary antibody (**Table 4-2**) overnight at 4°C, followed by secondary antibody incubation for 1 h at room temperature in the dark. Coverslips/slides were washed in the dark and mounted. Ten random fields on each slide were imaged under a fluorescence microscope, and the mean number of positive cells was determined.

Table 4-2. Primary and secondary antibody information for immunocytochemical staining.

Primary antibody	Target cells	Manufacturer	Optimal concentration	Secondary antibody
Anti-PGP9.5	Germ cell, gonocytes, SSCs	Abcam; ab72911	1:100	Goat anti-mouse IgG (1:200; Abcam)
Anti-Ki67	Proliferating marker, growth fraction	Abcam; ab15580	1:200	Goat anti-rabbit IgG (1:200; Abcam)
PLZF antibody	Germ cells, gonocytes, SSCs	Novus Biologicals; NBP2-19870	1:100	Goat anti-rabbit IgG (1:200; Abcam)
OCT4	Stem cells	Novus Biologicals; NB100-2379	1:100	Goat anti-rabbit IgG (1:200; Abcam)
Vimentin	Sertoli cells	Santa Cruz Biotechnology; sc-6260	1:200	Goat anti-mouse IgG (1:200; Abcam)

4.1.5 Cell apoptosis

A TUNEL (Promega DeadEnd; G3250) assay was used to measure DNA fragments in cells following the manufacturer's instructions, which was described in **Section 2.2.8**.

4.1.6 Statistical analysis

Data are presented as mean ± SD. GraphPad Prism 9.3.0 software for Mac software (GraphPad Software, San Diego, California, USA) was used to create graphs and perform tests for statistical significance. Statistical differences between groups were analysed by the student's *t*-test or by ANOVA. Differences were considered significant at $p<0.05$.

4.3 Results

Bovine abattoir testicular tissues were collected from slaughterhouse, which would be otherwise discarded. For the ethical aspect, Home Office licensing is not required in this case.

4.3.1 Isolation, enrichment, and identification of gonocytes

4.3.1.1 The two-step enzymatic method can isolate gonocytes effectively

I optimized the two-step enzymatic method by changing the incubation time. The results showed that 30 min incubation for each step on a shaker could effectively isolate testicular fragments (1-2 mm^3) into single cells while maintaining a high cell viability of 85.00± 4.00%. The presence of testicular cells was confirmed under a microscope. Incomplete tissue digestion occurred with 20 min incubation (**Figure 4-2A**), whereas single isolated cells were found following two-step enzymatic isolation and 30 min incubation (**Figure 4-2B**).

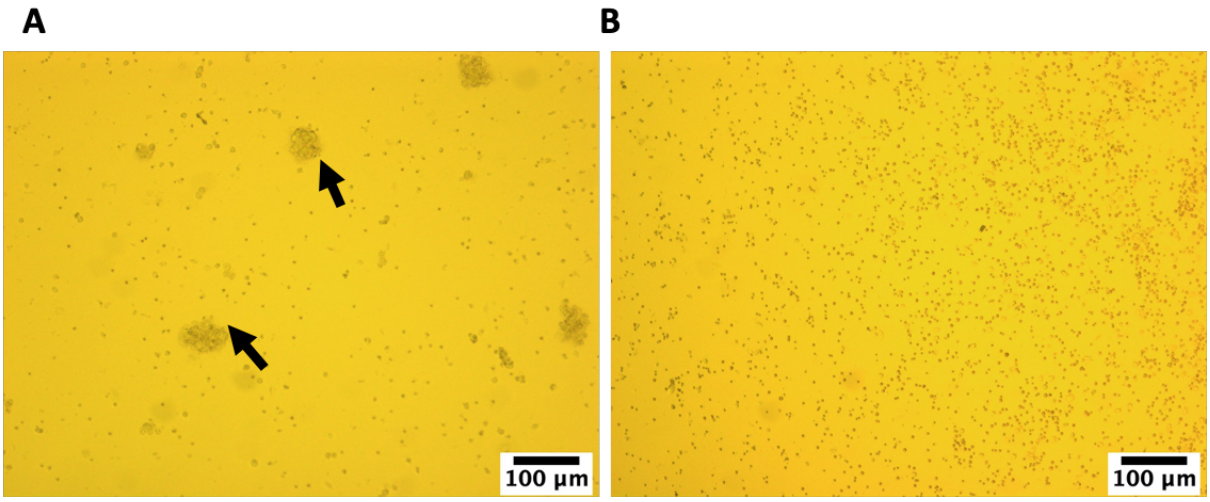

Figure 4-2. Cells isolated from cryopreserved neonatal bovine testicular samples using two-step enzymatic digestion. A) With 20 min incubation time in the first and second steps of the digestion process, small cell clumps occurred (white arrow). B) With 30 min incubation time for both steps of the digestion process, single isolated cells were observed. Scale bar= 100 µm. Three biological replicates were carried out (n=3).

4.3.1.2 Characterization of gonocytes

SSCs in single-cell suspension after isolation were identified based on their morphology under a microscope. After 3 days of culture in a culture dish, gonocytes/SSCs had a typical appearance: a larger cell size with a typical round shape and a higher nucleus/cytoplasm ratio (**Figure 4-3A**). Somatic cells formed a confluent flat mono-feeder layer to support gonocyte/SSC growth at the surface. Gonocytes were characterized by immunocytochemical staining using the GC marker PGP9.5 (**Figure 4-3B**). Immunocytochemical analysis revealed that gonocytes expressed the pluripotency stem cell marker Oct-4 (**Figure 4-3C**).

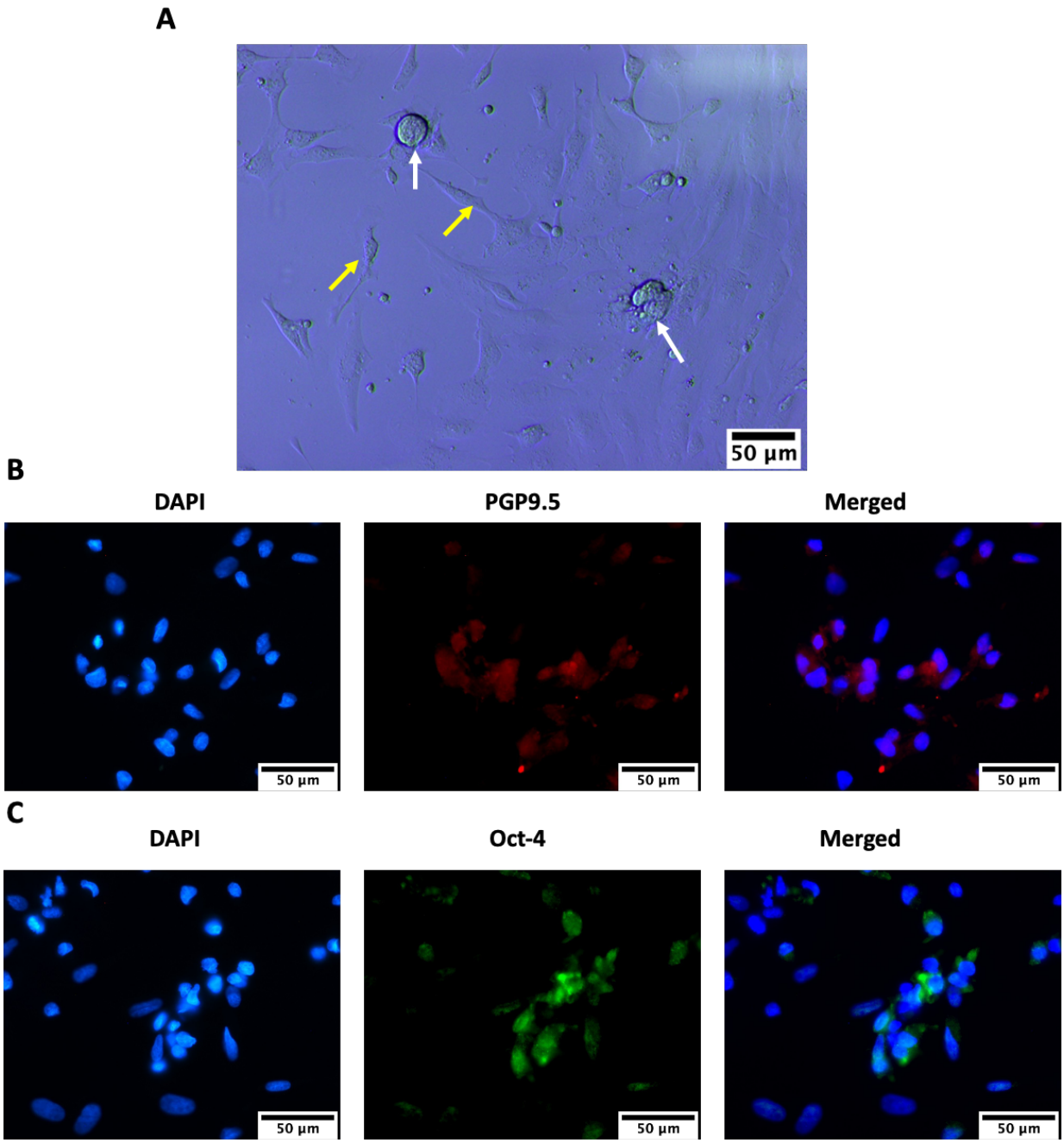

Figure 4-3. Characterization of gonocytes/SSCs. A) Bright-field image of enriched gonocytes/SSCs. White arrows indicate gonocytes/SSCs, yellow arrows indicate Sertoli somatic cells. B) Representative immunofluorescence images of enriched gonocytes/SSCs revealing the expression of PGP9.5 at day 3 of culture. C) Representative immunofluorescence images of gonocytes/SSCs revealing the expression of Oct-4 at day 3 of culture. Scale bar=50 µm. Three biological replicates were carried out (n=3).

4.3.1.3 Percoll density gradient centrifugation selection (30–40%) significantly enhanced gonocyte purification

Testicular tissues digested by two-step enzymatic digestion were isolated by a 20%, 30%, 35%, 40%, 45%, and 50% Percoll density gradients. The proportion of PGP9.5-positive cells in suspension was then used to determine the effectiveness of the Percoll density gradient for the enrichment of gonocytes/SSCs. The 30–45% Percoll fractions contained significantly higher percentages of PGP9.5-positive cells compared with other fractions, with values of 49.8% ± 1.833 in the 30% fraction, 42.36% ± 2.17 in the 35% fraction, 32.127% ± 3.4 in the 40% fraction, and 23.1% ± 1.49 in the 45% fraction, compared to that in total testicular cells groups (7.87 ± 2.215%) (p<0.05) (**Figure 4-4A**). The viabilities of cells selected from different fractions of the Percoll gradient were then evaluated using trypan blue. There was no significant difference in viability among testicular cells isolated in different fractions of the Percoll gradient (p>0.05) (**Figure 4-4B**).

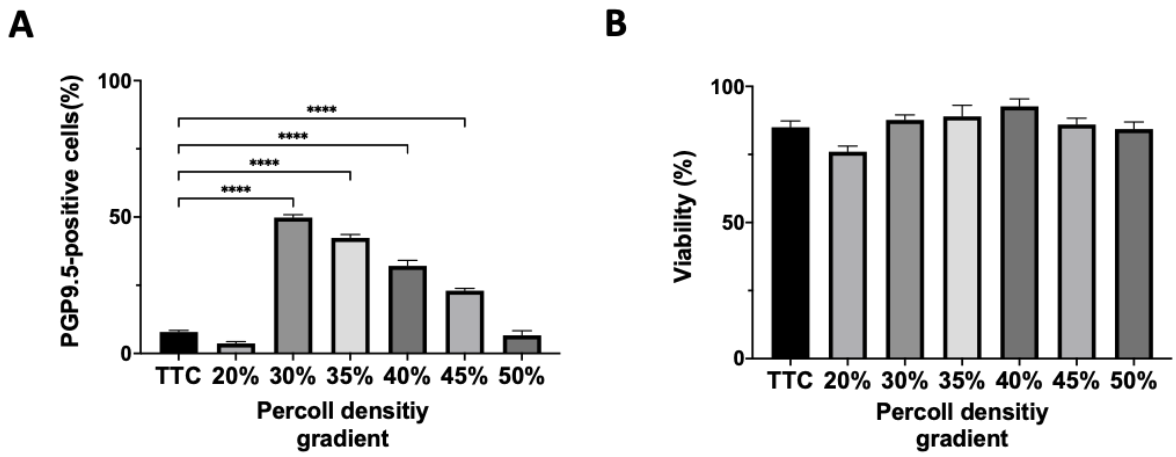

Figure 4-4. Bovine germ cell purification using discontinuous Percoll density gradient centrifugation selection. A) Proportion of PGP9.5 positive cells and B) viability of cells selected by 20%, 30%, 35%, 40%, 45%, and 50% Percoll density gradient. TTC, total testicular cells. ****p<0.0001. Three biological replicates were performed (n=3).

Therefore, 30–40% Percoll was used for GC enrichment owing to its effectiveness for selecting GCs and the high viability of the selected cells. The proportions of GCs and Sertoli cells were evaluated by immunocytochemical staining. The proportion of PGP9.5-positive cells was 45.10% ± 3.67 after 30–40% Percoll gradient enrichment, compared with 7.87% ± 2.215 in total testicular cells (p<0.001). There were no differences in cell viability and apoptosis in cells before and after Percoll selection (p>0.5) (**Figure 4-5 D, E**). Sertoli cells were evaluated by immunocytochemical staining using vimentin as a marker before and after 30–40% Percoll gradient selection. Percoll gradient (30–40%) centrifugation led to a significantly lower proportion (41.37% ± 2.62) of vimentin-positive cells (p<0.05) compared with that in total testicular cells before enrichment (81.72% ± 3.48) (**Figure 4-5A, B**). Cell viability and apoptosis were determined by trypan blue and TUNEL assays; the results showed no difference in viability or apoptosis before and after 30–40% Percoll selection (p>0.5) (**Figure 4-5D, E**).

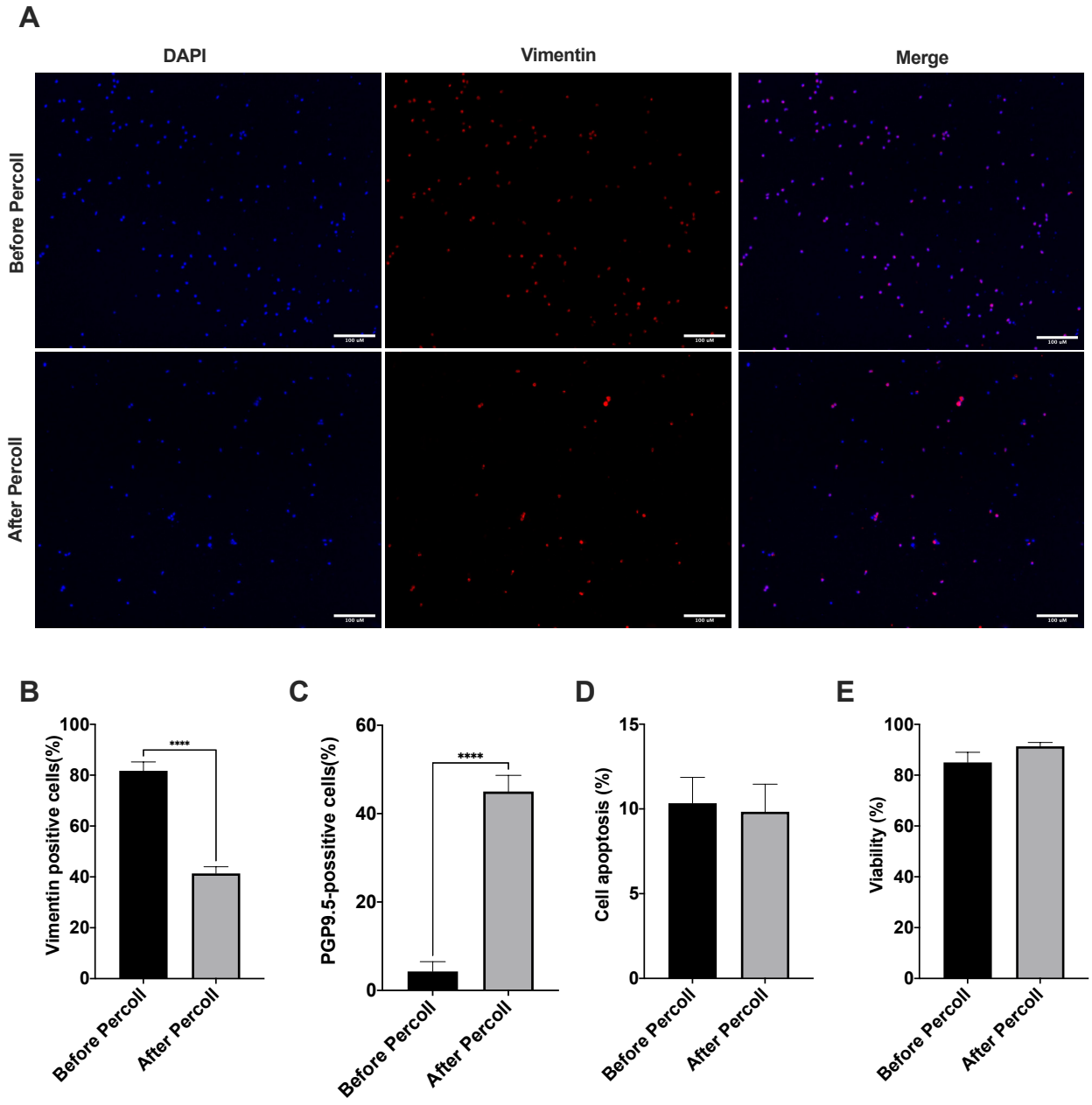
A
DAPI
Vimentin
Merge
Before Percoll
After Percoll
B
Vimentin positive cells(%)
****
Before Percoll
After Percoll
C
PGP9.5-possitive cells(%)
****
Before Percoll
After Percoll
D
Cell apoptosis (%)
Before Percoll
After Percoll
E
Viability (%)
Before Percoll
After Percoll

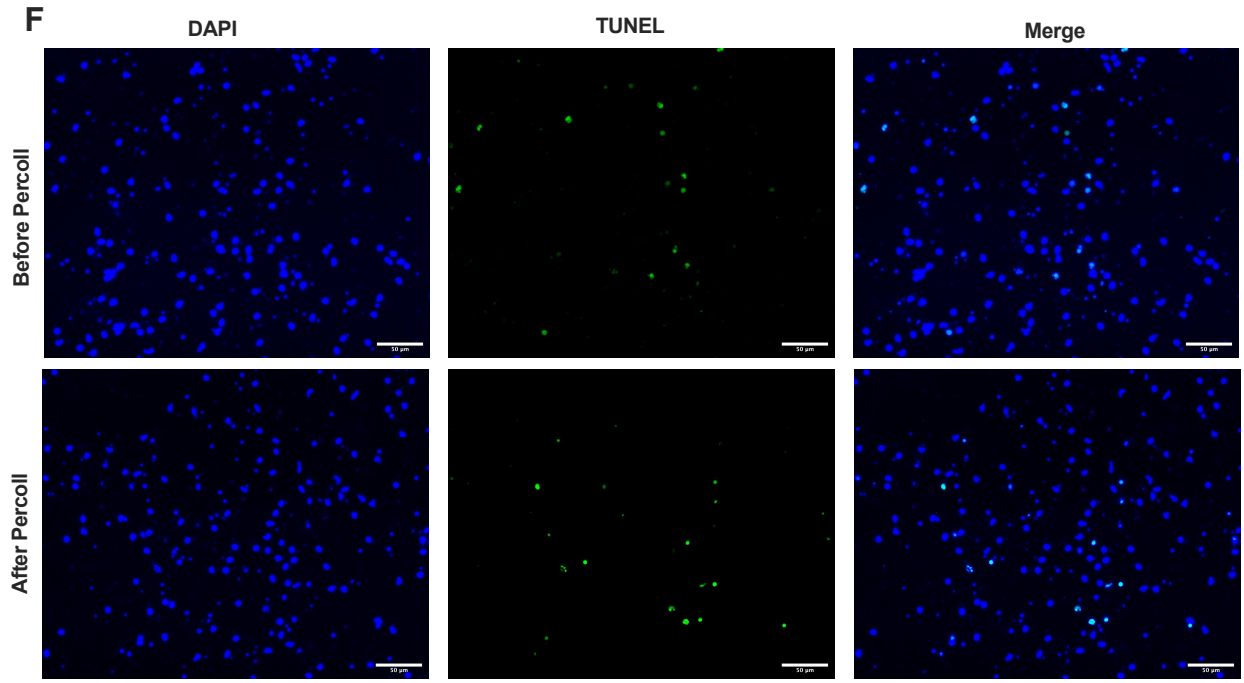

Figure 4-5. Evaluation of cells enriched by 30–40% Percoll density gradient. A, B) Percentage of vimentin-positive cells before and after Percoll gradient selection. Scale bar=100 µM. C) Proportion of PGP9.5-positive cells. D, F) Cell apoptosis assessed by TUNEL assay. Scale bar=50 µm. E) Viability of cells before and after Percoll selection. Three biological replicates were performed (n=3). Data are shown as means and standard deviations. GraphPad Prism 9.3.0 software was used to create graphs and to test for statistical significance. ****p<0.0001

4.3.1.4 The effects of differential plating on gonocyte purification

Differential plating has been proposed as a method to enrich SPG in testicular cell suspension. The initially isolated primary testicular cells were used in the initial group without any additional processes. Testicular cells were cultured for 3 h or overnight in uncoated or Matrigel-coated plates to enrich gonocytes and reduce the number of somatic cells. The bottom of the culture dish was examined by bright-field microscopy after the removal of suspended cells. After 3 h of primary cell culture, the bottom of Matrigel-coated or uncoated plates showed little cell attachment (**Figure 4-6A,C**). Increased levels of somatic cell attachment was observed on Matrigel-coated or uncoated plates subjected to overnight primary cell culture

(**Figure 4-6B,D**). Both round GCs and flat somatic cells were observed to be attached to the bottom of plates after the removal of suspended cells following overnight incubation with or without Matrigel coating on differential plates (**Figure 4-6B,D**). The proportion of gonocytes (PGP9.5 positive) in non-adherent cells in each group was assessed by immunocytochemical staining. The percentage of gonocytes was 14.00% ± 1.23 among non-adherent cells after overnight incubation on uncoated differential plates and 18.10% ± 1.02 among adherent cells after overnight incubation on Matrigel-coated differential plates; both these percentages were significantly higher than the value of 8.33% ± 1.53 in the initial group ($p<0.05$; **Figure 4-6E**).

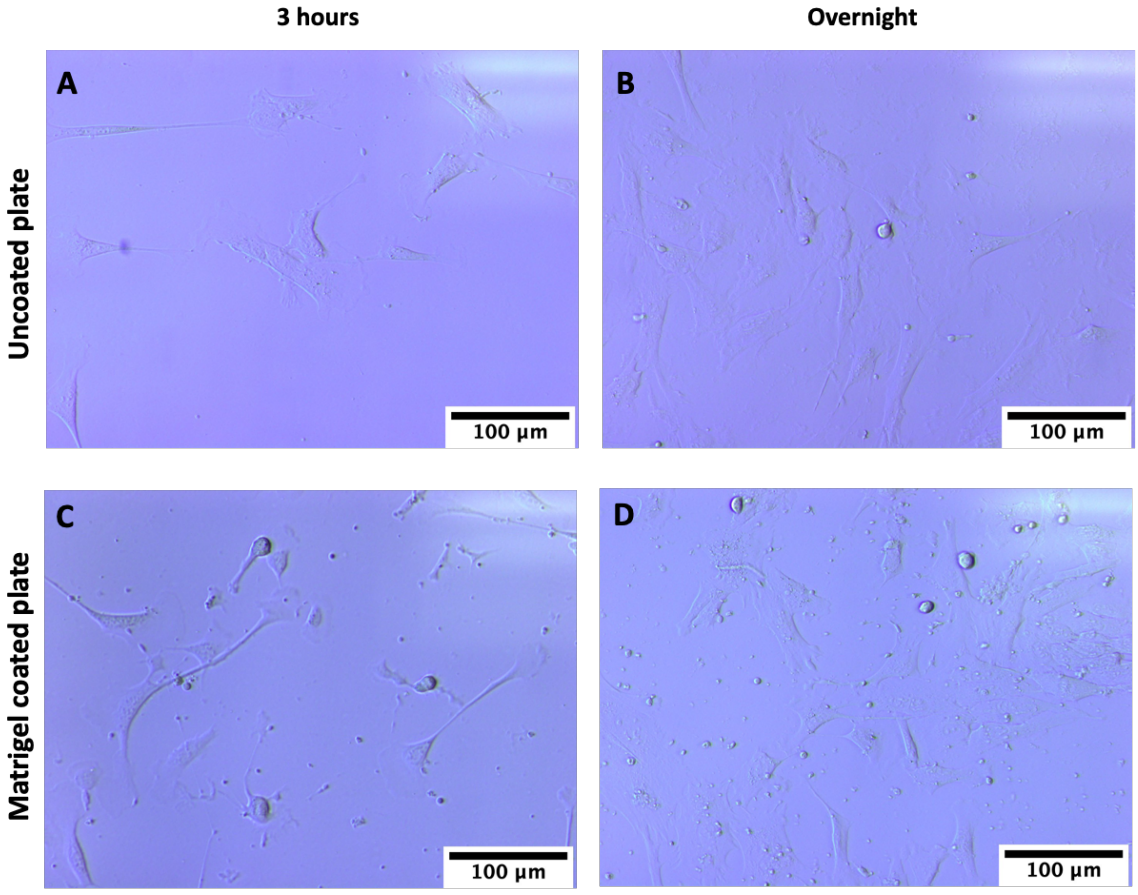

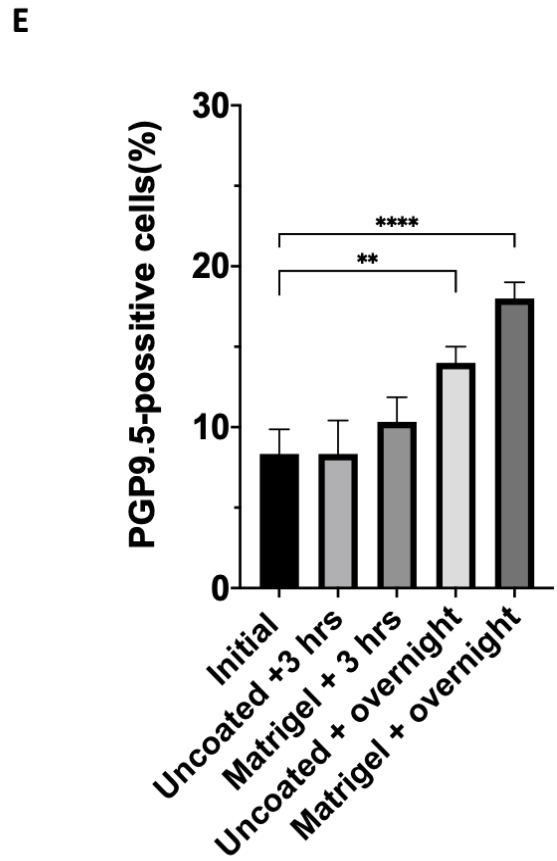

Figure 4-6. Enrichment of bovine gonocytes by differential plating. Dissociated neonatal bovine testicular cells were incubated for 3 h or overnight on uncoated or Matrigel-coated differential plates.

Cells attached at the bottom of the differential plastic dish were considered to be adherent cells and were examined by microscopy. Cells suspended in the culture medium were considered to be non-adherent cells. Representative bright-field images of adherent cells after A) 3 h incubation or B) overnight incubation on uncoated differential plates. Representative bright-field images of adherent cells after C) 3 h incubation or D) overnight incubation on Matrigel-coated differential plates. E) Proportions of PGP9.5-positive cells in initial group and groups of non-adherent cells on uncoated differential plates with 3 h incubation (uncoated + 3 h), Matrigel-coated plate with 3 h incubation (Matrigel + 3 h) group, uncoated plate with overnight incubation (uncoated ± overnight) group, and Matrigel-coated plate with overnight incubation (Matrigel + overnight). Scale bar=100 µm. ** $p<0.01$; **** $p<0.0001$ Three biological replicates were carried out (n=3).

4.3.1.5 Morphology-based selection for gonocyte purification

Isolated total testicular cells were cultured on Matrigel-coated culture dishes for 7 days until colonies appeared (**Figure 4-7A**). Gonocyte colonies were mechanically isolated using a glass pipette under a microscope and then transferred to a new freshly prepared culture dish (**Figure 4-7B**).

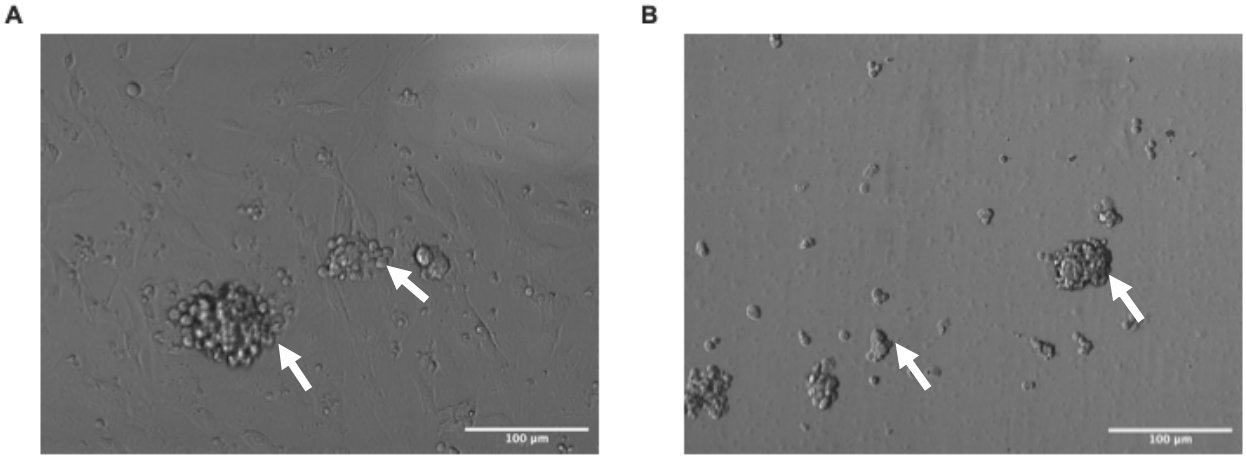

Figure 4-7. Representative bright-field images of gonocyte colonies. A) Formation of gonocyte colonies at day 7 after initial culture. B) Gonocyte colonies after being collected and transferred to a new fresh culture dish. Scale bar=100µm. Three biological replicates were carried out (n=3).

4.3.2 2D culture conditions for bovine gonocytes

4.3.2.1 The effects of cell seeding density on formation of germ cell colonies

This experiment aimed to determine the optimal seeding density for culturing neonatal gonocytes. Comparisons were made by seeding enriched testicular cells into 24-well plates at densities of 1.0×10^4 (group A), 5.0×10^4 (group B), or 1.0×10^5 (group C) cells/well; each well had a volume of 2 cm^2 and contained 1 ml of culture medium. Cells were cultured under similar conditions at 34°C, and the culture medium (MEM-α + 10% KSR) was changed every 2 days.

Cells in group C (1.0×10^5 cells/well) became confluent significantly earlier than those in group A (1.0×10^4 cells/well; $p<0.05$), reaching 90% confluence in 8.83 ± 0.75 days, whereas cells in group A and B took 13.67 ± 1.37 days and 11.33 ± 0.86 days to become confluent (**Table 4-3**). More cell–cell contacts were found in groups with higher seeding densities, i.e., groups B and C. The formation of cell colonies was observed in groups B and C but not in group A. Gonocyte colonies initially appeared at 7.31 ± 0.64 days in group C and 9.42 ± 1.45 days in group B. There was no significant difference in the time when colonies initially appeared when compared between groups B and C. In subsequent experiments, a seeding density of 1.0×10^5cells/well was used owing to the shorter confluency time and the appearance of colony formation.

Table 4-3. Effects of three cell seeding densities on the growth of testicular cells in culture.

	Group A (1.0×10^4 cells/well)	**Group B (5.0×10^4 cells/well)**	**Group C (1.0×10^5cells/well)**
Day confluency was reached	13.67 ± 1.37*	11.33 ± 0.86	8.83 ± 0.75*
Day colonies initially appeared	n/a	9.42 ± 1.45	7.31 ± 0.64
Viability (%)	90.33 ± 2.16	90.50 ± 2.42	92.50 ± 2.28

The results are shown as mean ± standard deviation. One-way ANOVA was used for statistical analysis, and multiple comparisons were performed for different columns within rows. *Data differed significantly ($p<0.05$) when compared. Three biological replicates were carried out (n=3).

4.3.2.2 The effects of culture medium and serum-free culture on gonocyte culture

Serum-free culture has been proposed for SSC culture. In this experiment, I compared the effects of two different culture media, DMEM/F12 and MEM-α, supplemented with 10% FBS or 10% KSR, on the formation of gonocyte colonies in 2D culture. Cells were seeded in 24-well plates and maintained for 10 days without passage. There were no significant differences between the confluency days in the four groups (**Table 4-4**). The formation of gonocyte colonies was only observed in the DMEM/F12 + 10% KSR and MEM-α + 10% KSR groups (**Figure 4-8**). Gonocytes colonies initially appeared at 8.15 ± 1.29 days in the DMEM/F12 + 10% KSR group, significantly later than the 7.13 ± 0.73 days for the MEM-α + 10% KSR group ($p<0.05$). The numbers and diameters of gonocyte colonies at day 7 were compared; this was because seeded cells started to become confluent at day 4 after culture. The mean number of gonocyte colonies was 7.42 ± 0.81 colonies/well in the MEM-α + 10% KSR group, significantly higher than the 2.75 ± 0.54 colonies/well in the DMEM/F12 + 10% KSR group ($p<0.05$). However, there was no significant difference in the mean colony diameter between the two groups. Therefore, MEM-α + 10% KSR was chosen for subsequent experiments.

Table 4-4. The effects of two culture media with and without serum on the formation of bovine gonocyte colonies.

	DMEM/F12 + 10% FBS	**DMEM/F12 + 10% KSR**	**MEM-α + 10% FBS**	**MEM-α + 10% KSR**
Day confluency was reached	8.72 ± 1.16	8.96 ± 0.71	8.65 ± 1.23	9.20 ± 0.80
Day colonies initially appeared	n/a	8.15 ± 1.29[a]	n/a	7.13 ± 0.73[a]
Number of colonies per well at day 7	n/a	2.75 ± 0.54[b]	n/a	7.42 ± 0.81[b]
Diameter of colonies at day 7 (µm)	n/a	60.53 ± 10.72	n/a	63.76 ± 11.27

MEM-α, Minimum Essential medium Alpha. DMEM/F12, Dulbecco's Modified Eagle medium nutrient mixture F-12. FBS, fetal bovine serum. KSR, knockout serum replacement. Data are mean ± standard deviation. Data labelled [a] or [b] were compared and significant difference was found, $p<0.05$. Three biological replicates were carried out (n=3).

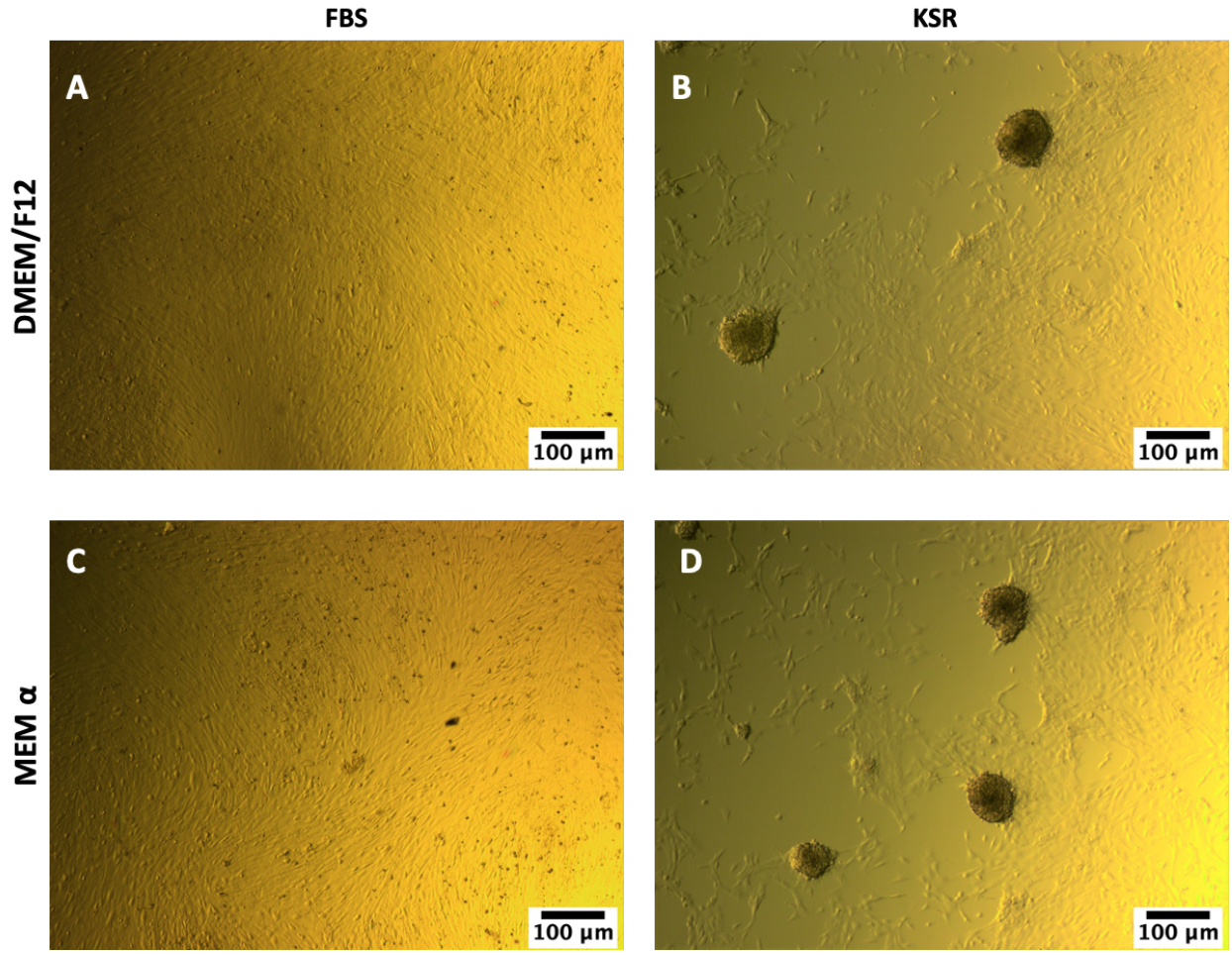

Figure 4-8. Representative bright-field images of formation of germ cell colonies at day 7. Representative images of enriched bovine gonocytes cultured in A) Dulbecco's Modified Eagle medium nutrient mixture F-12 (DMEM/F12) culture medium supplemented with fetal bovine serum (FBS) or B) knockout serum replacement (KSR). Representative images of enriched bovine gonocytes cultured in C) Minimum Essential medium Alpha (MEM-α) culture medium supplemented with FBS or D) KSR. Formation of colonies were found in B) and C). Scale bar=100µm. Three biological replicates were carried out (n=3).

4.3.2.3 The effect of incubation temperature

The objective of this experiment was to evaluate the effects of two different incubation temperature (34°C *versus* 37°C) on the growth of cultured testicular cells. Other culture conditions remained the same: cells were seeded at a density of 1.0×10^5cells/well in MEM-α + 10% KSR culture medium. There were no significant differences in the day at which cells reached confluency, the day at which colonies initially appeared, the numbers and diameters of colonies, or the viability of cells when compared between the two incubation temperature groups (**Table 4-5**). The mean spermatid cord temperature was approximately 34°C in bulls; therefore, 34°C was chosen for subsequent experiments.

Table 4-5. The effects of two incubation temperatures on the growth and viability of testicular cells in short-term culture.

	34 °C	**37 °C**
Day confluency was reached	9.12 ± 0.83	9.13 ± 0.79
Day colonies initially appeared	5.24 ± 1.10	5.95 ± 0.93
Number of colonies per well at day 7	7.15 ± 0.94	7.71 ± 1.02
Diameter of colonies at day 7	67.43 ± 11.32	62.01 ± 12.12
Viability (%)	92.31 ± 2.86	90.93 ± 3.30

Data are shown as mean ± standard deviation. *p<0.05, **p< 0.01, ***p<0.001, ****p<0.0001. Three biological replicates were carried out (n=3).

4.3.2.4 The effects of different ECMs on short-term *in vitro* gonocyte culture

In vivo, gonocytes are located in the centre of the seminiferous tubules, supported by Sertoli cells and extracellular matrices. The main components of the basement membrane are laminin, collagen IV, and fibronectin. This experiment aimed to evaluate the effects of four extracellular matrices, laminin, collagen IV, Matrigel, and fibronectin, on the culture of bovine gonocytes/SSCs.

Morphology changes of enriched bovine testicular cells in culture were evaluated for 7 days (**Figure 4-9A**). By 24 h after cell seeding, suspended cells started to adhere to the bottom of the culture dish. These cells were mostly somatic cells. In the next few days, dome-shaped, refractile colonies started to form, surrounded by flat somatic cells. Somatic cells in the collagen IV and fibronectin groups were flatter compared with those in the Matrigel and laminin groups. During culture, the adherence of colonies to the bottom of the culture dish was looser in the laminin group than in the other three groups. Colony transparency gradually decreased as colony size increased.

Assessment of colony numbers and diameters showed that the effects of the type of matrix and culture time were significant ($p<0.05$). In the laminin group, the number of SSC colonies per culture dish at day 3 was 44.00 ± 2.00, whereas only a few colonies had appeared in other groups by this time: 8.67 ± 0.57 in the collagen IV group, 9.00 ± 1.73 in the Matrigel group, and 7.00 ± 2.00 in the fibronectin group had appeared (**Figure 4-9AB**). The mean diameter of SSC colonies was 78.65 ± 19.71 μm in the laminin group at day 3, significantly higher than that in the other three groups ($p<0.05$). At day 5, there were significantly more gonocyte colonies in the laminin and Matrigel groups than in the other groups ($p<0.05$), with numbers of 40.67 ± 4.04 and 45.33 ± 4.16, respectively. No differences were found among the four

groups in terms of the diameter of colonies. At day 7, the number of SSC colonies were 38.67 ± 3.78 in the Matrigel group and 38.00 ± 6.24 in the laminin group, higher than those in the collagen IV (10.33 ± 1.52) and fibronectin (7.67 ± 1.58) groups ($p<0.05$). The mean diameter of colonies in the collagen group at day 7 was 162.3 ± 64.0 μm, significantly higher those in the other groups ($p<0.05$) (**Figure 4-9 C**). The diameters of colonies in the Matrigel and laminin groups increased at a steady rate, and the variation in colony size was smaller.

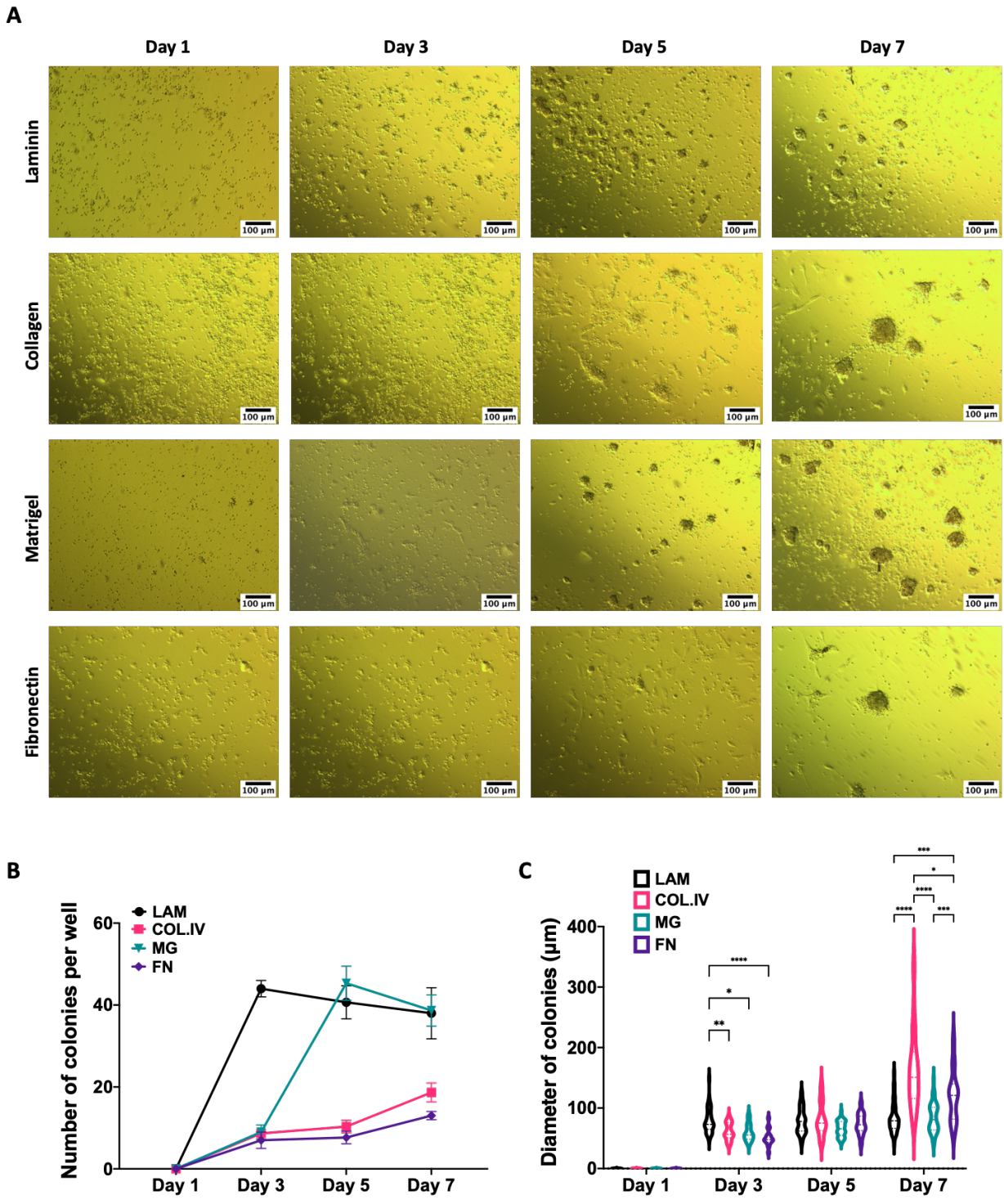

Figure 4-9. Growth of gonocytes/SSCs colonies on four extracellular matrices. A) Representative bright-field images of enriched gonocyte culture on LAM (laminin), COL.IV (collagen IV), MG (Matrigel), and FN (fibronectin) from day 1 to day 7 of culture. B) Numbers and C) diameters of colonies formed per well on the four extracellular matrices. Scale bar= 100 µm. *p<0.05, **p<0.01, ***p<0.001, ****p<0.0001. Three biological replicates were carried out (n=3).

Cell apoptosis was determined by TUNEL assays. TUNEL-positive cells were found both at the edges of the SSC colonies and among the uncolonized somatic cells. There were significant increases in cell apoptosis at day 7 of culture compared with day 1 in all four ECM groups (p<0.05) but no differences between the four groups at day 7 (**Figure 4-10**).

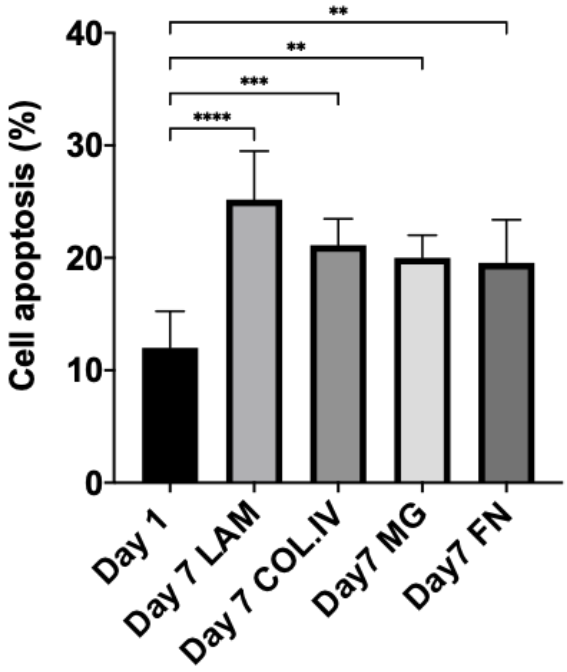

Figure 4-10. Cell apoptosis in gonocyte colonies in four extracellular matrix groups after 7 days of *in vitro* culture. Data are shown as mean ± standard deviation. *p<0.05, **p<0.01, ***p<0.001, ****p<0.0001. Three biological replicates were carried out (n=3).

At day 7 of culture, immunofluorescence analysis revealed that these colonies expressed PGP9.5 and PLZF, which are specific markers for gonocytes/SSCs. Ki-67, a marker of proliferating cells, was also found to be expressed in some PGP9.5-positive cells. Vimentin-positive cells were located at the outer layers of colonies, whereas PGP9.5- and PLZF-positive cells tended to be in the centres of colonies. There were no significant differences in the proportions of PGP9.5-positive, Ki67-positive, vimentin-positive, and PLZF-positive cells when compared between the four ECM groups (p>0.05; **Figure 4-11A, B, C, D**).

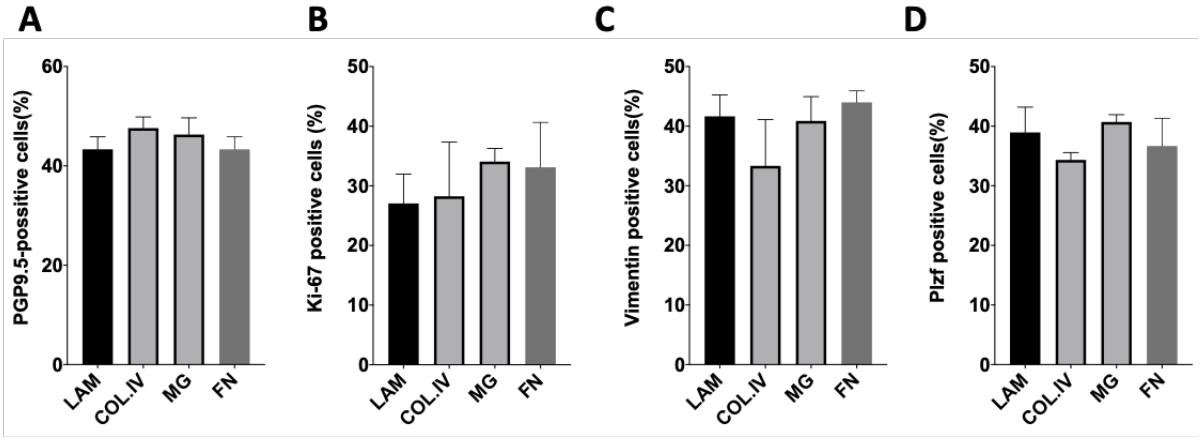

Figure 4-11. Immunocytochemical analysis of SSC colonies at day 7. Proportions of A) PGP9.5- B) vimentin-, C) Ki67-, and D) PLZF-positive cells at day 7 of culture. n=3 independent experiments, data are shown as mean ± standard deviation. *p<0.05, **p<0.01, ***p<0.001, ****p<0.0001.

Overall, enriched gonocytes formed higher numbers of moderate-sized colonies on laminin- and Matrigel-coated plates compared with the collagen IV and fibronectin groups. Matrigel was found to better maintain gonocyte colonies on plates for use in further procedures such as staining or collection; therefore, Matrigel was chosen for use in subsequent experiments.

4.3.2.5 The short-term culture of enriched neonatal bovine gonocytes

Dome-shaped gonocytes colonies normally appeared within a week after cell seeding at an appropriate density on Matrigel-coated plates. In order to provide gonocytes with more nutrition and more growing space, avoid the overgrowth of somatic cells, and reduced the loss of cells during the culture procedure, morphology-based selection was used during passage. Culture dishes were checked, and colonies were mechanically collected, sectioned, and transferred to new culture dishes during passages (**Figure 4-11**). After being transferred into the new culture dish, somatic cells around colonies were found to expend in the dish. Colonies tended to migrate slowly to the edges of the coverslips/culture dish. Gonocyte colonies expressed the SSC markers *PGP9.5* and *OCT4*, as confirmed by immunofluorescence (**Figure 4-11C**).

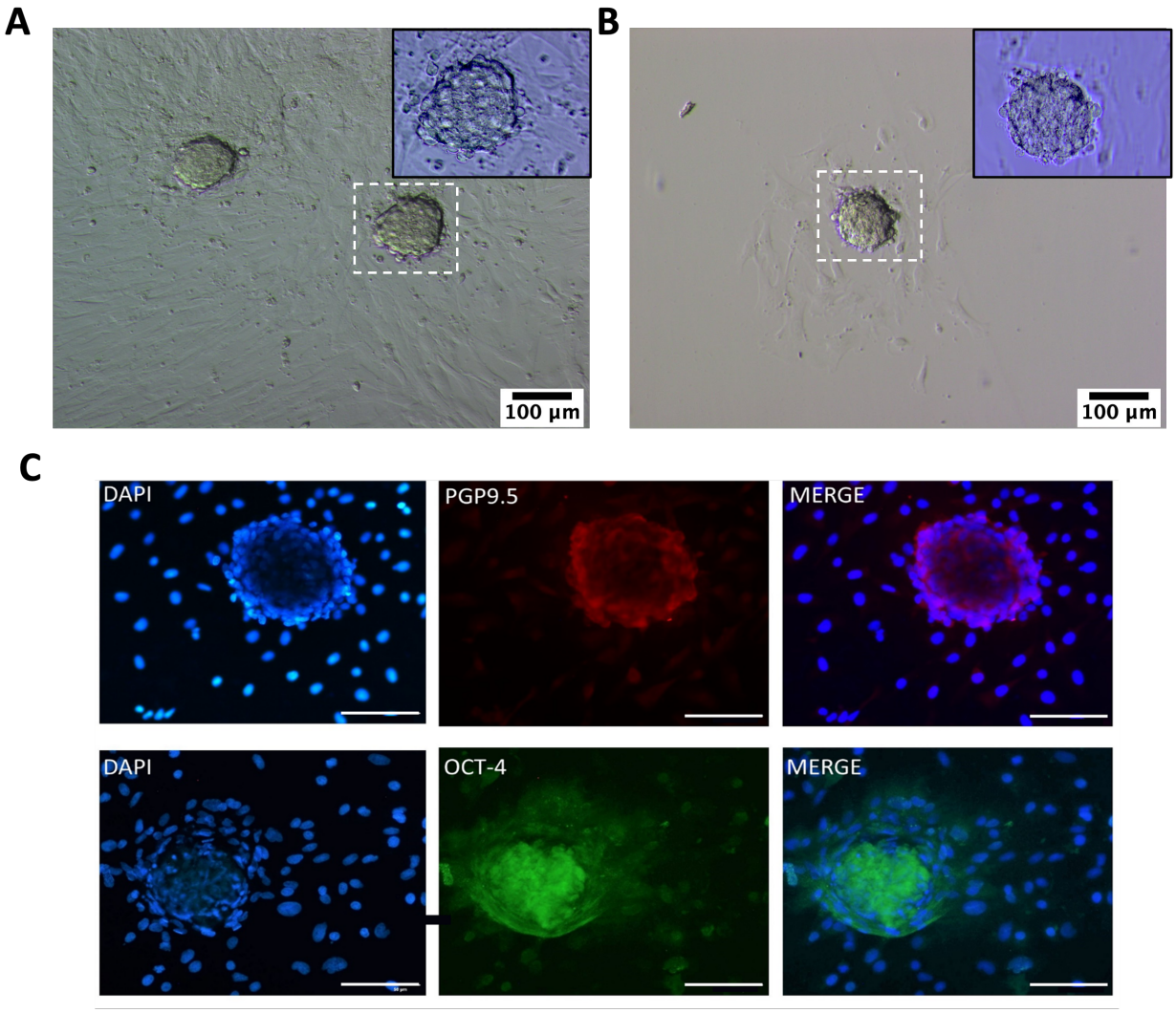

Figure 4-12. Subcultures of gonocyte colonies and immunofluorescence analysis of SSC colonies. A) Representative images of gonocyte colonies ready for subculture. Tightly packed dome-shaped gonocyte colonies with clear boundaries were picked for further culture. B) Representative images of subcultures of colonies that had been mechanically picked and transferred to a new culture dish. C) Immunofluorescence analysis of gonocyte colonies. Positive staining for the SSC marker PGP9.5. Positive staining for the stem cell marker OCT-4. Scale bar= 100 µm. Three biological replicates were carried out (n=3).

4.4 Discussion

Techniques for GC isolation and enrichment potentially enable GC transplantation or *in vitro* spermatogenesis. A two-step enzymatic method was first proposed for the isolation of prepubertal mouse testes in 1977 (Bellvé et al., 1977). This method has also been used to isolate testicular cells in humans (Moraveji et al., 2019), buffalo (Feng et al., 2016), sheep (Herrid et al., 2009), and mouse (Baazm et al., 2013). My results indicate that two-step enzymatic tissue dissociation with a 30 min incubation time is optimal for 2 mm^3 sections of neonatal testicular tissues and can completely dissociate tissue fragments into a single-cell suspension while maintaining high cell viability. The cell dissociation procedures included dispersion of the seminiferous cords *via* the degradation of the collagen surrounding the cords in the first step, and dissociation of the seminiferous epithelium into monodispersed cells in the second step. DNAse I was used to digest DNA that leaked from damaged cells into the dissociation medium, thereby protecting cells in the medium.

There are only very limited studies involving the isolation of gonocytes at earlier stages post-birth, such as from neonatal testes. Discontinuous Percoll density centrifugation selection and differential plating have been used to isolate gonocytes from 10- to 14-week-old prepubertal bull calves (Kim et al., 2014). In their study, gonocytes were collected from the interface of 20% and 40% Percoll density gradient layer with only 5% gonocytes in collected cells; while in differentiating plate with sequential incubation with laminin followed by gelatin, the percentage of gonocytes in selected cells reached 38%. However, my results in this chapter showed that Percoll density gradient centrifugation is more efficient than differential plating. Through discontinuous Percoll gradient density centrifugation, most gonocytes were retained in the 30–45% Percoll gradient fraction. My results also showed that gonocyte purificated by both Percoll gradient density and differential plating have similar cell viability or apoptosis

rate. Therefore, Percoll gradient density centrifugation selection is recommended as an effective method for gonocyte isolation from bovine neonatal testes.

Differential plates coated with laminin and gelatine have been used for the enrichment of bovine male gonocytes (Kim et al., 2014). Laminin has been proposed for SSC selection owing to the α-6 integrin receptors on the surfaces of mouse and bovine SSCs (Shinohara et al., 1999, de Barros et al., 2012). Giassetti et al. (2016) found higher percentages of GFRα-1 positive cells among non-adhered cells compared with adhered cells after incubation in laminin-coated, BSA-coated, and uncoated plates. Located in the centre of the seminiferous cords, gonocytes do not easily adhere or bind to ECM proteins; therefore, negative selection was used in my experiments to isolate gonocytes from somatic cells. Matrigel is a reconstituted extracellular matrix that mimics the natural basement membrane *in vitro*. The main protein components of Matrigel are laminin, collagen IV, and entactin. Therefore, Matrigel was used to coat differential plates to isolate gonocytes and somatic cells. The results indicated that differential plating helped to enrich bovine gonocytes and reduce the proportion of Sertoli cells. Increases in the proportion of gonocytes were observed among suspended cells after overnight incubation in both Matrigel-coated and uncoated differential plates. However, the suitable adherence time can vary and needs to be optimized; otherwise, a certain number of the gonocytes adhered to plates may be lost (He et al., 2015). The results of this study showed that gonocytes might adhere to the bottom of plates, which could lead to their loss. The somatic cell numbers remained relatively high compared with those obtained by Percoll density gradient centrifugation.

Morphology-based selection is a simple and low-cost method for gonocyte isolation. Sertoli cells grow faster than SSCs in culture; thus, it is necessary to check for and mechanically isolate SSC colonies for further passage and culture before the SSCs are overgrown by other cell types;

this requires an efficient technique (Guan et al., 2009). In some cases, colonies of gonocytes cannot be easily visualized or are mixed with somatic cells, which can lead to the loss of gonocytes. Moreover, some changes inside the cells can be missed if the first 7–10 days of cell culture is used for gonocyte enrichment in morphology-based selection. Therefore, discontinuous Percoll gradient density selection is regarded as a controllable, simple, and time-saving procedure for gonocyte enrichment. During cell passages, I mechanically collected gonocyte colonies to enrich the gonocyte number for further culture.

KSR has been commonly used in culture medium for the proliferation of embryonic stem cells in an undifferentiated state (Tsuji et al., 2008). My results indicated that KSR is a key factor in the formation of gonocyte colonies in 2D culture and 3D organoids, and that it affects the rate of cell migration inside the Matrigel dome and the boundary of organoids. For *in vitro* spermatogenesis, KSR has been used in culture medium to successfully induce the maturation of mice GCs to functional sperm. Sato et al. improved the culture medium from their previous experiment by replacing FBS with KSR after noting that FBS contains some factors that could suppress the progress of spermatogenesis (Sato et al., 2011a). These authors used KSR and B27 as serum replacements and found that KSR induced the expression of Acr-GFP (green fluorescent protein) and Gsg2-GFP, which are specific markers of meiosis and haploid cells. Lipid-rich BSA (AlbuMAX), one of the factors in KSR, was thought to be the most important critical component of KSR for the IVS of mice (Sato et al., 2011a). In 2015, rat ITTs cultured in KSR-supplemented medium were found to have increased seminiferous tubule diameter and induced the generation of spermatocytes and round spermatids (Liu et al., 2016a). SSCs grow efficiently, form “grape-shaped” colonies, and maintain their stemness *in vitro* with the support of KSR (Aoshima et al., 2013). In addition, primary cells are sensitive to some materials present in serum; thus, serum-free culture medium is a beneficial option for primary cell culture

(Aoshima et al., 2013). Reda et al. (2017) showed that KSR had a positive effect on the maturation of mouse GCs and on testosterone production. Gholami et al. (2018) found that the culture of GC colonies in soft agar with KSR and hormones enhanced the number and size of the colonies and promoted GC differentiation. KSR supplemented with melatonin and GlutaMAX has been successfully used for mouse IVS with an organ culture method (Reda et al., 2017). Therefore, KSR is recommended as a serum replacement for the culture of gonocytes in *in vitro* culture system.

In vivo, spermatogenesis occurs inside testes at a temperature that is 2–7°C lower than body temperature. My experimental results did not show any difference between the 34°C and 37°C groups in terms of cell viability and cell proliferation rate. This may have been because the experiments used neonatal (2-week-old) bovine testes. The results of an *in vitro* whole human testicular tissue culture indicated that an incubation temperature of 37°C led to an increased loss of tubular morphology and intratubular cell death at days 14 and 70 (Medrano et al., 2018). High temperatures were found to suppress self-renewal of SSCs but not cell apoptosis (Wang et al., 2019).

Gonocytes are located in the centre of the seminiferous cords and start to migrate to the basement membrane until 4–12 weeks after birth, when they start to transform into SSCs. Therefore in a 2-week-old calf, the majority of GCs are gonocytes. In mammals, the epithelial cells in testicular tubules exhibit an intimate relationship with ECM proteins (Alberts et al., 2002). The ECM provides essential physical support for cells, allowing cell–cell communications and cell migration. The components of the basement membrane of the seminiferous tubules include laminin, collagen IV, and fibronectin (Lai et al., 2002). Laminin and collagens support the migration of differentiating GCs from the basal lamina to the lumen by regulating junctional restructuring events. Changes in the localization of laminin and

collagen IV have been found in Sertoli-cell-only syndrome, cryptorchidism, and atrophy of the testes. This highlights the significance of the ECM for the normal functionality of the testes. Therefore, development of an appropriate *in vitro* culture system should include important ECM components to help the testicular cells to organize and interact in an appropriate manner. My results showed that four ECMs, laminin, collagen IV, Matrigel, and fibronectin, were beneficial in the formation of gonocytes colonies. Enriched cells cultured on laminin- or Matrigel-coated plates formed colonies faster; this may have been associated with interactions between the cell surface receptor integrin and laminin. Laminin was found to enhance cell proliferation and increase the activity and expression of stemness-related genes in neonatal mouse testicular cell colonies. Moreover, exposure to laminin can change the morphology of testicular cells and affect migration of cells during culture by upregulating the expression of molecules involved in cell migration, the secretion of cytokines, the induction of hypoxia response, and phosphatidylinositol-3-kinase (PI3K)/AKT and the mammalian target of rapamycin (mTOR) signalling (Au, Peng et al. 2021). ECM components play an important role in the microenvironment supporting the GCs; therefore, it is highly recommended that ECM components are used in gonocyte culture *in vitro*. More studies are needed to investigate the mechanism underlying the changes in GCs affected by ECM and other niche growth factors involved in self-renewal or differentiation.

4.5 Key findings

- Two-step digestion and a 30–40% Percoll gradient density gradient are efficient methods for dissociating testicular tissues and enriching bovine neonatal gonocytes.
- Enriched gonocytes from neonatal bovine testicular tissues form GC colonies characterized by GC markers PGP9.5 and PLZF and stem cell marker OCT4, with vimentin positive Sertoli cells forming a feeder layer at the outer edges. KSR significantly enhances the formation of gonocyte colonies in 2D culture.
- Laminin and Matrigel enhance the formation of gonocyte/GC colonies in 2D culture.

Chapter 5. The development of *in vitro* 3D organoid culture system for bovine gonocytes

5.1 Introduction

5.1.1 The formation and establishment of germ cell niche

SSCs are scattered throughout loops of seminiferous tubules in living animals, settling in the spaces between the basement membrane and the tight junctions of Sertoli cells. This niche allows them to provide support to SPG before they enter the meiosis stage. SSCs are regulated by the cells in the niches and factor regulation, which was described previously in **section 1.1.4.** SSC differentiation begins as these cells move away from a self-renewing niche to a differentiated niche and become dispersed over the entire basal compartment region of the seminiferous epithelium. The proper location and structure of the niche is essential for the fate of the GCs. In addition, evidence shows that this niche can be regenerated after tissue damage *in vivo*. This indicates that it is possible to reestablish the niche environment *in vitro* using tissue engineering technology.

Investigating the components of the GC niche is crucial for determining the regulation of spermatogenesis *in vivo* and the establishment of fertility restoration strategies using *in vitro* culturing techniques. The GC niche is essential for the regulation of stem cell self-renewal and differentiation abilities, ensuring a balance between these two processes (Lee et al., 2006). Located in the basal compartment of the seminiferous tubule, the niche supports and protects the most primitive SPG (Chiarini-Garcia et al., 2001b, Chiarini-Garcia et al., 2003). Undifferentiated SPG usually settle on the basement membrane next to the interstitial tissue and vasculature (Chiarini-Garcia et al., 2001a, Chiarini-Garcia et al., 2003, Yoshida et al., 2007a). The surrounding somatic cells that significantly contribute to the SSC niche include Sertoli cells, PMCs, peritubular macrophages, testicular endothelial cells, Leydig cells, and lymphatic endothelial cells; most of these cells provide support and produce factors to regulate

SSCs, directly or indirectly (Juho-Antti and Robin, 2019). For gonocytes, located in the center of the seminiferous tubules, the only cells that make direct contact are Sertoli cells. Sertoli cells are arguably the most important cellular components of the niche due to their direct contact with undifferentiated SPG (Oliver and Stukenborg, 2019) and they feed and support GCs. Sertoli cells secrete numerous paracrine factors, such as GDNF, which affects SSC behavior (de Rooij, 2009). PMCs provide structural support and also play a role in pushing luminal fluid towards the rete testis. In the interstitial tissue, the testosterone produced by Leydig cells influences the Sertoli cells and thus indirectly enhances colonization of SSCs in the testis (Ogawa et al., 1998). The maturation of somatic cells, and the establishment of the hypothalamus-pituitary-gonadal axis (HPGA) at puberty, lead to changes in the niche microenvironment, including the regulation of GDNF level and other endocrine factors; these events drive some SSCs in adult-type niches into differentiation (Shinohara et al., 2001, Tadokoro et al., 2002, Ventela et al., 2012).

The *in vitro* cultivation of GCs has been performed using different methods, including 2D, 3D, and organoid cultures. Physiological cell–cell and cell–matrix interactions are essential for regulating cell proliferation and differentiation, which contribute to maintaining the function and homeostasis of the tissue. While simplistic 2D monoculture models have their advantages, they lack proper representation of the cell–cell and cell–matrix interactions that are present in the natural tissue environment. The phenotype of purified primary cells is likely to change during culture in 2D culture systems. IVS has been achieved in rodents using organotypic and soft matrix culture systems. SSCs were able to proliferate and differentiate into spermatocytes after being cultured in a natural decellularized testicular 3D scaffold system (Rezaei Topraggaleh et al., 2019), indicating the importance of a reestablished SSC niche *in vitro*.

The ECM, consisting of a network of key macromolecules, modulates the maintenance,

proliferation, self-renewal, and differentiation of SSCs in the niches. It can also directly interact with stem cells through receptors for ECM–stem cell communication, and can also regulate SSC activities by presenting growth factors (Gattazzo et al., 2014). For this reason, the ECM has been used in 2D culture or 3D culture *in vitro* for regulating SSC self-renewal and differentiation. For example, a previous study showed that GCs from rats differentiated after 22 days of culture with ECM (Lee et al., 2006). 3D culture better mimics an *in vivo* situation by providing cells with a defined scaffold that resembles real living tissues in terms of their features and functions.

5.1.2 Factors that contribute to the niche

Similar to other adult stem cell niches, the gonocyte/SSC niche provides cells with proper architectural support as well as a growth factor milieu (Oatley and Brinster, 2012). During the prepubertal period, FSH, LH, and testosterone levels remain low; once puberty starts, AMH begins to decline while the serum levels of inhibin B, FSH, LH, and testosterone rise, thus resulting in testicular growth. Male puberty is initiated by the reactivation of HPGA, with major changes in the physiology of the testis, including increased testicular volume, hormonal and molecular modulation, and the initiation of spermatogenesis (Plant, 2015, Koskenniemi et al., 2017). The size and volume of the testis increase, and the tubular structure progressively forms clearly defined lamina and lumen (Rey, 1999). The process of spermatogenesis begins with a differentiating division of SSCs and SPG, followed by meiosis of the spermatocytes and finally the formation of round spermatids (Ogawa, 2001). GDNF (Naughton et al., 2006b, Chen and Liu, 2015), FGFs (Takashima et al., 2015b, Masaki et al., 2018), and RA (Raverdeau et al., 2012) are important growth factors that regulate SSC development. Pituitary hormones also

influence the behavior of testicular cells: FSH stimulates the proliferation of Sertoli cells and SPG, while testosterone and LH act more on completing spermatogenesis. In addition, the age of the niche cells themselves may also influence SSC behavior. The aging of niche cells can reduce the regenerative potential of stem cells, as shown for adult stem cells; exposure to systemic factors from younger individuals was shown to restore the regenerative function (Conboy et al., 2005). In addition, the limited supply of FGFs produced by lymphatic endothelial cells can regulate the self-organized density homeostasis of SSCs in the niche environment (Kitadate et al., 2019). To maintain the SSC population in the self-renewing state, exposure to a sufficiently high FGF stimulus is needed in the SSC niche. Proliferation of SSCs was enhanced when cultured *in vitro* with medium supplemented with LIF combined with GDNF (Wang et al., 2014).

The proliferation of gonocytes/SSCs has been successfully represented using 2D culture systems. However, in prepubertal/adult testes, gonocytes/SSCs are located within a 3D structure (seminiferous tubules), and direct cell-to-cell interactions play a critical role in their maintenance, proliferation, and development. Therefore, 3D representations of culture systems have been developed for the cultivation of cells or tissue fragments *in vitro*; these systems attempt to mimic the interactions and native arrangements between cells and the ECM. The two most commonly utilized 3D techniques for the culture of testicular cells *in vitro* are organ culture and supportive scaffolds in combination with dissociated cell culture. Organoids are 3D structures reconstructed by multiple cell types *in vitro* that have a similar cell architecture and functionality to *in vivo* native organs (Sakib, Voigt, *et al*., 2019). Organoid systems are based on the self-organizing capabilities of cells and create diverse multi-cellular tissue surrogates using novel bioengineering techniques (Yin *et al*., 2016). *In vitro* 3D organoid culture systems represent an attractive alternative for supporting the maintenance and

development of gonocytes/SSCs into their post-meiotic stages and therefore was investigated in this study.

In this Chapter, I report the development of 3D TOs in an *in vitro* culture system for the maintenance, proliferation, and possible spermatogenesis of gonocytes. The factors that affect the formation, storage, and development of gonocyte organoids were evaluated, including the optimal cell-seeding density, serum, replacement supplement, Matrigel ratio organoid cryopreservation, and growth factor treatments.

5.2 Methods

The collection of neonatal bovine testicular tissues was described in **Section 2.2.1.** Six testis from three different neonatal calves were used in this study. RT-qPCR analysis was described in **Section 2.2.4 and Section 2.2.5**. Digestion of freeze/thawed testicular tissues and enrichment of gonocytes/SSC using the Percoll density gradient were described in **Section 2.2.6** and **Section 4.2.1.**

5.2.1 3D culture of enriched gonocytes/SSCs

Enriched GCs were suspended in culture medium, mixed with Matrigel on ice at a ratio of 1:1, and then by carefully dispensed as 20 μL droplets on pre-warmed plates and incubated at 34°C for 30 min to polymerize the gel (**Figure 5-1**). A culture medium was added to cover the Matrigel dome after polymerization. Densities of 1×10^5 cells, 1×10^6 cells, and 1×10^7 cells per Matrigel droplet were used in the experiment. The basic culture medium was MEM-α medium, supplemented with 10% KSR and other supplements, as described in **Table 4-1**. Growth factors were added according to the experimental design (**Table 5-1**).

Table 5-1. Growth factors supplemented in culture medium for the culturation of testicular organoids (TOs).

Growth factor	Concentration	Manufacturer
FSH	10 IU/L	Sigma-Aldrich; T1500
Testosterone	10^{-6} M	Sigma-Aldrich; F4021
GDNF	20 ng/mL	Sigma-Aldrich; G1777
FGF2	2 ng/mL	Thermo Fisher; PHG0266
LIF	100 ng/mL	Thermo Fisher; PHC9484

FSH, follicle-stimulating hormone; GDNF, glial cell line-derived neurotrophic factor; FGF2, fibroblast growth factor 2; LIF, leukemia inhibitory factor.

The organoids were passaged by dissociating the Matrigel dome and reseeding cells (**Figure 5-1**). A pre-chilled 100 µL recovery solution was added to each well. The Matrigel matrix was destroyed by pipetting up and down gently using a pipette with wide bore tips. After mechanical separation, Matrigel with recovery solution was incubated at 4°C for 30–60 min. A depolymerized Matrigel matrix was checked by microscopy to determine whether organoids were floating free from the Matrigel. After a briefly centrifugation of the cultures, the recovery solution was removed, and organoids were washed with cold PBS. Then, organoids were dissociated using trypsin at 37°C and the level of dissociation was monitored under a

microscope. Dissociated TOs were washed with PBS and resuspended with a freshly made mixture of Matrigel and culture medium. The TOs easily adhered to the inside of pipette tips or tube walls, and therefore, the tips were pre-wetted with culture medium before the transfer of organoids to prevent organoid loss. Organoids were passaged every 10–14 days.

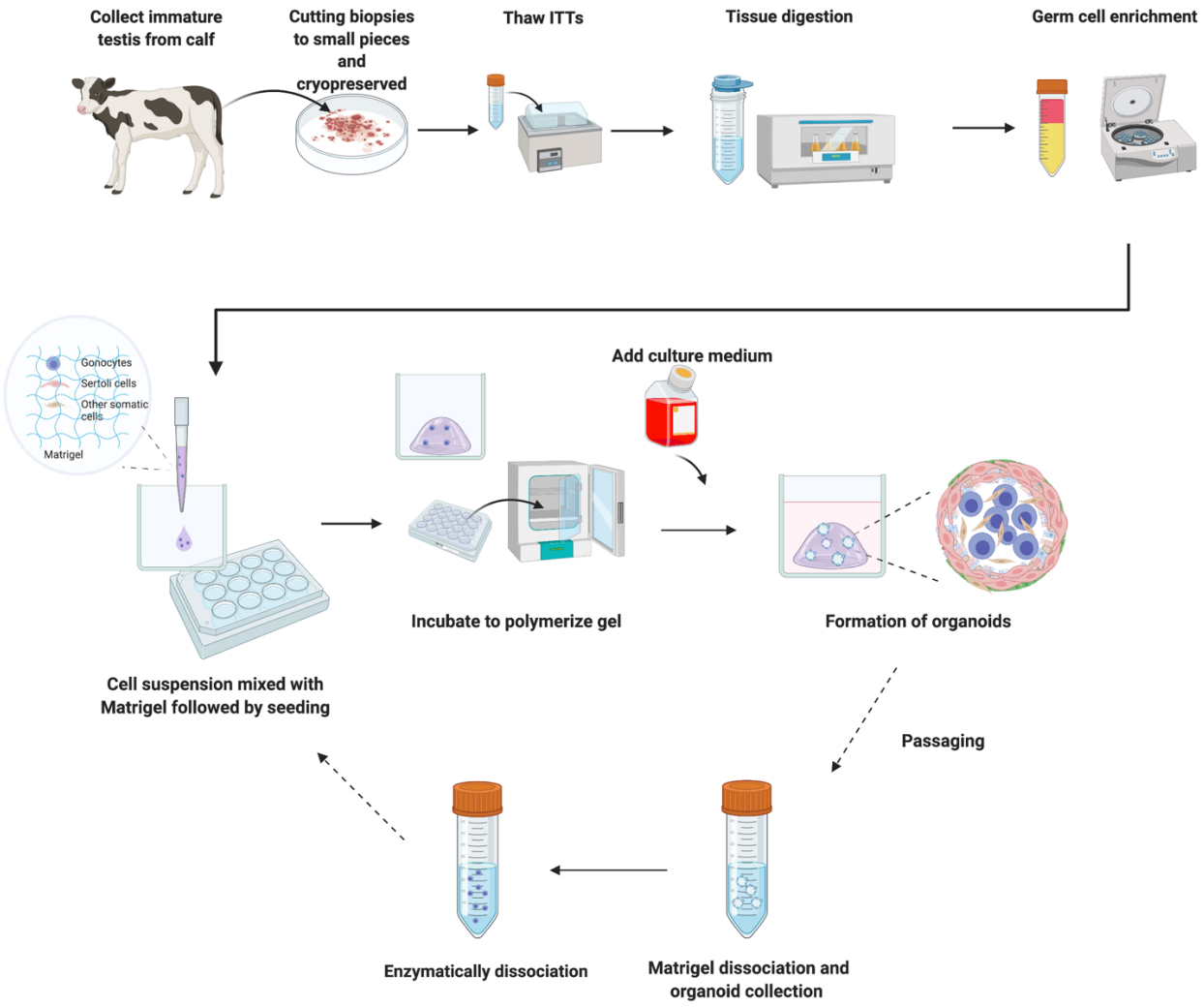

Figure 5-1. Establishment of 3D organoid *in vitro* culture system for gonocytes from neonatal bovine testis. After being frozen and thawed, the tissues were digested, and germ cells were enriched using a Percoll density gradient. The cells were suspended in culture medium and mixed with Matrigel on ice. The mixture was seeded as small droplets in 24-well culture dishes. The Matrigel-based 3D organoid culture system was put into the incubator for 30 min to allow the Matrigel to become gelled, and TOs were formed inside the Matrigel dome after a few days of *in vitro* culture. Organoids were passaged every 10–14 days. Matrigel was dissociated and removed, followed by enzymatic dissociation of organoids using trypsin. Dissociated cells and fragments were washed and resuspended in culture medium and seeded with Matrigel. Figure created by author on Biorander.com.

5.2.2 Cryopreservation and thawing of organoids

Organoids were cryopreserved intact in Matrigel fragments at a time point in the culture when they would otherwise be passaged. The number of organoids in each well was counted using a microscope. Mechanical separation of the Matrigel dome into fragments was performed by pipetting up and down gently with PBS-wetted 1000 µL tips. Matrigel fragments were washed with cold PBS before being transferred to cryovials. One mL of CPA was used in each cryovial with 50–100 organoids. Six cryoprotectants were used to cryopreserve organoids (**Table 5-2**). All cryovials were placed in a Mr. Frosty freezing container with isopropyl alcohol and transferred to a -80°C freezer for 24 h and then placed in LN_2 for long-term storage.

While the organoids were being thawed, cryovials were taken out from the LN_2 tank, immediately transferred to a 34°C water bath, and removed once thawed. To remove the remaining CPA, the organoids were washed in MEM-α medium with 0.1 M sucrose in a concentration of KSR or FSH that was consistent with the CPA used for cryopreservation.

Table 5-2. Cryoprotectant agents (CPAs) for cryopreservation of testicular organoids (TOs).

CPA		
Basic medium and supplement	MEMα, 0.1 M sucrose	
	DMSO	KSR or FBS
CPA 1	1 M	10% KSR
CPA 2	1 M	10% FBS
CPA 3	1 M	20% KSR
CPA 4	1 M	20% FBS
CPA 5	0.5 M	10% KSR
CPA 6	1.5 M	10% KSR

DMSO, dimethyl sulfoxide; FBS, fetal bovine serum; KSR, knockout serum replacement.

5.2.3 Cell viability and apoptosis in organoids

Cell viability was accessed using a live/dead cell image kit (Thermo Fisher; R37601), following the manufacturer's instructions. The cell apoptosis within the TOs was assessed using a DeadEnd Fluorometric TUNEL assay (Promega DeadEnd; G3250) in accordance with the manufacturer's instructions. Images were taken under a fluorescence microscope and analyzed with ImageJ (National Institutes of Health, Bethesda, Maryland, USA).

5.2.4 Immunocytochemical analysis of organoids

The immunocytochemical staining of TOs was optimized based on a protocol for all 3D organoids (Dekkers et al., 2019). To prevent the loss of organoids from sticking to the tips, 1% (wt/vol) PBS–BSA was used to precoat the tips used to transfer organoids. TOs were extracted from the Matrigel dome by incubating the dome with recovery solution at 4°C for 30 to 60 min. After washing with PBS, organoids were fixed by being immersed in 4% PFA for 30 min at room temperature. Organoid wash buffer (OWB) was used throughout the washing process during immunochemical staining, which contained 0.1% Triton X-100 and 0.1% BSA. To block the organoids, 1% (wt/vol) PBS–BSA was used for incubation at room temperature for 1 h. Primary antibodies (PGP9.5 and Vimentin) in optimized concentrations 1:100 diluted in OWB were used to incubate the organoids 24 h at 4°C. After three washes with OWB, an optimized concentration of secondary antibodies was used for 24 h incubation at 4°C, followed by three times washing and mounting using mounting medium with DAPI. Images were taken under fluorescence microscope or confocal microscope and were analyzed using and Volocity software (PerkinElmer, Waltham, Massachusetts, United States).

5.3 Results

Bovine abattoir testicular tissues were collected from slaughterhouse, which would be otherwise discarded. For the ethical aspect, Home Office licensing is not required in this case.

In vivo, GCs are located in a 3D niche in seminiferous tubules, where they are supported by Sertoli cells and membrane basements. In 2D culture, most cells appear in a flat monolayer, and GCs tend to form dome-shape colonies as described in **Section 4**. Therefore, after culturing gonocytes in a 2D culture system, I explored 3D culture for gonocytes, aiming to provide gonocytes with an *in vitro* microenvironment that is more similar to what appears *in vivo*. In a previous 2D ECM experiment, I compared the enriched growth of testicular cells on four ECM-coated plates and showed that Matrigel was the optimal ECM for the formation of gonocyte colonies. Moreover, Matrigel consists of multiple basement membrane proteins such as laminin and collagens, which make it suitable for rebuilding the microenvironment *in vitro*. Therefore, Matrigel was chosen for the subsequent 3D experiments. This section describes the optimization of the 3D Matrigel culture conditions for neonatal testicular cells, including seeding density, culture medium supplements, cell-seeding methods, organoid cryopreservation, and growing. Hormones were used to treat organoids to maintain the *in vitro* culture of gonocytes.

5.3.1 The effect of cell-seeding density on the formation of organoids

In 2D culture, gonocyte colonies were founded with an initial seeding density of 5×10^4 cells per well and 1×10^5 cells per well. To optimize the cell-seeding density in 3D culture and investigate the effects of cell density on the formation of organoids in 3D, three cell densities

were used: 1×10^5 cells, 1×10^6 cell, and 1×10^7 cell per Matrigel droplet (20ul) each well in 24-well-plate. The cell suspensions were mixed with Matrigel at a ratio of 1:1 to form a 20 ul dome-shape gel in each well; then, culture medium was added, and the system was incubated at 34°C. The formation of organoids was observed in all groups, beginning with the three seeding densities. After single-cell suspensions were seeded in Matrigel, gonocyte organoids started to form and show a boundary at day 2; therefore, the diameter and number of organoids were measured and counted. Organoids were passaged every 10 to 14 days, so at day 11 before organoid passage (**Figure 5-2A**), the diameter and number of the organoids in the three groups were compared. There were no differences in the diameter of organoids at day 2 among three groups. However, at day 11, the mean diameter of organoids in the 1×10^7 cell/well seeding group was 36.89±34.70 μm, significantly higher than the value of 28.76±26.99 μm in the 1×10^5 cell/well group ($p < 0.05$; **Figure 5-2B**). The typical diameter of 2-week-old neonatal testis tubules in vivo is 30-50μm. These results indicated that cells in the 1×10^7 cell/well group produced significantly more organoids than the other groups at day 2 and day 11 ($p < 0.05$, **Figure 5-2C**), with 5.41±1.79 /10^5 μm^2 at day 2 and 8.11±0.55/10^5 μm^2 at day 11.

The presence of GCs and Sertoli cells in TOs were confirmed by immunocytochemical staining with GC marker PGP9.5, PLZF and SC marker vimentin (**Figure 5-2D**). In 3D TO, a structure with GCs located at the centre of the organoids and most of the Sertoli cells in the surrounding was observed.

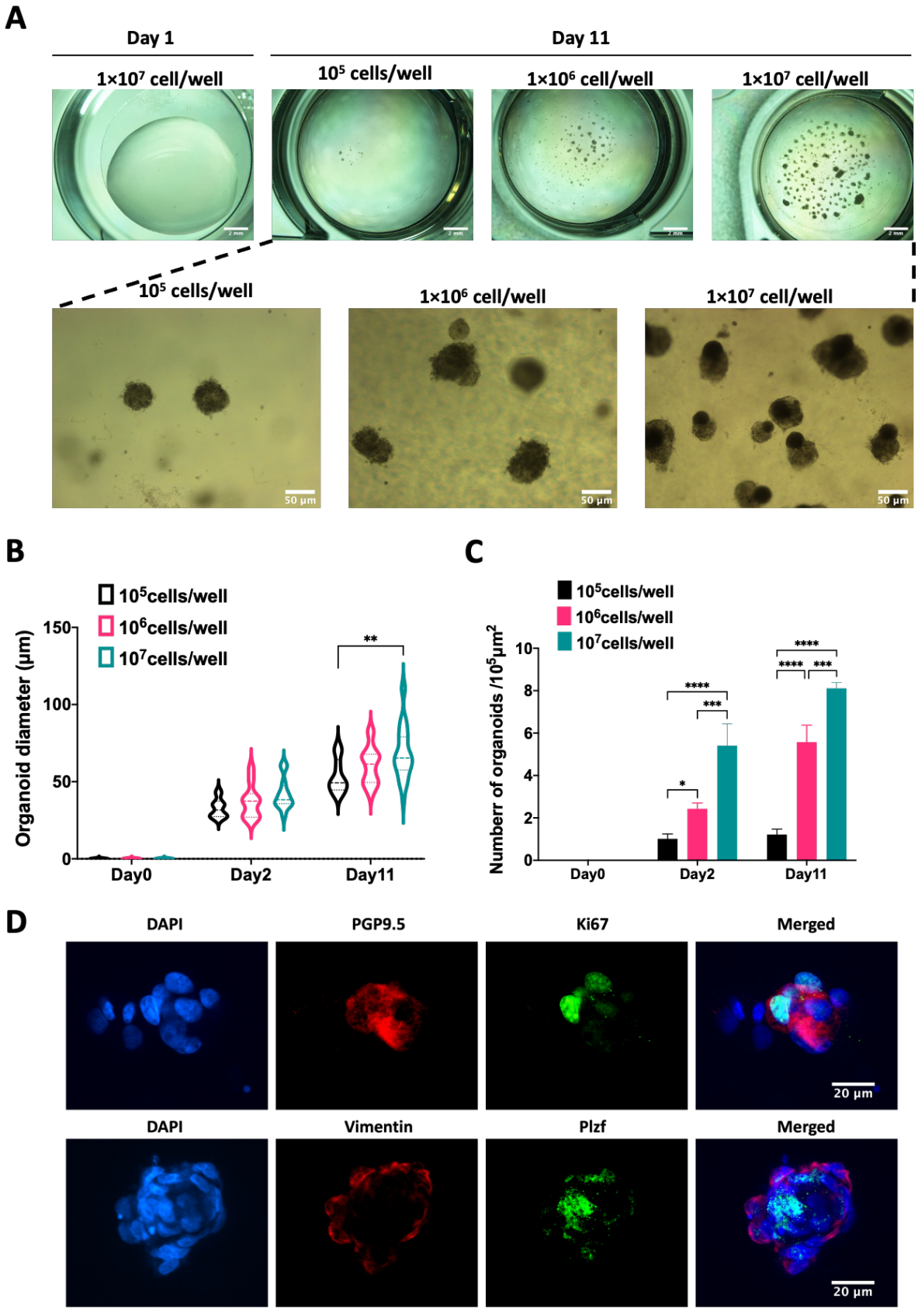
A
Day 1
Day 11
1×10⁷ cell/well
10⁵ cells/well
1×10⁶ cell/well
1×10⁷ cell/well
10⁵ cells/well
1×10⁶ cell/well
1×10⁷ cell/well
50 μm
50 μm
50 μm
B
10⁵cells/well
10⁶cells/well
10⁷cells/well
Organoid diameter (μm)
150
100
50
0
**
Day0
Day2
Day11
C
10⁵cells/well
10⁶cells/well
10⁷cells/well
Numberr of organoids /10⁵μm²
10
8
6
4
2
0
****
***
*
****
****
***
Day0
Day2
Day11
D
DAPI
PGP9.5
Ki67
Merged
20 μm
DAPI
Vimentin
Plzf
Merged
20 μm

Figure 5-2. Formation of organoids from enriched testicular cells seeded at different initial seeding densities in 3D Matrigel culture. A) Representative brightfield images of testicular organoids (TOs) after 1 day of culturing with initial seeding cells at 1×10^7 cell/mL. The Matrigel dome is clear and transparent. After 11 days of culturing, TOs were formed in three groups with 1×10^5 cell/mL, 1×10^6 cell/mL, and 1×10^7 cell/mL cell-seeding density. The scale bar in the top images = 2 mm. The scale bar in the bottom images = 50 µm. B) The diameters of organoids were measured for each group with different seeding densities. C) The number of organoids per 10^5 μm^2 was counted. D) Representative immunofluorescence images of TOs revealing the expression of PGP9.5, Ki67, vimentin and PLZF. Scale bar= 20µm. Three biological replicates were carried out (n=3). Data are shown as means ± standard deviations. *$p < 0.05$, **$p < 0.01$, ***$p < 0.001$, ****$p < 0.0001$.

5.3.2 The effect of serum-free culture on organoids

In this experiment, 10% FBS and 5%, 10%, and 15% KSR were used as supplements in culture medium as serum or serum replacement. Similar to the results for 2D culturing, no formation of organoids was observed in MEM-α + 10% FBS (**Figure 5-3A**). However, the formation of organoids was clearly observed in MEM-α+ 5% KSR, MEM-α+ 10% KSR, and MEM-α+ 15% KSR (**Figure 5-3B–D**).

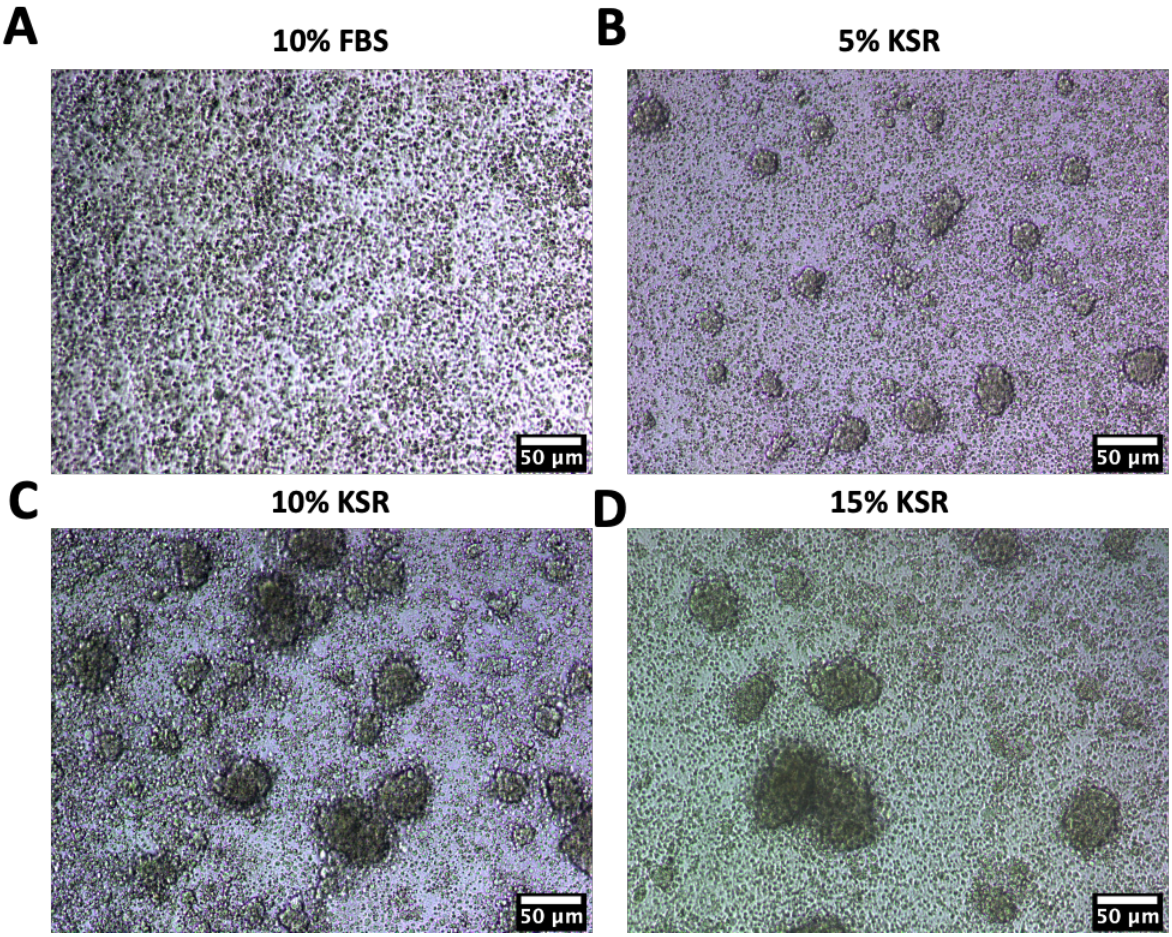

Figure 5-3. Formation of organoids cultured in culture medium supplemented with serum or serum replacement. A) No organoids formed in MEM-α medium with 10% fetal bovine serum (FBS) in the 3D Matrigel culture system. Organoids formed after 1 day of culturing in a 3D Matrigel culture system in MEM-α medium supplemented with 5% B), 10% C), or 15% D) knockout serum replacement (KSR). Scale bar = 50 µm. Three biological replicates were carried out (n=3).

5.3.3 The effect of cell-seeding method with Matrigel

Single-cell suspensions are usually mixed with Matrigel at a 1:1 ratio. In this experiment, I explored whether different mixtures of cell suspension and Matrigel would affect the formation of TOs. In a mixed-seed group, a single-cell suspension was mixed with the same volume of Matrigel at a 1:1 ratio to form an organoid mixture, and then one large droplet of mixture was carefully seeded into a plate and incubated at 37℃ for 10 min to allow the dome to polymerize. In an inside-seeding group and in an on-top-seeding group, a drop of Matrigel was incubated at 37℃ for 10 min for polymerization before the cell suspension was injected into the middle of or on top of the Matrigel dome. This process led to faster cell movement during culture to form organoids with clearer boundaries (**Figure 5-4**).

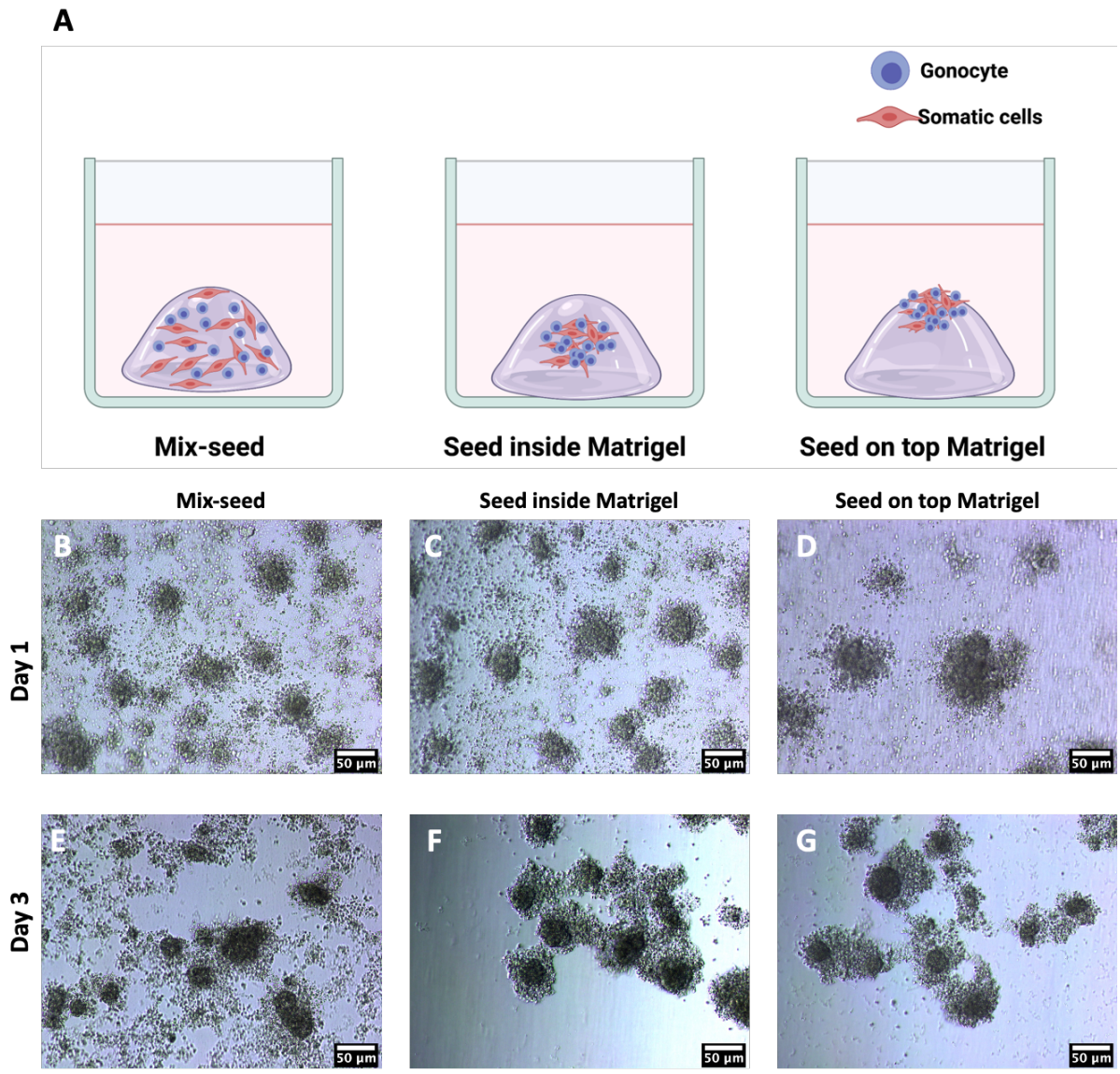

Figure 5-4. Formation of testicular organoids (TOs) in three cell-seeding methods in a 3D Matrigel culture system. A) Three methods of cell seeding. Testicular cell suspensions were mixed with the same volume of Matrigel (mixed seed) before cell seeding and cultured for 1 day B) and 3 days E). Cells were injected into Matrigel after 10 mins incubation (seed inside Matrigel) and were cultured for C) 1 day and F) 3 days. Cells were gently seeded on top of the Matrigel after 10 mins incubation (seed on top Matrigel) and cultured for D) 1 day and G) 3 days. Scale bar = 50 µm. Three biological replicates were carried out (n=3). Figure created by author on Biorander.com.

5.3.4 The cryopreservation of 3D organoids

Fresh testicular tissues are not always available, so frozen and thawed testicular tissues were used to generate organoids in this project. For clinical and practical purposes, a cryopreservation strategy is needed to preserve TOs. Cryopreservation is a promising method used to store and preserve organoids at cryogenic temperatures over the long term. In this experiment, TOs within a Matrigel dome were collected *in situ* and cryopreserved together using a slow-freezing method. In a previous experiment, KSR was found to be beneficial in the formation of gonocyte colonies or organoids, and could therefore be used as serum replacement in culture medium. Six CPAs were used to cryopreserve the organoids. After 30 days storage in LN_2, TOs were thawed, and their morphology, viability, and cell apoptosis were determined via brightfield microscopy, fluorescent live/dead cell staining, and TUNEL staining, followed by fluorescence microscopy. There was a significant difference between the viability of fresh organoids and post-cryopreserved organoids ($p < 0.05$; **Figure 5-5**). Cell viability in each group after cryopreservation was compared, and a significance difference was identified, with a cell viability 79.75±2.99% in the CPA3 group and 73.33±0.58% in the CPA5 group. Among the groups, the CPA3 group exhibited the highest cell viability, and was therefore chosen for the subsequent experiments.

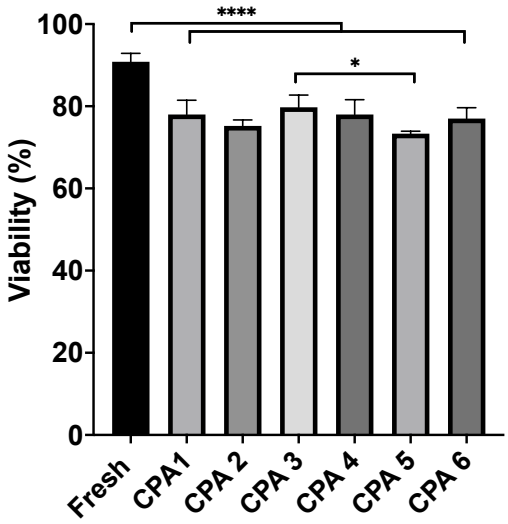

Figure 5-5. Cell viability before and after organoid cryopreservation. Cryoprotectant agent= CPA. *$p < 0.05$, **$p < 0.01$, ***$p < 0.001$, ****$p < 0.0001$. Three biological replicates were carried out (n=3).

5.3.5 The influence of growth factors on bovine gonocytes in Matrigel 3D culture

In this series of experiments, I investigated the effects of growth factors in the proliferation, stemness, and gene expression of enriched gonocytes in Matrigel 3D culture (**Figure 5-6A**). GDNF, FGF2, and LIF are important factors in the testis that regulate the self-renewal of GCs; FSH and testosterone are also associated with spermatogenesis. The basic culture medium consisted of MEM-α, additives (**Supplementary Table 1**), and 10% KSR. The basic culture medium was used in the control group. In the GDNF+FGF2+LIF (GFL) group, GDNF, FGF2, and LIF were added to the basic culture medium. In the FSH+ testosterone (FT) group, FSH and testosterone were added. The enriched gonocytes were cultured in a 3D Matrigel culture system and were able to form organoids in a short period of time, usually within 3 days after seeding. Cell viability was assessed at days 1, 7, 14, and 28 in the three groups, and dead cells

appeared in the centers of the organoids (**Figure 5-6B, D**). There was a significant difference in cell viability between the FT group and control group at day 28 of culture ($p < 0.05$). During culturing, the organoids in the three groups showed similar round shapes, with variation in size (**Figure 5-6C**). The mean size of the organoids was evaluated at days 3, 7, and 14 after cell seeding. Significant differences appeared between the three groups at days 7 and 14 ($p < 0.05$). The mean size of organoids at day 7 was 505.4±51.44 μm^2, 593.8±47.17 μm^2, and 380.0±40.25 μm^2 in the control, GFL, and FT groups, respectively. At day 14, the mean size of the organoids was 618.7±39.3 μm^2, 1030.00±116.5 μm^2, and 768.4±78.49 μm^2 in the control, GFL, and FT groups, respectively.

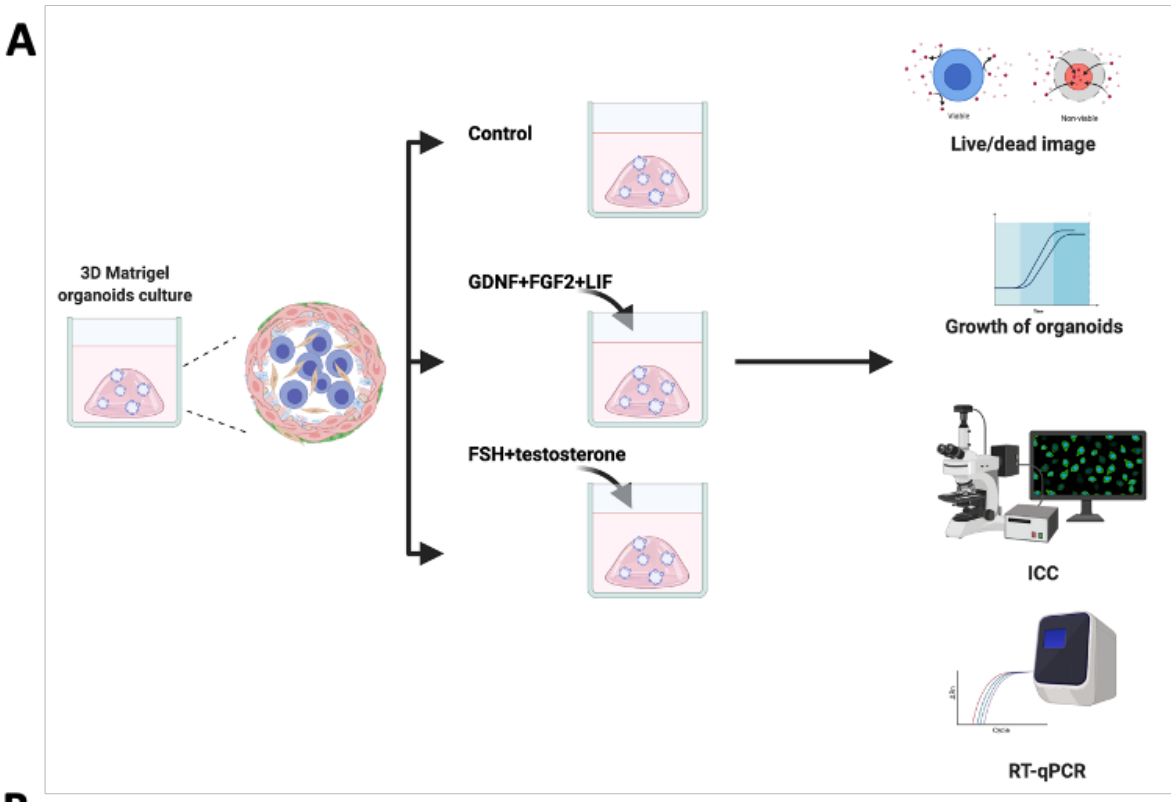
A
3D Matrigel
organoids culture
Control
GDNF+FGF2+LIF
FSH+testosterone
Live/dead image
Growth of organoids
ICC
RT-qPCR

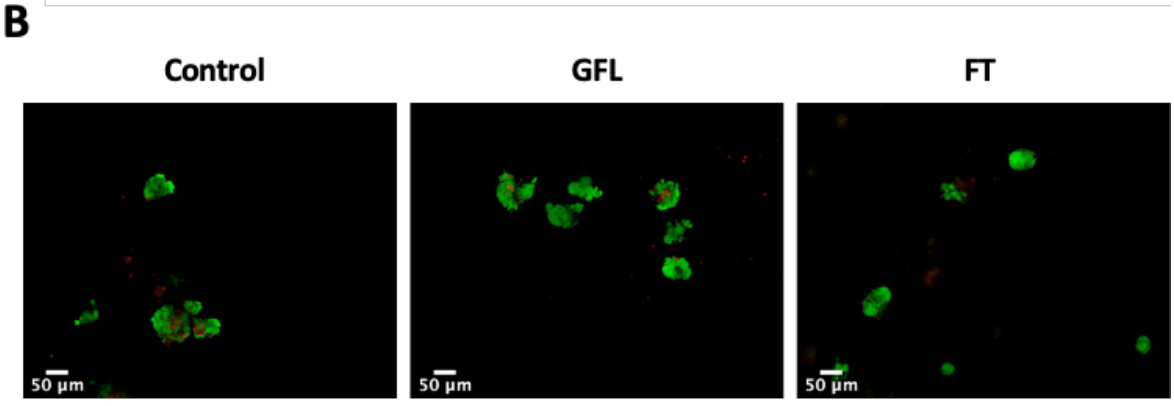
B
Control
GFL
FT
50 μm
50 μm
50 μm

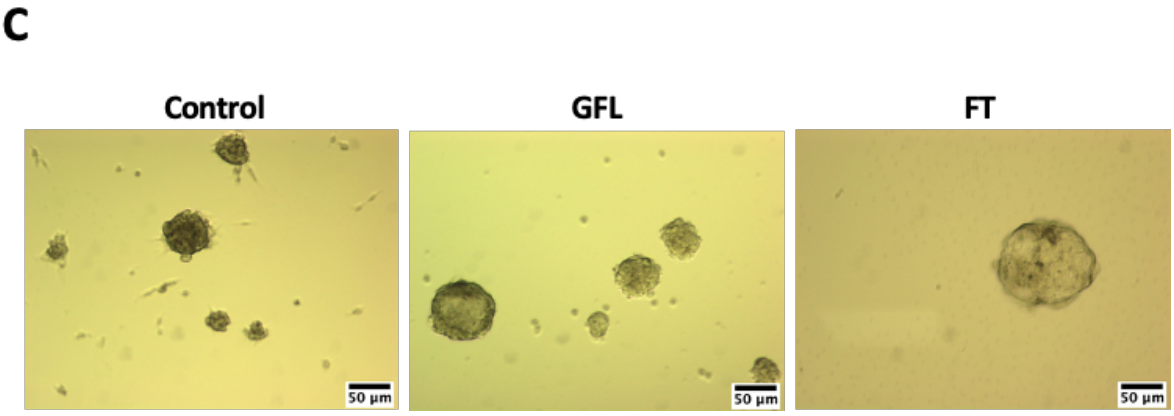
C
Control
GFL
FT
50 μm
50 μm
50 μm

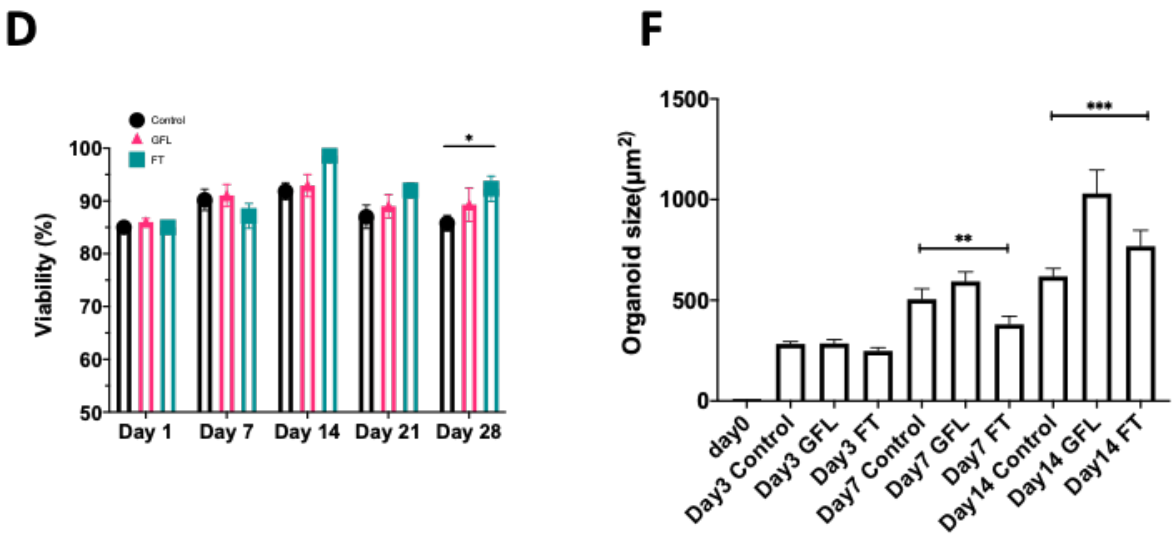

Figure 5-6. Effects of growth factors on testicular organoids (TOs) in *in vitro* growth. A) Experimental design: organoids were divided into three groups: the control group, GDNF+FGF2+LIF (GFL) group, and follicle-stimulating hormone (FSH) + testosterone (FT) group. All organoids were cultured for 28 days in a 3D Matrigel culture system. Figure created by author on Biorander.com. B) Representative viability images of organoids at day 28 of culture. C) Representative brightfield images of organoids at day 28 of culture. D) Viability of cells in organoids were accessed at days 1, 7, 14, 21, and 28. Data were presented as means ± SDs. E) Growth of organoids' size during the first 14 days after cell seeding in three groups. Scale bar = 50 μm. * $p < 0.05$, ** $p < 0.01$, *** $p < 0.001$, **** $p < 0.0001$. Three biological replicates were carried out (n=3).

Next, organoids were processed for immunocytochemistry to identify the types of cells within. Proliferating cells (Ki67 positive) were found in organoids at day 28 in the GFL group and the FT group, but fewer proliferating cells were found in the control group (**Figure 5-7A**). Gonocytes were identified in the GFL group but to a lesser degree in the control group and the FT group.

Rt-qPCR data showed that gonocyte markers and the expression levels of GFRα-1 level remained similar at day 14 after culturing in three groups but decreased significantly to 0.24±0.024 in the control group and 0.22±0.024 in the GFL group at day 28 ($p < 0.05$; **Figure**

5-7B). There was no significant change in the expression of the SSC marker gene *UCHL-1* (**Figure 5-7C**). The related gene expression level of *PLZF* was significantly reduced on day 14 in all three groups when compared to day 1 ($p < 0.05$; **Figure 5-7D**) and remained at a low level of expression at day 28. The expression of the spermatogenesis-related gene C-kit was 17.26±1.01 at day 28 in the GFL group was significantly higher than the gene expression level of 1.00±0.01 in the GFL group at day 1 and was 1.29±0.95 in the GFL group at day 14, 0.77±0.70 in the control group at day 28, and 0.43±0.15 in the FT group at day 28 ($p < 0.05$; **Figure 5-7F**).

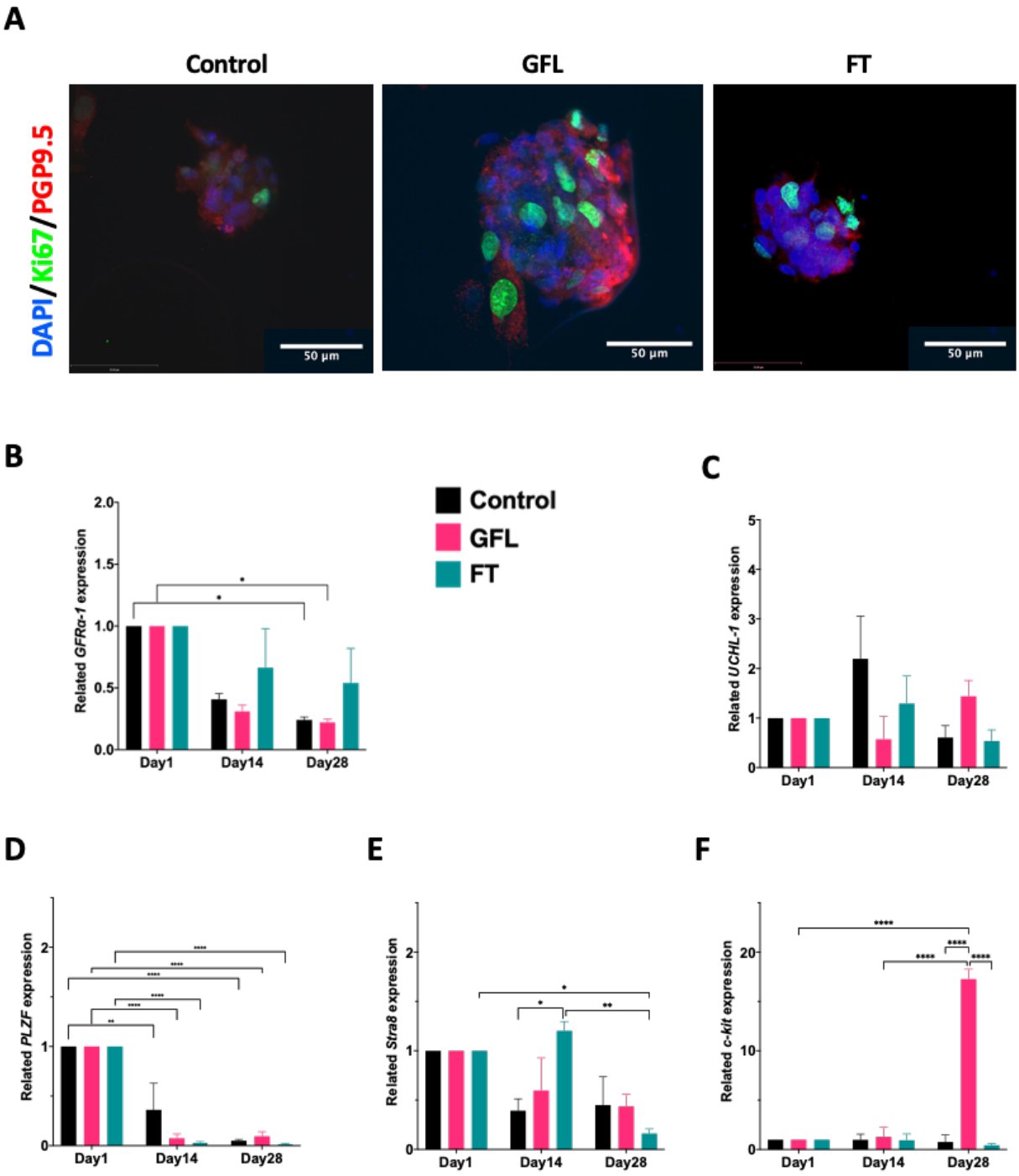

Figure 5-7. Immunocytochemical analysis and relative gene expression in gonocyte organoids in the control, GFL, and FT groups. A) Representative immunocytochemical analysis of gonocytes in three groups at culturing day 28. Positive staining for the germ cell marker PGP9.5 (red) and proliferating cell marker ki67 (green). The effects of different hormones on organoids were evaluated by comparing the expression levels of gonocyte-related genes: B) *GFRA-1*, C) *UCHL-1*, D) *PLZF*, E) *STRA8*, and spermatogenesis-related gene F) *C-KIT*. Three biological replicates were carried out (n=3). Data are presented as means ± SEMs. *$p < 0.05$, **$p < 0.01$, ***$p < 0.001$, ****$p < 0.0001$.

5.4 Discussion

In vitro culture provides a platform to study the cell behavior of cells. However, the development of sperm is a precisely controlled process of stepwise differentiation from the SSCs in the 3D microenvironment of the testes *in vivo*. The hierarchical nature of animals, including humans, makes the multi-level recapitulation of organoids achievable when cell–cell, cell-matrix, and cell–environment relationships are all found in a suitable model system (Yin *et al*., 2016). Significant progress in achieving complete spermatogenesis from SSCs to functional sperm has been made in mice through optimized classic organ culture *in vitro* (Sato *et al*., 2011). The *in vitro* cultivation of human SSCs has been developed using different methods, including 2D, 3D, and organoid means. The ECM is made up of a network of macromolecules that modulate the development and function of SSCs in the niche. ECM has been used in 2D and 3D cultures for SSC self-renewal and differentiation. A 3D culture mimics an *in vivo* situation by providing cells with a defined scaffold that is similar to that of real living tissues, incorporating the features and functions of different tissues. Physiological cell–cell and cell–matrix interactions are essential in cell proliferation and differentiation, which also maintain the function and homeostasis of the tissue.

If provided with an appropriate 3D scaffold and the necessary biochemical factors, cells from the testes self-organize to form tissue-specific organoids and provide GCs with a microenvironment that is similar to that which occurs *in vivo* (Alves-Lopes, Söder, and Stukenborg, 2017). Organoids are composed of cellular and non-cellular materials that are organized in a specific manner and exhibit internal and external interactions. In general, stem cells have the intrinsic capability to self-assemble into complex aggregates. Self-organized organoids including the intestine (Sato *et al*., 2009), the stomach (Barker *et al*., 2010), the prostate (Karthaus *et al*., 2014), and even prostate cancer (Boj *et al*., 2015) have all been

reproduced through the *in vitro* process. Stem cells are able to form organized clusters with specific structures when presented in a suitable matrix and optimal exogenous factors *in vitro* (Yin *et al*., 2016). *In vitro* culture systems provide the possibility for accessible observation, the retrieval of cells, controllable conditions, and multiple complex bioengineering approaches. An established organoid recapitulates a multitude of biological parameters in organs, such as cell–cell, cell–matrix, and cell–environment interactions, as well as spatial organization and physiological functions (Yin *et al*., 2016) and can therefore bridge the gap between *in vitro* culture and *in vivo* physiology by providing stable systems that can extend cultivation and manipulation.

The novel approach of developing TOs is the most promising method as it provides an SSC niche and cell–cell connections that mimic the *in vivo* microenvironment. In a previous study, primary human testicular cells were able to self-organize into functional organoids, where active niche cells and SPG could be maintained for up to 4 weeks (Baert *et al*., 2017). The newly formed organoids were able to secrete testosterone, inhibin B, and cytokines. Moreover, tight junction proteins have been found in Sertoli cells in organoids. Similarly, another study showed that human organoids from adult GCs, and immortalized Leydig and Sertoli cells cultured using the hanging drop method, could produce testosterone and support haploid GCs (Pendergraft *et al*., 2017). This 3D human-testis organoid model also has the potential to be used as a novel testicular toxicity-screening tool. In 2018, TOs were used to investigate Zika virus infections (Strange *et al*., 2018). Recently, researchers used a microwell culture system to generate a multicellular TO with a testes-specific morphology (Sakib, Uchida, *et al*., 2019), and found that GCs in the 3D TO experienced less cellular stress (a significantly lower amount of autophagosomes) than GCs in 2D culture. A 3D bioprinting method based on an alginate-based hydrogel was used as a novel culturing system to control scaffold design and cell

deposition, and post-meiotic cells were observed during cultivation (Baert *et al*., 2019). The 3D organoid was used in adult testicular culture and prepubertal testicular cell culture, but few studies have investigated gonocytes.

As described in this chapter, an *in vitro* Matrigel-based TO culture system derived from frozen/thawed neonatal bovine testicular cells was successfully developed. The initial cell-seeding density in each well is essential for organoid formation and the health of cells. In previously developed TO culture systems, varied initial cell-seeding densities, including 2.8 $\times 10^5$ cells/well, 5×10^5 cells/well, 6×10^5 cells/well, and 2×10^6 cells/well were used (Sakib et al., 2019, Edmonds and Woodruff, 2020, Cham et al., 2021). Higher concentration or after centrifugation were reported to promote the formation of seminiferous-tubule-like structures in rodents (Alves-Lopes et al., 2017). My results indicate that testicular cells self-assemble even in a relatively lower cell-seeding density in a culture platform. The requirement that a small number of testicular cells be used to initially form organoids might be helpful where only small tissues or limited testicular cells from humans or other species are available for research. A higher cell density, of 1×10^7 cell/well, increases the diameter and number of organoids formed in each well, but at the same time, may cause poor perfusion of nutrition and oxygen to cells inside the organoids. The diameter of organoids formed in the current 3D culture system is similar to the typical diameter of a neonatal testis tubule *in vivo* (30-50μm), which might reflect ease of nutrient and oxygen diffusion in the organoids formed *in vitro*. Dead cells and cellular apoptosis are easier to identify in the center of organoids with larger diameters using live/dead cell images and TUNEL staining data, which might be caused by lack of space, nutrient and oxygen for cells in the centre of organoids. Therefore, to better control the size and quality of organoids, a moderate cell-seeding density of 1×10^6 cell/well was considered an optimal initial cell-seeding density for generating neonatal bovine testis organoids.

Matrigel, a polymer-based gel, is commonly used in organoid culture. The biophysical features of Matrigel are highly dependent on the concentrations of polymer, which are crucial for the formation of organoids in different tissues. Knowing which conditions or properties are optimal for neonatal testicular cells was essential for my experiment. Matrigel is more fluid-like at low temperatures or shortly after incubation and becomes more solid-like over time, eventually settling to a consistent state after a few hours in an incubator. Furthermore, with an increase in polymer concentration, Matrigel exhibits progressively solid-like properties (Borries et al., 2020). In my preliminary experiments (data not shown), three concentrations of Matrigel (ratio) were tested: 33.3% (1:2), 50% (1:1), 66.7% (2:1). The organoids that grew in 66.7% Matrigel had visibly more branching at day 7, consistent with the pancreatic organoids in 75% Matrigel reported in a previous study (Borries et al., 2020). I also changed the way that initial cell seeding was performed to determine whether different seeding procedures would affect the formation of TOs. The cells migrated more rapidly when seeded on top or inside the Matrigel with 10 min incubation compared to cells suspended in culture medium and Matrigel mixture before incubation. This can be explained by the observation that when seeded inside or on top, the cells are suspended in culture medium and are freer and move more rapidly, making it easy for them to bind to each other and form cell clusters. Meanwhile, all cells/clusters are surrounded and supported by Matrigel, where they can maintain their 3D structure. Mixtures with 25% Matrigel or higher concentrations gradually become solid-like within 3 h and remain stable (Borries et al., 2020). Therefore, during the 10 min incubation at the beginning, the Matrigel dome was dominantly liquid-like, and the testicular cells injected within or on top of the Matrigel were able to migrate freely due the lower polymer concentration. It is possible that within a certain center region of the Matrigel dome, polymer concentrations are lower and thus cells in this area form organoids more rapidly. Interestingly, I found some cell bridges that

connect between nearby organoids. In some scenario, elongated cells tend to reach out and connect two organoids that were closed. But due to time limitations I was unable to investigate this further. More studies are needed to establish whether these are factors secreted by cells or from the ECM, which guides migration and changes the morphology of cells. It will also be interesting to see if there are some ways to encourage organoids to connect and form long tubules rather than symmetrical spheres, which might possibly be more physiological.

Cryopreservation strategies have been used to provide long-term storage options for organoids generated from different tissues, such as the colon, brain, intestines, and liver. The efficient and effective cryopreservation of organoids accelerates the development of organoid technology and clinical translation. The cryopreservation of intact organoids instead of dissociated organoids is recommended for intestinal organoids due to their better cell recovery (Han et al., 2017). During cryopreservation, cell morphology might change during the replacement of cryoprotectant inside cells. Therefore, to protect the structure of the organoids, I cryopreserved them *in situ* within the Matrigel dome. My results indicated that neonatal TOs could be generated from frozen/thawed neonatal testicular tissues and preserved by slow freezing. Uncontrolled slow freezing was performed in a Mr. Frosty freezing container for this experiment because this is a commonly used, easy, and cheap method of cryopreserving tissues or cells in a research laboratory. After thawing, over 70% of cells in the frozen/thawed organoids were viable, and their viability remained high in the subsequent culture. As noted previously, KSR is beneficial for forming gonocyte organoids. To maintain consistency with the organoid culture medium, KSR was used in the cryopreservation of prepubertal TOs for the first time and showed similar effectiveness to that of FBS without a loss of viability. Very few studies have investigated the cryopreservation of TOs. In a previous study, human adult TOs were cryopreserved by slow freezing and vitrification showed good viability after thawing

(Pendergraft et al., 2017). Vitrification has also been reported to efficiently cryopreserve porcine TOs and retain the defined interior-interstitial and exterior-seminiferous compartments (Sakib et al., 2019). However, the cited study reported reduced *GATA4* (Sertoli cell marker) expression and a more dispersed *SMA* (PMCs marker) distribution at day 7 of culture after thawing. My current cryopreservation strategy for preserving organoids within Matrigel provides an easy means of long-term storage for neonatal TOs. Cryopreservation of 3D organoids boosts their potential to be an accessible *in vitro* model for clinical use. In one study, better cell recovery and enhanced stem cell expansion were observed in frozen/thawed small intestine cell organoids within Matrigel, followed by encapsulation with an alginate shell (Lu et al., 2017). In the future, a Matrigel core within a hydrogel shell structure could be used for the large-scale culture and cryopreservation of whole organoids.

The main challenges for an *in vitro* GC culture system are survival, maintenance, proliferation, and maturation. In male GC cultures, growth factors are commonly used in short- and long-term SSC cultures. Only limited research has been performed on gonocyte cultures using growth factors. One reason for this may be that gonocytes only exist for a short time after birth, so their mechanisms are not fully understood. To study the possible maintenance and maturation of both gonocytes and Sertoli cells in TOs, growth factors, including GDNF, FGF2, LIF, FSH, and testosterone, were used for organoid culture. Sertoli cells play an important role in GC maintenance, self-renewal, and differentiation, as they are the only somatic cells to form a niche microenvironment in seminiferous tubules and directly interact with GCs. GDNF and FGF2 are important Sertoli cell growth factors that regulate the self-renewal of SSCs, and are commonly used in SSC cultures. GDNF regulates the self-renewal of SSCs through GDNF-RET-GFRA1 signaling (Naughton et al., 2006a, Jijiwa et al., 2008). GDNF/RET/GFRA1 activates the PI3K/AKT intercellular signaling pathways; this exerts influence on the

transcription factors *BCL6B, ETV5, LHX1, ID4,* and *POU3F1* that have been demonstrated to promote SSC self-renewal (Oatley et al., 2006, Lee et al., 2007a). FGF2, produced and released by mammalian Sertoli cells, drives *in vitro* SSC self-renewal by upregulating the *ETV5, BCL6B*, and *LHX1* genes *via* MAP2K1 activation (Ishii et al., 2012). SSC proliferation is also regulated by the autocrine activation of the PI3K/AKT and MAPK/ERK pathways by FGF2 (Zhang et al., 2012). FGF2 is involved in SSC expansion and the formation of GC colonies (Takashima et al., 2015a). LIF maintains the pluripotency of mouse embryonic stem cells and the self-renewal of SSCs. GDNF, FGF2, and LIF have been used for the long-term maintenance of porcine SSCs *in vitro* for up to 1 month in 2D cultures (Guan et al., 2006). I found that GDNF, FGF2, and LIF supplemented in culture medium resulted in larger organoids, consistent with the SSC expansion reported in a previous study (Takashima et al., 2015a). The increased size of GC colonies/organoids may be caused by the different cytoskeletal organizations due to GDNF and FGF2, which separately promote flat colony formation and colony clumping (Takashima et al., 2015a). A combination of the growth factors GDNF, FGF2, and LIF maintained the expression levels of the GC markers *UCHL-1* and *STRA8* and decreased the expression levels of the gonocyte marker *GFRα-1*, thus indicating the transformation from gonocytes to undifferentiated SSCs. Interestingly, a significant increase in *C-KIT* gene expression was observed at day 28 in organoids cultured with GDNF, FGF2, and LIF. *C-KIT* is thought to be associated with spermatogenesis. However, a previous study suggested that c-kit is associated with the migration of neonatal rat gonocytes to the basement membrane within 1 week after birth and is associated with the pseudopod that appear in gonocytes while migrating (Orth et al., 1997). It is possible that the expression of *c-kit* is suppressed and remains at a relatively low level in the testes of neonatal calves before the migration of gonocytes. When migration starts, the expression of the *c-kit* gene increases and

supports gonocyte migration *in vitro*. Immunocytochemical staining with the proliferating cell marker Ki67 showed a higher number of proliferating GCs (PGP9.5 positive) in organoids cultured with GDNF, FGF2, and LIF, thus indicating the transformation of gonocytes to proliferating SSCs.

After birth, the levels of FSH, LH, and testosterone increase during mini-puberty (Becker and Hesse, 2020). The FSH signaling pathway may be associated with gonocyte transformation in mice (Li et al., 2017). Testosterone can be generated by Leydig cells in immature mouse TOs as a result of LH stimulation during *in vitro* culture (Vermeulen et al., 2019, Edmonds and Woodruff, 2020) and it plays an important role in regulating SSC differentiation and spermatogenesis and is commonly used in SSC culture (Walker, 2011). In my 3D organoid culture system, gonocytes were enriched by Percoll gradients, and most selected cells were proven to be gonocytes and Sertoli cells, with only a very few Leydig cells remaining in enriched cells. Therefore, testosterone, instead of LH, was used as a supplemental growth factor in the culture medium. FSH and testosterone were added to supplement the culture medium to mimic the mini-puberty stage to induce gonocyte transformation into SSCs. Higher cell viability was detected at day 28 in the FSH and testosterone group, thus indicating that FSH and testosterone help to maintain the viability of testicular cells in organoid culture. The expression of the *STRA8* gene increased and then decreased during the 28 days of culture. However, no GC meiosis was detected during culture. The mean size of the organoids at 28 days was larger in cultured FSH and testosterone, and more Ki-67 positive cells were observed by immunocytochemical staining. These results indicated that FSH and testosterone stimulate the proliferation of cells in organoids. Further studies are now needed to investigate the mechanisms underlying the influence of gonadotrophin on the development of gonocytes.

5.5 Key findings

- For the first time, a 3D organoid culture system was developed for neonatal bovine gonocytes *in vitro*. Gonocytes in organoids were cultured *in vitro* up to 28 days. TOs were efficiently cryopreserved with good cell viability and little cell apoptosis for further use; 3D neonatal TOs are a novel tool for *in vitro* studies of GC development, cellular interactions, endocrinology, and toxicity.
- GDNF, FGF2, and LIF were found to promote the transformation of gonocytes into SSCs. FSH and testosterone were beneficial for maintaining the viability and proliferation of cells in organoids.

Chapter 6. Summary and future perspectives

As a result of the improvement in cancer therapies, the childhood cancer survival rate has been increasing in countries such as the UK (Ribeiro et al., 2008, Wasilewski-Masker et al., 2014b). An increasing number of cryopreservation centres worldwide are being established to provide reproductive tissue cryopreservation for young people with cancer to preserve their fertility. The recruitment of patients, collection and processing of tissues vary between different centres. So far, no global standard procedure has been set up for prepubertal reproductive tissue cryopreservation and tissue transportation. In **Chapter 2** of this thesis, I compared the effects of vitrification and slow freezing for the cryopreservation of bovine ITT.

When storing tissues, one of the most important things is the quality of tissues; this includes but is not limited to the following aspects: tissue quality during transportation and the cryopreservation process, tissue quality after thawing, and the potential for fertility restoration from the frozen/thawed tissues. To my knowledge, no study has investigated the effects of short-term storage before cryopreservation on neonatal testicular tissues. The study in **Chapter 3** investigated the tissue holding time before the cryopreservation process.

IVS is ideal for cancer patients, since this approach does not require immediate transplantation and avoids the risk of reintroducing cancer cells. To date, no study has reported *in vitro* complete spermatogenesis in ITTs from domestic animals, non-human primates or human. An effective *in vitro* platform is urgently needed to study the behaviour and regulation of GCs in their niches, and further development. To date, TOs have been established only in rodents, pigs, and humans. Studies in **Chapter 4 and 5** of this thesis shed light on a new bovine animal model to study TOs derived from neonatal testicular cells.

6.1 Vitrification as a potential alternative method for the cryopreservation of ITTs

The main goal of **Chapter 2** was to determine if vitrification could be a potential alternative cryopreservation method for prepubertal testicular tissues. In this study, vitrification was compared to traditional slow freezing methods with or without speed control in the cryopreserving neonatal bovine ITTs. USF is a commonly used method for cryopreserving tissues and CSF has been used in the OCTB. Different from mice, human and domestic animals such as bovine have a longer puberty period during which GCs are maintained in an undifferentiated stage. Therefore, the neonatal bovine ITTs used in this study are more similar and comparable to early-stage human ITTs. Results showed that there were no statistically significant differences between the three groups (vitrification, USF and CSF) in terms of GC and Sertoli cell evaluation through immunohistochemistry staining. Cell apoptosis was lower in vitrified testicular tissues than slow frozen tissues. However, when evaluating the effect of different cryopreservation methods on tissue structure, the percentage of seminiferous tubules attached to the basement membrane was lower in the vitrification group. *In vitro* culture showed similar results from the three groups. This study demonstrated that vitrification could effectively cryopreserve neonatal bovine testicular tissues that contain gonocytes, thus providing an alternative method for the cryopreservation of postnatal testicular tissues with gonocytes. The transformation from gonocytes to SSCs during the postnatal stage is important as this can directly affect the development of SSCs. The results of the current study are consistent with previous studies in Japanese quail (Liu et al., 2013), piglets (Kaneko et al., 2013), and new-born mice (Yokonishi et al., 2014a). Taken together, these findings suggest that vitrification could be used for the long-term storage of early-stage ITTs.

This study had two main limitations. Firstly, I evaluated the success of cryopreservation of calf neonatal testicular tissue only by evaluating *in vitro* culture; I did not evaluate the subsequent fertility function of these tissues. Secondly, only the expression levels of a few gonocyte-related genes were measured. It is now necessary to evaluate cryogenic damage during the long-term culture and transplantation of vitrified ITTs.

There are some questions that need to be answered before vitrification can be applied to human tissues. This study only tested vitrification on tissues from the postnatal stage. Since the structure of testicular tissues undergoes significant changes during the prepuberty period, whether vitrification is suitable for tissues at other stages remains unknown. Furthermore, the fertility function of vitrified tissues should be directly tested through xenografting or other approaches. Future research should aim to answer these questions using domestic animal models before application on human ITTs.

6.2 Short-term storage for up to 24 hours before cryopreservation could maintain ITTs in good condition

Generally, fresh human testicular biopsy should be sent for cryopreservation in tissue bank as soon as possible after collection to avoid compromising the samples. However, in some cases, a delay in the cryopreservation process is unavoidable. The purpose of **Chapter 3** of this thesis was to determine the effects of different tissue transportation times on ITTs. The tissue processing strictly followed the procedure for prepubertal human tissues at the OCTB in order to mimic the real conditions that human tissue biopsies will experience during tissue transportation and processing.

My results showed that there were no statistically significant differences in cell viability, percentage of Sertoli cells, the percentage of GCs and proliferating cells in tissues after the 48-hour transport period. However, the degradation in the structure of seminiferous cords increased in ITTs after 48 hours. Therefore, it is recommended that ITTs are processed for cryopreservation within 24 hours to protect their structure. The most important cells are the GCs, as these carry genetic information for the next generation. This study showed that SSC-related gene expression did not change for up to 48 hours of transportation time. However, the morphology of GCs, and the average occupied area of each GCs decreased after 48 hours. In previous studies, no neonatal testicular tissues have been investigated; this study shed light on the morphological changes in seminiferous tubules without formation the lumen. In Faes's study in 2017, adult human tissues were maintained for up to 3 days without the degradation of tissue morphology (Faes and Goossens, 2017). These authors also recommended keeping tissues in larger pieces to protect the morphology of tissues. During prepuberty, the size of the seminiferous tube, the formation of the lumen, and the age of patients, can all vary; thus, the effects of the length of transportation time on ITTs at different stages might also vary. It is possible that for testis in younger boys, the diameters of the seminiferous tubule in neonatal testes are smaller, immature Sertoli cells are more sensitive to the transport environment, therefore I detected significant changes in tissue morphology in the current study. Another reason may have caused morphology changes in the 48-hours group could be the size of the tissue fragments. The volume of the testes in prepubertal boys are smaller than those in adult; the amount of tissue that could be collected through surgery in clinic is limited. Therefore, small pieces of bovine ITTs were used in this study to be consistent with that in human ITTs.

It is unfortunate that this study did not include more biological replicates due the restricted access of tissues caused by the Covid-19 lockdown; more biological replicates are needed in

future. In practice, the success of a storage method should be measured by its ability to preserve a tissue's fertility function. Thus, xenotransplantation or IVS could be used as methods in the next step to examine the fertility function of frozen/thawed ITTs. The aim would be to ensure that human ITTs are in good condition and quality during and after transportation, therefore ideally this experiment should be repeated using human ITTs. Further studies need to investigate if testicular tissues from different age respond differently to delayed processing.

The findings of **Chapter 3** suggested that ITTs should be processed within 24 hours from collection to cryopreservation. However, the fertility function of these frozen/thawed ITTs with different delayed processing times has not yet been investigated and remain unknown. Tissue grafting or IVS could be used in subsequent experiments to explore the fertility function of these ITT fragments using the same bovine animal model. Further research should repeat the current experiment with prepubertal human testicular tissue from different ages that could represent different developed stages of testicular tissues.

6.3 3D testicular organoids (TOs) as *in vitro* models of germ cell biology

To address the lack of reliable 3D models of the neonatal testicular tissues, I optimized the dissociation and enrichment of GCs **(Chapter 4)** and developed a 3D organoid culture technique for neonatal testicular cells **(Chapter 5)**. For the first time, TOs were generated from bovine neonatal testicular cells.

There are two purposes to establish an *in vitro* culture system with an optimum microenvironment for testicular cells: i) for the propagation of GCs, and ii) for SSC

spermatogenesis. The GCs in neonatal testicular tissues are mainly gonocytes, which have the characteristics of both PGCs and SPGs. The isolation and enrichment of bovine gonocytes have not yet been fully understood. I optimized the protocols for isolating testicular cells from bovine ITTs using a two-step enzymic process that has been used for the isolation of testicular cells from rats ITTs (Alves-Lopes et al., 2018). A Percoll density gradient and differential plating were used for the enrichment of isolated GCs, and the expression of bovine GC markers was confirmed by immunocytochemical staining. In 2D culture, colonies of GCs were observed and confirmed by immunocytochemical staining with the GC marker PGP9.5. In addition, basic culture medium and serum replacement were also found to be directly associated with the formation of colonies in 2D culture. Culture medium MEM-α supplemented with 10% KSR was found to be the optimal basic culture medium to promote the formation of GC colonies and therefore was used for subsequent cell culture. Next, in order to select an optimal ECM for the culturation of GCs, I cultured enriched GCs on culture plates that were coated with four different ECMs (laminin, collagen IV, Matrigel and fibronectin). Matrigel was found to be the optimal ECM for GC culture because of a higher number and less variability in the size of the colonies formed in Matrigel coated plates. Immunocytochemical staining confirmed that GCs were located at the centre of the colonies surrounded by Sertoli cells at the outer layers.

Next, the *in vitro* culture system was shifted from 2D to a more complex 3D organoid system. This was necessary, as traditional 2D culture is not tractable and cannot provide long-term support for GCs. Matrigel was subsequently used in the formation of 3D TOs. To start with, I improved and simplified a method reported previously (Alves-Lopes et al., 2018) for bovine TOs by optimizing the cell seeding density and Matrigel ratio. In clinical practice, testicular biopsy fragments are small and only 10% of the tissue biopsy can be used for scientific research; therefore the amount of GCs available to human research is limited. In **Section 5.3.1,**

I confirmed that by using the optimized method designed in this thesis, TOs could be formed even with low cell density; this could be beneficial when this system is applied to human ITT fragments. Similar to the GC colonies in 2D culture, the organoids formed in 3D system had a structure with GCs located at the centre of the organoids and most of the Sertoli cells in the surrounding. Compared to normal serum FBS, the serum replacement KSR was found to promote the formation of TOs; this is consistent with results from 2D culture. However, the mechanism underlying this is not yet fully understood. Different cell-seeding methods were investigated in this study. Interestingly, incubating the Matrigel before cell seeding accelerated the formation of organoids; this can be explained by the effect of polymerization of Matrigel on the migration of cells within Matrigel.

Another important issue is the storage of the organoids. Previously, only one study has reported the cryopreservation of TOs in LN_2; this was for only 7 days (Pendergraft et al., 2017). In **Section 5.3.4**, I optimized the CPAs and proposed an optimal CPA for the long-term cryopreservation of ITT organoids. After thawing, the morphology of organoids remained good and cell viability remained over 70%. This optimized protocol for cryopreserving TOs could potentially be used for the storage and transportation of large-scale 3D organoid models.

As described in **Section 1.1.1**, the HPG axis and related growth factors play an important role in testis development, self-renewal, and the differentiation of SSC in niches. In **Section 5.3.5**, a number of growth factors that are essential for self-renewal, expansion and spermatogenesis of GCs was applied in the culture of TOs; these growth factors include GDNF, FGF2, LIF, FSH and testosterone. Size, morphology, and cell viability of TOs were evaluated. GDNF, FGF2 and LIF were found to be associated with the growth of organoid size and the transformation of gonocytes to SSCs. FSH and testosterone were found to improve cell viability of organoids and proliferation of testicular cells in a long-term culture.

In conclusion, the analysis of neonatal bovine TOs undertaken here has extended our knowledge of the in vitro culture of gonocytes and methodology for establishing a 3D TO culture system using a new domestic animal model; this 3D model provides a physiologically similar microenvironment that allows cell-cell contacts, cell re-aggregations, long-term *in vitro* culture and GC transformation into SSCs.

This study has some limitations. Firstly, due to the restriction on sample collection and access to the laboratory caused by Covid-19 lockdown, only a small number of biological replicates were included in this study. Secondly, only a few gonocyte-related genes expressions were evaluated in this study to examine changes of the GCs. Lastly, the fertility function of the GCs and potential maturation of other somatic cells were not investigated in this study due to time constraints.

6.3.1 Unanswered questions and future directions

There are a number of unanswered questions surrounding the role of TOs. For example, since cells are the most important components in TO, would the ratios of different types of testicular cells affect the self-assembly and other functions of the TOs? How do other vital soluble niche factors, such as RA, WNT and NOTCH, regulate TOs? To improve the TO system, would other organ culture methods such as the hanging drop approach and gas-liquid approach be beneficial to the culturation of TOs or promote the formation of a tubular-like structure?

This current TO model provided evidence that neonatal bovine testicular cells were able to self-assemble into organoids. In rats, the self-assembly of testicular cells appears to be age-dependent (Alves-Lopes et al., 2017). I would be interesting to know if testicular cells in

domestic animals or humans have similar characteristics. The self-assembly of testicular cells could provide the possibility to study GC biology in organoid systems with the potential for *in vitro* propagation and spermatogenesis. Therefore, further research might explore whether this organoid model could be applied to bovine testicular cells at different ages, and whether GCs at different stages could survive and develop in this re-established microenvironment.

The work in the current study mainly focused on GCs in the organoids; however, the roles of other somatic cells such as Sertoli cells and Leydig cells in organoids have not yet been fully investigated. As normal testicular tissues have the function of androgen secretion, experiments are needed to investigate the endocrine function of TOs as mini tissue units. In previous studies, the secretion of testosterone and inhibin B in prepubertal mice TOs (Edmonds and Woodruff, 2020) and adult and pubertal human TOs (Baert et al., 2017) have been reported. The prepubertal TOs developed in this thesis could be used to further investigate the endocrine function in a prepubertal TOs model in domestic animal models or humans.

Moving from animal models to humans, TOs could be used as i) a powerful *in vitro* research platform; ii) a potential fertility restoration strategy, and iii) an effective screening tool for drug toxicity detection. Since the gene profiles, signalling pathways and molecular regulation in human SSC niches (Mäkelä and Hobbs, 2019) have been increasingly revealed over recent years, this TO system could potentially be a useful platform that allows cell manipulation and monitoring for fundamental human GC biology research. An important potential future clinical application of human TOs is to provide the appropriate microenvironment for GC propagation and spermatogenesis (Pendergraft et al., 2017); this would help patients whose testicular tissues are contaminated by cancer cells to restore their fertility. In addition, similar to organoids derived from other organs, TOs could potentially replace the existing experimental models as

a more reliable and time-saving screening tool by providing mini tissue units that are highly similar to real human tissues.

List of references

Abofoul-Azab M, Lunenfeld E, Levitas E, Zeadna A, Younis JS, Bar-Ami S & Huleihel M. Identification of Premeiotic, Meiotic, and Postmeiotic Cells in Testicular Biopsies without Sperm from Sertoli Cell-Only Syndrome Patients. *International Journal of Molecular Sciences* 2019;20**,** 470.

Abrishami M, Anzar M, Yang Y & Honaramooz A. Cryopreservation of Immature Porcine Testis Tissue to Maintain Its Developmental Potential after Xenografting into Recipient Mice. *Theriogenology* 2010;73**,** 86-96.

Abu Elhija M, Lunenfeld E, Schlatt S & Huleihel M. Differentiation of Murine Male Germ Cells to Spermatozoa in a Soft Agar Culture System. *Asian Journal of Andrology* 2012;14**,** 285-293.

Al-Haboby AH. *Influence of Neonatal Hemiorchidectomy on Bovine Testicular Development and Plasma Hormone Levels*. University of Minnesota.1986.

Alberts B, Johnson A, Lewis J, Raff M, Roberts K & Walter P. *Molecular Biology of the Cell*. New York, Garland Science.2002.

Allen CM, Lopes F, Mitchell RT & Spears N. Comparative Gonadotoxicity of the Chemotherapy Drugs Cisplatin and Carboplatin on Prepubertal Mouse Gonads. *Molecular Human Reproduction* 2020;26**,** 129-140.

Alves-Lopes JP, Söder O & Stukenborg J-B. Use of a Three-Layer Gradient System of Cells for Rat Testicular Organoid Generation. *Nature Protocols* 2018;13**,** 248-259.

Alves-Lopes JP, Söder O & Stukenborg JB. Testicular Organoid Generation by a Novel In vitro Three-Layer Gradient System. *Biomaterials* 2017;130**,** 76-89.

Amann RP, Johnson L, Thompson DL & Pickett BW. Daily Spermatozoal Production, Epididymal Spermatozoal Reserves and Transit Time of Spermatozoa through the Epididymis of the Rhesus Monkey. *Biology of Reproduction* 1976;15**,** 586-592.

Aoshima K, Baba A, Makino Y & Okada Y. Establishment of Alternative Culture Method for Spermatogonial Stem Cells Using Knockout Serum Replacement. *PLoS ONE* 2013;8**,** e77715.

Aponte PM, Soda T, Teerds KJ, Mizrak SC, van de Kant HJ & de Rooij DG. Propagation of Bovine Spermatogonial Stem Cells in Vitro. *Reproduction* 2008;136**,** 543-557.

Arnold K, Sarkar A, Yram Mary A, Polo Jose M, Bronson R, Sengupta S, Seandel M, Geijsen N & Hochedlinger K. Sox2+ Adult Stem and Progenitor Cells Are Important for Tissue Regeneration and Survival of Mice. *Cell Stem Cell* 2011;9**,** 317-329.

Ashouri Movassagh S, Ashouri Movassagh S, Banitalebi Dehkordi M, Pourmand G, Gholami K, Talebi A, Esfandyari S, Jabari A, Samadian A & Abbasi M. Isolation, Identification and

Differentiation of Human Spermatogonial Cells on Three-Dimensional Decellularized Sheep Testis. *Acta Histochemica* 2020;122**,** 151623.

Awang-Junaidi AH & Honaramooz A. Optimization of Culture Conditions for Short-Term Maintenance, Proliferation, and Colony Formation of Porcine Gonocytes. *Journal of Animal Science and Biotechnology* 2018;9**,** 8.

Baazm M, Abolhassani F, Abbasi M, Habibi Roudkenar M, Amidi F & Beyer C. An Improved Protocol for Isolation and Culturing of Mouse Spermatogonial Stem Cells. *Cellular Reprogramming* 2013;15**,** 329-336.

Baert Y, De Kock J, Alves-Lopes JP, Söder O, Stukenborg JB & Goossens E. Primary Human Testicular Cells Self-Organize into Organoids with Testicular Properties. *Stem Cell Reports* 2017;8**,** 30-38.

Baert Y, Dvorakova-Hortova K, Margaryan H & Goossens E. Mouse in Vitro Spermatogenesis on Alginate-Based 3d Bioprinted Scaffolds. *Biofabrication* 2019a;11**,** 035011-035011.

Baert Y, Dvorakova-Hortova K, Margaryan H & Goossens E. Mouse in Vitro Spermatogenesis on Alginate-Based 3d Bioprinted Scaffolds. *Biofabrication* 2019b;11**,** 035011.

Baert Y & Goossens E *Preparation of Scaffolds from Decellularized Testicular Matrix.* 2018. Humana Press Inc.

Baert Y, Ruetschle I, Cools W, Oehme A, Lorenz A, Marx U, Goossens E & Maschmeyer I. A Multi-Organ-Chip Co-Culture of Liver and Testis Equivalents: A First Step toward a Systemic Male Reprotoxicity Model. *Human Reproduction* 2020;35**,** 1029-1044.

Baert Y, Stukenborg JB, Landreh M, De Kock J, Jörnvall H, Söder O & Goossens E. Derivation and Characterization of a Cytocompatible Scaffold from Human Testis. *Human Reproduction* 2015;30**,** 256-267.

Baert Y, Van Saen D, Haentjens P, In't Veld P, Tournaye H & Goossens E. What Is the Best Cryopreservation Protocol for Human Testicular Tissue Banking? *Human Reproduction* 2013;28**,** 1816-1826.

Bahadur G, Chatterjee R & Ralph D. Testicular Tissue Cryopreservation in Boys. Ethical and Legal Issues: Case Report. *Human Reproduction* 2000;15**,** 1416-1420.

Barker N, Huch M, Kujala P, van de Wetering M, Snippert HJ, van Es JH, Sato T, Stange DE, Begthel H, van den Born M, Danenberg E, van den Brink S, Korving J, Abo A, Peters PJ, Wright N, Poulsom R & Clevers H. Lgr5(+Ve) Stem Cells Drive Self-Renewal in the Stomach and Build Long-Lived Gastric Units in Vitro. *Cell Stem Cell* 2010;6**,** 25-36.

Becker M & Hesse V. Minipuberty: Why Does It Happen? *Hormone Research in Paediatrics* 2020;93**,** 76-84.

Bellve AR, Cavicchia J, Millette CF, O'brien DA, Bhatnagar Y & Dym M. Spermatogenic Cells of the Prepuberal Mouse: Isolation and Morphological Characterization. *Journal of Cell Biology* 1977;74**,** 68-85.

Bellvé AR, Cavicchia JC, Millette CF, O'Brien DA, Bhatnagar YM & Dym M. Spermatogenic Cells of the Prepuberal Mouse. Isolation and Morphological Characterization. *Journal of Cell Biology* 1977;74**,** 68-85.

Bergadá I, Milani C, Bedecarrás P, Andreone L, Ropelato MG, Gottlieb S, Bergadá C, Campo S & Rey RA. Time Course of the Serum Gonadotropin Surge, Inhibins, and Anti-Müllerian Hormone in Normal Newborn Males During the First Month of Life. *Jounal of Clinical Endocrinology & Metabolism* 2006;91**,** 4092-4098.

Bhakta N, Force LM, Allemani C, Atun R, Bray F, Coleman MP, Steliarova-Foucher E, Frazier AL, Robison LL, Rodriguez-Galindo C & Fitzmaurice C. Childhood Cancer Burden: A Review of Global Estimates. *The Lancet Oncology* 2019;20**,** e42-e53.

Bhang DH, Kim BJ, Kim BG, Schadler K, Baek KH, Kim YH, Hsiao W, Ding BS, Rafii S, Weiss MJ, Chou ST, Kolon TF, Ginsberg JP, Ryu BY & Ryeom S. Testicular Endothelial Cells Are a Critical Population in the Germline Stem Cell Niche. *Nature Communications* 2018;9.

Blendy JA, Kaestner KH, Weinbauer GF, Nieschlag E & Schütz G. Severe Impairment of Spermatogenesis in Mice Lacking the Crem Gene. *Nature* 1996;380**,** 162-165.

Boitani C, Politi MG & Menna T. Spermatogonial Cell Proliferation in Organ Culture of Immature Rat Testis1. *Biology of Reproduction* 1993;48**,** 761-767.

Borries M, Barooji YF, Yennek S, Grapin-Botton A, Berg-Sørensen K & Oddershede LB. Quantification of Visco-Elastic Properties of a Matrigel for Organoid Development as a Function of Polymer Concentration. *Frontiers in Physics* 2020;8.

Braye A, Tournaye H & Goossens E. Setting up a Cryopreservation Programme for Immature Testicular Tissue: Lessons Learned after More Than 15 Years of Experience. *Clinical Medicine Insights: Reproductive Health* 2019;13**,** 1179558119886342.

Brinster RL & Zimmermann JW. Spermatogenesis Following Male Germ-Cell Transplantation. *Proceedings of the National Academy of Sciences* 1994;91**,** 11298-11302.

Cai H, Tang B, Wu JY, Zhao XX, Wang ZZ, An XL, Lai LX, Li ZY & Zhang XM. Enrichment and in Vitro Features of the Putative Gonocytes from Cryopreserved Testicular Tissue of Neonatal Bulls. *Andrology* 2016;4**,** 1150-1158.

Cham T-C, Ibtisham F, Fayaz MA & Honaramooz A. Generation of a Highly Biomimetic Organoid, Including Vasculature, Resembling the Native Immature Testis Tissue. *Cells* 2021;10**,** 1696.

Chassot AA, Le Rolle M, Jourden M, Taketo MM, Ghyselinck NB & Chaboissier MC. Constitutive Wnt/Ctnnb1 Activation Triggers Spermatogonial Stem Cell Proliferation and Germ Cell Depletion. *Developmental Biology* 2017;426**,** 17-27.

Chen LY, Willis WD & Eddy EM. Targeting the Gdnf Gene in Peritubular Myoid Cells Disrupts Undifferentiated Spermatogonial Cell Development. *Proceedings of the National Academy of Sciences of the United States of America* 2016;113**,** 1829-1834.

Chen SR & Liu YX. Regulation of Spermatogonial Stem Cell Self-Renewal and Spermatocyte Meiosis by Sertoli Cell Signaling. *Reproduction* 2015;149**,** R159-167.

Chiarini-Garcia H, Hornick JR, Griswold MD & Russell LD. Distribution of Type a Spermatogonia in the Mouse Is Not Random. *Biology of Reproduction* 2001a;65**,** 1179-1185.

Chiarini-Garcia H, Hornick JR, Griswold MD & Russell LD. Distribution of Type a Spermatogonia in the Mouse Is Not Random1. *Biology of Reproduction* 2001b;65**,** 1179-1185.

Chiarini-Garcia H, Raymer AM & Russell LD. Non-Random Distribution of Spermatogonia in Rats: Evidence of Niches in the Seminiferous Tubules. *Reproduction* 2003;126**,** 669-680.

Clement P & Giuliano F *Chapter 3 - Anatomy and Physiology of Genital Organs – Men. In:* VODUŠEK, D. B. & BOLLER, F. (eds.) *Handbook of Clinical Neurology.* 2015. Elsevier.

Clevers H. Modeling Development and Disease with Organoids. *Cell* 2016;165**,** 1586-1597.

Clevers H & Watt FM. Defining Adult Stem Cells by Function, Not by Phenotype. *Annual Review of Biochemistry* 2018;87**,** 1015-1027.

Conboy IM, Conboy MJ, Wagers AJ, Girma ER, Weissman IL & Rando TA. Rejuvenation of Aged Progenitor Cells by Exposure to a Young Systemic Environment. *Nature* 2005;433**,** 760-764.

Corradi PF, Corradi RB & Greene LW. Physiology of the Hypothalamic Pituitary Gonadal Axis in the Male. *Urologic Clinics* 2016;43**,** 151-162.

Costoya JA, Hobbs RM, Barna M, Cattoretti G, Manova K, Sukhwani M, Orwig KE, Wolgemuth DJ & Pandolfi PP. Essential Role of Plzf in Maintenance of Spermatogonial Stem Cells. *Nature Genetics* 2004;36**,** 653-659.

Culty M. Gonocytes, the Forgotten Cells of the Germ Cell Lineage. *Birth Defects Research C Embryo Today* 2009;87**,** 1-26.

Curaba M, Poels J, van Langendonckt A, Donnez J & Wyns C. Can Prepubertal Human Testicular Tissue Be Cryopreserved by Vitrification? *Fertility and Sterility* 2011a;95**,** 2123.e2129-2123.e2112.

Curaba M, Verleysen M, Amorim CA, Dolmans MM, Van Langendonckt A, Hovatta O, Wyns C & Donnez J. Cryopreservation of Prepubertal Mouse Testicular Tissue by Vitrification. *Fertility and Sterility* 2011b;95**,** 1229-1234 e1221.

Curtis SK & Amann RP. Testicular Development and Establishment of Spermatogenesis in Holstein Bulls. *Journal of Animal Science* 1981;53**,** 1645-1657.

de Barros FR, Worst RA, Saurin GC, Mendes CM, Assumpção ME & Visintin JA. A-6 Integrin Expression in Bovine Spermatogonial Cells Purified by Discontinuous Percoll Density Gradient. *Reproduction in Domestic Animals* 2012;47**,** 887-890.

de Michele F, Poels J, Vermeulen M, Ambroise J, Gruson D, Guiot Y & Wyns C. Haploid Germ Cells Generated in Organotypic Culture of Testicular Tissue from Prepubertal Boys. *Frontiers in Physiology* 2018;9**,** 1413.

De Munck N & Vajta G. Safety and Efficiency of Oocyte Vitrification. *Cryobiology* 2017;78**,** 119-127.

de Rooij DG. The Spermatogonial Stem Cell Niche. *Microscopy Research and Technique* 2009;72**,** 580-585.

DeFalco T, Potter SJ, Williams AV, Waller B, Kan MJ & Capel B. Macrophages Contribute to the Spermatogonial Niche in the Adult Testis. *Cell Reports* 2015;12**,** 1107-1119.

Dekkers JF, Alieva M, Wellens LM, Ariese HCR, Jamieson PR, Vonk AM, Amatngalim GD, Hu H, Oost KC, Snippert HJG, Beekman JM, Wehrens EJ, Visvader JE, Clevers H & Rios AC. High-Resolution 3d Imaging of Fixed and Cleared Organoids. *Nature Protocols* 2019;14**,** 1756-1771.

Del Vento F, Vermeulen M, de Michele F, Giudice MG, Poels J, des Rieux A & Wyns C. Tissue Engineering to Improve Immature Testicular Tissue and Cell Transplantation Outcomes: One Step Closer to Fertility Restoration for Prepubertal Boys Exposed to Gonadotoxic Treatments. *International Journal of Molecular Sciences* 2018;19.

Devkota B, Sasaki M, Takahashi K-i, Matsuzaki S, Matsui M, Haneda S, Takahashi M, Osawa T & Miyake Y-i. Postnatal Developmental Changes in Immunohistochemical Localization of Alpha-Smooth Muscle Actin (Sma) and Vimentin in Bovine Testes. *The Journal of reproduction and development* 2006;52 1**,** 43-49.

Dix DJ, Allen JW, Collins BW, Mori C, Nakamura N, Poorman-Allen P, Goulding EH & Eddy E. Targeted Gene Disruption of Hsp70-2 Results in Failed Meiosis, Germ Cell Apoptosis, and Male Infertility. *Proceedings of the National Academy of Sciences* 1996;93**,** 3264-3268.

Eddy EM. Role of Heat Shock Protein Hsp70-2 in Spermatogenesis. *Reviews of Reproduction* 1999;4**,** 23-30.

Edmonds ME & Woodruff TK. Testicular Organoid Formation Is a Property of Immature Somatic Cells, Which Self-Assemble and Exhibit Long-Term Hormone-Responsive Endocrine Function. *Biofabrication* 2020;12**,** 045002.

Edmondson R, Broglie JJ, Adcock AF & Yang L. Three-Dimensional Cell Culture Systems and Their Applications in Drug Discovery and Cell-Based Biosensors. *Assay and Drug Development Technologies* 2014;12**,** 207-218.

El Ramy R, Verot A, Mazaud S, Odet F, Magre S & Le Magueresse-Battistoni B. Fibroblast Growth Factor (Fgf) 2 and Fgf9 Mediate Mesenchymal–Epithelial Interactions of Peritubular and Sertoli Cells in the Rat Testis. *Journal of Endocrinology* 2005;187**,** 135-147.

Ellis H & Mahadevan V. Scrotum, Testis and Epididymis. *Surgery (Oxford)* 2014;32**,** e9-e16.

Eyni H, Ghorbani S, Nazari H, Hajialyani M, Razavi Bazaz S, Mohaqiq M, Ebrahimi Warkiani M & Sutherland DS. Advanced Bioengineering of Male Germ Stem Cells to Preserve Fertility. *Journal of Tissue Engineering* 2021;12**,** 20417314211060590.

Faes K & Goossens E. Short-Term Hypothermic Preservation of Human Testicular Tissue: The Effect of Storage Medium and Storage Period. *Fertility and Sterility* 2016;105**,** 1162-1169. e1165.

Faes K & Goossens E. Short-Term Storage of Human Testicular Tissue: Effect of Storage Temperature and Tissue Size. *Reproductive Biomedicine Online* 2017;35**,** 180-188.

Fatehullah A, Tan SH & Barker N. Organoids as an in Vitro Model of Human Development and Disease. *Nature Cell Biology* 2016;18**,** 246-254.

Fayomi AP, Peters K, Sukhwani M, Valli-Pulaski H, Shetty G, Meistrich ML, Houser L, Robertson N, Roberts V, Ramsey C, Hanna C, Hennebold JD, Dobrinski I & Orwig KE. Autologous Grafting of Cryopreserved Prepubertal Rhesus Testis Produces Sperm and Offspring. *Science* 2019;363**,** 1314-1319.

Feng W, Chen S, Do D, Liu Q, Deng Y, Lei X, Luo C, Huang B & Shi D. Isolation and Identification of Prepubertal Buffalo (Bubalus Bubalis) Spermatogonial Stem Cells. *Asian-Australasian Journal of Animal Sciences* 2016;29**,** 1407-1415.

Forest MG & Cathiard AM. Pattern of Plasma Testosterone and Δ4-Androstenedione in Normal Newborns: Evidence for Testicular Activity at Birth. *The Journal of Clinical Endocrinology & Metabolism* 1975;41**,** 977-980.

Fujihara M, Kim SM, Minami N, Yamada M & Imai H. Characterization and in Vitro Culture of Male Germ Cells from Developing Bovine Testis. *Journal of Reproduction and Development* 2011;57**,** 355-364.

Fukuda T, Hedinger C & Groscurth P. Ultrastructure of Developing Germ Cells in the Fetal Human Testis. *Cell and Tissue Research* 1975;161**,** 55-70.

Gaskell TL, Esnal A, Robinson LL, Anderson RA & Saunders PT. Immunohistochemical Profiling of Germ Cells within the Human Fetal Testis: Identification of Three Subpopulations. *Biology of Reproduction* 2004;71**,** 2012-2021.

Gassei K, Ehmcke J, Wood MA, Walker WH & Schlatt S. Immature Rat Seminiferous Tubules Reconstructed in Vitro Express Markers of Sertoli Cell Maturation after Xenografting into Nude Mouse Hosts. *Molecular Human Reproduction* 2010;16**,** 97-110.

Gattazzo F, Urciuolo A & Bonaldo P. Extracellular Matrix: A Dynamic Microenvironment for Stem Cell Niche. *Biochimica et Biophysica Acta* 2014;1840**,** 2506-2519.

Gholami K, Pourmand G, Koruji M, Sadighigilani M, Navid S, Izadyar F & Abbasi M. Efficiency of Colony Formation and Differentiation of Human Spermatogenic Cells in Two Different Culture Systems. *Reproductive Biology* 2018;18**,** 397-403.

Giassetti MI, Ciccarelli M & Oatley JM. Spermatogonial Stem Cell Transplantation: Insights and Outlook for Domestic Animals. *Annual Review of Animal Biosciences* 2019;7**,** 385-401.

Giassetti MI, Goissis MD, de Barros F, Bruno AH, Assumpção M & Visintin JA. Comparison of Diverse Differential Plating Methods to Enrich Bovine Spermatogonial Cells. *Reproduction in Domestic Animals* 2016;51**,** 26-32.

Goel S, Fujihara M, Minami N, Yamada M & Imai H. Expression of Nanog, but Not Pou5f1, Points to the Stem Cell Potential of Primitive Germ Cells in Neonatal Pig Testis. *Reproduction* 2008;135**,** 785-795.

Goossens E, Jahnukainen K, Mitchell RT, van Pelt A, Pennings G, Rives N, Poels J, Wyns C, Lane S, Rodriguez-Wallberg KA, Rives A, Valli-Pulaski H, Steimer S, Kliesch S, Braye A, Andres MM, Medrano J, Ramos L, Kristensen SG, Andersen CY, Bjarnason R, Orwig KE, Neuhaus N & Stukenborg JB. Fertility Preservation in Boys: Recent Developments and New Insights (Dagger). *Human Reproduction Open* 2020;2020**,** hoaa016.

Green DM, Kawashima T, Stovall M, Leisenring W, Sklar CA, Mertens AC, Donaldson SS, Byrne J & Robison LL. Fertility of Male Survivors of Childhood Cancer: A Report from the Childhood Cancer Survivor Study. *Journal of Clinical Oncology* 2010;28**,** 332-339.

Green DM, Liu W, Kutteh WH, Ke RW, Shelton KC, Sklar CA, Chemaitilly W, Pui CH, Klosky JL, Spunt SL, Metzger ML, Srivastava D, Ness KK, Robison LL & Hudson MM. Cumulative Alkylating Agent Exposure and Semen Parameters in Adult Survivors of Childhood Cancer: A Report from the St Jude Lifetime Cohort Study. *Lancet Oncology* 2014;15**,** 1215-1223.

Guan K, Nayernia K, Maier LS, Wagner S, Dressel R, Lee JH, Nolte J, Wolf F, Li M, Engel W & Hasenfuss G. Pluripotency of Spermatogonial Stem Cells from Adult Mouse Testis. *Nature* 2006;440**,** 1199-1203.

Guan K, Wolf F, Becker A, Engel W, Nayernia K & Hasenfuss G. Isolation and Cultivation of Stem Cells from Adult Mouse Testes. *Nature Protocols* 2009;4**,** 143-154.

Guo J, Grow EJ, Mlcochova H, Maher GJ, Lindskog C, Nie X, Guo Y, Takei Y, Yun J, Cai L, Kim R, Carrell DT, Goriely A, Hotaling JM & Cairns BR. The Adult Human Testis Transcriptional Cell Atlas. *Cell Research* 2018;28**,** 1141-1157.

Guo J, Nie X, Giebler M, Mlcochova H, Wang Y, Grow EJ, Kim R, Tharmalingam M, Matilionyte G, Lindskog C, Carrell DT, Mitchell RT, Goriely A, Hotaling JM & Cairns BR. The Dynamic Transcriptional Cell Atlas of Testis Development During Human Puberty. *Cell Stem Cell* 2020;26**,** 262-276.e264.

Gurruchaga H, Saenz del Burgo L, Hernandez RM, Orive G, Selden C, Fuller B, Ciriza J & Pedraz JL. Advances in the Slow Freezing Cryopreservation of Microencapsulated Cells. *Journal of Controlled Release* 2018;281**,** 119-138.

Hadley MA, Byers SW, Suárez-Quian CA, Kleinman HK & Dym M. Extracellular Matrix Regulates Sertoli Cell Differentiation, Testicular Cord Formation, and Germ Cell Development in Vitro. *The Journal of Cell Biology* 1985;101**,** 1511-1522.

Hadley MA, Weeks BS, Kleinman HK & Dym M. Laminin Promotes Formation of Cord-Like Structures by Sertoli Cells in Vitro. *Developmental Biology* 1990;140**,** 318-327.

Han S-H, Shim S, Kim M-J, Shin H-Y, Jang W-S, Lee S-J, Jin Y-W, Lee S-S, Lee SB & Park S. Long-Term Culture-Induced Phenotypic Difference and Efficient Cryopreservation of Small Intestinal Organoids by Treatment Timing of Rho Kinase Inhibitor. *World Journal of Gastroenterology* 2017;23**,** 964-975.

Hayashi Y, Saitou M & Yamanaka S. Germline Development from Human Pluripotent Stem Cells toward Disease Modeling of Infertility. *Fertility and Sterility* 2012;97**,** 1250-1259.

He Y, Chen X, Zhu H & Wang D. Developments in Techniques for the Isolation, Enrichment, Main Culture Conditions and Identification of Spermatogonial Stem Cells. *Cytotechnology* 2015;67**,** 921-930.

Hermann BP, Sukhwani M, Winkler F, Pascarella JN, Peters KA, Sheng Y, Valli H, Rodriguez M, Ezzelarab M & Dargo G. Spermatogonial Stem Cell Transplantation into Rhesus Testes Regenerates Spermatogenesis Producing Functional Sperm. *Cell Stem Cell* 2012;11**,** 715-726.

Herrid M, Olejnik J, Jackson M, Suchowerska N, Stockwell S, Davey R, Hutton K, Hope S & Hill JR. Irradiation Enhances the Efficiency of Testicular Germ Cell Transplantation in Sheep. *Biology of Reproduction* 2009;81**,** 898-905.

Hiller-Sturmhöfel S & Bartke A. The Endocrine System - an Overview. *Alcohol Research and Health* 1998;22**,** 153-164.

Hiort O. Androgens and Puberty. *Best Practice & Research Clinical Endocrinology & Metabolism* 2002;16**,** 31-41.

Hoei-Hansen CE, Almstrup K, Nielsen JE, Brask Sonne S, Graem N, Skakkebaek NE, Leffers H & Rajpert-De Meyts E. Stem Cell Pluripotency Factor Nanog Is Expressed in Human Fetal Gonocytes, Testicular Carcinoma in Situ and Germ Cell Tumours. *Histopathology* 2005;47**,** 48-56.

Hofmann M-C, Narisawa S, Hess RA & Mill n JL. Immortalization of Germ Cells and Somatic Testicular Cells Using the Sv40 Large T Antigen. *Experimental Cell Research* 1992;201**,** 417-435.

Honaramooz A, Snedaker A, Boiani M, Schöler H, Dobrinski I & Schlatt S. Sperm from Neonatal Mammalian Testes Grafted in Mice. *Nature* 2002;418**,** 778-781.

Huch M, Bonfanti P, Boj SF, Sato T, Loomans CJ, Van De Wetering M, Sojoodi M, Li VS, Schuijers J & Gracanin A. Unlimited in Vitro Expansion of Adult Bi-Potent Pancreas Progenitors through the Lgr5/R-Spondin Axis. *The EMBO journal* 2013;32**,** 2708-2721.

Huleihel M, Nourashrafeddin S & Plant TM. Application of Three-Dimensional Culture Systems to Study Mammalian Spermatogenesis, with an Emphasis on the Rhesus Monkey (Macaca Mulatta). *Asian Journal of Andrology* 2015;17**,** 972.

Hynes RO. The Extracellular Matrix: Not Just Pretty Fibrils. *Science (New York, N.Y.)* 2009;326**,** 1216-1219.

Ibtisham F, Awang-Junaidi AH & Honaramooz A. The Study and Manipulation of Spermatogonial Stem Cells Using Animal Models. *Cell Tissue Research* 2020;380**,** 393-414.

Ishii K, Kanatsu-Shinohara M, Toyokuni S & Shinohara T. Fgf2 Mediates Mouse Spermatogonial Stem Cell Self-Renewal Via Upregulation of Etv5 and Bcl6b through Map2k1 Activation. *Development* 2012;139**,** 1734-1743.

Izadyar F, Spierenberg G, Creemers L, Ouden Kd & De Rooij D. Isolation and Purification of Type a Spermatogonia from the Bovine Testis. *Reproduction* 2002a;124**,** 85-94.

Izadyar F, Spierenberg G, Creemers L, Ouden Kd & De Rooij D. Isolation and Purification of Type a Spermatogonia from the Bovine Testis. *REPRODUCTION-CAMBRIDGE-* 2002b;124**,** 85-94.

J Costa GM, Avelar GF, S N Lacerda SM, A Figueiredo AF, Tavares AO, Rezende-Neto JV, P Martins FG & França LR. Horse Spermatogonial Stem Cell Cryopreservation: Feasible Protocols and Potential Biotechnological Applications. *Cell and Tissue Research* 2017;370.

Jijiwa M, Kawai K, Fukihara J, Nakamura A, Hasegawa M, Suzuki C, Sato T, Enomoto A, Asai N & Murakumo Y. Gdnf-Mediated Signaling Via Ret Tyrosine 1062 Is Essential for Maintenance of Spermatogonial Stem Cells. *Genes to Cells* 2008;13**,** 365-374.

Johnson L. Spermatogenesis and Aging in the Human. *Journal of Andrology* 1986;7**,** 331-354.

Jørgensen A, Nielsen J, Perlman S, Lundvall L, Mitchell R, Juul A & Rajpert-De Meyts E. Ex Vivo Culture of Human Fetal Gonads: Manipulation of Meiosis Signalling by Retinoic Acid Treatment Disrupts Testis Development. *Human Reproduction* 2015;30**,** 2351-2363.

Jørgensen A, Young J, Nielsen J, Joensen UN, Toft BG, Rajpert-De Meyts E & Loveland K. Hanging Drop Cultures of Human Testis and Testis Cancer Samples: A Model Used to Investigate Activin Treatment Effects in a Preserved Niche. *British Journal of Cancer* 2014;110**,** 2604-2614.

Juho-Antti M & Robin MH. Molecular Regulation of Spermatogonial Stem Cell Renewal and Differentiation. *Reproduction* 2019;158**,** R169-R187.

Kaneko H, Kikuchi K, Men NT, Dang-Nguyen TQ, Oyadomari M, Touma S, Suzuki N & Katagiri Y. Embryo Production by Intracytoplasmic Injection of Sperm Retrieved from Neonatal Testicular Tissue of Agu Pigs after Cryopreservation and Grafting into Nude Mice. *Anim Sci J* 2020;91**,** e13479.

Kaneko H, Kikuchi K, Nakai M, Somfai T, Noguchi J, Tanihara F, Ito J & Kashiwazaki N. Generation of Live Piglets for the First Time Using Sperm Retrieved from Immature Testicular Tissue Cryopreserved and Grafted into Nude Mice. *PLoS ONE* 2013;8**,** e70989.

Keros V, Hultenby K, Borgström B, Fridström M, Jahnukainen K & Hovatta O. Methods of Cryopreservation of Testicular Tissue with Viable Spermatogonia in Pre-Pubertal Boys Undergoing Gonadotoxic Cancer Treatment. *Human Reproduction* 2007;22**,** 1384-1395.

Keros V, Rosenlund B, Hultenby K, Aghajanova L, Levkov L & Hovatta O. Optimizing Cryopreservation of Human Testicular Tissue: Comparison of Protocols with Glycerol, Propanediol and Dimethylsulphoxide as Cryoprotectants. *Human Reproduction* 2005;20**,** 1676-1687.

Kierszenbaum AL, Crowell JA, Shabanowitz RB, DePhilip RM & Tres LL. Protein Secretory Patterns of Rat Sertoli and Peritubular Cells Are Influenced by Culture Conditions. *Biology of Reproduction* 1986;35**,** 239-251.

Kim J, Koo B-K & Knoblich JA. Human Organoids: Model Systems for Human Biology and Medicine. *Nature Reviews Molecular Cell Biology* 2020;21**,** 571-584.

Kim KJ, Cho CM, Kim BG, Lee YA, Kim BJ, Kim YH, Kim CG, Schmidt JA & Ryu BY. Lentiviral Modification of Enriched Populations of Bovine Male Gonocytes. *Journal of Animal Science* 2014;92**,** 106-118.

Kim YH, Choi YR, Kim BJ, Jung SE, Kim SM, Jin JH, Yun MH, Kim SU, Kim YH, Hwang S, Pang MG & Ryu BY. Gdnf Family Receptor Alpha 1 Is a Reliable Marker of Undifferentiated Germ Cells in Bulls. *Theriogenology* 2019;132**,** 172-181.

Kitadate Y, Jörg DJ, Tokue M, Maruyama A, Ichikawa R, Tsuchiya S, Segi-Nishida E, Nakagawa T, Uchida A, Kimura-Yoshida C, Mizuno S, Sugiyama F, Azami T, Ema M, Noda C, Kobayashi S, Matsuo I, Kanai Y, Nagasawa T, Sugimoto Y, Takahashi S, Simons BD & Yoshida S. Competition for Mitogens Regulates Spermatogenic Stem Cell Homeostasis in an Open Niche. *Cell Stem Cell* 2019;24**,** 79-92.e76.

Kofman AE, Huszar JM & Payne CJ. Transcriptional Analysis of Histone Deacetylase Family Members Reveal Similarities between Differentiating and Aging Spermatogonial Stem Cells. *Stem Cell Reviews and Reports* 2013;9**,** 59-64.

Komeya M, Hayashi K, Nakamura H, Yamanaka H, Sanjo H, Kojima K, Sato T, Yao M, Kimura H & Fujii T. Pumpless Microfluidic System Driven by Hydrostatic Pressure Induces and Maintains Mouse Spermatogenesis in Vitro. *Scientific reports* 2017;7(1).

Komeya M, Kimura H, Nakamura H, Yokonishi T, Sato T, Kojima K, Hayashi K, Katagiri K, Yamanaka H & Sanjo H. Long-Term Ex Vivo Maintenance of Testis Tissues Producing Fertile Sperm in a Microfluidic Device. *Scientific reports* 2016a;6**,** 1-10.

Komeya M, Kimura H, Nakamura H, Yokonishi T, Sato T, Kojima K, Hayashi K, Katagiri K, Yamanaka H, Sanjo H, Yao M, Kamimura S, Inoue K, Ogonuki N, Ogura A, Fujii T & Ogawa T. Long-Term Ex Vivo Maintenance of Testis Tissues Producing Fertile Sperm in a Microfluidic Device. *Scientific reports* 2016b;6**,** 21472.

Köse S, Yersal N, Önen S & Korkusuz P *Comparison of Hematopoietic and Spermatogonial Stem Cell Niches from the Regenerative Medicine Aspect.* 2018. Springer New York LLC.

Koskenniemi JJ, Virtanen HE & Toppari J. Testicular Growth and Development in Puberty. *Current Opinion in Endocrinology, Diabetes and Obesity* 2017;24**,** 215-224.

Kuijper EA, van Kooten J, Verbeke JI, van Rooijen M & Lambalk CB. Ultrasonographically Measured Testicular Volumes in 0- to 6-Year-Old Boys. *Human Reproduction* 2008;23**,** 792-796.

Kuiri-Hänninen T, Seuri R, Tyrväinen E, Turpeinen U, Hämäläinen E, Stenman UH, Dunkel L & Sankilampi U. Increased Activity of the Hypothalamic-Pituitary-Testicular Axis in Infancy Results in Increased Androgen Action in Premature Boys. *Journal of Clinical Endocrinolology & Metabolism* 2011;96**,** 98-105.

Kulibin AY & Malolina EA. Only a Small Population of Adult Sertoli Cells Actively Proliferates in Culture. *Reproduction* 2016;152**,** 271-281.

Kvist K, Thorup J, Byskov A, Høyer P, Møllgård K & Yding Andersen C. Cryopreservation of Intact Testicular Tissue from Boys with Cryptorchidism. *Human Reproduction* 2006;21**,** 484-491.

Lai L, Kolber-Simonds D, Park KW, Cheong HT, Greenstein JL, Im GS, Samuel M, Bonk A, Rieke A, Day BN, Murphy CN, Carter DB, Hawley RJ & Prather RS. Production of Alpha-1,3-Galactosyltransferase Knockout Pigs by Nuclear Transfer Cloning. *Science* 2002;295**,** 1089-1092.

Lakhoo K, Davies J, Chakraborty S, Berg S, Tennyson R, Fowler D, Manek S, Verrill C & Lane S. Development of a New Reproductive Tissue Cryopreservation Clinical Service for Children: The Oxford Programme. *Pediatric Surgery International* 2019a;35**,** 1271-1278.

Lakhoo K, Davies J, Chakraborty S, Berg S, Tennyson R, Fowler D, Manek S, Verrill C & Lane S. Development of a New Reproductive Tissue Cryopreservation Clinical Service for Children: The Oxford Programme. *Pediatric Surgery International* 2019b;35**,** 1271-1278.

Lam CG, Howard SC, Bouffet E & Pritchard-Jones K. Science and Health for All Children with Cancer. *Science* 2019;363**,** 1182-1186.

Lancaster MA & Knoblich JA. Organogenesis in a Dish: Modeling Development and Disease Using Organoid Technologies. *Science* 2014;345**,** 1247125.

Lee DR, Kaproth MT & Parks JE. In Vitro Production of Haploid Germ Cells from Fresh or Frozen-Thawed Testicular Cells of Neonatal Bulls1. *Biology of Reproduction* 2001;65**,** 873-878.

Lee J, Kanatsu-Shinohara M, Inoue K, Ogonuki N, Miki H, Toyokuni S, Kimura T, Nakano T, Ogura A & Shinohara T. Akt Mediates Self-Renewal Division of Mouse Spermatogonial Stem Cells. *Development* 2007a;134**,** 1853-1859.

Lee JH, Gye MC, Choi KW, Hong JY, Lee YB, Park DW, Lee SJ & Min CK. In Vitro Differentiation of Germ Cells from Nonobstructive Azoospermic Patients Using Three-Dimensional Culture in a Collagen Gel Matrix. *Fertility and Sterility* 2007b;87**,** 824-833.

Lee JH, Kim HJ, Kim H, Lee SJ & Gye MC. In Vitro Spermatogenesis by Three-Dimensional Culture of Rat Testicular Cells in Collagen Gel Matrix. *Biomaterials* 2006;27**,** 2845-2853.

Lee JH, Oh JH, Lee JH, Kim MR & Min CK. Evaluation of in Vitro Spermatogenesis Using Poly(D,L-Lactic-Co-Glycolic Acid) (Plga)-Based Macroporous Biodegradable Scaffolds. *Journal of Tissue Engineering and Regenerative Medicine* 2011a;5**,** 130-137.

Lee JH, Oh JH, Lee JH, Kim MR & Min CK. Evaluation of in Vitro Spermatogenesis Using Poly(D,L-Lactic-Co-Glycolic Acid) (Plga)-Based Macroporous Biodegradable Scaffolds. *Journal of Tissue Engineering and Regenerative Medicine* 2011b;5**,** 130-137.

Legendre A, Froment P, Desmots S, Lecomte A, Habert R & Lemazurier E. An Engineered 3d Blood-Testis Barrier Model for the Assessment of Reproductive Toxicity Potential. *Biomaterials* 2010;31**,** 4492-4505.

Li R, Vannitamby A, Yue SSK, Handelsman D & Hutson J. Mouse Minipuberty Coincides with Gonocyte Transformation into Spermatogonial Stem Cells: A Model for Human Minipuberty. *Reproduction, Fertility and Development* 2017;29**,** 2430-2436.

Lima DBC, Silva L & Comizzoli P. Influence of Warming and Reanimation Conditions on Seminiferous Tubule Morphology, Mitochondrial Activity, and Cell Composition of Vitrified Testicular Tissues in the Domestic Cat Model. *PLoS ONE* 2018;13**,** e0207317.

Lima DBC, Silva L, Marinari P & Comizzoli P. Long-Term Preservation of Testicular Tissue Integrity and Viability Using Vitrification in the Endangered Black-Footed Ferret (Mustela Nigripes). *Animals (Basel)* 2020;10.

Liu F, Cai C, Wu X, Cheng Y, Lin T, Wei G & He D. Effect of Knockout Serum Replacement on Germ Cell Development of Immature Testis Tissue Culture. *Theriogenology* 2016a;85**,** 193-199.

Liu J, Cheng KM & Silversides FG. Production of Live Offspring from Testicular Tissue Cryopreserved by Vitrification Procedures in Japanese Quail (Coturnix Japonica)1. *Biology of Reproduction* 2013;88.

Liu Z, Nie Y-H, Zhang C-C, Cai Y-J, Wang Y, Lu H-P, Li Y-Z, Cheng C, Qiu Z-L & Sun Q. Generation of Macaques with Sperm Derived from Juvenile Monkey Testicular Xenografts. *Cell Research* 2016b;26**,** 139-142.

Livak KJ & Schmittgen TD. Analysis of Relative Gene Expression Data Using Real-Time Quantitative Pcr and the 2(-Delta Delta C(T)) Method. *Methods* 2001;25**,** 402-408.

Lord T, Oatley MJ & Oatley JM. Testicular Architecture Is Critical for Mediation of Retinoic Acid Responsiveness by Undifferentiated Spermatogonial Subtypes in the Mouse. *Stem Cell Reports* 2018;10**,** 538-552.

Lu YC, Fu DJ, An D, Chiu A, Schwartz R, Nikitin AY & Ma M. Scalable Production and Cryostorage of Organoids Using Core-Shell Decoupled Hydrogel Capsules. *Advanced Biosystems* 2017;1.

Luo J, Megee S, Rathi R & Dobrinski I. Protein Gene Product 9.5 Is a Spermatogonia-Specific Marker in the Pig Testis: Application to Enrichment and Culture of Porcine Spermatogonia. *Molecular Reproductive Development* 2006;73**,** 1531-1540.

Mäkelä JA & Hobbs RM. Molecular Regulation of Spermatogonial Stem Cell Renewal and Differentiation. *Reproduction* 2019;158**,** R169-r187.

Masaki K, Sakai M, Kuroki S, Jo JI, Hoshina K, Fujimori Y, Oka K, Amano T, Yamanaka T, Tachibana M, Tabata Y, Shiozawa T, Ishizuka O, Hochi S & Takashima S. Fgf2 Has Distinct Molecular Functions from Gdnf in the Mouse Germline Niche. *Stem Cell Reports* 2018;10**,** 1782-1792.

Masliukaite I, Hagen JM, Jahnukainen K, Stukenborg JB, Repping S, van der Veen F, van Wely M & van Pelt AMM. Establishing Reference Values for Age-Related Spermatogonial Quantity in Prepubertal Human Testes: A Systematic Review and Meta-Analysis. *Fertility and Sterility* 2016.

McLachlan RI, Rajpert-De Meyts E, Hoei-Hansen CE, de Kretser DM & Skakkebaek NE. Histological Evaluation of the Human Testis—Approaches to Optimizing the Clinical Value of the Assessment: Mini Review. *Human Reproduction* 2006;22**,** 2-16.

Medrano JV, Vilanova-Pérez T, Fornés-Ferrer V, Navarro-Gomezlechon A, Martínez-Triguero ML, García S, Gómez-Chacón J, Povo I, Pellicer A, Andrés MM & Novella-Maestre E. Influence of Temperature, Serum, and Gonadotropin Supplementation in Short- and Long-Term Organotypic Culture of Human Immature Testicular Tissue. *Fertility and Sterility* 2018;110**,** 1045-1057.e1043.

Menon S, Rives N, Mousset-Siméon N, Sibert L, Vannier JP, Mazurier S, Massé L, Duchesne V & Macé B. Fertility Preservation in Adolescent Males: Experience over 22 Years at Rouen University Hospital. *Human Reproduction* 2009;24**,** 37-44.

Milazzo JP, Vaudreuil L, Cauliez B, Gruel E, Massé L, Mousset-Siméon N, Macé B & Rives N. Comparison of Conditions for Cryopreservation of Testicular Tissue from Immature Mice. *Human Reproduction* 2008;23**,** 17-28.

Miller SC, Bowman BM & Rowland HG. Structure, Cytochemistry, Endocytic Activity, and Immunoglobulin (Fc) Receptors of Rat Testicular Interstitial-Tissue Macrophages. *American Journal of Anatomy* 1983;168**,** 1-13.

Misell L, Holochwost D, Boban D, Santi N, Shefi S, Hellerstein M & Turek P. A Stable Isotope-Mass Spectrometric Method for Measuring Human Spermatogenesis Kinetics in Vivo. *Journal of Urology* 2006;175**,** 242-246.

Mitchell RT, Camacho-Moll M, Macdonald J, Anderson RA, Kelnar CJ, O'Donnell M, Sharpe RM, Smith LB, Grigor KM, Wallace WHB, Stoop H, Wolffenbuttel KP, Donat R, Saunders PT & Looijenga LH. Intratubular Germ Cell Neoplasia of the Human Testis: Heterogeneous Protein Expression and Relation to Invasive Potential. *Modern Pathology* 2014;27**,** 1255-1266.

Mohammadzadeh E, Mirzapour T, Nowroozi MR, Nazarian H, Piryaei A, Alipour F, Modarres Mousavi SM & Ghaffari Novin M. Differentiation of Spermatogonial Stem Cells by Soft Agar

Three-Dimensional Culture System. *Artificial Cells, Nanomedicine, and Biotechnology* 2019;47**,** 1772-1781.

Moraveji SF, Esfandiari F, Sharbatoghli M, Taleahmad S, Nikeghbalian S, Shahverdi A & Baharvand H. Optimizing Methods for Human Testicular Tissue Cryopreservation and Spermatogonial Stem Cell Isolation. *Journal of Cellular Biochemistry* 2019;120**,** 613-621.

Mori C, Nakamura N, Dix DJ, Fujioka M, Nakagawa S, Shiota K & Eddy EM. Morphological Analysis of Germ Cell Apoptosis During Postnatal Testis Development in Normal and Hsp70-2 Knockout Mice. *Developmental dynamics: an official publication of the American Association of Anatomists* 1997;208**,** 125-136.

Mouttham L & Comizzoli P. The Preservation of Vital Functions in Cat Ovarian Tissues During Vitrification Depends More on the Temperature of the Cryoprotectant Exposure Than on the Sucrose Supplementation. *Cryobiology* 2016;73**,** 187-195.

Nagy ZP, Shapiro D & Chang CC. Vitrification of the Human Embryo: A More Efficient and Safer In vitro Fertilization Treatment. *Fertility and Sterility* 2020;113**,** 241-247.

Naughton C, Jain S, Strickland A, Gupta A & Milbrandt J. Glial Cell-Line Derived Neurotrophic Factor-Mediated Ret Signaling Regulates Spermatogonial Stem Cell Fate. *Biology of Reproduction* 2006a;74**,** 314-321.

Naughton CK, Jain S, Strickland AM, Gupta A & Milbrandt J. Glial Cell-Line Derived Neurotrophic Factor-Mediated Ret Signaling Regulates Spermatogonial Stem Cell Fate. *Biology of Reproduction* 2006b;74**,** 314-321.

Nickkholgh B, Mizrak SC, van Daalen SK, Korver CM, Sadri-Ardekani H, Repping S & van Pelt AM. Genetic and Epigenetic Stability of Human Spermatogonial Stem Cells During Long-Term Culture. *Fertility and Sterility* 2014;102**,** 1700-1707. e1701.

Ntemou E, Kadam P, Van Saen D, Wistuba J, Mitchell RT, Schlatt S & Goossens E. Complete Spermatogenesis in Intratesticular Testis Tissue Xenotransplants from Immature Non-Human Primate. *Human Reproduction* 2019;34**,** 403-413.

Oatley J, Avarbock M, Telaranta A, Fearon D & Brinster R. Identifying Genes Important for Spermatogonial Stem Cell Self-Renewal and Survival. *PNAS* 2006;103**,** 9524-9529.

Oatley JM & Brinster RL. The Germline Stem Cell Niche Unit in Mammalian Testes. *Physiological Reviews* 2012;92**,** 577-595.

Oatley JM, Oatley MJ, Avarbock MR, Tobias JW & Brinster RL. Colony Stimulating Factor 1 Is an Extrinsic Stimulator of Mouse Spermatogonial Stem Cell Self-Renewal. *Development* 2009;136**,** 1191-1199.

Oatley MJ, Racicot KE & Oatley JM. Sertoli Cells Dictate Spermatogonial Stem Cell Niches in the Mouse Testis. *Biology of Reproduction* 2011;84**,** 639-645.

Ogawa T. Spermatogonial Transplantation: The Principle and Possible Applications. *Journal of Molecular Medicine* 2001;79**,** 368-374.

Ogawa T, Dobrinski I, Avarbock MR & Brinster RL. Leuprolide, a Gonadotropin-Releasing Hormone Agonist, Enhances Colonization after Spermatogonial Transplantation into Mouse Testes. *Tissue Cell* 1998;30**,** 583-588.

Ohta H & Wakayama T. Generation of Normal Progeny by Intracytoplasmic Sperm Injection Following Grafting of Testicular Tissue from Cloned Mice That Died Postnatally1. *Biology of Reproduction* 2005;73**,** 390-395.

Oliver E & Stukenborg JB. Rebuilding the Human Testis in Vitro. *Andrology* 2019**,** andr.12710-andr.12710.

Onofre J, Baert Y, Faes K & Goossens E. Cryopreservation of Testicular Tissue or Testicular Cell Suspensions: A Pivotal Step in Fertility Preservation. *Human Reproduction Update* 2016;22**,** 744-761.

Orth JM, Qiu J, Jester WF, Jr. & Pilder S. Expression of the C-Kit Gene Is Critical for Migration of Neonatal Rat Gonocytes in Vitro. *Biology of Reproduction* 1997;57**,** 676-683.

Pan F, Chi L & Schlatt S. Effects of Nanostructures and Mouse Embryonic Stem Cells on in Vitro Morphogenesis of Rat Testicular Cords. *PLoS ONE* 2013;8**,** e60054.

Paniagua R & Nistal M. Morphological and Histometric Study of Human Spermatogonia from Birth to the Onset of Puberty. *Journal of Anatomy* 1984;139 (Pt 3)**,** 535-552.

Pendergraft SS, Sadri-Ardekani H, Atala A & Bishop CE. Three-Dimensional Testicular Organoid: A Novel Tool for the Study of Human Spermatogenesis and Gonadotoxicity in Vitro † Summary Sentence. *Biology of Reproduction* 2017;96**,** 720-732.

Perrard M-H, Sereni N, Schluth-Bolard C, Blondet A, d'Estaing SG, Plotton I, Morel-Journel N, Lejeune H, David L & Durand P. Complete Human and Rat Ex Vivo Spermatogenesis from Fresh or Frozen Testicular Tissue1. *Biology of Reproduction* 2016;95.

Phillips SM, Padgett LS, Leisenring WM, Stratton KK, Bishop K, Krull KR, Alfano CM, Gibson TM, de Moor JS, Hartigan DB, Armstrong GT, Robison LL, Rowland JH, Oeffinger KC & Mariotto AB. Survivors of Childhood Cancer in the United States: Prevalence and Burden of Morbidity. *Cancer Epidemiology, Biomarkers & Prevention* 2015;24**,** 653-663.

Picton HM, Wyns C, Anderson RA, Goossens E, Jahnukainen K, Kliesch S, Mitchell RT, Pennings G, Rives N, Tournaye H, van Pelt AM, Eichenlaub-Ritter U & Schlatt S. A European Perspective on Testicular Tissue Cryopreservation for Fertility Preservation in Prepubertal and Adolescent Boys. *Human Reproduction* 2015;30**,** 2463-2475.

Pietzak EJ, 3rd, Tasian GE, Tasian SK, Brinster RL, Carlson C, Ginsberg JP & Kolon TF. Histology of Testicular Biopsies Obtained for Experimental Fertility Preservation Protocol in Boys with Cancer. *Journal of Urology* 2015;194**,** 1420-1424.

Plant TM. Neuroendocrine Control of the Onset of Puberty. *Frontiers in Neuroendocrinology* 2015;38**,** 73-88.

Poels J, Van Langendonckt A, Dehoux JP, Donnez J & Wyns C. Vitrification of Non-Human Primate Immature Testicular Tissue Allows Maintenance of Proliferating Spermatogonial Cells after Xenografting to Recipient Mice. *Theriogenology* 2012;77**,** 1008-1013.

Poels J, Van Langendonckt A, Many M-C, Wese F-X & Wyns C. Vitrification Preserves Proliferation Capacity in Human Spermatogonia. *Human Reproduction* 2013;28**,** 578-589.

Poganitsch-Korhonen M, Masliukaite I, Nurmio M, Lähteenmäki P, van Wely M, van Pelt AMM, Jahnukainen K & Stukenborg JB. Decreased Spermatogonial Quantity in Prepubertal Boys with Leukaemia Treated with Alkylating Agents. *Leukemia* 2017;31**,** 1460-1463.

Pukazhenthi BS, Nagashima J, Travis AJ, Costa GM, Escobar EN, França LR & Wildt DE. Slow Freezing, but Not Vitrification Supports Complete Spermatogenesis in Cryopreserved, Neonatal Sheep Testicular Xenografts. *PLoS ONE* 2015;10**,** e0123957.

Quadrato G, Nguyen T, Macosko EZ, Sherwood JL, Yang SM, Berger DR, Maria N, Scholvin J, Goldman M & Kinney JP. Cell Diversity and Network Dynamics in Photosensitive Human Brain Organoids. *Nature* 2017;545**,** 48-53.

Rajpert-De Meyts E. Developmental Model for the Pathogenesis of Testicular Carcinoma in Situ: Genetic and Environmental Aspects. *Human Reproduction Update* 2006;12**,** 303-323.

Raverdeau M, Gely-Pernot A, Feret B, Dennefeld C, Benoit G, Davidson I, Chambon P, Mark M & Ghyselinck NB. Retinoic Acid Induces Sertoli Cell Paracrine Signals for Spermatogonia Differentiation but Cell Autonomously Drives Spermatocyte Meiosis. *Proceedings of the National Academy of Sciences of the United States of America* 2012;109**,** 16582-16587.

Reda A, Albalushi H, Montalvo SC, Nurmio M, Sahin Z, Hou M, Geijsen N, Toppari J, Söder O & Stukenborg JB. Knock-out Serum Replacement and Melatonin Effects on Germ Cell Differentiation in Murine Testicular Explant Cultures. *Annals of Biomedical Engineering* 2017;45**,** 1783-1794.

Reda A, Hou M, Landreh L, Kjartansdóttir KR, Svechnikov K, Soder O & Stukenborg J-B. In Vitro Spermatogenesis–Optimal Culture Conditions for Testicular Cell Survival, Germ Cell Differentiation, and Steroidogenesis in Rats. *Frontiers in Endocrinology* 2014;5**,** 21.

Reddy MSB, Ponnamma D, Choudhary R & Sadasivuni KK. A Comparative Review of Natural and Synthetic Biopolymer Composite Scaffolds. *Polymers (Basel)* 2021;13.

Reuter K, Ehmcke J, Stukenborg JB, Simoni M, Damm OS, Redmann K, Schlatt S & Wistuba J. Reassembly of Somatic Cells and Testicular Organogenesis in Vitro. *Tissue Cell* 2014;46**,** 86-96.

Rey R. Histology and Histopathology from Cell Biology to Tissue Engineering the Prepubertal Testis: A Quiescent or a Silently Active Organ? *Histology and Histopathology* 1999;14**,** 991-1000.

Rezaei Topraggaleh T, Rezazadeh Valojerdi M, Montazeri L & Baharvand H. A Testis-Derived Macroporous 3d Scaffold as a Platform for the Generation of Mouse Testicular Organoids. *Biomaterials Science* 2019;7**,** 1422-1436.

Rheinwald J & Green H. Seria Cultivation of Strains of Human Epidemal Keratinocytes: The Formation Keratinizin Colonies from Single Cell Is. *Cell* 1975;6**,** 331-342.

Ribeiro RC, Steliarova-Foucher E, Magrath I, Lemerle J, Eden T, Forget C, Mortara I, Tabah-Fisch I, Divino JJ, Miklavec T, Howard SC & Cavalli F. Baseline Status of Paediatric Oncology Care in Ten Low-Income or Mid-Income Countries Receiving My Child Matters Support: A Descriptive Study. *The Lancet Oncology* 2008;9**,** 721-729.

Richer G, Baert Y & Goossens E. In-Vitro Spermatogenesis through Testis Modelling: Toward the Generation of Testicular Organoids. *Andrology* 2020;8**,** 879-891.

Richer G, Hobbs RM, Loveland KL, Goossens E & Baert Y. Long-Term Maintenance and Meiotic Entry of Early Germ Cells in Murine Testicular Organoids Functionalized by 3d Printed Scaffolds and Air-Medium Interface Cultivation. *Frontiers in Physiology* 2021;12.

Rienzi L, Gracia C, Maggiulli R, LaBarbera AR, Kaser DJ, Ubaldi FM, Vanderpoel S & Racowsky C. Oocyte, Embryo and Blastocyst Cryopreservation in Art: Systematic Review and Meta-Analysis Comparing Slow-Freezing Versus Vitrification to Produce Evidence for the Development of Global Guidance. *Human Reproduction Update* 2016;23**,** 139-155.

Rienzi L, Gracia C, Maggiulli R, LaBarbera AR, Kaser DJ, Ubaldi FM, Vanderpoel S & Racowsky C. Oocyte, Embryo and Blastocyst Cryopreservation in Art: Systematic Review and Meta-Analysis Comparing Slow-Freezing Versus Vitrification to Produce Evidence for the Development of Global Guidance. *Human Reproduction Update* 2017;23**,** 139-155.

Roulet V, Denis H, Staub C, Le Tortorec A, Delaleu B, Satie AP, Patard JJ, Jégou B & Dejucq-Rainsford N. Human Testis in Organotypic Culture: Application for Basic or Clinical Research. *Human Reproduction* 2006;21**,** 1564-1575.

Sakib S, Uchida A, Valenzuela-Leon P, Yu Y, Valli-Pulaski H, Orwig K, Ungrin M & Dobrinski I. Formation of Organotypic Testicular Organoids in Microwell Culture. *Biology of Reproduction* 2019;100**,** 1648-1660.

Salian SR, Pandya RK, Laxminarayana SLK, Krishnamurthy H, Cheredath A, Tholeti P, Uppangala S, Kalthur G, Majumdar S, Schlatt S & Adiga SK. Impact of Temperature and Time Interval Prior to Immature Testicular-Tissue Organotypic Culture on Cellular Niche. *Reproductive Sciences* 2021;28**,** 2161-2173.

Salonia A, Rastrelli G, Hackett G, Seminara SB, Huhtaniemi IT, Rey RA, Hellstrom WJG, Palmert MR, Corona G, Dohle GR, Khera M, Chan Y-M & Maggi M. Paediatric and Adult-Onset Male Hypogonadism. *Nature Reviews Disease Primers* 2019;5**,** 38.

Sato T, Katagiri K, Gohbara A, Inoue K, Ogonuki N, Ogura A, Kubota Y & Ogawa T. In Vitro Production of Functional Sperm in Cultured Neonatal Mouse Testes. *Nature* 2011a;471**,** 504-508.

Sato T, Katagiri K, Kubota Y & Ogawa T. In Vitro Sperm Production from Mouse Spermatogonial Stem Cell Lines Using an Organ Culture Method. *Nature Protocols* 2013;8**,** 2098-2104.

Sato T, Stange DE, Ferrante M, Vries RG, Van Es JH, Van Den Brink S, Van Houdt WJ, Pronk A, Van Gorp J & Siersema PD. Long-Term Expansion of Epithelial Organoids from Human Colon, Adenoma, Adenocarcinoma, and Barrett's Epithelium. *Gastroenterology* 2011b;141**,** 1762-1772.

Sato T, Vries RG, Snippert HJ, Van De Wetering M, Barker N, Stange DE, Van Es JH, Abo A, Kujala P & Peters PJ. Single Lgr5 Stem Cells Build Crypt-Villus Structures in Vitro without a Mesenchymal Niche. *Nature* 2009;459**,** 262-265.

Schlatt S, De Kretser DM & Loveland KL. Discriminative Analysis of Rat Sertoli and Peritubular Cells and Their Proliferation in Vitro: Evidence for Follicle-Stimulating Hormone-Mediated Contact Inhibition of Sertoli Cell Mitosis. *Biology of Reproduction* 1996;55**,** 227-235.

Schlatt S, Honaramooz A, Boiani M, Schöler HR & Dobrinski I. Progeny from Sperm Obtained after Ectopic Grafting of Neonatal Mouse Testes. *Biology of Reproduction* 2003;68**,** 2331-2335.

Schofield R. The Relationship between the Spleen Colony-Forming Cell and the Haemopoietic Stem Cell. *Blood Cells* 1978;4**,** 7-25.

Shinohara T, Avarbock MR & Brinster RL. Beta1- and Alpha6-Integrin Are Surface Markers on Mouse Spermatogonial Stem Cells. *Proceedings of the National Academy of Sciences of the United States of America* 1999;96**,** 5504-5509.

Shinohara T, Inoue K, Ogonuki N, Kanatsu-Shinohara M, Miki H, Nakata K, Kurome M, Nagashima H, Toyokuni S, Kogishi K, Honjo T & Ogura A. Birth of Offspring Following Transplantation of Cryopreserved Immature Testicular Pieces and in-Vitro Microinsemination. *Human Reproduction* 2002a;17**,** 3039-3045.

Shinohara T, Inoue K, Ogonuki N, Kanatsu-Shinohara M, Miki H, Nakata K, Kurome M, Nagashima H, Toyokuni S, Kogishi K, Honjo T & Ogura A. Birth of Offspring Following Transplantation of Cryopreserved Immature Testicular Pieces and in-Vitro Microinsemination. *Human Reproduction* 2002b;17**,** 3039-3045.

Shinohara T, Orwig KE, Avarbock MR & Brinster RL. Remodeling of the Postnatal Mouse Testis Is Accompanied by Dramatic Changes in Stem Cell Number and Niche Accessibility. *Proceedings of the National Academy of Sciences of the United States of America* 2001;98**,** 6186-6191.

Skinner R, Mulder RL, Kremer LC, Hudson MM, Constine LS, Bardi E, Boekhout A, Borgmann-Staudt A, Brown MC, Cohn R, Dirksen U, Giwercman A, Ishiguro H, Jahnukainen K, Kenney LB, Loonen JJ, Meacham L, Neggers S, Nussey S, Petersen C, Shnorhavorian M, van den Heuvel-Eibrink MM, van Santen HM, Wallace WH & Green DM. Recommendations for Gonadotoxicity Surveillance in Male Childhood, Adolescent, and Young Adult Cancer Survivors: A Report from the International Late Effects of Childhood Cancer Guideline Harmonization Group in Collaboration with the Pancaresurfup Consortium. *Lancet Oncology* 2017;18**,** e75-e90.

Smart E, Lopes F, Rice S, Nagy B, Anderson RA, Mitchell RT & Spears N. Chemotherapy Drugs Cyclophosphamide, Cisplatin and Doxorubicin Induce Germ Cell Loss in an in Vitro Model of the Prepubertal Testis. *Scientific reports* 2018;8**,** 1773.

Sohni A, Tan K, Song HW, Burow D, de Rooij DG, Laurent L, Hsieh TC, Rabah R, Hammoud SS, Vicini E & Wilkinson MF. The Neonatal and Adult Human Testis Defined at the Single-Cell Level. *Cell Reports* 2019;26**,** 1501-1517.e1504.

Sousa M, Cremades N, Alves C, Silva J & Barros A. Developmental Potential of Human Spermatogenic Cells Co-Cultured with Sertoli Cells. *Human Reproduction* 2002;17**,** 161-172.

Southard JH & Belzer FO. Organ Preservation. *Annual Review of Medicine* 1995;46**,** 235-247.

Steinberger A & Steinberger E. Differentiation of Rat Seminiferous Epithelium in Organ Culture. *Reproduction* 1965;9**,** 243-248.

Steinberger A & Steinberger E. Replication Pattern of Sertoli Cells in Maturing Rat Testis in Vivo and in Organ Culture1. *Biology of Reproduction* 1971;4**,** 84-87.

Steinberger A, Steinberger E & Perloff W. Mammalian Testes in Organ Culture. *Experimental Cell Research* 1964;36**,** 19-27.

Strange DP, Zarandi NP, Trivedi G, Atala A, Bishop CE, Sadri-Ardekani H & Verma S. Human Testicular Organoid System as a Novel Tool to Study Zika Virus Pathogenesis Correspondence. *Emerging Microbes & Infections* 2018;7.

Stukenborg J-B, Jahnukainen K, Hutka M & Mitchell RT. Cancer Treatment in Childhood and Testicular Function: The Importance of the Somatic Environment. *Endocrine Connections* 2018;7**,** R69-R87.

Stukenborg J-B, Schlatt S, Simoni M, Yeung C-H, Elhija MA, Luetjens CM, Huleihel M & Wistuba J. New Horizons for in Vitro Spermatogenesis? An Update on Novel Three-Dimensional Culture Systems as Tools for Meiotic and Post-Meiotic Differentiation of Testicular Germ Cells. *Molecular Human Reproduction* 2009;15**,** 521-529.

Stukenborg JB, Wistuba J, Luetjens CM, Elhija MA, Huleihel M, Lunenfeld E, Gromoll J, Nieschlag E & Schlatt S. Coculture of Spermatogonia with Somatic Cells in a Novel Three-Dimensional Soft-Agar-Culture-System. *Journal of Andrology* 2008;29**,** 312-329.

Sun M, Yuan Q, Niu M, Wang H, Wen L, Yao C, Hou J, Chen Z, Fu H, Zhou F, Li C, Gao S, Gao W-Q, Li Z & He Z. Efficient Generation of Functional Haploid Spermatids from Human Germline Stem Cells by Three-Dimensional-Induced System. *Cell Death & Differentiation* 2018;25**,** 749-766.

Suzuki N, Yoshioka N, Takae S, Sugishita Y, Tamura M, Hashimoto S, Morimoto Y & Kawamura K. Successful Fertility Preservation Following Ovarian Tissue Vitrification in Patients with Primary Ovarian Insufficiency. *Human Reproduction* 2015;30**,** 608-615.

Szczepny A, Hogarth CA, Young J & Loveland KL. Identification of Hedgehog Signaling Outcomes in Mouse Testis Development Using a Hanging Drop-Culture System. *Biology of Reproduction* 2009;80**,** 258-263.

Tadokoro Y, Yomogida K, Ohta H, Tohda A & Nishimune Y. Homeostatic Regulation of Germinal Stem Cell Proliferation by the Gdnf/Fsh Pathway. *Mechanisms of Development* 2002;113**,** 29-39.

Takashima S, Kanatsu-Shinohara M, Tanaka T, Morimoto H, Inoue K, Ogonuki N, Jijiwa M, Takahashi M, Ogura A & Shinohara T. Functional Differences between Gdnf-Dependent and Fgf2-Dependent Mouse Spermatogonial Stem Cell Self-Renewal. *Stem Cell Reports* 2015a;4**,** 489-502.

Takashima S, Kato J, Hiraoka S, Nakarai A, Takei D, Inokuchi T, Sugihara Y, Takahara M, Harada K, Okada H, Tanaka T & Yamamoto K. Evaluation of Mucosal Healing in Ulcerative Colitis by Fecal Calprotectin Vs. Fecal Immunochemical Test. *American Journal of Gastroenterology* 2015b;110**,** 873-880.

Takebe T, Sekine K, Enomura M, Koike H, Kimura M, Ogaeri T, Zhang R-R, Ueno Y, Zheng Y-W & Koike N. Vascularized and Functional Human Liver from an Ipsc-Derived Organ Bud Transplant. *Nature* 2013;499**,** 481-484.

Tan K, Song H-W & Wilkinson MF. Single-Cell Rnaseq Analysis of Testicular Germ and Somatic Cell Development During the Perinatal Period. *Development* 2020;147**,** dev183251.

Tanaka A, Nagayoshi M, Awata S, Mawatari Y, Tanaka I & Kusunoki H. Completion of Meiosis in Human Primary Spermatocytes through in Vitro Coculture with Vero Cells. *Fertility and Sterility* 2003;79**,** 795-801.

Tao Y, Sanger E, Saewu A & Leveille M-C. Human Sperm Vitrification: The State of the Art. *Reproductive Biology and Endocrinology* 2020;18**,** 17.

Tesarik J & Bahceci M. Restoration of Fertility by in-Vitro Spermatogenesis. *The Lancet* 1999;353**,** 555-556.

Tesarik J, Balaban B, Isiklar A, Alatas C, Urman Bl, Aksoy S, Mendoza C & Greco E. In-Vitro Spermatogenesis Resumption in Men with Maturation Arrest: Relationship with in-Vivo Blocking Stage and Serum Fsh. *Human Reproduction* 2000;15**,** 1350-1354.

Tournaye H, Dohle GR & Barratt CL. Fertility Preservation in Men with Cancer. *Lancet* 2014;384**,** 1295-1301.

Tsuji Y, Yoshimura N, Aoki H, Sharov AA, Ko MSH, Motohashi T & Kunisada T. Maintenance of Undifferentiated Mouse Embryonic Stem Cells in Suspension by the Serum- and Feeder-Free Defined Culture Condition. *Developmental Dynamics* 2008;237**,** 2129-2138.

Tung PS & Fritz IB. Interactions of Sertoli Cells with Myoid Cells in Vitro. *Biology of Reproduction* 1980;23**,** 207-217.

Valli-Pulaski H, Peters KA, Gassei K, Steimer SR, Sukhwani M, Hermann BP, Dwomor L, David S, Fayomi AP, Munyoki SK, Chu T, Chaudhry R, Cannon GM, Fox PJ, Jaffe TM, Sanfilippo JS, Menke MN, Lunenfeld E, Abofoul-Azab M, Sender LS, Messina J, Klimpel LM, Gosiengfiao Y, Rowell EE, Hsieh MH, Granberg CF, Reddy PP, Sandlow JI, Huleihel M & Orwig KE. Testicular Tissue Cryopreservation: 8 Years of Experience from a Coordinated Network of Academic Centers. *Human Reproduction* 2019;34**,** 966-977.

Ventela S, Come C, Makela JA, Hobbs RM, Mannermaa L, Kallajoki M, Chan EK, Pandolfi PP, Toppari J & Westermarck J. Cip2a Promotes Proliferation of Spermatogonial Progenitor Cells and Spermatogenesis in Mice. *PLoS ONE* 2012;7**,** e33209.

Vermeulen M, Del Vento F, Kanbar M, Pyr Dit Ruys S, Vertommen D, Poels J & Wyns C. Generation of Organized Porcine Testicular Organoids in Solubilized Hydrogels from Decellularized Extracellular Matrix. *International Journal of Molecular Sciences* 2019;20**,** 5476.

von Kopylow K, Schulze W, Salzbrunn A, Schaks M, Schäfer E, Roth B, Schlatt S & Spiess AN. Dynamics, Ultrastructure and Gene Expression of Human in Vitro Organized Testis Cells from Testicular Sperm Extraction Biopsies. *Molecular Human Reproduction* 2018;24**,** 123-134.

Walker WH. Testosterone Signaling and the Regulation of Spermatogenesis. *Spermatogenesis* 2011;1**,** 116-120.

Wang J, Gao W-J, Deng S-L, Liu X, Jia H & Ma W-Z. High Temperature Suppressed Ssc Self-Renewal through S Phase Cell Cycle Arrest but Not Apoptosis. *Stem Cell Research & Therapy* 2019;10**,** 227.

Wang P, Suo LJ, Wang YF, Shang H, Li GX, Hu JH & Li QW. Effects of Gdnf and Lif on Mouse Spermatogonial Stem Cells Proliferation in Vitro. *Cytotechnology* 2014;66**,** 309-316.

Ward ZJ, Yeh JM, Bhakta N, Frazier AL & Atun R. Estimating the Total Incidence of Global Childhood Cancer: A Simulation-Based Analysis. *The Lancet Oncology* 2019a;20**,** 483-493.

Ward ZJ, Yeh JM, Bhakta N, Frazier AL, Girardi F & Atun R. Global Childhood Cancer Survival Estimates and Priority-Setting: A Simulation-Based Analysis. *Lancet Oncology* 2019b;20**,** 972-983.

Ward ZJ, Yeh JM, Bhakta N, Frazier AL, Girardi F & Atun R. Global Childhood Cancer Survival Estimates and Priority-Setting: A Simulation-Based Analysis. *Lancet Oncology* 2019c;20**,** 972-983.

Wasilewski-Masker K, Seidel KD, Leisenring W, Mertens AC, Shnorhavorian M, Ritenour CW, Stovall M, Green DM, Sklar CA & Armstrong GT. Male Infertility in Long-Term Survivors of Pediatric Cancer: A Report from the Childhood Cancer Survivor Study. *Journal of Cancer Survivorship* 2014a;8**,** 437-447.

Wasilewski-Masker K, Seidel KD, Leisenring W, Mertens AC, Shnorhavorian M, Ritenour CW, Stovall M, Green DM, Sklar CA, Armstrong GT, Robison LL & Meacham LR. Male

Infertility in Long-Term Survivors of Pediatric Cancer: A Report from the Childhood Cancer Survivor Study. *Journal of Cancer Survivorship* 2014b;8**,** 437-447.

Winter JS, Faiman C, Hobson WC, Prasad AV & Reyes FI. Pituitary-Gonadal Relations in Infancy. I. Patterns of Serum Gonadotropin Concentrations from Birth to Four Years of Age in Man and Chimpanzee. *Journal of Clinical Endocrinology & Metabolism* 1975a;40**,** 545-551.

Winter JSD, Faiman C, Hobson WC, Prasad AV & Reyes FI. Pituitary-Gonadal Relations in Infancy. I. Patterns of Serum Gonadotropin Concentrations from Birth to Four Years of Age in Man and Chimpanzee. *The Journal of Clinical Endocrinology & Metabolism* 1975b;40**,** 545-551.

World Health O. *Cureall Framework: Who Global Initiative for Childhood Cancer: Increasing Access, Advancing Quality, Saving Lives*. Geneva, World Health Organization.2021.

Wowk B. Thermodynamic Aspects of Vitrification. *Cryobiology* 2010;60**,** 11-22.

Wrobel K-H, Schilling E & Zwack M. Postnatal Development of the Connexion between Tubulus Seminiferus and Tubulus Rectus in the Bovine Testis. *Cell and Tissue Research* 1986;246**,** 387-400.

Wrobel KH. Prespermatogenesis and Spermatogoniogenesis in the Bovine Testis. *Anatomy and Embryology* 2000;202**,** 209-222.

Wyns C, Curaba M, Petit S, Vanabelle B, Laurent P, Wese JF & Donnez J. Management of Fertility Preservation in Prepubertal Patients: 5 Years' Experience at the Catholic University of Louvain. *Human Reproduction* 2011;26**,** 737-747.

Wyns C, Curaba M, Vanabelle B, van Langendonckt A & Donnez J. Options for Fertility Preservation in Prepubertal Boys. *Human Reproduction Update* 2010;16**,** 312-328.

Wyns C, Van Langendonckt A, Wese F-X, Donnez J & Curaba M. Long-Term Spermatogonial Survival in Cryopreserved and Xenografted Immature Human Testicular Tissue. *Human Reproduction* 2008;23**,** 2402-2414.

Yamanaka H, Komeya M, Nakamura H, Sanjo H, Sato T, Yao M, Kimura H, Fujii T & Ogawa T. A Monolayer Microfluidic Device Supporting Mouse Spermatogenesis with Improved Visibility. *Biochemical and Biophysical Research Communications* 2018;500**,** 885-891.

Yang D, Zhang M, Gan Y, Yang S, Wang J, Yu M, Wei J & Chen J. Involvement of Oxidative Stress in Zno Nps-Induced Apoptosis and Autophagy of Mouse Gc-1 Spg Cells. *Ecotoxicology and Environmental Safety* 2020;202**,** 110960.

Yang Q-E & Oatley JM *Chapter Nine - Spermatogonial Stem Cell Functions in Physiological and Pathological Conditions. In:* RENDL, M. (ed.) *Current Topics in Developmental Biology.* 2014. Academic Press.

Yang S, Ping P, Ma M, Li P, Tian R, Yang H, Liu Y, Gong Y, Zhang Z, Li Z & He Z. Generation of Haploid Spermatids with Fertilization and Development Capacity from Human Spermatogonial Stem Cells of Cryptorchid Patients. *Stem Cell Reports* 2014;3**,** 663-675.

Yang Y & Honaramooz A. Effects of Medium and Hypothermic Temperatures on Preservation of Isolated Porcine Testis Cells. *Reproduction, Fertility and Development* 2010;22**,** 523-532.

Yang Y, Steeg J & Honaramooz A. The Effects of Tissue Sample Size and Media on Short-Term Hypothermic Preservation of Porcine Testis Tissue. *Cell Tissue Research* 2010;340**,** 397-406.

Yavin S & Arav A. Measurement of Essential Physical Properties of Vitrification Solutions. *Theriogenology* 2007;67**,** 81-89.

Yildiz C, Mullen B, Jarvi K, McKerlie C & Lo KC. Comparison of Cryosurvival and Spermatogenesis Efficiency of Cryopreserved Neonatal Mouse Testicular Tissue between Three Vitrification Protocols and Controlled-Rate Freezing. *Cryobiology* 2018;84**,** 4-9.

Yokonishi T, Sato T, Katagiri K, Komeya M, Kubota Y & Ogawa T. In Vitro Reconstruction of Mouse Seminiferous Tubules Supporting Germ Cell Differentiation1. *Biology of Reproduction* 2013;89.

Yokonishi T, Sato T, Komeya M, Katagiri K, Kubota Y, Nakabayashi K, Hata K, Inoue K, Ogonuki N, Ogura A & Ogawa T. Offspring Production with Sperm Grown in Vitro from Cryopreserved Testis Tissues. *Nature Communications* 2014a;5**,** 4320.

Yokonishi T, Sato T, Komeya M, Katagiri K, Kubota Y, Nakabayashi K, Hata K, Inoue K, Ogonuki N, Ogura A & Ogawa T. Offspring Production with Sperm Grown in Vitro from Cryopreserved Testis Tissues. *Nature Communications* 2014b;5.

Yoshida S. Stem Cells in Mammalian Spermatogenesis. *Development, Growth & Differentiation* 2010;52**,** 311-317.

Yoshida S. Open Niche Regulation of Mouse Spermatogenic Stem Cells. *Dev Growth Differ* 2018;60**,** 542-552.

Yoshida S, Sukeno M & Nabeshima Y. A Vasculature-Associated Niche for Undifferentiated Spermatogonia in the Mouse Testis. *Science* 2007a;317**,** 1722-1726.

Yoshida S, Sukeno M & Nabeshima YI. A Vasculature-Associated Niche for Undifferentiated Spermatogonia in the Mouse Testis. *Science* 2007b;317**,** 1722-1726.

Yu X, Sidhu JS, Hong S & Faustman EM. Essential Role of Extracellular Matrix (Ecm) Overlay in Establishing the Functional Integrity of Primary Neonatal Rat Sertoli Cell/Gonocyte Co-Cultures: An Improved in Vitro Model for Assessment of Male Reproductive Toxicity. *Toxicological Sciences* 2005;84**,** 378-393.

Zeng W, Snedaker AK, Megee S, Rathi R, Chen F, Honaramooz A & Dobrinski I. Preservation and Transplantation of Porcine Testis Tissue. *Reproduction, Fertility and Development* 2009;21**,** 489-497.

Zhang J, Hatakeyama J, Eto K & Abe S. Reconstruction of a Seminiferous Tubule-Like Structure in a 3 Dimensional Culture System of Re-Aggregated Mouse Neonatal Testicular Cells within a Collagen Matrix. *General and Comparative Endocrinology* 2014;205**,** 121-132.

Zhang L, Tang J, Haines CJ, Feng H, Lai L, Teng X & Han Y. C-Kit and Its Related Genes in Spermatogonial Differentiation. *Spermatogenesis* 2011;1**,** 186-194.

Zhang XG, Li H & Hu JH. Effects of Various Cryoprotectants on the Quality of Frozen-Thawed Immature Bovine (Qinchuan Cattle) Calf Testicular Tissue. *Andrologia* 2017;49.

Zhang XM. Gfrα-1 Is a Reliable Marker of Bovine Gonocytes/Undifferentiated Spermatogonia: A Mini-Review. *Anatomia Histologia Embryologia* 2021;50**,** 13-14.

Zhang Y, Wang S, Wang X, Liao S, Wu Y & Han C. Endogenously Produced Fgf2 Is Essential for the Survival and Proliferation of Cultured Mouse Spermatogonial Stem Cells. *Cell Research* 2012;22**,** 773-776.

Ziloochi Kashani M, Bagher Z, Asgari HR, Najafi M, Koruji M & Mehraein F. Differentiation of Neonate Mouse Spermatogonial Stem Cells on Three-Dimensional Agar/Polyvinyl Alcohol Nanofiber Scaffold. *Systems Biology in Reproductive Medicine* 2020;66**,** 202-215.

Zogbi C, Tesser RB, Encinas G, Miraglia SM & Stumpp T. Gonocyte Development in Rats: Proliferation, Distribution and Death Revisited. *Histochemistry and Cell Biology* 2012;138**,** 305-322.

Appendix I

Research output

Publications

Tang S, Jones C, Coward K. Dissociation, enrichment, and colony formation for bovine gonocytes in vitro. (In preparation)

Tang S, Jones C, Davies J, Lane S, Coward K. A comparison between vitrification and two methods of slow freezing for the cryopreservation of gonocyte-containing neonatal calf testicular tissue. (In preparation)

Tang S, Jones C, Davies J, Lane S, Coward K. Effects of transport delay upon the process of cryopreservation on immature testicular tissue. (In preparation)

Tang S, Jones C, Coward K. Three-dimensional organoid culture for spermatogonial stem cell in vitro maintenance and spermatogenesis. (In preparation)

Presentations

Oral presentations at national and international conferences

Tang S, Jones C, Coward K. Fertility preservation in pre-pubertal boys with cancer: the cryopreservation of immature testicular tissue and the isolation of spermatogonial stem cells to encourage in vitro spermatogenesis in frozen/thawed testicular samples. Molecular Andrology, Giessen, Germany. Sept 2019 (Oral Presentation)

Tang S, Jones C, Coward K. Fertility preservation in pre-pubertal boys with cancer: developing a three-dimensional scaffolding system to encourage in vitro spermatogenesis in frozen/thawed testicular samples. British Andrology Society 2019, London, UK. Sept 2019 (Oral Presentation)

Poster presentations

Tang S, Jones C, Coward K. Fertility preservation in pre-pubertal boys with cancer: A three-dimensional prepubertal testicular organoid for in vitro spermatogonial stem cell propagation and spermatogenesis. 37th European Society of Human Reproduction and Embryology (ESHRE) annual meeting, Jun 2021 (ePoster Presentation)

Tang S, Jones C, Coward K. Development and optimization of a three-dimensional organoid culture system for prepubertal testicular cells to support spermatogonial stem cells. Fertility 2021, Feb 2021 (ePoster presentation)

Tang S, Jones C, Coward K. Fertility preservation in pre-pubertal boys with cancer: cryopreserving immature testicular tissue and developing a three-dimensional scaffolding system to encourage in vitro spermatogenesis. 36th ESHRE, Jul 2020 (ePoster Presentation)

Tang S, Jones C, Coward K. Fertility preservation in pre-pubertal boys with cancer: developing a three-dimensional scaffolding system to encourage in vitro spermatogenesis in frozen/thawed testicular samples. Annual Oxford Developmental Biology Symposium Programme, Oxford, UK. Dec 2019 (Poster Presentation)

Awards

- ✧ Clarendon Scholarship, University of Oxford (2018-2021)
- ✧ Goodger & Schorstein Scholarship, Medical division, University of Oxford (2021)
- ✧ Graduates' Research Fund, Lincoln college Oxford (2019, 2020)
- ✧ Sir Alec Turnbull Travelling Scholarship, Nuffield Department of Women's & Reproductive Health, University of Oxford (2019)
- ✧ Travel grant by the Society of Reproduction and Fertility (2020)
- ✧ Travel grant, Molecular Andrology conference, Giessen, Germany (2019)